

14/9/76

"D₃ CHROMOPHORES -
geometric distortion in trigonal-dihedral transition metal
chromophores and its relevance to optical circular dichroism."

a thesis submitted for the
Degree of Doctor of Philosophy
at the University of Adelaide
in May, 1973.

by KEITH RAYMOND BUTLER, B.Sc. (Hons.)

Department of Physical and Inorganic Chemistry.

PART II

PART II

ANALYSIS OF STRUCTURAL DATA



CHAPTER 6 ML₆ TRANSITION METAL CHROMOPHORES: SPECTRAL THEORY.

6.1 INTRODUCTORY REMARKS

The low resolution visible absorption spectra of transition metal complexes were early^{ier 12)} shown to be characteristic of the ML_n first coordination sphere (or chromophore).[?] Although the broad spectral features of the pseudo-octahedral complexes can be qualitatively explained in terms of the number and symmetry of the electronic transitions expected for an O_h symmetric ML₆-core the question arises as to the level at which the lowered-symmetry of a chelate complex becomes manifest in the electromagnetic properties. The long wavelength *d-d* transitions of transition metals are triply degenerate in O_h symmetry and any lowering of the chromophore symmetry should result in at least partial lifting of this degeneracy. ✓

Measurement of the CD spectra of chiral complexes suggests that the degenerate components of the pseudo-octahedral transitions are resolved in favourable instances. Therefore assignment of the absolute configuration of chiral transition metal complexes from their circular dichroism spectra, other than by an empirical correlation of curve shape, requires a knowledge of the symmetry and energy ordering of the optically active electronic transitions. The accepted interpretation of the "trigonal-splitting" of the octahedrally-based degenerate transitions in D₃ chromophores has been questioned and it is worthwhile at this stage to review the treatment adopted in this work.

In section 6.2 the relevant spectral theory of pseudo-octahedral

ML_6 chromophores, particularly of Cr^{III} and Co^{III} , is outlined and in section 6.3 the theoretical interpretation of the ORD and CD spectra of the trigonal-dihedral complexes of these metals is discussed.

6.2 ABSORPTION SPECTRA

6.2.1 Octahedral Symmetry (O_h)

Coordination of six identical ligands, L, to a transition metal to give an octahedral ML_6 -core (O_h symmetry) partially lifts the five-fold degeneracy of the d -orbitals of the isolated spherical metal ion; three orbitals of t_{2g} symmetry and two of e_g symmetry result, the e_g orbitals lying at energy Δ (or $10 Dq$) above the t_{2g} orbitals. The $d-d$ spectra of transition metal complexes result from electronic transitions between these split d orbitals.

Octahedral Cr^{III} has the ground electronic configuration ${}^4A_{2g}(t_{2g}^3)$; application of group theory predicts²¹⁷ three major absorption bands for Cr^{III} in an octahedral environment due to spin-allowed electronic transitions from the non-degenerate ground state. In order of increasing energy these are ${}^4A_{2g} \rightarrow {}^4T_{2g}(t_{2g}^2 e_g^1)$, ${}^4A_{2g} \rightarrow {}^4T_{1g}(t_{2g}^2 e_g^1)$ and ${}^4A_{2g} \rightarrow {}^4T_{1g}(t_{2g}^1 e_g^2)$, the latter two-electron jump being of low intensity and normally submerged under a strong charge transfer band.²¹⁸ Three low intensity quartet-doublet ($t_{2g}^3 \rightarrow t_{2g}^3$) zero-electron jumps are also predicted to occur in the region of the low energy transitions and are observed in low resolution spectra as band asymmetries; they will not be further considered in this discussion as they can have no allowed rotatory strength. The two one-electron

transitions each give rise to a broad band in the visible spectral region (330-780 nm); the transition symmetries are determined as the product of the ground and excited electronic state representations and are $T_{1g}({}^4A_{2g} \rightarrow {}^4T_{2g})$ and $T_{2g}({}^4A_{2g} \rightarrow {}^4T_{1g})$ in order of increasing energy.

The ground state of octahedral Co^{III} is the totally symmetric diamagnetic ${}^1A_{1g}(t_{2g}^6)$, except for high spin $[\text{CoF}_6]^{3-}$ which has a paramagnetic ${}^5T_{2g}(t_{2g}^4e_g^2)$ ground state.^{66,81} Analogous to the case of Cr^{III} , two "relatively" strong (weak by comparison with charge transfer bands; $\epsilon_{d-d} = 10-200$) absorption bands are observed in the visible region of the spectrum (13,000-30,000 cm^{-1}); in order of increasing energy the one-electron transitions responsible are ${}^1A_{1g} \rightarrow {}^1T_{1g}(t_{2g}^5e_g^1)$ and ${}^1A_{1g} \rightarrow {}^1T_{2g}(t_{2g}^5e_g^1)$, of symmetry T_{1g} and T_{2g} respectively. Several much less intense spin-forbidden singlet-triplet transitions also occur.

The low extinction coefficients of the visible absorption bands in octahedral transition metal complexes are an example of the Laporte selection rule which predicts zero electric-dipole strength (D_{ba}) for a transition between two orbitals of the same type within a single quantum shell.^{66,219} Although the spectra of metal complexes are a feature of the whole complex, the low resolution visible absorption spectra are largely characteristic of the transition metal ion, its oxidation state and the nature of the first coordination sphere,²²⁰ except in cases of chelation by unsaturated ligands (e.g. phen and dipy) where low lying ligand π -orbitals are of importance. Spectral details

of some relevant complexes are given in Table 6.1.

TABLE 6.1 *d-d* VISIBLE ABSORPTION BANDS OF $M^{III}L_6$ CHROMOPHORES

(M = Co, Cr; L = O, N).

<i>Complex</i>	<i>T_{1g} band</i>	<i>T_{2g} band</i>	<i>Refs.</i>
	ν_{max}^a (ϵ_{max})	ν_{max} (ϵ_{max})	
Co ³⁺ in α -Al ₂ O ₃ ^b	15.56	22.98	221
Co(H ₂ O) ₆ ³⁺	16.50 (40)	24.95 (50)	66,222
Co(CO ₃) ₃ ³⁻	15.75 (154)	22.73 (166)	159,223
Co(ox) ₃ ³⁻	16.60 (153)	23.70 (204)	27,222
Co(mal) ₃ ³⁻	16.45 (148)	23.60 (127)	154
Co(NH ₃) ₆ ³⁺	21.20 (56)	29.55 (46)	66,222
Co(en) ₃ ³⁺	21.30 (84)	29.40 (74)	27
Co(acac) ₃	16.8	ca. 25.0	224
Cr ³⁺ in α -Al ₂ O ₃ ^b	17.80 (40)	24.55 (60)	66,217
Cr(H ₂ O) ₆ ³⁺	17.40 (13)	24.60 (15)	66,217
Cr(ox) ₃ ³⁻	17.50 (74)	23.70 (97)	27,222
Cr(mal) ₃ ³⁻	17.40 (30)	23.40 (24)	27
Cr(NH ₃) ₆ ³⁺	21.46 (41)	28.25 (34)	225
Cr(en) ₃ ³⁺	21.74 (74)	28.33 (65)	27
Cr(tn) ₃ ³⁺	21.53 (55)	28.19 (48)	167
Cr(acac) ₃	17.9	-	224

a. frequency, $\times 10^3$ cm⁻¹.

b. positions of absorption bands vary with concentration of "impurity" ion.

Non-zero intensities for the visible absorption bands of the ideally octahedral hexaquo- and hexamine- Cr^{III} and Co^{III} complex ions arise from *u*-symmetric vibrations of the ML_6 -core, i.e. those vibrations which do not retain the octahedral centre of inversion;^{226,227} this vibronic contribution to the electric-dipole strength is common to chromophores of any symmetry.²¹⁹ Where the chromophore symmetry is already hemihedric (i.e. in the static geometry), as in ruby,²²⁸ the dipole-strength of the spin-allowed transitions is increased²¹⁹ as shown by the extinction coefficients listed in Table 6.1 or more correctly by comparison of band areas. It is this loss of inversion centre which is responsible for the increased dipole-strength of the allowed transitions of chiral tris-bidentate complexes of Co^{III} and Cr^{III} relative to the hexaquo- and hexamine-complexes.

Tris-bidentate complexes have idealized D_3 symmetry ($C_3 + 3C_2$ axes perpendicular) and the pure electronic selection rules can be expected to be dominant.²²⁹ However, the intensity of the ruby (Cr^{3+} corundum) absorption bands compared with those of $\text{Cr}(\text{H}_2\text{O})_6^{3+}$ suggests that static *ungerade* distortion of the CrO_6 core may contribute significant additional dipole-strength, even without consideration of the chiral ligand displacement. Comparison of the band intensities for the five- and six-membered chelate ring complexes (e.g. tris(ox) with tris(mal), tris(en) with tris(tn)) indicates generally reduced dipole-strengths for the larger ring ions; in these ions the ML_6 -core conforms most closely to an holohedric geometry (see Chapter 8). Various explanations of this "ring size effect" (both in absorption and

rotatory dispersion spectra) have been proposed^{25,60,65} but it should be realized that the ML_6 -core of most D_3 complexes is not O_h symmetric and electronic effects due to this static core distortion are usually inseparable from those due to the geometry of the complex as a whole.

6.2.2 Distortion from O_h Symmetry

The excited states (T) of octahedral Co^{III} and Cr^{III} discussed in section 6.2.1 are triply degenerate and further reduction, either static or dynamic, of the chromophore symmetry should lift this degeneracy (partially or completely) resulting in a splitting of the spectral bands: often the splitting of the excited state is small compared with the width of the absorption band envelope and band broadening or asymmetry only are observed.

Application of group theory gives^{229,230} the following breakdown of octahedral representations under the influence of a trigonal distortion of the ML_6 -core, i.e. elongation or compression along one C_3 axis of the parent octahedron. The resultant geometry has D_{3d} symmetry and

O_h	D_{3d}	D_3	C_3
A_{1g}	A_{1g}	A_1	A
A_{2g}	A_{2g}	A_2	A
T_{1g}	$A_{2g} + E_g$	$A_2 + E$	$A + E$
T_{2g}	$A_{1g} + E_g$	$A_1 + E$	$A + E$

retains the octahedral centre of inversion; hence the trigonal states

remain *gerade*. D_3 geometry is achieved by a twist of one pair of opposing trigonal faces of the parent octahedron, with or without concomitant axial elongation. Splitting of absorption bands due to static trigonal distortion of the ML_6 -core is usually not observed in ambient temperature solution spectra of tris(bidentate) complexes. This situation should be contrasted with that found for chromophores of the type CoA_4B_2 where splitting of the low energy T_1 band is particularly marked for the *trans*-complex^{219,231} when A and B are well separated in the spectrochemical series (e.g. *trans*- $[Co en_2F_2]^+$ (ref. 81), bis(aminoacidato) Co^{III} complexes^{232,233}), and for electronic configurations having strong Jahn-Teller distortion of the ground (e.g. Cu^{2+} , Mn^{3+} salts)^{81,234} or excited states (e.g. $[CoF_6]^{3-}$).^{81,235}

For Cr^{III} trigonal-dihedral (D_3) complexes ${}^4A_{2g} \rightarrow {}^4T_{2g}$ becomes ${}^4A_2 \rightarrow {}^4A_1 + {}^4E_a$ and ${}^4A_{2g} \rightarrow {}^4T_{1g}$ splits into ${}^4A_2 \rightarrow {}^4A_2 + {}^4E_b$ where the *a* and *b* subscripts of the doubly degenerate *E* components indicate the lower and higher energy transitions only and have no symmetry significance; analogously for Co^{III} the low energy transition becomes ${}^1A_1 \rightarrow {}^1A_2 + {}^1E_a$ and the high energy ${}^1A_1 \rightarrow {}^1A_1 + {}^1E_b$. For the present work the trigonal splitting parameter, *K*, is defined as $\nu_{E_a} - \nu_A$ for the T_1 symmetric lower energy octahedral transition and is negative when the non-degenerate *A* component lies higher in energy (i.e. shorter in wavelength) than E_a .^{†1}

^{†1} a) The T_2 transition should show similar splitting.

b) Elsewhere^{35,207,228} the trigonal splitting of the E_a and *A* component frequencies is symbolised as $3K'/2$ since the components are theoretically displaced $\pm \nu'$ and $\mp 2\nu'$ respectively to opposite sides of the unperturbed frequency: $3K'/2$ is therefore equivalent to the *K* defined here.

The following electric-dipole selection rules apply where the terms "parallel" and "perpendicular" define the polarization of the transition relative to the C_3 axis of the D_3 symmetric chromophore:

$$\begin{array}{lll} A_1 \rightarrow A_1 \} \text{ forbidden,} & A_1 \rightarrow A_2 \} \text{ parallel,} & A_1 \rightarrow E \} \text{ perpendicular.} \\ A_2 \rightarrow A_2 \} & A_2 \rightarrow A_1 \} & A_2 \rightarrow E \} \end{array}$$

For C_3 symmetry the $A \rightarrow A$ components are electric-dipole allowed in the parallel polarization and for D_{3d} symmetry ($C_3 + 3$ parallel mirror planes) all the trigonal component transitions are vibronically allowed but dipole forbidden because the inversion centre remains. Cotton²²⁹ argued that the polarized absorption spectrum of $\text{Cr}(\text{ox})_3^{3-}$ (ref. 207) follows the selection rules for D_3 symmetry, validating consideration of the whole complex ion rather than just the D_{3d} CrO_6 -core; in so doing, however, he neglected the relative twisting of the oxygen trigonal faces which in itself is sufficient to destroy the assumed centric symmetry of CrO_6 (see Chapter 8).

For exact D_3 symmetry the intensity of the high energy T_2 octahedral band should derive entirely from the E_g symmetric trigonal component. In the static crystal field approximation the intensity of the T_1 symmetric transition is partitioned between the A_2 and E_g components in the ratio 4:1;^{34,35,228,236} elsewhere^{192,237,238} this ratio is incorrectly quoted as 2:1. Rarely, the splitting of the T_1 transition has been decided from Gaussian analysis of the absorption band asymmetry but the observed dipole strength ratios often show marked divergence from the theoretical values.^{34,192} More usually the sign of the trigonal splitting is determined by means of plane-

polarized single crystal absorption spectra.^{29,35,173,207,239} The theory is most readily applied^{219,240} in the case of uniaxial crystals (trigonal, hexagonal, tetragonal) of known structure but the technique has also been successfully used in studying monoclinic crystals^{173,239,241,242,243} where the orientation of the pseudo-symmetry axes of the complex relative to the crystal optic axes is known. Considering the uniaxial case,²⁴⁴ and more particularly trigonal and hexagonal, two types of spectra are measurable;

- 1) *axial*; where the direction of propagation of the polarized (or unpolarized) light is parallel to the unique axis, c , the electric vector vibrating perpendicular to c .
- 2) *orthoaxial*; the incident plane-polarized light travels perpendicular to c . Here the electric vector can be parallel to the unique axis (π spectrum; $\underline{E} // c, \underline{H} \perp c$) or perpendicular (σ spectrum; $\underline{E} \perp c, \underline{H} // c$).

The *axial* and σ spectra should be coincident for an electric dipole mechanism,^{207,244} the $A_{1,2} \rightarrow E_{a,b}$ transitions being excited; the π spectrum should largely result from the $A_1 \rightarrow A_2$ ($A_2 \rightarrow A_1$) transition under the low energy octahedral absorption band. Note that only for a trigonal or hexagonal structure will K be trivially derived as $\nu_\sigma - \nu_\pi$.

The differentiation of E and A symmetric components by the use of plane-polarized light is not applicable to complexes in solution and it is questionable whether the splitting determined for the chromophore in a specific crystal environment is transferable within the solid state or to solution studies. The trigonal components of the long wavelength

T_1 octahedral band are supposedly distinguishable in the CD spectrum by virtue of their opposite signs (see section 6.3.1) but often (e.g. Cr(en)_3^{3+} , ref. 27, 60; Cr(tn)_3^{3+} , ref. 60, 67, 190; Co(ox)_3^{3-} , ref. 27, 184) one CD component only is observed in the solution spectrum and further "assumptions" must be made. Oriented single-crystal CD spectra can be used to identify the E symmetry components and by deduction the A trigonal component of the long wavelength transition. Few oriented single crystal CD spectra have been published; for Co(ox)_3^{3-} and Cr(ox)_3^{3-} in a $\text{NaMg[Al ox}_3\text{]}\cdot 9\text{H}_2\text{O}$ host lattice the polarized crystal spectra²⁰⁷ and single crystal CD spectra^{27,184} give a consistent sign for the trigonal splitting parameter K . However, for Co(en)_3^{3+} conflicting assignments have been made from the two types of spectra for the complex ion in various host lattices^{192,193,245-247} and in solution.^{192,248}

The more recently applied technique of magnetic circular dichroism promises²⁴⁹⁻²⁵¹ a means of distinguishing transitions from non-degenerate ground states to non-degenerate excited states from those to degenerate upper states; the technique is applicable both in solution and solid states. Further discussion of this technique will not be made here other than to indicate that Russell and Douglas^{180,252} have derived an extremely large trigonal splitting ($K = -1500 \text{ cm}^{-1}$) for $[\text{Co en}_3]^{3+}$ in solution from analysis of the MCD curve, in contrast to earlier studies^{246,249,253} which suggested only a very small splitting consistent with a vibronic (Jahn-Teller) mechanism. This inability to make a consistent assignment of the trigonal splitting, or for that

matter to decide whether the spectral splitting is a consequence of static distortion or *ungerade* vibronic coupling, is the major obstacle to current attempts to describe theoretically the optical rotatory properties of D_3 transition metal complexes; this point is discussed further in sections 6.3.1 and 8.3.3.

Another important question is the level at which reduced chromophore symmetry shows in the spectral properties. Just as the aqueous solution spectrum of a D_3 complex exhibits the broad bands characteristic of the octahedral chromophore so the polarized absorption spectrum of a tris-bidentate complex distorted from D_3 geometry is close to that expected for the undistorted symmetry: often, however, some intensity is observed under the high energy T_2 octahedral absorption band in the π spectrum (i.e. the ${}^1A_1 \rightarrow {}^1A_1$ (${}^4A_2 \rightarrow {}^4A_2$) transition is no longer electric-dipole forbidden for C_3 or lower symmetry) which, together with band asymmetry suggests that a D_3 representation of the chromophore is inadequate or that vibronic and covalency complications are significant.

As with transition dipole strength, so with energy level splitting it is important to appreciate the limiting description of the chromophore necessary to interpret the phenomenon. Simple electrostatic crystal-field treatments^{219,254} indicate that trigonal elongation (or compression) of the ML_6 -core along a C_3 axis of the octahedron is sufficient condition to split a triplet (T) excited state into a singlet (A) and a doublet (E). However, the sign of the splitting (K) for a compressed chromophore (θ , the polar angle, $\gg 54.74^\circ$; see Chapter 7) is inconsistently derived from the various theoretical treatments; the

point-charge ionic model gives K positive^{173,254} but introduction of significant σ - and π -bonding can reverse the predicted energy ordering of the trigonal components.^{191,241,254,255} As indicated above, the experimental assignments are equally inconsistent.

There are numerous examples of theoretical interpretations of spectral and magnetic properties in terms of trigonal distortion of an ideally octahedral ML_6 -core; for example, the ground state crossover from low spin ($^1A_{1g}$) to high spin ($^5T_{2g}$) and consequent splitting of the triplet state observed for several Fe^{II} complexes,^{256,257} and the splitting of the octahedral transitions in tris(oxalato) metal(III) complex ions^{207,258} (but not the $M^{III}(acac)_3$ complexes) and several tris(diethyldithiocarbamate) metal(III) complexes²⁴¹ (these assignments are further discussed in section 8.3.3). The polarized crystal spectra of trivalent "impurity" ions in the distorted C_3 MO_6 environment of $\alpha-Al_2O_3$ (corundum) have often been interpreted^{259,260} simply in terms of a trigonal compression with^{219,221} or without consideration of the predicted Jahn-Teller distortion of the excited state.²⁶¹

A recent interpretation²⁶² of the powder magnetic susceptibility data for $[Ti(urea)_6]I_3$ in terms of a trigonal twist of the TiO_6 -core about an octahedral C_3 axis raises an important query. An earlier analysis in terms of θ had not been entirely satisfactory and was questioned when the crystal structure determination²⁶³ showed negligible trigonal compression of the D_3 chromophore. How valid is it then to ignore the trigonal twist of a D_3 chromophore and interpret the spectral

splitting solely in terms of axial elongation or compression, especially when for most tris(four-) and tris(five-membered ring) complexes the former is the larger relative distortion (see the tables of section 8.1)?

6.3 OPTICAL ACTIVITY

6.3.1 Configurational Activity

Tris-bidentate transition metal complexes, $M(L-L)_3$, are the highest symmetry molecules (D_3) which can exist in two enantiomeric forms; the higher the enantiomer symmetry the theoretically less complex the ORD and CD spectra.²⁵

For a molecule to exist as two non-superimposable mirror image forms it must not possess a rotary inversion axis, S , as a symmetry element;^{58,59} a helix lacks such an axis and it is instructive to consider a D_3 complex as a short finite helix. Any two non-intersecting skew lines define a helix, a right-handed helix being said to have the opposite chirality to a left-handed helix. In the now accepted nomenclature^{127,128} a left-hand helix is designated Λ and a right-handed helix Δ ; Piper²⁶⁴ had previously used this symbolism to describe the chirality of D_3 complexes relative to the C_3 axis. The chirality of a helix perpendicular to the helix axis is opposite that parallel to the axis; thus a D_3 complex Λ with respect to C_3 is Δ relative to the perpendicular C_2 axes. Alternative symbols (e.g. $R(C_3)S(C_2)$,⁶⁸ $M(C_3)P(C_2)$ ^{27,265}) have been proposed to indicate this dual helicity but since definition of the chirality relative to C_3 necessarily implies an opposite skew about the C_2 axes the dual specification is unnecessary.

The rotational strength, $R_{b\alpha}$, of an optically active transition determines the contribution which that transition makes to the total rotatory power at any frequency. $R_{b\alpha}$ is a pseudo-scalar product of the electric- and magnetic-dipole moment operators for a particular transition and therefore should exhibit the largest values for those transitions which are both magnetic- and electric-dipole allowed. Returning to the O_h symmetric ML_6 -core, it was indicated in section 6.2.1 that for both Co^{III} and Cr^{III} the lowest energy spin-allowed one-electron transition has T_{1g} symmetry while the next highest has T_{2g} symmetry. The magnetic-dipole operator transforms as T_1 in O_h and therefore the low-energy band is magnetic-dipole allowed whereas the T_{2g} symmetric transition is magnetic-dipole forbidden.^{25,58,266}

This simplified description suggests that for a D_3 Co^{III} or Cr^{III} complex the major part of the rotatory power derives from the transitions of E_α and A symmetry under the first octahedral absorption band, these transitions being both electric- and magnetic-dipole allowed.²⁵ The higher energy E_b transition, however, being magnetic-dipole forbidden, should have zero rotational strength;^{†2} that it does not is attributed^{25,58,268} to a borrowing of magnetic-dipole strength by this transition from others of E symmetry (e.g. E_α , charge transfer) thus gaining a small second-order

^{†2} It has been argued²⁶⁷ that consideration of the symmetry of the "parent" octahedral transition is incorrect and that the symmetry of the trigonal components only is relevant. Since the magnetic-dipole selection rules in D_3 symmetry are identical with the electric-dipole selection rules given in section 6.2.2 the E_b component should then have an inherent non-vanishing rotatory strength.

rotational strength. In the D_3 formalism the high energy A component of the T_2 band is both magnetic- and electric-dipole forbidden and should have zero rotational strength. The magnetic-dipole "allowedness" of the trigonal component transitions can be tested in a manner analogous to that used for the determination of the electric-dipole characteristics but with regard to the plane of polarization of the magnetic vector, \underline{H} , of the incident light.²⁴⁴ These experiments and the weak rotatory-strength of the E_b component in most CD spectra of D_3 complexes suggest the "parent" octahedral formalism is basically correct.

For C_3 symmetry the A and E components of both the T_1 and T_2 octahedral transitions are magnetic- and electric-dipole allowed. ORD and CD are two of the most sensitive techniques (certainly in organic chemistry) for distinguishing small structural changes in a chiral chromophore; even so, the CD spectrum of the C_3 symmetric $\Lambda(+)[Co(+)pn_3]^{3+}$ ion is virtually identical with that of the potentially D_3 symmetric $\Lambda(+)[Co en_3]^{3+}$ ion, both spectra showing a single minor positive peak under the envelope of the high energy ${}^1A_{1g} \rightarrow {}^1T_{2g} Co^{III}$ band,^{27,269} In contrast, the D_3 symmetric $\Lambda(\leftarrow)[Co ox_3]^{3\leftarrow}$ anion shows three components under this high energy band.²⁷ Again there is the question of the level at which the reduced structural symmetry should become observable in the electromagnetic properties.

The E and A component transitions are polarized perpendicular and parallel to the C_3 axis respectively (μ and ρ being parallel for each) and to first order should have equal but oppositely signed

rotatory strengths,^{34,41} i.e. $R(E_a) = -R(A)$, reflecting the opposing chiralities parallel and perpendicular to the three-fold axis.^{58,270} Incomplete cancellation of these oppositely signed components was considered to be due to a finite trigonal splitting^{34,191} (see also Chapter 7) but in some cases one component only is observed in the CD spectrum. However, although the total rotatory strength summed over all optically active transitions should vanish to zero^{238,246,271} the strength of an individual octahedral transition may be non-zero⁶⁵ and more recent theoretical models^{41,272} taken to second-order perturbation predict a dominant rotational strength for the E_a component of the long wavelength T_1 band in $D_3 Co^{III}$ and Cr^{III} complexes, in agreement with the empirical correlations adopted earlier (see Chapter 7).

Partial mutual cancellation of the A_2 and E_a components is indicated^{191,192} from a comparison of the solution and single-crystal CD spectra for $Co(en)_3^{3+}$; the solution rotatory strength is an order of magnitude lower. The use of oriented single-crystal CD spectra to identify the trigonal components was mentioned in section 6.2.2; for structures in which the C_3 axes of the tris-bidentate complex molecules are aligned parallel (or nearly so) to the optic axis of a uniaxial crystal, passing circularly polarized light along the optic axis, i.e. corresponding to the *axial* polarized light spectrum, excites only the E symmetric components. As with the plane-polarized spectral assignments, however, there remains the question of the validity of comparing these solid state CD assignments, often derived for the complex diluted in a host lattice of uncertain structure, with the solution spectra. No

orthoaxial CD spectra have been reported; uniaxial crystals are anisotropic perpendicular to the unique axis.

The aqueous solution spectrum¹⁹² of $\Lambda(+)$ Co(en)_3^{3+} has a dominant positive low energy CD component and a smaller negative component at higher energy under the ${}^1A_{1g} \rightarrow {}^1T_{1g}$ octahedral absorption band; there is a small positive component under the T_{2g} band envelope. *c* axis CD spectra of the complex ion in a tetragonal²⁷³ and hexagonal^{192,193} lattice show only the two positive components, their rotatory strengths being approximately ten times those in aqueous solution.¹⁹¹ The three solution components can therefore be assigned as E_α , A_2 and E_b to increasing energy. This interpretation of the observed CD bands as trigonal component transitions arising from "static" splitting of the triplet octahedral symmetry states has been questioned, it being inferred from single crystal CD/MCD^{249,253} and polarized spectral studies^{246,247,274} that the small splitting of the octahedral states reflects dynamic Jahn-Teller distortion of the first triplet excited state rather than partial removal of the degeneracy due to a static trigonal field. More recent discussions^{13,41,275} suggest that although this vibronic mechanism dominates²²⁷ the electric-dipole strength of Co(en)_3^{3+} it makes only a small contribution to the total rotatory strength,^{12,25} the dominant factor here being the chiral nature of the static *ungerade* ligand field (see also Chapters 7 and 8). The vibronic contribution to R_{T_1} for D_3 Co^{III} and Cr^{III} complexes is usually considered negligible²⁷⁶ but is probably responsible for the non-vanishing rotatory-strength of the E_b component.^{13,268,277} Thorough consideration of the role of

vibronic coupling,^{277,278} i.e. with *ungerade* vibrations of the ML_6 -core, in inducing rotatory-strength in the transition metal *d-d* transitions is of prime importance since if it is a significant contributing factor there can be no straightforward correlation between the absolute configuration of the complex, or the chirality of the static ML_6 -core distortion, and the signed rotatory strength.^{12,276}

It is not possible here to give a detailed discussion of vibronic effects or to comment on the modified intensity profile of degenerate states resulting from incorporation of spin-orbit coupling,^{219,244} ligand π -bonding^{173,224,254} and covalency^{255,279,280} in the ionic crystal-field model. For tris(acac)- and to a lesser extent tris(ox)-complexes the ligand π -orbitals overlap the metal t_{2g} -orbitals; delocalized ligand-metal π -bonding can reverse the component splitting order, i.e. change the sign of K , predicted from the point-charge crystal-field model and can promote appreciable dipole strength in the otherwise electric-dipole forbidden high energy ${}^4A_2 \rightarrow {}^4A_2$ and ${}^1A_1 \rightarrow {}^1A_1$ transitions. Allowance for spin-orbit coupling is important in evaluating the magnetic parameters of Cr^{III} systems^{219,222} but it has been argued that it can be neglected in spectral discussions since the Cr^{III} complexes exhibit spectra closely similar to those of Co^{III} for which there is no first-order spin-orbit coupling of the singlet states.^{276,281,282}

In the following chapters the formalism of the static crystal-field model is adopted. This is because, apart from its comparative simplicity, irrespective of the uncertainty as to the origin of the octahedral band

splitting the polarizations of the resultant components generally conform to that predicted for trigonally split octahedral T_1 and T_2 one-electron transitions on trigonal distortion of the static charge approximation of the O_h symmetric ML_6 -core.

6.3.2 Vicinal, Conformational and Environmental Effects

At what level must a transition metal complex be chiral in order that the $d-d$ transitions have non-vanishing rotatory strength? This question forms the basis of the present study, particularly as it relates to chiral distortion of the ML_6 -core as opposed to the configurational chirality of a D_3 complex as a whole and this aspect is discussed more fully in Chapters 7 and 8. In the present section our concern is with mechanisms other than configuration by which the transition metal ion $d-d$ transitions become optically active.

For optical activity to be observable in solution at least a partial resolution of the complex must be achieved (but even this is not an absolute requirement, see for example the comments on the Pfeiffer effect in sections 8.3.1 and 8.3.4); this is not so in the solid state where dissymmetric perturbation of ideally holohedric transition metal ML_6 units by the chiral crystal environment is sufficient condition to induce finite rotatory strength in the metal $d-d$ transitions. One example is α - $[Ni(H_2O)_6]SO_4 \cdot 6H_2O$ which crystallizes^{283,284} in the enantiomorphous space groups $P_{4_3}2_12/P_{4_1}2_12$; the NiO_6 core remains closely octahedral in the static approximation and the rotatory power is attributed^{285,286} to electronic interaction with the chiral crystal

environment. However, vibronic interactions are considered^{13,287} appreciable in this system although their contribution to the rotatory strength is disputed.²⁸⁵

Pronounced changes in the CD spectra attributed to specific interaction of a chiral complex with solvent molecules are well known;¹⁶⁵ the effect is not simply due²⁸⁸ to conformational lability of the chromophoric group since similar changes have been observed for conformationally rigid organic^{19,289} and inorganic chiral chromophores in optically-inactive solvents.^{269,282} This effect is analogous to the so-called "gegenion" or "outer-sphere" effects induced by certain counter-ions in aqueous solution, e.g. the effect of phosphate and selenite ions on the rotatory strengths of the $d-d$ transitions of Co^{III} and Cr^{III} tris(diamines).^{60,190,248,290,291} However, it is still uncertain to what extent these latter changes in component rotatory strength reflect a change in conformer distribution^{269,292} rather than enhancement of specific transition dipole strengths, as proposed^{248,291} (see section 8.3.1 for further comment on this point). A related solution effect is observed with optically active counter-ions (the Pfeiffer effect),^{71,293} the results not always being explicable^{294,295} merely in terms of displacement of the enantiomer equilibrium.

Of greater relevance is a recent solid-state CD study²⁹⁶ of $[\text{Co}(\text{NH}_3)_6]^{3+}$ crystallized as the (+) bromocamphorsulphonate; the microcrystalline KBr disc CD spectrum was weaker than that of (+) $[\text{Co en}_3]^{3+}$ and it seems probable that the rotatory strength of the metal $d-d$ transitions is induced solely by the chiral anion which must lie outside

the first coordination sphere; of course, the CoN_6 -core may also be hemihedric.

The importance of conformational contributions to the rotatory strength of transition metal complexes has been well demonstrated by the variable temperature studies of Co^{III} diamine complexes in aqueous solution. Chelated diamines (e.g. en, tn) can adopt relatively low energy skew forms in which the C-C bond of en or the CCC plane of tn is inclined to the CoNN donor atom plane; there are two limiting chiral forms, λ and δ ,^{127,128} of the bidentate ligand and they should make oppositely signed mirror symmetric contributions to the overall rotatory strength throughout the frequency range, provided it is valid to consider each ring in "electromagnetic isolation", i.e. provided there is no inter-ligand coupling on chelation of the second and third ligands. The conformational contribution to the rotatory strength is particularly important in attempting assignments of the absolute configurations of polydentate systems,¹⁶⁵ e.g. complexes of ethylenediamine-tetraacetic acid and its derivatives.

The presence of an asymmetric (chiral) centre in a ligand can induce finite rotatory strength in the $d-d$ transitions.²⁹⁷ This *vicinal* effect²⁹⁸ usually occurs with a concomitant conformational contribution,²⁹⁹ especially if the asymmetric atom is incorporated in the chelate ring, e.g. complexes of pn. However, in one notable example it has been stated^{300,301} that the optical activity of the bis-(tridentate) complex $\text{trans}[\text{Co dien}_2]^{3+}$ (dien = diethylenetriamine) is induced solely by a chiral displacement of the *trans*-(N-H) bonds in the chelated "linear"

tridentate ligands; the intra-ligand conformational contributions were argued to be self-cancelling but the relative inter-ligand conformational chirality and probable¹⁶⁵ hemihedric distortion of the $\text{Co}^{\text{III}} \text{N}_6$ core were not considered.

The rotatory strength of the Co^{III} and Cr^{III} $d-d$ transitions was long considered^{269,302} to be dominated by the configurational arrangement of chelated ligands about the metal ion but in view of the results of a recent variable temperature study²⁹² of $[\text{Co}(\text{tn}_3)]^{3+}$ it now seems that this simplifying assumption is untenable. All three effects (configurational, conformational, vicinal) produce noticeable changes throughout the visible-charge-transfer region of the CD spectrum;^{269,303} Douglas and co-workers^{298,304,305} and Mason et al^{306,307} have demonstrated the additivity of the rotatory strengths arising from these contributions and criteria for making conformational assignments based on the charge-transfer rotatory strength have been proposed.^{269,302,303}

From these necessarily brief comments it can be appreciated that not only is the theoretical treatment somewhat artificial with its neglect of covalency, vibronic effects and spin-orbit coupling but the interpretation of the long wavelength components of the CD spectrum as being largely free of specific solvent effects and conformational and vicinal contributions, i.e. reflecting solely a configurational or ML_6 -core distortion effect, is equally simplistic.

primary references for this chapter

refs. 25, 66-68, 217, 219, 229, 308.

CHAPTER 7 MODELS FOR CORRELATING THE SIGNED ROTATORY STRENGTHS OF D_3 TRANSITION METAL CHROMOPHORES.

The sign of the Cotton effect of a chiral molecule is opposite for its two enantiomeric forms. This property promised a ready method of assigning the absolute configurations of chiral chromophores and several models have been proposed for application to transition metal complexes and more particularly trigonal-bidentates of pseudo- D_3 symmetry. This work attempts (section 8.3) an empirical assessment of the predictive validity of one such model, the trigonal-distortion model of Piper and Karipides. It has not been possible to make such a detailed examination of the other relevant models in the present work; instead they are briefly reviewed in section 7.1.

7.1 SUMMARY OF RELEVANT MODELS

(1) *a priori* prediction of the sign of the Cotton effect for a particular electronic transition of a chiral transition metal complex proved uncertain. X-ray crystallographic determination³⁰⁹ of the absolute configuration of (+) $\text{Co}(\text{en})_3^{3+}$ as Λ provided the needed reference complex: (+) $\text{Co}(\text{en})_3^{3+}$ had previously been shown to have a dominant positive Cotton effect at long wavelength. Oriented single crystal CD spectra^{192,193,273} of the tris-complex ion in favourable host lattices suggested that the dominant positive component observed in the solution spectrum was E_g symmetric and that the smaller negative component under the envelope of the low energy octahedral transition had A_2 symmetry.

A minor positive component at still higher energy (under the T_{2g} absorption band) was confirmed as E_g symmetric.

Prior to this structural assignment of absolute configuration several methods had been proposed for correlating the configurations of chemically similar complexes. The method of least-soluble diastereoisomers applied by Werner¹⁴⁸ is reliable only where precipitation of one enantiomer occurs to the total exclusion of the other to give a crystalline diastereoisomer isostructural with a reference compound (see section 5.1). Incorrect correlation^{28,202} of the tris(phen)- and tris(dipy)-complexes of Ni(II), Ru(II) and Fe(II) as the antimony (+) tartrates is a pertinent example of failure to establish isomorphism. Delepine used the method of active racemates^{145,310} in relating the absolute configurations of (+) $\text{Co(ox)}_3^{3-} \equiv (-)_{546} \text{Rh(ox)}_3^{3-} \equiv (-) \text{Ir(ox)}_3^{3-}$. Jaeger¹⁴⁹ later applied the method to the tris(en) complexes of Co(III), Rh(III) and Cr(III) and his assignments have been verified by a more recent application¹⁴⁷ of the same method. Although Werner's and Delepine's methods are useful, both suffer from the limitation of relating only chemically similar complexes of the same charge and for reliable results optically pure samples must be used.

Correlation of absolute configurations via synthetic pathways has been more commonly applied to organic chromophores than to transition metal complexes but an important recent study²⁰⁴ has been the conversion, with retention of configuration, of (+) Ru(phen)_3^{2+} to (+) Ru(dipy)_3^{2+} (see section 5.3).

It was early realized in the synthesis of transition metal complexes

that linear diamines could adopt puckered conformations on chelation, the lowest energy conformer being that in which the substituents (be they hydrogen, methyl or more bulky groups) on the carbon-nitrogen ligand backbone atoms are maximally staggered, i.e. *gauche*. Where the coordinating ligand is optically active the conformational energy difference may favour formation of one complex ion structural isomer over an alternative form; if the ligand absolute configuration is known that of the complex may often be assigned. The stereospecific chelation of (+)/(-) pn to Co(III) studied by Dwyer and co-workers^{150,195,213,311} and the theoretical treatment by Corey and Bailar,¹ which predicted that for Co(en)_3^{3+} the conformer having all three C-C bonds parallel to the C_3 axis has the lowest enthalpy in the vapour state, are well known. Conformational energy calculations are now considerably more sophisticated than those of Corey and Bailar and the use of NMR has facilitated identification of the various isomers. A recent application has been in the study of six-membered diamine ring complexes, e.g. Co(tn)_3^{3+} (refs. 94, 312, 313): tris-complexes of *meso*- and *racemic*-2,4-diaminopentane have been prepared and their CD spectra correlated with the predicted absolute configurations based on the ring conformations indicated by the solution NMR spectra³¹⁴ (see section 8.3.3). Stereospecific coordination studies have been extended^{3,195,282,315} to polydentate complexes (e.g. of PDTA) and complexes containing the less puckered amino acid chelate rings.

Early attempts⁷ to correlate absolute configurations through the sign of the measured rotation at a fixed wavelength were unsuccessful

because the dispersion of optical rotation with wavelength was not appreciated. Comparison of ORD (or CD) curves without an understanding of the electronic transitions involved is similarly unrealistic except for electronically identical chromophores. The similar shapes observed for the ORD curves of $\Lambda(-)$ $\text{Co(ox)}_3/(\text{mal})_3^{3-}$, $\Lambda(+)$ $\text{Cr(ox)}_3/(\text{mal})_3^{3-}$ and $\Lambda(+)$ $\text{Cr(en)}_3/(-)$ Cr(tn)_3^{3+} complexes have already been discussed (section 5.3); the absolute configurations of several tris(ox), tris(en) and tris(phen) transition metal complexes had previously been related on the basis of the sign of the first inflexion in the ORD curve taken to decreasing wavelength (see e.g. refs. 150, 179). The inflexion point in the ORD spectrum of $\Lambda(-)$ Co(ox)_3^{3-} lies ca. 130 nm to longer wavelength than that of $\Lambda(+)$ Co(en)_3^{3+} ; the ORD curves of these two ions are qualitatively similar as are their CD spectra (Figure 5.5). The relative wavelength shift in the ORD and CD spectra of these two complex ions correlates well with the displacement of the ${}^1A_{1g} \rightarrow {}^1T_{1g}$ Co(III) absorption band (Table 6.1): since this is the magnetic-dipole allowed T_1 symmetric transition it should make a dominant contribution to the optical rotatory power at the long wavelength end of the spectrum. For these complexes, correlating the shapes of the ORD curves predicts the correct relative absolute configurations regardless of the nature of the ML_6 -core or the size of the chelate rings (see section 5.3). It would be interesting to extend this comparison to other complexes of Co(III) and Cr(III) (e.g. tris(carbonato), tris(acac), tris(biguanide)); regrettably the increasing availability of circular dichrographs and the expectation that CD spectra

offer greater potential resolution of the optically active transition components have resulted in a reluctance to publish even qualitative ORD curves.

(2) The probable resolution of E_a , A and E_b component rotatory strengths in the CD spectra of trigonal-dihedral Co(III) and Cr(III) chromophores stimulated the proposing of several models. At the same time it became necessary to determine the energy ordering of the E_a and A components of the $T_1(O_h)$ symmetric transition before some of these models could be tested. More importantly, the possible assignment of individual transition rotatory strengths promised a means of deriving the absolute configurations of low symmetry complexes from that of a related D_3 symmetric chromophore.

Observation that the positive long wavelength CD component of $\Lambda(+)$ Co(en)_3^{3+} was E_a symmetric prompted Mason to propose^{58,192,193} that related chromophores having a positive E_a or E_a -derivative component have a Λ configuration. This model has provided the greatest stimulus to determination of the absolute configurations of chiral transition metal complexes. It has been applied to many tris(five-membered chelate-ring) systems^{70,191,240} and to polydentates^{316,317} and bidentate complexes lacking trigonal symmetry^{282,318,319} where the observed components are interpreted as resulting from further removal of the degeneracy of the triply-degenerate excited octahedral states. Two important failures of the model are known, namely the assignment of Λ configurations to $(+)$ Co(tn)_3^{3+} (refs. 36, 96, 189, 190)

and (\ominus) $\text{Cr}(\text{mal})_3^{3-}$ (refs. 27, 28, 93).

Several variations of this basic model have been suggested: in some cases^{27,184} (e.g. (+) $\text{Co}(-)\text{pn}_3^{3+}$, (\ominus) $\text{Co}(\text{ox})_3^{3-}$) a single broad component only is observed under the envelope of the T_1 band and is labelled E_α in agreement with the general hypothesis that this component has the dominant rotatory strength,^{58,191} an assumption not followed^{67,190} in making the original assignment for (+) $\text{Co}(\text{tn})_3^{3+}$. Elsewhere it has been proposed that (a) the sign of the longest wavelength component be taken as reference^{67,204,320} or that (b) the signed net rotatory strength of the low-energy transition^{41,272} be considered diagnostic of the absolute configuration;^{61,232,233,282,321,322} proposition (b) follows the method of comparison of the long wavelength ORD spectra.^{150,216} No attempt has been made to assign relative absolute configurations on the basis of the rotatory strength of the E_D component alone (the rotatory strength of this component is probably most sensitive to vibronic effects) although a questionable correlation³²³ of charge-transfer CD spectra has been published.

The E_α sign model relates complex ion absolute configurations only and takes no account of vicinal or conformational effects. Hawkins and Larsen^{306,324} proposed an octant sign rule (similar to that applied^{18,325} to organic compounds having optically-active carbonyl groups) for correlating the sign of the Cotton effect for identified transitions of D_3 and lower symmetry chromophores. In applying³²⁴ this model monodentate ligands and exocyclic substituents on the chelate rings were considered to make no contribution but the ligand conformation was explicitly

included; any displacement of the donor atoms from exact orthogonality was ignored (application of the octant model, to the ML_6 donor atom cores considered in section 8.1, through program OCTANT (Appendix V) gave completely random correlations). The model simply sums the product terms for the ligand backbone atoms without any consideration of the electrostatic charge distribution.

The success of a hexadecal sector rule^{†1} in relating the signs of the CD components in pseudo-tetragonal transition metal chromophores has been re-emphasized^{275,306,326,327} in recent studies; the octant sign rule has been found less satisfactory for this class of chromophore.^{297,306} At the same time Mason³⁰⁶ has proposed a sextant rule applicable to D_3 complexes; this rule is elaborated in section 7.2. For complexes lacking either trigonal or tetragonal symmetry but having a "regular" octahedral ML_6 -core the nodal properties of the rotatory power are represented by the octahedral sector rule, $F(O_h)$.^{275,306} This function

^{†1} The various sector rules which have been proposed are:

octant sign: ³⁰⁶	$Z(X^2 - Y^2)$. N.B. - this orientation of the complex with respect to the orthogonal reference axes differs from that of ref. 324.
$F(D_{4h})$ /hexadecal: ^{275,306,326}	$XYZ(X^2 - Y^2)$.
$F(O_h)$ /octahedral: ^{275,306}	$XYZ(X^2 - Y^2)(Y^2 - Z^2)(Z^2 - X^2)$. (But see the alternative formulation of ref. 165.)
$F(C_3)$ /sextant: ³⁰⁶	$X(3Y^2 - X^2)$.

where X, Y, Z are the coordinates of all ligand atom perturbors taken individually.

is considered^{165,306} to represent the conformational contribution of puckered chelate rings to the optical activity of pseudo-octahedral transition metal chromophores. Electrostatic charge distributions are not explicitly incorporated in the regional functions which serve only to define the nodal properties of the rotatory power; neglect of the charges associated with the perturber atom sites can lead to conflicting conclusions^{41,306} (see section 7.2). Application of the regional rules to a complex of known structure requires that the chromophore be correctly oriented with respect to the Cartesian reference axes: this was the original purpose of program OCTANT.

(3) Whereas the above approaches attempted to relate the sign of the observed Cotton effect to the chiral distribution of chelating ligands about the transition metal atom, the distortion model developed by Moffitt²⁵ and others attributed the optical rotatory power of the $d-d$ transitions solely to a static *ungerade* distortion of the ML_6 -core from O_h symmetry; it is a corollary of this model that tris-bidentate complexes having the same chiral distribution of ligands but opposite senses of distortion of the ML_6 -core should show enantiomeric Cotton effects. The important features of this trigonal-distortion model as it applies to trigonal-dihedral (D_3) transition metal chromophores are outlined in section 7.2.

Shinada³²⁸ developed an ionic model for the Cotton effect of D_3 transition metal complexes in which the ligand chelation effects were incorporated as effective dipole moments. The ORD and CD curve shapes

were calculated for (+) Co(en)_3^{3+} and (+) Cr(ox)_3^{3-} using trigonal splittings (K) of $+100 \text{ cm}^{-1}$ and $+250 \text{ cm}^{-1}$ respectively; although the experimental curves were well reproduced in the latter case, the theoretical curves for (+) Co(en)_3^{3+} showed an inversion in energy ordering about λ_{max} of the long wavelength absorption band, this inversion being unaltered by a change in the sign of K . However, without knowing the effective dipole moments the signed rotatory strength cannot be calculated for a given absolute configuration of a D_3 complex using this model.

Another description developed concurrently with the trigonal-distortion model is the orbital-mismatch model of Liehr.^{65,329,330} This model was developed in two parts, the first⁶⁵ applicable to D_3 transition metal complexes and the second³²⁹ to organic and inorganic compounds of lower symmetry; the "universality" of Liehr's molecular-orbital treatment is appealing in that no matter what the symmetry or chemical nature of the chromophore the optical rotatory power derives from a similar source, namely a mismatch of the bonding orbitals rather than chiral displacement of atomic nuclei. However, the requirement for relatively complete wave functions and the complexity of the resultant integrals make application of the model to transition metal complexes extremely difficult. Here we are more concerned with the qualitative aspects of the model as applied to D_3 complexes.

Liehr's model^{65,330} is similar to the trigonal-distortion model of Piper and Karipides (section 7.2) in considering the optical rotatory power of D_3 complexes to reflect the dissymmetry of the first-coordination,

or donor-atom, sphere. Although ligand conformational and vicinal effects are of major importance in digonal-dihedral and lower symmetry complexes they are credited³²⁹ with making only a minor contribution to R_{ba} in the D_3 geometry and cannot alter the sign of the metal atom activity (c.f. Richardson's model, section 7.2). The rotatory strength derives from a mismatch of the metal d and donor atom σ orbitals measured as the "angle of cant", α_c ; O_h symmetry of the ML_6^- core does not impose a zero α_c and hence, unlike the first order trigonal-distortion model, the rotatory strength for this centric arrangement of donor atom nuclei is non-vanishing. Note that although ML_6 was taken as O_h symmetric for the detailed derivation relaxation of this restriction does not alter the qualitative predictions, resulting only in an increase in the electric-dipole strengths due to the hemihedric field. Zero angle of cant gives zero rotatory power but reversing the sign does not invert the sign of the rotational strength due to a compensating sign change in the covalency parameters; the larger the angle of cant, the greater the rotational strength. In applying the model to $Cu(en)_3^{2+}$ and $Cu(ox)_3^{4-}$ Liehr showed that the mathematical treatment required for σ -bonded and σ, π -bonded complexes was essentially identical, a conclusion worthy of note in evaluating the experimental data with respect to other models.

Piper and Karipides³³¹ concluded that the experimental electric-dipole strengths for $Cu(en)_3^{2+}$ and $Co(en)_3^{3+}$ were more closely represented by the trigonal-distortion (molecular orbital) model than by Liehr's orbital-mismatch model; however, in analysing the experimental data they

invoked a trigonal-bidentate model having ligand angles at the metal atom greater than 90° (clearly not the case for either complex ion, see Table 8.1) and did not apportion the spectral intensity between the vibronic and static hemihedric sources. As for the E_α -sign model, the negative E_α component observed³⁶ for $\Lambda(-) \text{Co}(\text{tn})_3^{3+}$ is at variance with the predictions of the orbital-mismatch model since the sign of the rotatory strength of a chiral D_3 molecule is supposedly³²⁹ independent of the sign of the angle of cant for a given absolute configuration. The reduced rotational strengths observed for the tris(six-membered-ring) complexes (e.g. mal, tn) compared with the five-membered ring complexes (e.g. ox, en) offers some support for Liehr's model (since α_c decreases with increasing chain length⁶⁵) as opposed to the second-order trigonal-distortion model developed by Richardson⁴¹ (see section 7.2). Both models predict oppositely signed unequal rotational strengths for the A and E_α trigonal components of the T_1 symmetric octahedral transition, the theoretical rotatory strengths²⁵ being twice as large for $\text{Co}(\text{III}) (d^6)$ as for $\text{Cr}(\text{III}) (d^3)$ chromophores.

Schäffer²⁷⁶ has applied the "angular-overlap" model to an analysis of the CD spectra of tris- and *cis*-bis(bidentate) coordination complexes of $\text{Co}(\text{III})$ and $\text{Cr}(\text{III})$. As in the "trigonal-distortion" and "orbital-mismatch" models, the chirality of the chromophore is described in terms of the displacement of the six donor atoms from regular O_h symmetry. Evaluation of this model is not attempted here but it should be noted that the positive distortion parameters, ϵ and δ , as defined in Figure

1 of ref. 276, when extended within the D_3 framework of a Δ tris-bidentate complex correspond to a flattened (in terms of β , sections 7.3 and 8.2) trigonal-dihedral CoL_6 -core, an uncommon distortion in tris-bidentate complexes and certainly not the case in tris(en) cations (Table 8.1). The more common distortion in the direction of a trigonal prism is intimated elsewhere in ref. 276.

(4) Finally, a formalism of particular relevance to the interpretation of the optical rotatory spectra of transition metal complexes containing unsaturated ligands (e.g. phen, dipy, acac)^{21-24,199} is that based on the electric-dipole/electric-dipole coupled oscillator mechanism.^{271,321,332} Intense electric-dipole allowed $\pi \rightarrow \pi^*$ ligand transitions occur in the near ultra-violet region and dominate the spectral absorption at high frequency; the ligand field $d-d$ transitions in the visible region are partially obscured by intense charge transfer bands.¹⁹⁹ Consequently, correlation of absolute configurations of tris(phen) and tris(dipy) M(II) and M(III) complexes is commonly based on comparison of the rotatory strengths of the long-axis polarized ligand transitions.^{21,199,333} For the Co and Cr complexes the metal $d-d$ transitions are less obscured by the charge-transfer band and the predictions of the E_a -sign model and the exciton theory can be tested on the one complex;^{24,334,335} there has been no structural determination of the absolute configuration of these complexes as yet.

For tris(β -diketone) complexes the long wavelength absorption and CD spectra are often treated as typical $d-d$ ligand field transitions,

ignoring the complication of ligand- π -bonding and covalency effects and enabling direct comparison with the corresponding tris-oxalates.

7.2 DEVELOPMENT OF THE TRIGONAL-DISTORTION MODEL

(1) The "trigonal-distortion" model for optical activity in D_3 symmetric transition metal chromophores developed by Piper and Karipides^{34,35} had as its foundation the crystal-field model originally proposed by Moffitt.²⁵ An error²⁵ in the sign of the angular momentum matrix elements for the one-electron rotatory strength led Moffitt to predict a non-vanishing first-order rotatory strength for tris-bidentate transition metal complexes; Sugano³³⁶ identified the source of error and proved by symmetry argument that Moffitt's distortion model could not account for the rotatory power of these complexes.^{219,281}

Moffitt²⁵ attributed the optical activity of the $3d$ electronic spectra of the D_3 chromophores $M(en)_3^{3+}$ and $M(ox)_3^{3-}$, ($M = Co(III), Cr(III)$), to a mixing of the $3d$ and $4p$ orbitals of the coordinated transition metal and stressed that the small rotational strengths of magnetic-dipole forbidden transitions ($Cr(III), {}^4A_{2g} \rightarrow {}^4T_{1g}$; $Co(III), {}^1A_{1g} \rightarrow {}^1T_{2g}$) most probably arose from vibronic distortion of the nuclear framework and spin-orbit coupling; the activity of E_b supposedly^{34,192} derived from intermixing with E_a in the trigonal field (section 6.3.1). Although the chiral distribution of the three bidentate ligands around the central metal defines the absolute configuration of the tris-complex, the ligand backbone was not explicitly introduced into the detailed derivation of the rotatory

strength. The potential field was taken as octahedral³³⁷ having a subsidiary trigonal perturbation, v_3 ,^{†2} combining angular and radial functions (polar coordinate description) of the $3d$ orbitals. Moffitt claimed that the sign of the transition rotational strengths derived from the sign of v_3 , or more precisely from that of the angular function. The angular function reduces to components of the two polar angles θ and ϕ ; θ is the angle of inclination of the metal-ligand atom vector (or the M-L bond when considering only the ML_6 -core) to the trigonal axis of the D_3 system, i.e. θ is the polar angle, and ϕ is an angle in the plane perpendicular to the C_3 axis and thus is a measure of the deviation of the ML_6 -core from D_{3d} symmetry; Moffitt calls ϕ the *azimuthal* angle.^{†3}

Without details of the relative energies of the trigonally split components of the octahedral $d-d$ transitions, Moffitt²⁵ was restricted to the prediction that for $Co(en)_3^{3+}$ and $Cr(en)_3^{3+}$ of the same

$$†2 \quad v_3 = \sum \{ Y_3^{-3}(\theta_i, \phi_i) - Y_3^3(\theta_i, \phi_i) \} R_3(r_i) \quad \text{refs. 25, 34.}$$

v_3 is the *ungerade* trigonal field potential where the Y are spherical harmonics (after the formalism of Condon and Shortley³³⁷) dependent on the angular coordinates of the chromophoric electron and r_i is the electron radial coordinate, the summation being taken over all perturber atom sites.

†3 The term *azimuth* has been used throughout the development of the trigonal-distortion model; its use to refer to an angle in the plane perpendicular to the C_3 axis is confusing since, by definition,³³⁸ it denotes an arc of longitude, not latitude, e.g. see Piper's inconsistent usage in reference to both the polar angle³³⁹ and the horizontal twist angle.³⁵ We have chosen⁹⁶ to break with tradition and call the angle in the plane perpendicular to C_3 the *trigonal twist angle*; this angle is given the symbol ω to avoid confusion.

configuration the rotational strengths of the T_1 symmetric transitions should be of the same sign but about twice as active⁶⁵ for the Co(III) complex as for Cr(III). Piper²⁶⁴ concluded that, despite the error in Moffitt's derivation, the sign of the rotation should correlate with the sign of the trigonal potential: further, he proposed that the necessary *ungerade* field could be generated by distortion of the ML_6 first coordination sphere such that the angle α subtended by the bidentate ligand at the metal was no longer 90° , the sign of the rotational strength depending on the sign of $\Delta\alpha = 90 - \alpha$, i.e. complexes having the same absolute configuration would have oppositely signed R_{ba} if in one $\Delta\alpha > 0$ and in the other $\Delta\alpha < 0$. However, the sign of the observed trigonal splitting, K , could not^{207,264} be correlated with the sign of $\Delta\alpha$.

(2) Sugano³³⁶ and Hamer²⁸¹ showed by symmetry argument that $3d - 4p$ orbital mixing could make no first-order contribution to the net rotatory strength of the $d-d$ transitions of $(+)$ $Co(en)_3^{3+}$; Piper's²³⁶ conclusion that $3d - 4f$ mixing could account for the observed rotatory strength was shown by Karipides^{34,236} to result from an error in the matrix elements for the one-electron rotatory strength. The $d-p$ mixing gave a better representation of the electric-dipole strengths of the trigonal components than did the $d-f$ approximation^{34,264} and it was concluded^{34,275} that the latter mixing made little contribution to either the dipole- or rotatory-strengths. However, the $3d - 3d$ one-electron transitions were shown³⁴ to have finite rotatory strength

in the $d-p$ treatment if the t_{2g}^0 (i.e. a_1') and t_{2g}^\pm (i.e. e') orbitals had appreciably different radial parameters, i.e. if trigonal splitting of the t_{2g} orbitals occurred.

A major purpose of this research has been an attempted qualitative evaluation of the predictive worth of the $3d - 4p$ ionic (crystal-field) model detailed by Piper and Karipides³⁴ (hereafter variously termed the "PK-model" or the "trigonal distortion model") for correlating the signed rotatory strengths of D_3 symmetric transition metal complexes with the structural distortion of their ML_6 -cores; its relevance to various complexes is discussed in section 8.3. We are primarily concerned with the symmetry or nodal features of this model since an electrostatic crystal-field representation is inappropriate for making quantitative calculations of the rotatory strength. A molecular-orbital model developed by the same authors³⁵ gave improved values for the predicted electric-dipole strengths of the $Co(en)_3^{3+}$ electronic transitions but the nodal properties are identical with those of the PK-model and joint discussion is warranted.

For the PK-model the D_3 complex is described by the static distortion of the ML_6 -core from O_h symmetry, the six donor atoms each carrying point charge, z . The difficulty in evaluating the radial parameters (Moffitt's model) necessitates their being treated as semi-empirical constants. The earlier analysis²⁶⁴ in terms of the ligand angle, α , was not entirely satisfactory and these more complete treatments^{34,35} are in terms of the polar angles (θ, ϕ) introduced by Moffitt.²⁵ Evaluation³⁴ of the *ungerade* trigonal potential, v_3 ,

yielded as the constant coefficient

$$c = e z \left(\frac{3}{7}\right) \sqrt{35\pi} \cdot \sin^3 \theta \cdot \sin 3\delta \quad (\text{eq. 7.1})$$

where e is the electronic charge

θ is the polar angle subtended at the C_3 axis by the M-L bond, and

δ , the so-called *azimuthal* distortion constant, is defined positive for a Δ complex having contraction of the angle α within the chelate ring in projection on the plane defined by the three dihedral axes of the D_3 complex. In our nomenclature $\delta = (60 - \omega)$, 60° being the value of the trigonal twist angle, ω , in the holohedric D_{3d} symmetry (of which O_h is a special case, see section 7.3).

The sign of c is determined by δ and z , since θ has values approximating 54.74° (or $\pi - 54.74^\circ$), the value for an octahedron.

In the PK-model the trigonal splitting, K , and the rotational strength are respectively determined by the polar and trigonal twist distortions of the donor atom nuclei from O_h symmetry.^{35,41} The nodal position in the angular function determining the rotatory strength is $\delta = 0^\circ$ ($\omega = 60^\circ$): the trigonal splitting should be zero for $\theta = 54.74^\circ$ (or $\pi - 54.74^\circ$). As indicated in section 6.2.2, on the basis of the electrostatic crystal-field model K should be positive for an axially compressed ($54.74^\circ < \theta < 125.26^\circ$) ML_6 -core but this certainly seems not to be the case in the single-crystal CD spectrum^{192,273} of $Co(en)_3^{3+}$ where K is negative and $\theta > 54.74^\circ$ (see Table 8.1) nor in the oriented single-crystal CD spectrum³⁶ of the "supposedly" axially elongated

$\text{Co}(\text{tn})_3^{3+}$ ion where K is positive.

Prediction of the sign of the net rotatory strength of the T_1 symmetric octahedral transition was considered^{34,35,236} unreliable since experimentally it is the resultant of an almost complete cancellation of two trigonal components having much larger, oppositely signed rotational strengths. Fixing⁴¹ a residual negative charge on each ligator, L, gives a positive constant coefficient, c , for a Δ complex having $\delta > 0^\circ$. The discussion³⁴ of the signs expected for the radial parameters determining the rotatory strengths of the trigonal components is confusing; the sign of the rotatory strength derived from the PK-model effectively depends solely on δ ,³⁵ the ligator atom charge being taken as negative for all ligand types.⁴¹ The PK-model predicts³⁴ that a Δ complex having $\delta > 0^\circ$ (i.e. $\omega < 60^\circ$, trigonal twist contraction) should show a negative Cotton effect in the non-degenerate A component and a positive effect in the E_α component of the T_1 transition but this prediction is based on a polarized single-crystal assignment²⁴⁵ of the trigonal components of $\text{Co}(\text{en})_3^{3+}$ which is at variance with the single-crystal CD measurements^{192,273} showing K to be negative and R_{E_α} to be positive for the Δ configuration. Burer²⁵⁵ has shown that introduction of ligand covalency, π or σ , could effectively reverse the energy ordering of ${}^1E_\alpha$ and 1A_2 for the axially compressed ML_6 -core, without changing the nodal properties of the trigonal splitting or the rotatory strength.

In developing the molecular orbital model³⁵ the distortion was restricted to an expansion or contraction of the ligand angle, α ,

maintaining interligand plane dihedral angles $\gamma = 90^\circ$ (see sections 7.3 and 8.2); the Δ configuration was again treated but this time with trigonal twist expansion ($\omega > 60^\circ$). The non-donor atoms were not considered and π -bonding and spin-orbit coupling effects were neglected. Because of this inability to incorporate π -bonding contributions the PK-model was considered³⁵ inapplicable to tris(phen) and tris(dipy) complexes and of limited relevance⁴¹ to complexes having coordinated β -diketones, e.g. acac, as ligands.

The most significant corollary of the PK-model, ionic³⁴ and molecular-orbital,³⁵ is that two D_3 complexes of opposite absolute configuration should have rotational strengths of the same sign if in one the ML_6 -core is trigonal-twist expanded and in the other trigonal-twist contracted. Since the model does not yield a correct *a priori* calculation of the sign of the optical activity a reference complex is still required.³⁵

(3) Recently Richardson^{41,272} has extended the electrostatic PK-model to second-order in the trigonal perturbation and has incorporated the non-donor atoms in the derived potential function. This "R-model" is the most detailed discussion of the crystal-field treatment so far but still lacks an explicit discussion of vibronic effects; these are presently being included in a further refinement of the model.³⁴⁰ A summary of the R-model follows.

Richardson⁴¹ follows Moffitt²⁵ and Piper and Karipides^{34,35} in treating the tris-bidentate complex as pseudo-octahedral; however, the perturbing trigonal potential is attributed to the chiral arrangement

of the three bidentate ligands around the metal atom rather than solely to distortion of the ML_6 -core from O_h symmetry. To first-order in the *ungerade* trigonal potential the one-electron rotatory strength for the $d-d$ transition manifold vanishes to zero,^{270,281,336} but extension to second-order results in a residual rotatory strength.^{41,191,281} The trigonal components of the low energy octahedral transition (T_1 symmetry) are predicted^{34,270,281} to have equal (to first-order) but oppositely signed rotatory strengths, the sign being determined⁴¹ as

$$R'_{E_a} = e \left(\frac{35\pi}{14} \right)^{\frac{1}{2}} \sum_i^N q_i \sin^3 \theta_i \cos 3\phi_i / r_i^4 \quad (\text{the } \textit{ungerade} \text{ function})$$

(eq. 7.2)

where the summation is taken over all ligand atoms ($i \rightarrow N$)

excluding hydrogens,

q_i is the signed ligand atom charge,

θ_i is the polar angle subtended by the metal-ligand atom vector at the C_3 axis,

ϕ_i is the angular distortion constant in the plane of the three C_2 axes measured from one of the dihedral axes (see ref. 41),

and r_i is the metal-ligand atom distance.

The nodal properties of this function are identical with those of the constant c (eq. 7.1), $\cos 3\phi_i$ being the equivalent of $\sin 3\delta$. Richardson concluded⁴¹ that for the tris(diamine) complexes of Co(III) and Cr(III) the non-donor atoms should make a dominant contribution to

the first-order rotatory strength because of their larger polar angles and greater displacement from the ϕ nodal planes: if q_{CARBON} is positive, R'_{Ea} is positive for a Λ absolute configuration having "contracted" ligands. However, even though the ligating nitrogen atoms are closer to the octahedral positions resulting in smaller angular terms (especially $\cos^3\phi_i$), unless they lie precisely on the ϕ nodal planes (i.e. $\cos^3\phi_i = 0$) their contribution to R'_{Ea} may still be appreciable since

- a) they have smaller radial parameters, r_i , than the backbone carbon atoms, e.g. in Co(en)_3^{3+} : $\text{Co-N} \approx 2 \text{ \AA}$, $r_N^{-4} = 0.063$: $\text{Co}\dots\text{C} \approx 3 \text{ \AA}$, $r_C^{-4} = 0.012$, and
- b) in saturated chelate rings the electrostatic charge localized on the ligand backbone atoms is usually considered small relative to that on the donor atoms.

The *gerade* potential (polar distortion) of the R-model gives a finite trigonal splitting of the triply degenerate excited states; the sign of this splitting is obtained as

$$K = -\left(\frac{1}{14}\right)e \sum_i^N q_i (3\cos^2\theta_i - 1)/r_i^3 \quad (\text{eq. 7.3})$$

where $K = 0$ for $\theta_i = 54.74^\circ$. For $q_{CARBON} > 0$, K is negative for compression of the chromophore parallel to the C_3 axis, i.e. for $\theta_i > 54.74^\circ$; $K = \nu_E - \nu_A$, therefore the non-degenerate A component lies at higher energy as observed in the Co(en)_3^{3+} CD spectra.

Although a non-vanishing rotatory strength was predicted in the PK-model³⁴ due to the different radial wave functions of the trigonally

split components, calculation of the sign of the net-rotation was uncertain. The R-model results in a non-vanishing rotatory strength for both the T_1 and T_2 bands of D_3 symmetric Co(III) and Cr(III) complexes; this rotatory strength arises entirely from second-order contributions²⁸¹ and the sign is determined⁴¹ as

$$R''_{net T_1} = \left(\frac{1}{28}\right)^{\frac{1}{2}} \pi \sum_i^N \sum_j^N q_i q_j (3 \cos^2 \theta_i - 1) \sin^3 \theta_j \cos^3 \phi_j / r_i^3 r_j^4 \quad (\text{eq. 7.4})$$

being the double summation over all perturber sites (i, j) of the product of the *gerade* and *ungerade* functions. Since this second-order extension of the electrostatic crystal-field model involves product functions taken over two perturber sites at a time a knowledge of the electrostatic charge distribution as well as the detailed stereochemistry of the complex is required²⁷² for an evaluation of equation 7.4 unless considering charges of the same sign only, as for example when considering the ML_6 -core with all q_L negative.

In the derivation⁴¹ of the net rotatory strengths of the T_1 and T_2 symmetric transitions an error has arisen in transferring the $d-f$ # mixing terms but the relation that

$$R''_{net T_1} = a + b$$

and

$$R''_{net T_2} = R''_{E_b} = a + 4b \quad (\text{eq. 7.5})$$

holds good. Since the a and b terms have the same sign, R''_{E_b} and $R''_{net T_1}$ should have the same sign with R''_{E_b} being the larger rotatory strength; there is no first-order contribution to the rotatory strength

of the E_b component. There are several instances where this relationship between $R''_{net T_1}$ and $R''_{net T_2}$ seems not to hold (e.g. (+) Cr(en)_3^{3+} where the two absorption T_1 and T_2 bands each show a single CD component in aqueous solution, R''_{T_1} is large (+) and R''_{T_2} smaller (-);⁶⁰ similarly for the Co(ptn)_3^{3+} complexes and the tris(biguanides) of Co(III) and Cr(III) - see Tables 8.15 and 8.16): it should be remembered, of course, that the rotatory-strength of the magnetic-dipole forbidden high-energy T_2 symmetric transition is probably most sensitive to the effects of vibronic coupling.²⁶⁸

(4) A rigorous evaluation of the R-model is not possible in this work because of the requirement of knowing the electrostatic charge distribution over all perturber sites where these encompass both donor and backbone atoms of the bidentate ligands. Since both the PK- and R-models derive from the crystal-field approximation of a transition metal complex it is to be expected that the nodal properties of the first-order rotatory strength and the trigonal splitting would be identical when applied to the isolated ML_6 -core. The sign of the second-order rotatory strength derived from the R-model reflects the sense of both the polar (θ) and twist (ϕ) distortions; the predictions of the two models as applied to a D_3 symmetric ML_6 -core ($q_i < 0$) are summarized in Table 7.1. Consideration of only the methylene carbon atoms of an ethylenediamine ligand ($q_c > 0$) yields the following signs for a Λ trigonally-compressed/twist-contracted complex (e.g. $\Lambda(+)$ Co(en)_3^{3+}):

$$R'_{E_a} (+), K(-), R''_{net T_1} (+).$$

TABLE 7.1 PREDICTIONS OF THE PK- AND R-CRYSTAL FIELD MODELS.

Λ CONFIGURATION: ML_6 only: $q_L < 0$.

ML ₆ -core distortion	PK- and R- models		R- only
	R'_{E_a}	K	$R''_{net T_1}$
1. trigonal compression, $\theta > 54.74^\circ$			
twist contraction, $\omega < 60^\circ$	-	+	+
2. trigonal compression,			
twist expansion, $\omega > 60^\circ$	+	+	-
3. trigonal elongation, $\theta < 54.74^\circ$			
twist contraction	-	-	-
4. trigonal elongation,			
twist expansion	+	-	+

First-order rotatory strengths are orders of magnitude larger than the second-order activities; thus $R''_{191,192 net T_1}$ observed in solution CD spectra is a small residual of the overlap of two strongly rotating trigonal components of opposite sign and R''_{E_b} is seen to be smaller than R'_{E_a} when this overlap reduction is considered. Attributing the optical activity solely to the positively charged carbon atoms of $Co(en)_3^{3+}$ gives a second-order rotatory strength which supplements R'_{E_a} but diminishes R'_{A_2} ; E_a should be the dominant component under the T_1 band in agreement with the earlier empirical correlations.^{58,191} However, six-membered

chelate rings are predicted⁴¹ to induce larger rotatory strength than the corresponding five-membered rings in contradiction of the observed ring size effect^{60,182} (but contrast ref. 272). The trigonal splitting should also be larger for the larger ring complexes but the opposite seems to hold for four-, five- and six-membered ring derivatives (see section 8.3). The tris(1e1)^{†4} conformer of Co(en)_3^{3+} , e.g. $\Lambda(\delta\delta\delta)$, should show reduced trigonal splitting compared with tris(ob)- Co(en)_3^{3+} , i.e. $\Lambda(\lambda\lambda\lambda)$, contrary to empirical CD correlations:^{269,341} the predicted changes in net rotatory strength are more subtle — no sign change is predicted.^{41,272}

Richardson⁴¹ predicts, on the basis of the R-model, that substitution of the ligand hydrogen atoms will increase the net rotatory strength without sign change but examination of Dreiding models indicates that for substituents having charges of the same sign as the backbone atoms the rotatory strength will be diminished if the substituent group lies outside the sector spanned by the ligand, or at polar angles $\theta < 54.74^\circ$: this consideration is most relevant for substitution on the donor atoms rather than on the backbone atoms since

^{†4} Corey and Bailar¹ used the abbreviation "1e1" to refer to that conformer of Co(en)_3^{3+} having the three C-C bonds of the en ligands parallel to the C_3 -axis of the complex ion; tris(1e1) is an obvious extension of this terminology which recognizes the independence of the three chelate rings. tris(ob) refers to the Co(en)_3^{3+} conformer having the three C-C bonds oblique to the C_3 axis. The nomenclature is readily extended⁹⁶ to the six-membered ring complexes, e.g. Co(tn)_3^{3+} , for which the orientation of the C-C-C ligand backbone plane is the relevant geometrical parameter.

in the latter case the reciprocal radial vector term is diminishingly small.

Irrespective of component symmetry assignments the net negative rotatory strength observed for the ${}^1A_{1g} \rightarrow {}^1T_{1g}$ transition in the solution CD spectra^{36,60,190,292} of $\Lambda(-)$ $\text{Co}(\text{tn})_3^{3+}$ and^{111,342} $\Lambda(1e1)_3(-)$ $\text{Co}((+)\text{cptn})_3^{3+}$ contradicts the primary result of Richardson's second-order perturbation treatment,^{41,272} namely that D_3 -tris(bidentate) complexes of Λ configuration should exhibit a positive net rotatory strength, R''_{netT_1} , for this low energy transition regardless of ring size, conformation or vicinal effects: R'_{E_a} and R''_{E_b} should also be positive. Further, the prediction⁴¹ that two D_3 -complexes having similar, in terms of charge distribution, five- and six-membered chelate rings should show trigonal splittings of the same sign if all ligand backbone atoms have $\theta > 54.74^\circ$ contradicts the more generally observed dependence on the ML_6 -core distortion (see sections 6.2, 8.3).

(5) Various sector rules relevant to transition metal chromophores were mentioned in section 7.1. One of these, the sextant rule, $F(C_3)$, derived by Mason³⁰⁶ prescribes the nodal properties of the configurational contribution to the optical activity of trigonally symmetric chiral chromophores. The function $X(3Y^2 - X^2)$ has nodes at $n\pi/3$ degrees ($n = 0, 1, 2, \dots$) in the plane orthogonal to the C_3 axis; this corresponds to the nodal properties of the first-order crystal-field model (eq. 7.1 and 7.2) but lacks the polar nodal plane at $\theta = 54.74^\circ$ arising from the *gerade* function incorporated in the equation (eq. 7.5)

for the second-order rotatory strength of the R-model.

Since sector rules are based strictly on group theoretical arguments they predict only the "relative" signs of the CD components between complexes. Application³⁰⁶ of the sextant rule (without consideration of the distribution of the electrostatic charge) to the $\Lambda(+)$ $\text{Co}(\text{en})_3^{3+}$ and $\Lambda(-)$ $\text{Co}(\text{tn})_3^{3+}$ cations prompted Mason to conclude that the opposite signs for the observed rotatory strengths of the E_α components^{36,192,292} are a consequence of the donor-nitrogen atoms occupying different sextants in the two complexes. His conclusion that the configurational effect of the donor NH_2 groups dominates that due to the methylene CH_2 functions is at variance with an analysis of the R-model⁴¹ but in agreement with the more general assumption of backbone atom non-involvement made in applying the PK-model.^{34,35} The NH_2 and CH_2 contributions to the configurational rotatory strength were considered³⁰⁶ additive for the five-membered ring, in support of a larger rotational strength for the E_α component of $\text{Co}(\text{en})_3^{3+}$. In applying the sextant rule to $\text{Co}(\text{tn})_3^{3+}$ Mason has effectively assumed that a ligand angle $\alpha > 90^\circ$ implies a projected angle $\omega > 60^\circ$; the values listed in Table 8.2 suggest that this is probably the case for the tris(chair) conformer but the implicit assumption of ligand plane orthogonality in tris(bidentate) complexes is not supported by the structural data (sections 8.1 and 8.2).

(6) On the basis of an earlier treatment³²⁶ of pseudo-tetragonal transition metal chromophores, Richardson concluded that the one-electron

formalism adopted⁴¹ in deriving the rotatory strength of the ligand field transitions using the R-model was identical in nodal symmetry to the more rigorous electric-magnetic coupled oscillator (e-mCO) description. For conjugated ligands (e.g. β -diketones, dipy, phen) having intense electric-dipole allowed $\pi \rightarrow \pi^*$ transitions in the near ultra-violet region the oscillating electric-dipole can couple with the magnetic oscillator localized on the metal atom and the e-mCO mechanism will make a large contribution to the ligand-field rotatory strengths. However, the nodal properties should remain unaltered and provided the $d-d$ rotatory strength can be distinguished from that of the intense intra-ligand transitions (i.e. as in Co(III) and Cr(III) complexes) the R-model should remain qualitatively applicable.

This two-electron contribution to the rotatory strength is relatively less significant for the tris(oxalate) complexes and negligible for the essentially σ -bonded tris(diamines).

(7) To summarize the electrostatic crystal-field model of optical activity as embodied in the PK- and R-models:

First-order contributions (eq. 7.1, 7.2) dominate the rotatory strengths of the trigonal components of the T_1 symmetric magnetic-dipole allowed transition of chiral D_3 symmetric Co(III) and Cr(III) pseudo-octahedral chromophores giving rise, in the trigonal-field description, to an E_a and A component having equal but oppositely signed rotatory strengths: the first-order rotatory strength summed over the complete manifold of $d-d$ transitions is zero.

The net rotatory strengths of the T_1 and T_2 transitions are due solely to a second-order contribution (eq. 7.4, 7.5) not considered in the PK-model. As Richardson²⁷² has indicated, a structure-rotatory strength correlation based on the signs and relative intensities of the separate trigonal components would be preferable to correlation via the net rotatory strength of the T_1 manifold with its more complicated second-order dependence; the difficulty is, of course, that the spectral component assignments are often not available or are ambiguous.

In evaluating the validity of the PK-model (section 8.3) we are therefore concerned to apply the ML_6 -core geometries of relevant transition metal complexes to equations 7.1 (or 7.2) and 7.3, i.e. examining its success (or otherwise) in relating both the rotatory strength of the E_a trigonal component and the sign of the trigonal splitting parameter, K , to the precise distortion of the ML_6 first-coordination sphere. The evaluation is qualitative only and since the *a priori* predictions of this model are at best doubtful, we take as reference the trigonally-compressed, twist-contracted $\Lambda(+)$ $Co(en)_3^{3+}$ ion having R_{E_a} , $R_{net_{T_1}}$ and R_{E_b} all positive and $K = \nu_{E_a} - \nu_{A_2}$ negative: donor atoms for all complexes discussed are assumed to bear a residual negative charge.

For a D_3 symmetric ML_6 -core the sign of $R''_{net_{T_1}}$ (eq. 7.4) is derived as $-R'_{E_a} \times K$. All three equations (7.2, 7.3, 7.4) must be summed within the total complex ion framework for an evaluation of the R-model. Since the donor and non-donor atoms most probably bear electrostatic



charges of different magnitude and opposite sign, the determination of the relative signs of R'_E , K and $R''_{net T_1}$ is then more complex and can no longer be made in a qualitative manner.

7.3 THE TRIGONAL-DISTORTION PROGRAM: AZIMUTH

Program AZIMUTH was written in Fortran IV for use on a CDC 6400 computer. It was developed to facilitate determination of the geometric distortion parameters of the ML_6 -cores of tris-bidentate complexes, particularly those angular parameters of the coordination polyhedron relevant to an evaluation of the PK-model of optical activity as applied to trigonal-dihedral transition-metal chromophores. A copy of the program listing and typical printout follow this brief outline.

For D_3 symmetry, the geometric distortion of the six donor atoms of the ML_6 -core from regular octahedral positions can be fully specified by two angles; description in terms of inter-donor atom distances is equally satisfactory and has been used elsewhere (see section 8.2) but in this work we follow the more historical angular description which is immediately applicable to a qualitative discussion of the spectral and magnetic properties of tris-bidentate complexes. There are four characteristic angles (defined by Figure 7.1); specification of any two defines the others. α , the ligand angle, is that angle subtended by the bidentate ligand (L-L) at the metal atom, ω , the trigonal-twist angle, is the projection of α on the plane containing the three digonal axes,⁹⁶ θ , the polar angle, is the angle subtended by the M-L bond at the trigonal axis and β , the angle of

inclination, is the angle at which the ligand plane (defined as the plane L.M.L, where the donor atoms L are of the same bidentate ligand) is inclined to the plane containing the three digonal axes.

The four angles are related as follows:

$$\sin\theta = \cos(\alpha/2)/\cos(\omega/2) \quad (\text{eq. 7.6})$$

$$\cos\theta = \sin\beta.\sin(\alpha/2) \quad (\text{eq. 7.7})$$

$$\cos\beta = \tan(\omega/2)/\tan(\alpha/2) \quad (\text{eq. 7.8})$$

$$1/\tan\beta = \tan\theta.\sin(\omega/2) \quad (\text{eq. 7.9})$$

For O_h symmetry the angular values are $\alpha = 90^\circ$, $\omega = 60^\circ$, $\theta = \beta = 54^\circ 44.14'$ (approx. 54.74°); for trigonal prismatic (D_{3h}) geometry $\omega = 0^\circ$, $\beta = 90^\circ$ and $\theta = (\pi - \alpha)/2$. The unrealistic completely flattened geometry has $\alpha = \omega$, $\beta = 0^\circ$ and $\theta = 90^\circ$: for the meaningless geometry having $\alpha = 180^\circ$, ω is also 180° (except for D_{3h} when $\omega = 0^\circ$) and equations 7.6 and 7.8 are undefined — equations 7.7 and 7.9 give the correct equality for such a case, namely $\theta = \pi/2 - \beta$. Analogous equations connecting the angular parameters have recently been independently derived by Holm and co-workers;³⁴³ all angles have been used previously in discussing distortion of ML_6 -cores from O_h symmetry (see e.g. Gerloch,^{257,344} Piper,^{34,35} Tomlinson,²⁴¹ Kepert⁴²).

The program input consists of the crystallographic unit cell constants and the positional coordinates of the seven atoms of the ML_6 -core; trivial modification would permit inclusion of the whole D_3 complex but such an extension is not warranted for evaluation of the PK-model. Since the majority of tris-bidentate complex structures published in the crystallographic literature lack trigonal symmetry

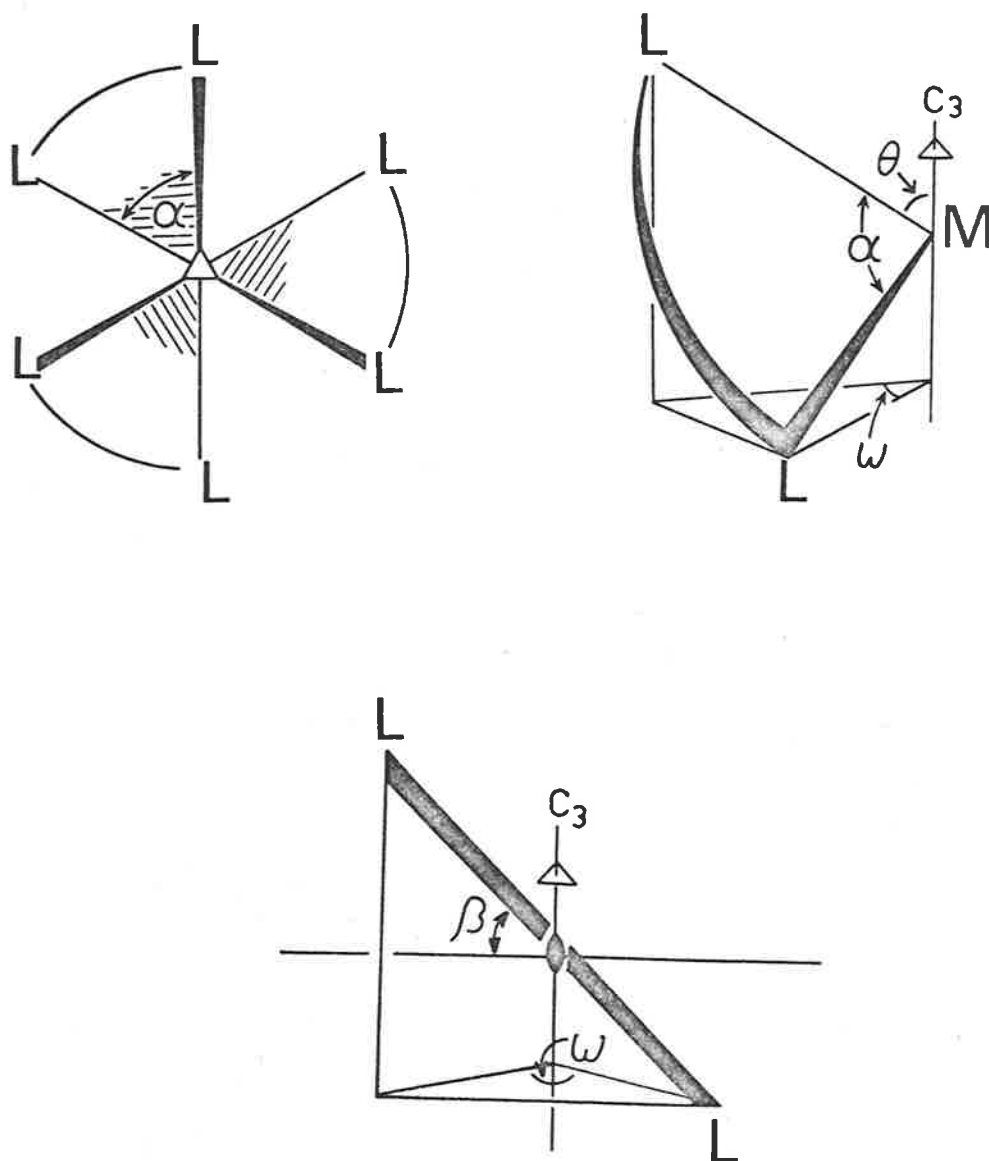


FIGURE 7.1: MODEL OF A TRIS-BIDENTATE COMPLEX IN THE A CONFIGURATION.

the most critical feature of any geometrical analysis such as that reported in this work is definition of the pseudo- C_3 axis: the approach adopted here has been to calculate the plane through the metal atom corresponding to the average of the planes through the two opposing sets of three non-linked ligator atoms. This plane is taken as the plane of reference for the determination of ω , θ and β , the C_3 axis being taken perpendicular to it and coincident with the metal atom. Other specifications are possible, e.g. the line through the "pseudo-centroids" of the opposing "trigonal" faces could be taken as reference axis but the metal atom would usually be displaced from such a line in cases lacking C_3 symmetry. The average plane treatment seems the most suitable without taking cognizance of the positional coordinate standard deviations.^{†5}

Program AZIMUTH outputs the individual α, θ, ω and β values and the sum averages of these are listed in section 8.1, except where divergence from the mean is considered worthy of note, e.g. θ for the corundum structures. This averaging of distortion parameters implies a linear relationship between them and the dependent electromagnetic properties; this is unrealistic as can be seen from equations 7.1-7.4 which all involve a trigonometric function of the distortion parameter. Ideally,

^{†5} A program for orienting pseudo-symmetric complexes with respect to a framework of exact symmetry so as to maximize the fit is currently being developed elsewhere.³⁴⁵ This program is reported to incorporate the standard deviations of the positional parameters of all atoms of the complex and the approach would be superior to the method of defining the C_3 axis used here.

in evaluating the polar and trigonal twist distortion functions the contribution of each donor atom should be individually computed for tris-bidentate complexes which lack exact D_3 symmetry.

In addition to α , θ , ω and β , program AZIMUTH estimates the degree of elongation (or compression) of the ML_6 -core along its pseudo- C_3 axis; this parameter is not quoted in the tables of section 8.1 as it is simply an extension of the information contained in $\beta^{\dagger 6}$ (sections 8.1 and 8.2). Since, in evaluating the PK-model we are concerned only with the distortion of the ML_6 -core from O_h symmetry, the ligand planes are represented as L.M.L, but in discussing the geometry of tris-bidentate complexes the average ligand planes should be used, preferably without inclusion of the coordinated metal atom since often this is significantly displaced from the ligand plane (see section 8.2). In either case distortion of the complex, or the ML_6 -core, toward a D_{3h} geometry can be expressed in terms of $\beta > 54.74^\circ$ or inter-ligand dihedral angles $\gamma > 90^\circ$; the limiting values for γ are $-D_{3h}$, trigonal prismatic, $120^\circ - O_h$, octahedral, 90° — completely flattened, 0° .

For the current data analysis, in cases of special interest where a preliminary communication only is in print, an effort has been made to acquire atomic positional coordinates from the authors. Where this was

^{†6} This measure of axial elongation (i.e. in terms of β) should not be confused with changes in the polar angle, θ , e.g. a D_3 complex having inter-ligand dihedral angles $\gamma = 90^\circ$ (i.e. $\beta = 54.74^\circ$) will have $\theta < 54.74^\circ$ for $\alpha > 90^\circ$ and $\theta > 54.74^\circ$ for $\alpha < 90^\circ$. Complexes with $\alpha < 90^\circ$ and $\theta > 54.74^\circ$ can still have $\beta > 54.74^\circ$ (see section 8.2) and can be described as distorted toward trigonal prismatic geometry. β is simply a measure of the degree of parallelism between the ligand plane, L.M.L, and the C_3 axis.

not possible a set of orthogonalized coordinates was calculated from the literature bond lengths and interatom vectors using program OCTANT (Appendix V). In its present format program AZIMUTH is restricted to seven atoms and for complexes having exact D_3 symmetry several of the calculation steps are unnecessarily repetitive.

Summary of the Mathematical Sequence -

- 1) Orthogonalization of the crystal coordinates, in Å.
- 2) Calculation of the planes (as fourth-order determinants)^{74,346,347} through the two sets of three non-bonded donor atoms and averaging of the coefficients to give the plane of reference through the metal atom.
- 3) Calculation of the six M-L bond lengths, a .
- 4) Calculation of the distances of the seven atoms (ML_6) from the reference plane.
- 5) Calculation of the ligand bites, i.e. L...L, b .
- 6) Calculation of ω .
- 7) Calculation of α .
- 8) Calculation of θ and $\sin^3\theta$.^{†7}

^{†7} Both the polar angle function ($\sin^3\theta$) and the trigonal twist function ($\sin 3\delta$) of Piper's constant (eq. 7.1) are computed from the averaged values of θ and ω , but are not quoted in Chapter 8 since the angular parameters are readily applied to a qualitative discussion of the nodal properties.

- 9) Calculation of β and estimation of the per cent axial elongation (or compression) for each ligand in terms of β ; $h = b\sin\beta$.
- 10) Determination of average α , α and ω ,^{†8} calculation of the inter-trigonal plane distance, h , in terms of these three parameters, namely

$$h = 2a(\sin^2(\alpha/2) - \cos^2(\alpha/2)\tan^2(\omega/2))^{1/2},$$

and estimation of the per cent elongation (compression) from the orthogonal arrangement having $\gamma = 90^\circ$ and $\beta = 54.74^\circ$. h could more easily have been calculated from the average β value.

†⁸ The version of program AZIMUTH listed hereafter determines the unsigned values of ω and β . For chiral pseudo-octahedral complexes averaging of the three independent values in those cases lacking exact C_3 symmetry is straightforward since the positive value is taken in the chiral-sense of the molecule with respect to the pseudo- C_3 axis, the three values for each parameter (i.e. ω and β) having identical signs. However, for pseudo trigonal prismatic complexes in which the ML_6 -core geometry is not precisely D_{3h} , the bidentate ligands often twist in the opposite chiral sense and the relative signs of the independent values must be considered in determining the ω and β averages. This is the case in the $V(dpd)_3$,^{348,349} $Re(dpd)_3$,^{350,351} and $Er(thd)_3$ ³⁵² structures (see notes on Tables 8.5 and 8.6 in section 8.1).

PROGRAM AZIMUTH(INPUT,OUTPUT)

C
 C INPUT FROM CARDS,CALC OF AZIMUTHAL ANGLES IN DISTORTED OCTAHEDRON
 C LOOKING DOWN THREE-FOLD AXIS PIPERS THEORY OF COTTON EFFECTS
 C CHIRALITY OF COMPLEX ION TAKEN AS ABS CONFIG OF LIGANDS
 C NOTE PIPERS THEORY DOES NOT CONSIDER LIGAND CHIRALITY BUT ONLY DISTORTION OF
 C IMMEDIATE SIX LIGAND ATOMS FROM IDEAL OCTAHEDRAL SYMMETRY BUTLER 1970
 C CRYSTAL COORDS. TRANSFORMED TO ORTHOGONAL COORDS. IN ANGSTROMS
 C DATA SET CARD 1.NUMBER OF DATA SETS
 C CARD 2.TITLE
 C CARD 3.UNIT CELL PARAS.NUMBER OF ATOMS,C3 INDICATOR
 C CARD 5.CRYSTAL ATOMIC COORDS.
 C ATOMS SHOULD BE SUPPLIED IN ORDER METAL,3 NONBONDED LIGATORS
 C SPANNING ONE TRIGONAL FACE,THE OTHER 3 NONBONDED LIGATORS SPANNING
 C THE OPPOSITE TRIGONAL FACE IN THE SAME ORDER AS FOR FACE1.
 C BUTLER JULY 1970-1972
 C

COMMON TITLE(8),X(7),Y(7),Z(7),XT(7),YT(7),ZT(7),BLEN(10),N(4),
 1PDIST(10),DISTL(10),ATOM(10),OMEGA(7),ALPHA(7),COSMU(7),AMU(7),
 2BMU(7),SINMU(7),COSBA(7),BET(7),BETA(7),SINB(7),EXPANS(7),CONTR(7)
 9000 FORMAT(8A10)
 9001 FORMAT(6F10.4,2I2)
 9002 FORMAT(A6,3F10.6)
 9003 FORMAT(1H1,8A10)
 9004 FORMAT(1H0,8X,1HA,8X,1HB,8X,1HC,7X,4HCOSA,7X,4HCOSB,7X,4HCOSC,2X,
 14HNATH,3X,3HNC3/X,3F9.4,3F11.5,2I6)
 9005 FORMAT(1H0,7X,*ATOM*,10X,*X*,8X,*Y*,8X,*Z*,7X,*XT*,7X,*YT*,7X,*ZT
 1*)
 9006 FORMAT(8X,A6,6F9.5)
 9008 FORMAT(1H0,X,* BOND LENGTH ATOM 1 TO *,A6,* IS *,F9.5,* ANGSTROM*)
 9009 FORMAT(1H0,X,* DISTANCE OF ATOM *,A6,* FROM PLANE *,F9.5,* ANGSTRO
 1M*)
 9010 FORMAT(1H0,X,* INTRALIGAND DISTANCE *,A6,* TO *,A6,* IS *,F9.5,
 1*ANGSTROM*)
 9011 FORMAT(1H0,X,* TRIGONAL ANGLE OMEGA *,A6,* TO *,A6,* IS *,F9.5,*
 1DEGREES*)
 9012 FORMAT(* DENOMINATOR ZERO*)
 9013 FORMAT(* AZIMUTH END*)
 9014 FORMAT(5X,*DEN=*,F9.5,*DUM=*,F9.5)
 9015 FORMAT(5X,*DIFP=*,F9.5,*PARR=*,F9.5,*PLAN=*,F9.5,*PLON=*,F9.5)
 9016 FORMAT(1H0,X,*LIGAND ANGLE ALPHA*,3X,A6,*TO*,3X,A6,F9.5,*DEGREES*/
 15X,*SUMP*,F9.5,*DUMP*,F9.5)
 9018 FORMAT(I4)
 9019 FORMAT(1H0,X,* EQUATION OF PLANE THROUGH METAL ATOM *//X,F9.5,
 1*XT*,F9.5,*YT*,F9.5,*ZT*,F9.5,*=0*)
 9020 FORMAT(1H0,X,*CA= *,F9.5,*CB= *,F9.5,*CC= *,F9.5,*CD= *,F9.5,
 1*CAA= *,F9.5,*CBB= *,F9.5,*CCC= *,F9.5,*CDD= *,F9.5)
 9021 FORMAT(1H0,X,* POLAR ANGLE THETA OF METAL *,A6,* BOND WITH C3 AXIS
 1*/6X,*COSMU= *,F10.6,*SINMU= *,F10.6,*AMU= *,F10.6,*THETA= *,
 2F10.6,*DEGREES*)
 9022 FORMAT(1H0,42H PIPERS POLAR ANGLE TERM (SIN(THETA))**3 =,F20.15)
 9023 FORMAT(1H0,* ELEVATION ANGLE BETA OF LIGAND PLANE *,A6,X,A6,* IS *
 1,F10.6,*DEGREES. SINB= *,F10.6)
 9024 FORMAT(X,*ROUGH ESTIMATE OF PER CENT EXPANSION IN TERMS OF BETA *,
 1F10.6)
 9025 FORMAT(X,*ROUGH ESTIMATE OF PER CENT CONTRACTION IN TERMS OF BETA
 1*,F10.6)
 9026 FORMAT(1H0,* AVERAGE BOND LENGTH *,F10.6,* ANGSTROMS */X,
 1* AVERAGE LIGAND ANGLE *,F9.6,* RADIANS*/X,
 2* AVERAGE TRIGONAL ANGLE*,F9.6,* RADIANS*)
 9027 FORMAT(1H0,X,* DISTANCE BETWEEN TRIGONAL PLANES FOR AVERAGE MODEL
 1*,F10.6,* ANGSTROMS*/,* A=*,F10.6,* C=*,F10.6,* D=*,F10.6,* E=*,
 2F10.6)

```

9028 FORMAT(1H0,/,X,* IDEALIZED TWIST ANGLE,OMIDR=*,F10.6,* DEGREES*)
9029 FORMAT(1H0,X,* HEIGHT OF IDEALIZED OCTAHEDRON,LIGAND ANGLE ALPHA,
1DOCTI=*,F10.6,* ANGSTROMS*,/X,* HEIGHT OF TRIGONAL PRISM,LIGAND AN
2GLE ALPHA,DTPI=*,F10.6,* ANGSTROMS*)
9030 FORMAT(1H0,X,* PER CENT EXPANSION OVER IDEALIZED OCTAHEDRON= *,
1F10.6)
9031 FORMAT(1H0,X,* PER CENT CONTRACTION FROM IDEALIZED OCTAHEDRON=*,
1F10.6)
9032 FORMAT(1H0,X,* HEIGHT OF OH OCTAHEDRON,ALPHA 90 DEGREES,IS *,
1F9.6,* ANGSTROMS*,/X,* HEIGHT OF TRIGONAL PRISM,ALPHA 90 DEGREES,
2IS*,F9.6,* ANGSTROMS*)
9033 FORMAT(1H0.5X,* PIPERS VARIABLE PRODUCT=*,F20.18)
9040 FORMAT(2X,I4)
      RAD=57.2957795131
      READ 9018,IDAT
      PRINT 9040,IDAT
      DO 1000 NCYC=1,IDAT
      READ 9000,TITLE
      PRINT 9003,TITLE
      READ 9001,A,B,C,COSA,COSB,COSC,NATM,NC3
      PRINT 9004,A,B,C,COSA,COSB,COSC,NATM,NC3

```

C

C CALCULATION OF TRANSFORMED COORDS.

```

      SG=SQRT(1.-COSC*COSC)
      CR=(COSA-COSB*COSC)/SG
      CP=SQRT(1.-COSB*COSB-CR*CR)
      PRINT 9005
      DO 1 I=1,NATM
      READ 9002,ATOM(I),X(I),Y(I),Z(I)
      XT(I)=A*X(I)+B*COSC*Y(I)+C*COSB*Z(I)
      YT(I)=B*SG*Y(I)+C*CR*Z(I)
      ZT(I)=C*CP*Z(I)
      PRINT 9006,ATOM(I),X(I),Y(I),Z(I),XT(I),YT(I),ZT(I)
1 CONTINUE

```

C

C CALCULATION OF PLANES THROUGH ATOMS 2,3,4 AND 5,6,7

```

      I=2 $ M=3 $ N=4
300 CAA=+YT(I)*ZT(M)+YT(M)*ZT(N)+YT(N)*ZT(I)
      1-YT(N)*ZT(M)-YT(M)*ZT(I)-YT(I)*ZT(N)
      CBB=-XT(I)*ZT(M)-XT(M)*ZT(N)-XT(N)*ZT(I)
      1+XT(N)*ZT(M)+XT(M)*ZT(I)+XT(I)*ZT(N)
      CCC=+XT(I)*YT(M)+XT(M)*YT(N)+XT(N)*YT(I)
      1-XT(N)*YT(M)-XT(M)*YT(I)-XT(I)*YT(N)
      CDD=-XT(I)*YT(M)*ZT(N)-XT(M)*YT(N)*ZT(I)-XT(N)*YT(I)*ZT(M)
      1+XT(N)*YT(M)*ZT(I)+XT(M)*YT(I)*ZT(N)+XT(I)*YT(N)*ZT(M)
      CNORM=CAA**2+CBB**2+CCC**2
      CNORM=SQRT(CNORM)
      CAA=CAA/CNORM $ CBB=CBB/CNORM $ CCC=CCC/CNORM $ CDD=CDD/CNORM
      IF(I.EQ.2)404,405
404 CA=CAA $ CB=CBB $ CC=CCC $ CD=CDD
      I=5 $ M=6 $ N=7
      GO TO 300

```

C

C CALCULATION OF AVERAGE PLANE THROUGH METAL ATOM

```

405 PRINT 9020,CA,CB,CC,CD,CAA,CBB,CCC,CDD
      CA=(CA+CAA)/2. $ CB=(CB+CBB)/2. $ CC=(CC+CCC)/2.
      CNOR=CA**2+CB**2+CC**2
      CNOR=SQRT(CNOR)
      CA=CA/CNOR $ CB=CB/CNOR $ CC=CC/CNOR
      CD=- (CA*XT(1)+CB*YT(1)+CC*ZT(1))
      PRINT 9019,CA,CB,CC,CD

```

C

C METAL LIGAND BOND DISTANCES BLEN(M)

```

301 DO 10 M=2,7
      BLEN(M)=SQRT((XT(1)-XT(M))**2+(YT(1)-YT(M))**2+(ZT(1)-ZT(M))**2)
      PRINT 9008,ATOM(M),BLEN(M)

```

```

10 CONTINUE
C
C DISTANCE OF ALL ATOMS FROM AVERAGE PLANE PDIST(I)
DEN=SQRT(CA*CA+CB*CB+CC*CC)
303 DO 20 I=1,7
313 DUM=CA*XT(I)+CB*YT(I)+CC*ZT(I)+CD
PDIST(I)=ABS(DUM/DEN)
PRINT 9009,ATOM(I),PDIST(I)
PRINT 9014,DEN,DUM
20 CONTINUE
C
C INTRALIGAND DISTANCES BETWEEN ATOMS ON OPPOSITE TRIGONAL FACES DISTL(M)
DO 30 I=2,4
M=I+3
DISTL(M)=SQRT((XT(I)-XT(M))**2+(YT(I)-YT(M))**2+(ZT(I)-ZT(M))**2)
PRINT 9010,ATOM(M),ATOM(I),DISTL(M)
30 CONTINUE
C
C TRIGONAL ANGLE OMEGA SUBTENDED ON AVERAGE PLANE PERPENDICULAR TO C3
C AXIS BY LIGAND.
307 DO 56 I=5,7
M=I-3
PLAN=SQRT(BLEN(I)**2-PDIST(I)**2)
PARR=SQRT(BLEN(M)**2-PDIST(M)**2)
DIFP=PDIST(I)+PDIST(M)
PLON=SQRT(DISTL(I)**2-DIFP**2)
500 DUM=PARR**2+PLAN**2-PLON**2
DEN=2*PARR*PLAN
IF(DEN.EQ.0)100,48
48 COST=DUM/DEN
ANG=ACOS(COST)
OMEGA(M)=ANG
ANG=ANG*RAD
PRINT 9011,ATOM(I),ATOM(M),ANG
PRINT 9015,DIFP,PARR,PLAN,PLON
PRINT 9014,DEN,DUM
56 CONTINUE
C
C CALC OF LIGAND ANGLE ALPHA
320 DO 50 I=2,4
M=I+3
SUMP=BLEN(I)**2+BLEN(M)**2-DISTL(M)**2
DUMP=2*BLEN(I)*BLEN(M)
YANG=SUMP/DUMP
DANG=ACOS(YANG)
ALPHA(I)=DANG
ALPHD=DANG*RAD
PRINT 9016,ATOM(M),ATOM(I),ALPHD,SUMP,DUMP
50 CONTINUE
C
C CALC OF POLAR ANGLES SUBTENDED AT C3 AXIS BY BONDS THETA
201 DO 204 I=2,7
COSMU(I)=PDIST(I)/BLEN(I)
AMU(I)=ACOS(COSMU(I))
BMU(I)=AMU(I)*RAD
SINMU(I)=(SIN(AMU(I)))**3
204 CONTINUE
DO 205 I=2,7
PRINT 9021,ATOM(I),COSMU(I),SINMU(I),AMU(I),BMU(I)
205 CONTINUE
C
C CALC OF AVERAGE VALUES. (SIN(THETA))**3
AVSIN=(SINMU(2)+SINMU(3)+SINMU(4)+SINMU(5)+SINMU(6)+SINMU(7))/6.0
PRINT 9022,AVSIN
C
C CALC OF ELEVATION ANGLES OF LIGAND PLANES FROM TRIGONAL PLANE. BETA

```

```

DO 210 I=2,4
M=I*3
COSBA(I)=TAN(OMEGA(I)/2.0)/TAN(ALPHA(I)/2.0)
BET(I)=ACOS(COSBA(I))
BETA(I)=BET(I)*RAD
SINB(I)=SIN(BET(I))
PRINT 9023,ATOM(I),ATOM(M),BETA(I),SINB(I)
C
C ROUGH EVALUATION OF EXPANSION/CONTRACTION IN TERMS OF SIN(BETA)
IF(SINB(I).GE.0.8165)211,212
211 EXPANS(I)=(SINB(I)-0.8165)*100/0.1835
PRINT 9024,EXPANS(I)
GO TO 210
212 CONTR(I)=(0.8165-SINB(I))*100/0.8165
PRINT 9025,CONTR(I)
210 CONTINUE
C
C CALC OF DISTANCE BETWEEN TRIGONAL PLANES FOR AVERAGE MODEL
SUM=BLEN(2)+BLEN(3)+BLEN(4)+BLEN(5)+BLEN(6)+BLEN(7)
AVB=SUM/6.0
AVA=(ALPHA(2)+ALPHA(3)+ALPHA(4))/3.0
DAVO=(OMEGA(2)+OMEGA(3)+OMEGA(4))/3.0
PRINT 9026,AVB,AVA,DAVO
A=(SIN(AVA/2.0))**2
C=(COS(AVA/2.0))**2
D=(TAN(DAVO/2.0))**2
E=SQRT(A-C*D)
DTRIG=2*AVB*E
PRINT 9027, DTRIG,A,C,D,E
C
C CALC OF IDEALIZED TRIGONAL ANGLE. DIHEDRAL ANGLES 90 DEGREES AND
C LIGAND ANGLE AVERAGE(ALPHA). AVERAGE BOND LENGTH.
OD=TAN(AVA/2.0)
OD=0.5774*OD
OMID=2*ATAN(OD)
OMIDR=OMID*RAD
PRINT 9028,OMIDR
C
C CALC OF HEIGHT OF IDEALIZED OCTAHEDRON. DIHEDRAL ANGLES 90 DEGREES.
C LIGAND ANGLE AVERAGE(ALPHA). AVERAGE BOND LENGTH.
D=TAN(OMID/2.0)**2
DE=SQRT(A-C*D)
DOCTI=2*AVB*DE
C
C CALC OF HEIGHT OF TRIGONAL PRISM OF LIGAND ANGLE ALPHA
DTPI=2*AVB*SQRT(A)
PRINT 9029,DOCTI,DTPI
C
C CALC OF PER CENT EXPANSION/CONTRACTION FROM IDEALIZED OCTAHEDRON ALONG C3
IF(DTRIG.GE.DOCTI)220,221
220 PCEX=(DTRIG-DGCTI)/(DTPI-DOCTI)
PCEX=100*PCEX
PRINT 9030,PCEX
GO TO 222
221 PCCON=(DOCTI-DTRIG)/DOCTI
PCCON=100*PCCON
PRINT 9031,PCCON
222 CONTINUE
C
C CALC OF HEIGHT OF OH OCTAHEDRON
C BOND LENGTH AVB,ALPHA 90 DEG,DIHEDRAL ANGLE 90 DEG
DOH=1.1546*AVB
C
C CALC OF HEIGHT OF TRIGONAL PRISM,ALPHA 90 DEG
DTP=1.4142*AVB
PRINT 9032,DOH,DTP

```

```
C
C CALC OF PIPERS VARIABLE TERM. ((SIN(THETA))**3)*(SIN(3*(60-OMEGA)))
  CONST=60.0/RAD
  DELTA=CONST-DAVO
  DDTA=3*DELTA
  PIPER=AVSIN*SIN(DDTA)
  PRINT 9033,PIPER
  GO TO 1000
100 PRINT 9012
1000 CONTINUE
101 PRINT 9013
  END
```

K.CA.(+)589.(CO(THIOX)3).4H2O FINAL LS PARAS R1=0.062 BUTLER 1972

A	B	C	COSA	COSB	COSC	NATM	NC3
12.3810	12.7910	11.8010	0.00000	0.00000	0.00000	7	1

ATOM	X	Y	Z	XT	YT	ZT
CO	.07737	-.01378	.21300	.95793	-.17626	2.51362
S1	-.03710	-.11908	.11870	-.45932	-1.52309	1.40073
S5	.21779	-.08689	.12041	2.69647	-1.11146	1.42102
S4	.09761	-.13838	.34341	1.20857	-1.77003	4.05262
S3	.05583	.10848	.07667	.69126	1.38757	.90478
S6	.19104	.09608	.29973	2.36530	1.22895	3.53714
S2	-.05293	.05875	.31714	-.65533	.75141	3.74255

CA= .12850 CB= -.97672 CC= -.17177 CD= -1.18800 CAA= .14436
 CBB= -.97798 CCC= -.15074 CDD= 1.39360
 EQUATION OF PLANE THROUGH METAL ATOM

.13644XT -.97743YT -.16127ZT .10238=0

BOND LENGTH ATOM 1 TO S1 IS 2.24969 ANGSTROM

BOND LENGTH ATOM 1 TO S5 IS 2.25631 ANGSTROM

BOND LENGTH ATOM 1 TO S4 IS 2.22967 ANGSTROM

BOND LENGTH ATOM 1 TO S3 IS 2.25943 ANGSTROM

BOND LENGTH ATOM 1 TO S6 IS 2.23671 ANGSTROM

BOND LENGTH ATOM 1 TO S2 IS 2.23011 ANGSTROM

DISTANCE OF ATOM CO FROM PLANE 0.00000 ANGSTROM
 DEN= 1.00000DUM= 0.00000

DISTANCE OF ATOM S1 FROM PLANE 1.30254 ANGSTROM
 DEN= 1.00000DUM= 1.30254

DISTANCE OF ATOM S5 FROM PLANE 1.32751 ANGSTROM
 DEN= 1.00000DUM= 1.32751

DISTANCE OF ATOM S4 FROM PLANE 1.34381 ANGSTROM
 DEN= 1.00000DUM= 1.34381

DISTANCE OF ATOM S3 FROM PLANE 1.30547 ANGSTROM
 DEN= 1.00000DUM= -1.30547

DISTANCE OF ATOM S6 FROM PLANE 1.34653 ANGSTROM
 DEN= 1.00000DUM= -1.34653

DISTANCE OF ATOM S2 FROM PLANE 1.32504 ANGSTROM
 DEN= 1.00000DUM= -1.32504

INTRALIGAND DISTANCE S3 TO S1 = 3.16887 ANGSTROM

INTRALIGAND DISTANCE S6 TO S5 = 3.17256 ANGSTROM

INTRALIGAND DISTANCE S2 TO S4 = 3.15086 ANGSTROM

TRIGONAL ANGLE OMEGA S3 TO S1 IS 58.59490 DEGREES
 DIFP= 2.60800PARR= 1.83425PLAN= 1.84413PLON= 1.80001
 DEN= 6.76519DUM= 3.52524

TRIGONAL ANGLE OMEGA S6 TO S5 IS 56.42811 DEGREES

DIFP= 2.67404 PARR= 1.82445 PLAN= 1.78598 PLON= 1.70723
 DEN= 6.51688 DUM= 3.60372

TRIGONAL ANGLE OMEGA S2 TO S4 IS 55.90511 DEGREES
 DIFP= 2.66885 PARR= 1.77921 PLAN= 1.79379 PLON= 1.67486
 DEN= 6.38307 DUM= 3.57812

LIGAND ANGLE ALPHA S3 TO S1 89.29878 DEGREES
 SUMP .12441 DUMP 10.16603

LIGAND ANGLE ALPHA S6 TO S5 89.83735 DEGREES
 SUMP .02865 DUMP 10.09341

LIGAND ANGLE ALPHA S2 TO S4 89.90250 DEGREES
 SUMP .01692 DUMP 9.94483

POLAR ANGLE THETA OF METAL S1 BOND WITH C3 AXIS
 COSMU= .578985 SINMU= .542017 AMU= .953313 THETA= 54.620786 DEGREES

POLAR ANGLE THETA OF METAL S5 BOND WITH C3 AXIS
 COSMU= .588357 SINMU= .528692 AMU= .941771 THETA= 53.959489 DEGREES

POLAR ANGLE THETA OF METAL S4 BOND WITH C3 AXIS
 COSMU= .602695 SINMU= .508115 AMU= .923922 THETA= 52.936830 DEGREES

POLAR ANGLE THETA OF METAL S3 BOND WITH C3 AXIS
 COSMU= .577784 SINMU= .543717 AMU= .954785 THETA= 54.705150 DEGREES

POLAR ANGLE THETA OF METAL S6 BOND WITH C3 AXIS
 COSMU= .602013 SINMU= .509099 AMU= .924777 THETA= 52.985810 DEGREES

POLAR ANGLE THETA OF METAL S2 BOND WITH C3 AXIS
 COSMU= .594157 SINMU= .520395 AMU= .934579 THETA= 53.547426 DEGREES

PIPERS POLAR ANGLE TERM (SIN(THETA))*3 = .525339448965468

ELEVATION ANGLE BETA OF LIGAND PLANE S1 S3 IS 55.387384 DEGREES
 ROUGH ESTIMATE OF PER CENT EXPANSION IN TERMS OF BETA 3.548402 SINB= .823011

ELEVATION ANGLE BETA OF LIGAND PLANE S5 S6 IS 57.449932 DEGREES
 ROUGH ESTIMATE OF PER CENT EXPANSION IN TERMS OF BETA 14.398696 SINB= .842922

ELEVATION ANGLE BETA OF LIGAND PLANE S4 S2 IS 57.889657 DEGREES
 ROUGH ESTIMATE OF PER CENT EXPANSION IN TERMS OF BETA 16.635413 SINB= .847026

AVERAGE BOND LENGTH 2.243654 ANGSTROMS
 AVERAGE LIGAND ANGLE 1.565203 RADIANS
 AVERAGE TRIGONAL ANGLE .994420 RADIANS

DISTANCE BETWEEN TRIGONAL PLANES FOR AVERAGE MODEL 2.651412 ANGSTROMS
 A= .497204 C= .502796 D= .294507 E= .590869

IDEALIZED TWIST ANGLE, OMIDR= 59.727127 DEGREES

HEIGHT OF IDEALIZED OCTAHEDRON, LIGAND ANGLE ALPHA, DOCTI= 2.583382 ANGSTROMS
 HEIGHT OF TRIGONAL PRISM, LIGAND ANGLE ALPHA, DTPI= 3.164120 ANGSTROMS

PER CENT EXPANSION OVER IDEALIZED OCTAHEDRON= 11.714405

HEIGHT OF OH OCTAHEDRON, ALPHA 90 DEGREES, IS 2.590522 ANGSTROMS
 HEIGHT OF TRIGONAL PRISM, ALPHA 90 DEGREES, IS 3.172975 ANGSTROMS

PIPERS VARIABLE PRODUCT= .082831989284025020
 AZIMUTH END

CHAPTER 8 ANALYSIS OF ML_6 -CORE GEOMETRY OF D_3 COMPLEXES.

8.1 THE STRUCTURAL DATA

The distortion parameters derived from the crystal coordinates using program AZIMUTH are tabulated at the beginning of this chapter, the complexes being subdivided according to the nature of the donor atoms (i.e. N or O, S) and the size of the chelate rings (four-, five- or six-membered rings). Some miscellaneous structures, e.g. the corundums and bis-tridentate complexes, are tabulated separately. The geometries are discussed in sections 8.2 and 8.3.

The complex characterized by the distortion parameters is listed first (formal charge given) followed by the remaining molecular or ionic groups comprising the structure: [A] means the complex molecule (ion) as written first and is included in the structure formula only where there is more than one unit of the complex per structural unit. The lengths $M-L$ ($\equiv a$), $L-L$ ($\equiv b$) and the angles α , θ , ω and β have been defined in section 7.3; h , the intertrigonal plane distance is also calculated by program AZIMUTH but is not tabulated since it is readily estimated as $b\sin\beta$. No attempt has been made to compute the errors in the tabulated parameters from the estimated standard deviations of the atomic positional coordinates but where available the standard deviations of $M-L$ and α have been abstracted from the literature and are given in parentheses: these esd's are the average of those quoted for the individual bond lengths and angles, not the estimated standard deviation of the mean. These errors give a more

meaningful indication of the accuracy of the structure refinement from which the positional coordinates were taken than does the least-squares residual, R_1 . Even so, such an indication of the success of a refinement is clearly limited: a more rigorous assessment would require comparison of the chemically equivalent bond parameters, the thermal parameters, the degree of sophistication of the model (e.g. anisotropic thermal parameters, inclusion of the hydrogen atoms, adjustment of the scattering factor curves for anomalous dispersion effects) and details of the number and type of reflection data (e.g. counter, film, visual, absorption corrected) included in the least-squares refinement cycles. It is impossible to include this information here for each structure: when it is required reference should be made to the primary source as indicated in the final column of each table.

Some of the structure refinements are of such low accuracy as to warrant exclusion but in several cases these are the very complexes which served as a basis for the development of the electrostatic crystal-field model in tris(bidentate) complexes and it is of interest to compare their distortion parameters with those of the more accurately refined structures. In most cases the number of digits included in the tabulated lengths and angles exceeds that justified by the accuracy of the refinement; the most accurate refinements referenced here support three post-decimal digits in $M-L$ and two in α , particularly for complexes having the metal atom fixed at a crystallographic special position. For consistency, and to allow for truncation effects, all interatom vectors have therefore been listed to three decimal places

and all distortion angles to two places.

Some points of additional interest are included in the supplementary notes collected at the end of these tables.

TABLE 8.1 TRIS-BIDENTATE COMPLEXES, CHELATION THROUGH NITROGEN: FIVE-MEMBERED RINGS.

Complex : structure	M-L (Å)	L-L (Å)	α (deg.)	θ (deg.)	ω (deg.)	β (deg.)	Ref.
1. (+) Co(en) ₃ ³⁺ : Cl ₃ ·H ₂ O	1.974(7)	2.678	85.43(30)	55.88	54.89	55.77	353
2. (+) Co(en) ₃ ³⁺ : Br ₃ ·H ₂ O	2.006	2.765	87.17	56.01	58.21	54.18	354
3. Co(en) ₃ ³⁺ : Cl ₃ ·3H ₂ O	2.001	2.837	90.31	54.42	59.77	55.14	355
4. (-) Co(en) ₃ ³⁺ : 2[A]·Cl ₆ ·NaCl·6H ₂ O	1.996	2.760	87.51	53.87	53.14	58.50	356
5. Co(en) ₃ ³⁺ : Cu ₂ Cl ₈ ·Cl ₂ ·2H ₂ O	1.969(12)	2.635	84.02(50)	56.56	54.12	55.44	357
6. Co(en) ₃ ³⁺ : 2[A]·(HPO ₄) ₃ ·9H ₂ O	1.963(4)	2.677	85.98(20)	55.49	54.84	56.18	358
7. Co(en) ₃ ³⁺ : Cr(CN) ₅ NO ³⁻ ·2H ₂ O	1.968(10)	2.650	84.63(40)	56.35	54.67	55.39	132
8. Co(en) ₃ ³⁺ : 2[A]·CdCl ₆ ·Cl ₂ ·2H ₂ O	1.972(6)	2.680	85.63(20)	55.19	53.39	57.13	359
9. (-) Co(-)pn ₃ ³⁺ : Br ₃	2.000(30)	2.741	86.52(1.5)	53.89) 56.18)	54.61	56.73	360
10. (-) Co(-)pn ₃ ³⁺ : (+) Cr(mal) ₃ ³⁻ ·3H ₂ O	1.964(10)	2.609	83.24(81)	54.91	47.99	59.93	Ch.2
11. (-) Co(+)cptn ₃ ³⁺ : Cl ₃ ·4H ₂ O	2.004(20)	2.756	86.89(87)	54.63	54.14	57.34	111
12. (-) Co(+)chxn ₃ ³⁺ : Cl ₃ ·5H ₂ O	2.012(24)	2.768	86.92(93)	54.37	53.48	57.88	361
13. Cr(en) ₃ ³⁺ : Co(CN) ₆ ³⁻ ·6H ₂ O	2.081(9)	2.725	81.81(37)	56.64	50.35	57.13	97
14. Cr(en) ₃ ³⁺ : Ni(CN) ₅ ³⁻ ·7H ₂ O	2.076(7)	2.723	81.95(29)	57.01	51.63	56.14	92
15. As for 14, complex ion 2.	2.075(8)	2.744	82.79(31)	56.20	50.93	57.28	92
16. Ni(en) ₃ ²⁺ : SO ₄	2.124(6)	2.788	82.04(20)	56.44	50.24	57.39	362
17. Ni(en) ₃ ²⁺ : (NO ₃) ₂	2.120(13)	2.790	82.29(1.0)	57.19	52.72	55.45	363
18. Ni(en) ₃ ²⁺ : Si ₂ O ₅ ²⁻ , 8.7H ₂ O	2.125(14)	2.831	83.55	56.44	52.97	56.08	364
19. Cu(en) ₃ ²⁺ : SO ₄	2.150(2)	2.790	80.91(10)	56.75	49.03	57.67	365
20. Cd(en) ₃ ²⁺ : S ₂ O ₃ ²⁻	2.433) 2.413)	3.032	77.47	51.17) 60.74)	39.63	63.31	366
21. Ru(en) ₃ ³⁺ : Cl ₃ ·4H ₂ O	2.110(18)	2.758	81.64(68)	57.32	51.91	55.70	367

(contd.)

TABLE 8.1 (contd.)

	<i>Complex : structure</i>	<i>M-L (Å)</i>	<i>L-L (Å)</i>	<i>α (deg.)</i>	<i>θ (deg.)</i>	<i>ω (deg.)</i>	<i>β (deg.)</i>	<i>Ref.</i>
22.	Co(en) ₃ : (lel) ₃	1.972	2.732	87.67	54.85	56.20	56.22	109
23.	Co(en) ₃ : (ob) ₃	1.972	2.720	87.21	55.16	56.18	55.92	109
24.	Co(pn) ₃ : (lel) ₃	1.973	2.732	87.63	54.86	56.13	56.24	109
25.	Co(pn) ₃ : (ob) ₃	1.973	2.720	87.13	55.13	55.94	56.06	109
26.	Co(en) ₃ ³⁺ : Fe(CN) ₆ ³⁻ · 2H ₂ O	2.010(21)	2.778	87.39(1.5)	54.54	54.75	57.18	368
27.	Zn(en) ₃ ²⁺ : S ₂ O ₃ ²⁻	2.315) 2.089)	2.891	81.87	51.61) 59.31)	47.16	59.79	369
28.	Cd(en) ₃ ²⁺ : SSeO ₃ ²⁻	2.586) 2.084)	2.764	71.65	49.57) 71.10)	43.21	56.72	369

TABLE 8.2 TRIS-BIDENTATE COMPLEXES, CHELATION THROUGH NITROGEN: SIX-MEMBERED RINGS.

Complex : structure	M-L (Å)	L-L (Å)	α (deg.)	θ (deg.)	ω (deg.)	β (deg.)	Ref.
1. (-) $\text{Co}(\text{tn})_3^{3+} : \text{Br}_3 \cdot \text{H}_2\text{O}$	2.000(30)	2.937	94.49(1.0)	52.59	62.49	55.87	120
2. (+) ₅₄₆ $\text{Co}(\text{R,R-ptn})_3^{3+} : \text{Cl}_3 \cdot \text{H}_2\text{O}$	1.988	2.767	88.21(1.3)	54.40	55.94	56.77	370, 371
3. $\text{Co}(\text{tn})_3 : (\text{lel-skew})_3$	1.984	2.768	88.45	54.51	56.68	56.35	372
4. $\text{Co}(\text{tn})_3 : (\text{chair})_3$	1.998	2.916	93.73	53.86	64.31	53.91	372
5. $\text{Co}(\text{tn})_3 : (\text{ob-skew})_3$	2.003	2.786	88.11	54.60	56.30	56.43	372
6. $\text{Ni}(\text{tn})_3^{2+} : \text{Ni}(\text{tn})_2(\text{H}_2\text{O})_2^{2+} \cdot \text{Cl}_4 \cdot \text{H}_2\text{O}$	2.145(6)	2.964	87.42(10)	54.67	55.24	56.82	121

TABLE 8.3 TRIS 1,10-PHENANTHROLINE AND 2,2'-DIPYRIDYL COMPLEXES: MN_6 .

1. (+) $\text{Ni}(\text{phen})_3^{2+} : \text{K} \cdot \text{Co}(\text{ox})_3^{3-} \cdot 2\text{H}_2\text{O}$	2.104(40)	2.710	80.14(1.4)	56.20	45.89	58.79	87
2. $\text{V}(\text{dipy})_3$	2.100(30)	2.694	79.82(1.5)	59.02	53.05	53.36	373
3. $\text{Ni}(\text{phen})_3^{2+} : [\text{Mn}(\text{CO})_5^-]_2$	2.090(5)	2.669	79.37(30)	57.49	48.19	57.34	374

TABLE 8.4 TRIS-BIDENTATE COMPLEXES, CHELATION THROUGH SULPHUR: FOUR-MEMBERED RINGS.

<i>Complex : structure</i>		<i>M-L (Å)</i>	<i>L-L (Å)</i>	<i>α (deg.)</i>	<i>θ (deg.)</i>	<i>ω (deg.)</i>	<i>β (deg.)</i>	<i>Ref.</i>
1.	Co(exan) ₃	2.276(4)	2.805	76.10(15)	57.90	43.24	59.58	137
2.	Co(dtc) ₃	2.258(3)	2.786	76.19(12)	57.98	43.68	59.25	135
3.	Fe(exan) ₃	2.375(20)	2.930	76.13(70)	56.46	38.33	63.65	375
4.	In(dtpa) ₃	2.603(6)	2.935	68.64(20)	60.37	36.11	61.39	376
5.	V(etp) ₃	2.450(20)	3.184	81.07	54.36	41.49	63.71	377
6.	Ni(bdtc) ₃ ⁺ : Br	2.261	2.794	76.32	58.45	45.37	57.89	378
7.	Fe(btxan) ₃	2.296(3)	2.801	75.17(8)	58.19	42.30	59.81	379
8.	Fe(pdtc) ₃	2.406(10)	2.911	74.44(30)	57.25	37.38	63.53	380
9.	Fe(mdtc) ₃	2.312(9)	2.819	75.13(30)	57.75	40.67	61.14	380
10.	Co(mtp) ₃	2.322(3)	3.108	84.03(10)		see notes		138
11.	Cr(exan) ₃	2.393(3)	2.888	74.22(8)	58.27	40.70	60.64	381
12.	Co(xan) ₃ , complex 1	2.398(4)	2.890	74.11(10)	58.76	42.01	59.41	139
13.	As for 12, complex 2	2.398(4)	2.891	74.15(10)	58.79	42.13	59.31	139
14.	Cr(etp) ₃	2.424(3)	3.195	82.43(10)	55.07	46.84	60.36	382
15.	V(etp) ₃	2.454(6)	3.208	81.65(23)	54.09	41.74	63.81	383
16.	Co(dtc) ₃	2.260(3)	2.806	76.72(11)	57.75	43.99	59.31	136

TABLE 8.5 TRIS-BIDENTATE COMPLEXES, CHELATION THROUGH OXYGEN OR SULPHUR: FIVE-MEMBERED RINGS.

	<i>Complex : structure</i>	<i>M-L (Å)</i>	<i>L-L (Å)</i>	<i>α (deg.)</i>	<i>θ (deg.)</i>	<i>ω (deg.)</i>	<i>β (deg.)</i>	<i>Ref.</i>
1.	(-) $\text{Co(ox)}_3^{3-} : \text{K.Ni(phen)}_3^{2+} \cdot 2\text{H}_2\text{O}$	1.922(30)	2.580	84.27(1.5)	56.36	54.08	55.65	87
2.	$\text{Cr(ox)}_3^{3-} : (\text{NH}_4)_3 \cdot 2\text{H}_2\text{O}$	1.965	2.591	82.36	56.30	50.34	57.50	384
3.	(+) $\text{Co(thiox)}_3^{3-} : \text{Ca.K.}4\text{H}_2\text{O}$	2.244(4)	3.164	89.68(15)	53.79	56.98	56.91	Ch.3
4.	$\text{Rh(ox)}_3^{3-} : \text{K}_3 \cdot 4.5\text{H}_2\text{O}$	2.020	2.678	83.03	57.36	54.46	54.45	385
5.	$\text{Si(cat)}_3^{2-} : [\text{C}_5\text{H}_5\text{NH}^+]_2$	1.784(3)	2.493	88.67(13)	54.09	55.95	57.08	386
6.	Fe(trop)_3	2.008(3)	2.522	77.80(15)	55.55	38.62	64.26	387
7.	$\text{Cr(ox)}_3^{3-} : \text{K}_3 \cdot 3\text{H}_2\text{O}$	1.896	2.407	78.89	58.92	51.11	54.29	388
8.	V(dpd)_3	2.338(4)	3.059	81.71(13)	49.30	see notes		348
9.	Re(dpd)_3	2.325(10)	3.032	81.40(37)	49.40	see notes		350
10.	Mo(tfs)_3	2.491(2)	3.315	83.42(10)	48.29	0.0	90.0	389
11.	Fe(nph)_3	1.999	2.447	75.45	55.60	31.46	68.29	390

TABLE 8.6 TRIS-BIDENTATE COMPLEXES, CHELATION THROUGH OXYGEN OR SULPHUR: SIX-MEMBERED RINGS.

	Complex : structure	M-L (Å)	L-L (Å)	α (deg.)	θ (deg.)	ω (deg.)	β (deg.)	Ref.
1.	(+) Cr(mal) ₃ ³⁻ : (-) Co(-)pn ₃ ³⁺ .3H ₂ O	1.953(7)	2.808	91.91(68)	53.47	60.19	55.91	Ch.2
2.	α -V(acac) ₃	1.979(8)	2.749	87.98(60)	54.40	55.50	56.96	391
3.	β -V(acac) ₃	1.987(8)	2.745	87.38(60)	54.68	55.19	56.83	391
4.	Fe(acac) ₃	1.992(6)	2.744	87.06(32)	54.33	53.57	57.87	392
5.	Cr(acac) ₃	1.956(7)	2.792	91.10(60)	54.48	61.50	54.29	112
6.	Cr(acac) ₃	1.898	2.674	89.60	55.30	60.67	53.90	393, 394
7.	Mn(acac) ₃	1.872(8)	2.805	97.04(60)	53.03	68.00	53.39	86
8.	Ni(acac) ₃ ⁻ : Ag ₃ (NO ₃) ₂ ⁺ .H ₂ O	2.043(60)	2.899	90.37(3.0)	55.34	62.02	53.22	395
9.	Cu(hfac) ₃ ⁻ : C ₁₄ H ₁₉ N ₂ ⁺	2.067(9)	2.863	87.63(40)	55.35	57.30	55.19	396
10.	Mg(hfac) ₃ ⁻ : C ₁₄ H ₁₉ N ₂ ⁺	2.058(9)	2.771	84.66(30)	55.77	53.18	56.66	396
11.	(+) Cr(+)atc ₃	1.968(10)	2.831	91.96(10)	54.53	62.70	53.83	114, 115
12.	Co(OMPA) ₃ ²⁺ : (ClO ₄) ₂	2.084(3)	2.894	87.96(10)	55.17	57.54	55.33	397
13.	Mg(OMPA) ₃ ²⁺ : (ClO ₄) ₂	2.060(2)	2.815	86.21(10)	55.56	55.42	55.86	397
14.	Cu(OMPA) ₃ ²⁺ : (ClO ₄) ₂	2.065(2)	2.879	88.40(10)	55.11	58.14	55.14	397
15.	Fe(sacsac) ₃	2.254(5)	3.269	92.98	52.35	59.12	57.38	398, 399
16.	Pt(S ₅) ₃ ²⁻ : (NH ₄) ₂ .2H ₂ O	2.390(7)	3.447	92.33(30)	53.09	60.04	56.30	400, 401

223.

(contd.)

TABLE 8.6 (contd.)

	<i>Complex : structure</i>	<i>M-L (Å)</i>	<i>L-L (Å)</i>	<i>α (deg.)</i>	<i>θ (deg.)</i>	<i>ω (deg.)</i>	<i>β (deg.)</i>	<i>Ref.</i>
17.	Co(acac) ₃	2 x 1.923(3) 4 x 1.885(8)	2.849	97.32(18)	52.80	67.94	53.64	85
18.	Al(acac) ₃	1.892(8)	2.718	91.82(11)	53.79	60.85	55.33	85
19.	Rh(sacsac) ₃	2.321(3)	3.486	97.33(10)	52.41	67.10	54.32	398, 402
20.	Er(thd) ₃	2.223(11)	2.671	73.86(33)	53.19	see notes		352

TABLE 8.7 THE CORUNDUM-TYPE STRUCTURES: M(III)O₆ CHROMOPHORES.

1.	Cr ₂ O ₃	2.013 1.963	2.735	86.92	48.86 61.38	56.10	55.79	403
2.	α-Al ₂ O ₃	1.971 1.858	2.622	86.39	47.70 63.08	56.10	55.42	403
3.	Fe ₂ O ₃	2.087 1.960	2.756	85.77	46.36 64.42	55.28	55.68	403
4.	Ti ₂ O ₃	2.084 2.013	2.802	86.30	51.56 60.94	57.63	54.07	403
5.	V ₂ O ₃	2.127 2.024	2.901	88.62	49.13 59.84	57.35	55.93	403

TABLE 8.8A MISCELLANEOUS STRUCTURES.

Complex : structure	M-L (Å)	L-L (Å)	α (deg.)	θ (deg.)	ω (deg.)	β (deg.)	Ref.
1. (+) ₅₄₆ Co(TRI) ₂ ³⁺ : I ₃ .3H ₂ O	1.923(10)	2.711	89.61(50)	52.21	52.26	60.40	33
2. Ni(TRI)(H ₂ O) ₂ NO ₃ ⁺ : NO ₃ /NiN ₃ O ₃ core	N, 2.095(10) O, 2.029(10)	2.971	92.17	51.41 53.18	57.53	58.09	404
3. Co(tame) ₂ : $\Lambda\Lambda$	1.966	2.728	87.88	54.71	56.18	56.37	372
4. Co(tame) ₂ : $\Lambda\Lambda$	1.971	2.795	90.30	54.53	60.00	54.94	372
5. Cr(gly) ₃ : H ₂ O	N, 2.068(1) O, 1.964(1)	2.640	81.77(10)	59.01 56.77	53.61	54.29	113
6. (-) Co(acac)(tn) ₂ ²⁺ : (As(+)-tartrate) ₂ .H ₂ O	N, 1.984 O, 1.886	2.944 2.796	95.81 95.66	53.13 52.42	66.16 64.21	53.93 55.37	122, 405
7. (+) ₅₄₆ Co(mal) ₂ en ⁻ : Na.2H ₂ O	N, 1.925(24) O, 1.897(19)	2.639 2.764	86.56(1.1) 93.56(82)	56.54 52.99	58.46 61.88	53.54 55.69	Ch.1
8. Fe(dtc) ₂ (tfd)	dtc, 2.310(3) tfd, 2.195(3)	2.798 3.049	74.54(10) 87.99(10)	56.14 50.40	33.23 41.97	66.91 66.60	406
9. Co[Co(OH) ₂ en ₂] ₃ ⁶⁺ : (S ₂ O ₆) ₃ .8H ₂ O	1.910(20)	2.540	83.33(90)	57.66	55.66	53.61	407
10. (+) Co(mal) ₂ en ⁻ : (-)[Co(NO ₂) ₂ en ₂] ⁺	N, 1.943(20) O, 1.901(20)	2.640 2.821	85.57(1.0) 95.79(1.0)	55.05 52.64	52.91 64.96	57.48 54.87	89
11. Cr(ox) ₂ en ⁻ : [Cr(ox)en ₂] ⁺ .2H ₂ O	N, 2.063(6) O, 1.971(5)	2.736 2.605	83.06(30) 82.75(20)	56.22 56.50	51.51 51.73	56.99 56.61	408
12. Cr(ox)en ₂ ⁺ : [Cr(ox) ₂ en] ⁻ .2H ₂ O	N, 2.067(6) O, 1.958(5)	2.718 2.595	82.22(10) 83.02(20)	55.99 58.08	49.28 56.18	58.29 52.92	408
13. [Ti(urea) ₆] ³⁺ : I ₃ /TiO ₆ ⁻ core	2.014(5)	2.758	86.40(30)	55.08	54.48	55.07	263
14. Ferrichrome-A : 4H ₂ O/FeO ₆ ⁻ core	2.007	2.534	78.29	56.13	41.78	62.01	409
15. [Ti(urea) ₆] ³⁺ : (ClO ₄) ₃	2.035(10)	2.821	87.76(50)	54.41	55.17	57.09	410
16. [V(urea) ₆] ³⁺ : I ₃ (at 300°K)	1.983(20)	2.686	85.24(1.0)	55.26	52.86	57.30	411
17. As for no. 16 (at 90°K)	1.935(10)	2.682	87.77(20)	53.46	52.47	59.18	411

TABLE 8.8B MISCELLANEOUS STRUCTURES.

	<i>Complex : structure</i>	<i>M-L (Å)</i>	<i>L-L (Å)</i>	<i>α (deg.)</i>	<i>θ (deg.)</i>	<i>ω (deg.)</i>	<i>β (deg.)</i>	<i>Ref.</i>
1.	(+) Co(-)chxn ₃ ³⁺ : Cl ₃ ·H ₂ O	1.982(4)	2.658	84.19(14)	55.16	50.59	58.46	412
2.	(+) Co(en) ₃ ³⁺ : (NO ₃) ₃	1.967(7)	2.667	85.33(31)	55.69	54.19	56.28	413
3.	Mn(dtc) ₃	2.450(8)	2.908	72.79(20)	59.03	40.16	60.24	234
4.	Cu(dipy) ₃ ²⁺ : (ClO ₄) ₂	2.133(7)	2.675	77.49(30)	59.76	50.88	53.52	414
5.	Al(trop) ₃	1.888(1)	2.487	82.43(6)	55.62	48.50	59.01	415

Supplementary Notes on Tables 8.1-8.8TABLE 8.1

a) Crystallographic point symmetry of the complex.

D_3 3,10,16,17,19,22,23

C_3 4,9,20,21,24,25,27,28

C_2 1,2,11,13

C_1 5-8,12,14,15,18,26

b) Absolute configuration of the complex.

Λ 1,2,11,12

Δ 4,9,10

c) Ligand conformations.

$1e1_3$ 1-4,6,8-12,16-22,24,26-28

ob_3 13,23,25

$(1e1)_2ob$ 15

$1e1(ob)_2$ 5,7,14

d) Complexes 22-25 energy minimized by P.F. Crossing^{95,109} using a modification of Boyd's procedure,⁴¹⁶ extended by M.R. Snow.⁴¹⁷ Energies at convergence 10.39, 10.97, 11.94, 12.59 kcal mol⁻¹ respectively; energy differences only are meaningful, not the absolute values.

TABLE 8.2

- a) Crystallographic point symmetry of the complex.
- D_3 3,5
- C_3 4
- C_1 1,2,6
- b) Complex ions nos. 1 and 2 have a Λ absolute configuration.
- c) Ligand conformations.
- tris(chair) 1,4,6
- tris(ob-skew) 2,5
- tris(1el-skew) 3
- d) Complexes 3-5 energy minimized by R.J. Geue,^{94,372} as for the Co(en)_3 complexes of Table 8.1. Energies at convergence 28.21, 28.98 and 34.04 kcal mol⁻¹ respectively.
- e) For structure no. 1, z_{Co} should be³¹³ 0.4393 rather than 0.4293 as quoted in the original structure report.¹²⁰
- f) The crystal structure of $(-)[\text{Co tn}_3]\text{Cl}_3 \cdot \text{H}_2\text{O}$ has recently been determined;⁴¹⁸ it is isomorphous with the monoclinic tribromide salt (no. 1). Structural parameters and coordinates have not yet been published: $\alpha = 91.2 (2)^\circ$, ω ca. 62° .

TABLE 8.2 (contd.)

- g) Complex ion no. 6 has C_1 site symmetry in the lattice. However, the published coordinates do not correspond to the published bond lengths and angles and a set of orthogonalized coordinates was calculated — this was not entirely satisfactory.
- h) The structure of $(-)[Cr \text{ bgH}_3]$ d-10-camphorsulphonic acid trihydrate has been solved³²³ but the refinement is incomplete and structural parameters are not available.⁴¹⁹

TABLE 8.3

- a) Crystallographic point symmetry of the complex.
- | | |
|-------|---|
| D_3 | 2 |
| C_3 | 1 |
| C_1 | 3 |
- b) Complex ion no. 1 has a Λ absolute configuration.
- c) Structure no. 2 was solved³⁷³ by projection methods and is of low accuracy: the Ti^0 and Cr^0 complexes were quoted as being isostructural. The structures of $[Ni \text{ dipy}_3]SO_4 \cdot 7H_2O$ ⁴²⁰ and $[Cu \text{ dipy}_3]Cl_2 \cdot 7H_2O$ ⁴²¹ were both quoted by Piper¹⁷³ but the full structure reports are unavailable. Accurate determinations of several tris(dipy) and tris(phen) structures are required.

TABLE 8.3 (contd.)

- d) The structure of (+)[Fe phen₃](antimony-(+)-tartrate)₂.8H₂O has been refined²⁶ to convergence at $R_1 = 0.070$ but the structural coordinates have not been published. Holm and co-workers³⁴³ quote $\alpha = 83^\circ$ and $\omega = 56^\circ$ for the cation in this structure; they also list $\alpha = 80^\circ$, $\omega = 50^\circ$ for the cation⁴²² in [Ni phen₃][S₂P(OCH₃)₂]₂.

TABLE 8.4

- a) Crystallographic point symmetry of the complex.

D₃ 5,6

C₃ 1,3,11

C₂ 2,10,14-16

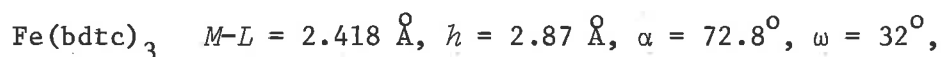
C₁ 4,7-9,12,13

- b) All complexes listed in this table are zero-charged, apart from complex ion no. 6. The chelated metal has a formal +3 oxidation state except for Ni(IV) in no. 6. Note that complex ion 6 has $\beta = 57.89^\circ$ which is the closest of any of these tris(complexes) to the orthogonal geometry having interligand plane dihedral angles of 90° and $\beta = 54.74^\circ$.
- c) Structure no. 5 is a preliminary report of no. 15. In general, reference to a preliminary communication of a structure which has subsequently been published in full is not made in these tables.

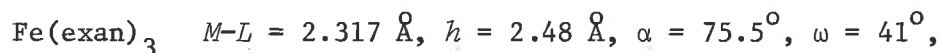
TABLE 8.4 (contd.)

d) The coordinates listed for atom S_3 of structure no. 10 are in error; the calculated bond lengths and angles involving this atom do not correspond to the published values. The average values of $M-L$, $L-L$ and α have been abstracted from the structure report. Furthermore, the value given for the unit cell β angle is 98.81° in the abstract but 97.81° in the text; this does not account for the discrepancy in bond values involving atom S_3 .

e) The following angular parameters are given in the preliminary structure communications -



(ref. 423):



(ref. 424).

TABLE 8.5

a) Crystallographic point symmetry of the complex.

D_{3h} 10

D_3 6

C_3 1

C_2 5,7,8

C_1 2,3,4,9,11

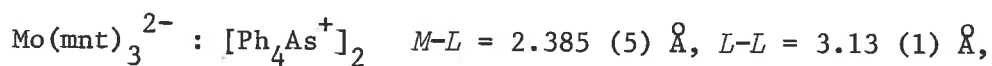
TABLE 8.5 (contd.)

- b) Complex ions 1 and 3 have the Λ absolute configuration.
- c) van Niekerk and Schoening⁴²⁵ also solved the structure of $\text{Rb}_3[\text{Cr ox}_3] \cdot 3\text{H}_2\text{O}$ and found it to be isostructural with the tri-potassium salt (no. 7); the angular distortion parameters for the former structure are not included in this table.
- d) The neutral dithiolate complexes nos. 8 and 9 are pseudo trigonal-prismatic. However, both lack exact C_3 symmetry and one chelate ring twists in the opposite chiral sense to the other two relative to the pseudo- C_3 axis. The ω and β values for the three chelate rings are -
- Structure no. 8, C_2 -symmetric,
for the two ligands skewed in the same direction $\omega = 7.20^\circ$,
 $\beta = 85.82^\circ$: for the third ligand $\omega = -8.52^\circ$ and $\beta = 85.07^\circ$
but in the opposite chiral sense.
- Structure no. 9, no symmetry,
for two ligands $\omega = 5.50^\circ$, 8.40° and $\beta = 86.82^\circ$, 85.11° : the
third ligand has $\omega = -3.70^\circ$ and $\beta = 87.82^\circ$, again in the opposite
sense.
- e) Although the MoSe_6 core in complex 10 has D_{3h} symmetry³⁸⁹ the complex "as a whole" has only C_{3h} symmetry since the Se_2C_2 ligand plane is inclined at a dihedral angle of $18.6 (5)^\circ$ to the MoSe_2 plane: the plane

TABLE 8.5 (contd.)

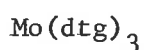
defined by the ethylene and trifluoromethyl carbons deviates 6° from the Se_2C_2 plane but in the opposite sense.

f) The following parameters are given in the preliminary structure reports -



$$h = 3.00 \text{ \AA}, \quad \alpha = 82 (1.0)^\circ,$$

$$\omega = 27^\circ, \quad (\text{ref. 426}):$$



$$M-L = 2.33 (2) \text{ \AA}, \quad L-L = 3.1 \text{ \AA},$$

$$\alpha = 82.5^\circ, \quad \omega = 0^\circ, \quad (\text{ref. 427}).$$

In the latter complex the dihedral angle between the MoS_2 plane and the S_2C_2 ligand plane = 18° ; as for $\text{Mo}(\text{tfs})_3$ the core symmetry is D_{3h} but the whole complex conforms only to C_{3h} symmetry.

TABLE 8.6

a) Crystallographic point symmetry of the complex.

m 20

D_3 1,12-14

C_2 15

C_1 2-11,16-19

b) Complexes 1 and 11 have a Λ absolute configuration.

TABLE 8.6 (contd.)

- c) For structure no. 6 the coordinates were taken from ref. 393 and the unit cell parameters from ref. 394. There is gross disparity between the bond angles quoted in the literature and those calculated from the published coordinates: the bond lengths are in agreement. The bond lengths and angles calculated from the coordinates of an earlier structure solution⁴²⁸ of $\text{Cr}(\text{acac})_3$ show even greater divergence from the published values.
- d) Structure no. 7 is reported⁴²⁹ to be that of the $\text{Co}(\text{III})$ rather than the $\text{Mn}(\text{III})$ derivative. It is surprising that complex 17 shows an apparent tetragonal elongation, expected for a Jahn-Teller distorted $\text{Mn}(\text{III})$ acac_3 complex^{430,431} but not predicted for $\text{Co}(\text{III})$. Much of the available data on tris(acac) structures is collated in ref. 432.
- e) The structure of $\text{Rh}(\text{III})\text{acac}_3$ has been solved by J.C. Morrow (1964) - see ref. 112 - but does not seem to have been published.
- f) For structure no. 16 the published⁴⁰⁰ crystallographic β angle of the monoclinic unit cell was 92.74° . However, the published bond lengths and angles correspond to $\beta = 87.26^\circ$ and from the internal agreement it seems^{401,433} that the structure refinement has been carried through with β acute. The complex ion has a tris(chair) conformation.

TABLE 8.6 (contd.)

- g) Complex no. 20 is mirror symmetric with one chelate ring coincident with the mirror plane.³⁵² The complex lacks exact C_3 symmetry and the other two chelate rings (i.e. those related by the mirror) have opposite chiral twist senses relative to the pseudo- C_3 axis. For the mirror related ligands $\omega = \pm 7.92^\circ$, $\beta = +84.61^\circ$; the average ω and β over the three ligands are 0° and 90° respectively for a mirror symmetric complex.

TABLE 8.7

- a) All $M(\text{III})O_6$ polyhedra are C_3 symmetric: the crystal lattice conforms to the centric space group $R\bar{3}c$.
- b) The positional coordinates of the metal and oxide ions are identical in refs. 403 and 434 but the lattice constants are marginally different. Those from ref. 403 have been used in computing the distortion parameters tabulated here.
- c) The metal atom is significantly displaced along the crystallographic c axis away from the shared trigonal face of the oxide ion interstice: hence the two values for $M-L$ and θ . The larger $M-L$ value corresponds to the smaller θ .
- d) Naturally α , β and ω do not correspond to bidentate chelate rings but they are still indicative of the precise MO_6 core distortion.

TABLE 8.8A

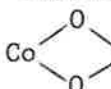
- a) Crystallographic point symmetry of the complex.
- S_6 4
- D_3 3,13,15-17
- C_2 8,11,12
- C_1 1,2,5-7,9,10,14
- b) Absolute configuration of the complex.
- Λ 1,14 (ref. 409, 435)
- Δ 6,7,10
- c) Complexes nos. 1-4 are bis(tridentates). α , ω and β do not correspond to a bidentate ligand but still give information about the distortion of the ML_6 -core; for structures 1-3 they are taken in the chiral sense of the tridentate ligand.
- d) Complexes 3 and 4 energy minimized by R.J. Geue³⁷² — $\Lambda\Lambda$, *chiral*, and $\Lambda\Delta$, *meso*, respectively; the computed energies at convergence were 25.1 and 26.8 kcal mol⁻¹.
- e) Complex ion no. 6 is in the bis(chair) conformation.
- f) Complex ion no. 9 comprises a central Co(III) atom coordinated through six bridging hydroxyl groups to three $[Co(en)_2(OH)_2]^+$ residues: the central CoO_6 -core thus comprises three four-membered  rings.

TABLE 8.8A (contd.)

- g) In complex no. 16 the Fe atom is chelated to three hydroxamate residues in the branched ligand chain forming three five-membered chelate rings bidentate through oxygen.
- h) For complexes other than tris(bidentates) listed in this table α , β and ω naturally do not correspond to a bidentate ligand. The α , ω distortion parameters for complexes 5 and 9 were plotted in Figure 8.3A and the average α , ω values for complex 6 on Figure 8.3B. No other values from this table were plotted.

TABLE 8.8B

- a) The published structure reports of these tris(bidentate) complexes were located too late to permit their inclusion on Figure 8.3A. Structure no. 4 shows appreciable divergence from the theoretical ω_{min} vs α line: the cation exhibits a significant static Jahn-Teller tetragonal elongation.⁴¹⁴
- b) Crystallographic point symmetry of the complex.
- | | |
|-------|-------|
| C_2 | 1,5 |
| C_1 | 2,3,4 |
- c) Both complexes 1 and 2 have the Λ absolute configuration.
- d) Complex no. 1 has the ob_3 conformation and no. 2 the lel_3 conformation.

8.2 GEOMETRY OF TRIS-BIDENTATE COMPLEXES

The lowest energy geometry of tris-bidentate transition metal complexes is often implicitly considered to be that in which the three chelate rings are positioned orthogonally, i.e. a pseudo-octahedral^{436,437} or trigonal anti-prismatic conformation of the ML_6 -core. Deviation from this arrangement was found^{348-351,389,427} for certain zero-charged tris-dithiolene type complexes which adopt a closely trigonal prismatic (D_{3h}) geometry, the five-membered chelate rings lying approximately parallel to the C_3 axis. This distortion from an orthogonal geometry was rationalized in terms of specific inter-ring S...S attractions between the three sulphur donor atoms of each "non-bonded" trigonal face.^{348,349,438} However, electrically neutral tris(complexes) containing four-membered chelate rings bidentate through sulphur were less distorted toward a D_{3h} geometry (Table 8.4) and more generally resembled the charged species containing five- and six-membered chelate rings.

A possible mechanism for the intra-molecular racemization of optically-active tris(bidentate) transition metal complexes is a "trigonal-twist" of one triangular face about the C_3 axis relative to the opposing face:^{436,439,440} passing through a supposedly higher energy pseudo-trigonal prismatic transition state, the antiprism absolute configuration inverts from Λ to Δ . On a simplistic analysis this mechanism could be considered most probable for those complexes which already show significant distortion towards trigonal-prismatic geometry in the ground state, although the existence of such static distortion implies nothing about the favourability of possible bond rupture processes.⁴⁴¹

Stiefel and Brown⁴⁴² have recently analysed the geometric distortion of the ML_6 donor atom polyhedra in several tris-bidentate complexes and concluded that complexes containing ligands of small bite are less likely to racemize via a trigonal-twist mechanism than are those containing large-bite ligands. This conclusion is contrary to that which would be drawn from a comparison of the β values tabulated in section 8.1. In section 8.2.1 Stiefel and Brown's data are reworked and are shown to be consistent with a distortion of all the complexes toward trigonal-prismatic geometry.

Having illustrated the reality of this distortion the question remains as to why the majority of tris-bidentate complexes listed in section 8.1 should distort in this way. An analysis in terms of a repulsive electrostatic potential is given in section 8.2.2; comparison is made with an almost identical treatment developed independently by Kepert.⁴² Again, contrary to the conclusions of Stiefel and Brown,⁴⁴² the smaller the ligand bite the more energetically favourable a distortion from antiprismatic toward trigonal-prismatic geometry.

8.2.1 Critique of Stiefel and Brown's Analysis

In discussing the distortion of a tris(bidentate) complex towards D_{3h} geometry it is important to define the ML_6 -core consistent with the coordination positions spanned by the ligands; the metal atom and the two donor atoms of a given ligand are thus taken to define the average plane through the metal and the chelate ring. This definition is unsatisfactory where the metal atom is displaced from the mean ligand plane

and in such cases the planes through the ligands only should be considered.

The common characteristic of trigonal-prismatic tris-bidentate complexes of ideal D_{3h} symmetry, irrespective of the size of the ligand bite, is the parallelism of the ligand backbone to the C_3 axis; the interplanar dihedral angles, γ , are ideally 120° but it is possible for the three ligands to remain parallel to a pseudo- C_3 axis without this axis being exact, provided the horizontal mirror is maintained. The deviation of the ligand plane from the parallel position is indicated by β in the tables of section 8.1, being 90° for an ideally parallel ligand and 54.74° for an orthogonal disposition of the three chelate rings. For D_{3h} symmetry the opposing trigonal faces are eclipsed and the trigonal twist angle, ω , is zero; since $\cos\beta = \tan(\omega/2)/\tan(\alpha/2)$ — (eq. 7.8), either ω or β can be quoted as an indicator of the extent of distortion towards D_{3h} geometry (see section 8.2.2).

Stiefel and Brown's⁴⁴² use of the ratio s/h (where s = length of the side of the equilateral triangular non-bonded donor atom face, h = distance between the opposing parallel triangular faces) is unfortunate. Although it is directly related to the polar angle ($\theta = \arctan[(s/h)2/\sqrt{3}]$) this ratio does not indicate the extent of the trigonal-prismatic distortion without the specification of an additional parameter; for this other parameter Stiefel and Brown chose the trigonal twist angle which we have given the symbol ω . From equation 7.9 the relationship between θ , β and ω is $1/\tan\beta = \tan\theta \cdot \sin(\omega/2)$. The relationships between $s, h, \omega, \alpha(M-L)$ and $b(L-L)$ given by Stiefel and Brown are

$$(4/3)s^2 \sin^2(\omega/2) + h^2 = b^2$$

and $s^2/3 + h^2/4 = a^2$.

As limiting geometry they took a trigonal prism of square face ($s/h = 1.00$, $\omega = 0^\circ$);^{†1} for O_h geometry $s/h = 1.22$ and $\omega = 60^\circ$.

All the complexes listed (Table 8.9) have $\omega < 60^\circ$ but fall into two groups with respect to $s/h = 1.22$, namely (i) those with $s/h < 1.22$ and (ii) those with $s/h > 1.22$. Stiefel and Brown suggest that group (ii) comprises those complexes where the ligand bite, b , is too short to span an octahedron and that they are more compressed than a regular octahedron; however, $\text{Mo}(\text{mnt})_3^{2-}$ which has $s/h = 1.09$ and a geometry⁴²⁶ intermediate between trigonal prismatic (TP) and trigonal anti-prismatic (TAP), also has a small ligand bite, $b/a = 1.31$, corresponding to $\alpha = 82^\circ$. The analysis of s/h in terms of ligand bite (or more readily, α) is inconsistent; it is shown in section 8.2.2 that the inconsistency results from use of the ratio s/h rather than from comparison

^{†1} In this geometry the bidentate ligand subtends an angle of 81.80° at the metal atom (calculated as $\alpha = 2 \arcsin(b/2a)$). Stiefel and Brown assign this idealized geometry on the basis of valence-bond theory⁴⁴³ and the structures of the tris-dithiolenes which have angles $\alpha = 81.4^\circ$, $\text{Re}(\text{dpd})_3$,^{350,351} 81.7° , $\text{V}(\text{dpd})_3$,^{348,349} 82.5° , $\text{Mo}(\text{dtg})_3$,⁴²⁷ and 83.4° , $\text{Mo}(\text{tfs})_3$.³⁸⁹ Whether or not such an idealized D_{3h} configuration is a valid limiting geometry for comparison of other tris-bidentates of fixed bite is doubtful.⁴¹⁵ The adoption of D_{3h} geometry by these four complexes is not solely a steric adjustment (see section 8.2.2) and it is questionable to what extent the precise geometry of the trigonal prismatic ML_6 -cores reflect the apparently unusual electronic properties of these complexes.

More generally,^{42,415,444} the dimensions of the chelate ring are taken to be invariant in discussing antiprismatic (D_{3d}) \rightarrow trigonal prismatic (D_{3h}) interconversion; applying the restriction that the trigonal prism have square faces makes this possible only for chelate rings having $\alpha = 81.80^\circ$. See also ref. 445 where the surprising restriction that $\theta = 54.74^\circ$ is proposed, independent of the value of ω .

of α values.

Using the values tabulated by Stiefel and Brown, analysis in terms of β , the angle of inclination of the metal-donor atom plane to the plane orthogonal to the pseudo- C_3 axis (i.e. $90^\circ - \beta$ is the tilt of the L.M.L plane from the C_3 axis) reveals a distortion similar to that indicated by the data tabulated in section 8.1, namely the complexes are significantly distorted toward a trigonal prismatic geometry of the ML_6 -core. Furthermore, apart from the seemingly special case of the tris(dithiolenes), the distortion towards D_{3h} geometry is greater the smaller the ligand angle, α . The reworked data are presented in Table 8.9: ω and s/h were abstracted from ref. 442, α values were taken from the primary references and β was calculated as $\arcsin(h/b)$. Complexes are listed in the order in which they appear in Table 1 of ref. 442.

Some minor truncation effects are noticeable, e.g. ω for $Re(dpd)_3$ is 3° but $h = b = 3.03 \text{ \AA}$ resulting in $\beta = 90^\circ$ for which ω must equal zero. In an orthogonal arrangement of three bidentate ligands $\beta = 54.74^\circ$; for $\beta > 54.74^\circ$ the distortion of the ML_6 -core is toward D_{3h} symmetry. The last two entries in Table 8.9 have $\beta < 54.74^\circ$ and merit some comment. The complex $Y(bzac)_3 \cdot H_2O$ is seven coordinate;⁴⁴⁶ although the molecular symmetry is closely C_3 , one triangular oxygen face is significantly distorted by the water molecule which coordinates along the pseudo- C_3 axis causing a flattening of the three bidentate ligands, as indicated by $\beta = 49.2^\circ$. It is included in Table 8.9 only for completeness.

TABLE 8.9 STIEFEL AND BROWN'S DATA REWORKED.

<i>Complex</i>	<i>s/h</i>	α (deg.)	ω (deg.)	β (deg.)	<i>Ref.</i>
^a Re(dpd) ₃	1.01	81.4	3	90	350,351
Mo(dtg) ₃	1.00	82.5	0	90	427
^a V(dpd) ₃	1.01	81.7	3	85.4	348,349
Mo(tfs) ₃	0.97	83.4	0	90	389
Mo(mnt) ₃ ²⁻	1.09	82	28	74.1	426
Fe(exan) ₃	1.43	75.5	41	62.3	424
Co(exan) ₃	1.38	76.1	43	59.5	137
Ni(bdtc) ₃ ⁺	1.36	76.4	45	61.4	378
Cr(ox) ₃ ³⁻	1.30	85	50	57.3	384
Fe(acac) ₃	1.21	87.1	54	57.5	392
V(acac) ₃	1.21	87.7	56	56.8	391
Si(cat) ₃ ²⁻	1.26	88.7	59	54.2	386
Y(bzac) ₃ ·H ₂ O	1.62	74.7	53	49.2	446

a. see footnote †⁸, section 7.3, and supplementary notes to Table 8.5.

The complex ion $\text{Si}(\text{cat})_3^{2-}$ contains three catechol ligands bidentate through oxygen to give five-membered chelate rings;³⁸⁶ the relevant geometric parameters derived using program AZIMUTH are given in Table 8.5. The complex ion has C_2 site symmetry and although the ligand angles range 86.4° - 89.8° the two independent β angles agree more closely being 57.3° and 57.0° (Average = 57.1°). Average values for a , b , h and ω obtained from AZIMUTH are 1.784 Å, 2.493 Å, 2.093 Å and 55.95° respectively; the corresponding values given by Stiefel and Brown are 1.79 Å, 2.49 Å, 2.02 Å and 59° . The conflicting values of β obtained for this ion are symptomatic of the uncertainty which can arise where crystallographic C_3 symmetry is lacking; the differences result from the alternative methods used to determine the distance, h , between the triangular faces in cases where these are no longer parallel. For this reason the values listed in Table 8.8A for those trigonal-bidentate complexes containing three non-identical ligands should be interpreted with particular caution.

Finally, Stiefel and Brown⁴⁴² intimate that the complex $[\text{Fe}(\text{mdtc})_2(\text{tfd})]$ falls into the highly compressed class and that attainment of a trigonal-prismatic transition state is improbable, contrary to the conclusion based on NMR averaging patterns.⁴⁴⁷ Using program AZIMUTH, the distortion parameters for the related complex $[\text{Fe}(\text{dte})_2(\text{tfd})]$ ⁴⁰⁶ are as given in Table 8.8A: the distance between the trigonal sulphur faces was taken as 2.655 Å and the β values were 66.9° and 66.6° respectively for the four (2 times) and five-membered

chelate rings. On the β criterion this complex is significantly distorted toward trigonal-prismatic geometry and the attainment of a trigonal-prismatic transition state maintaining the same dimensions of the chelate rings seems highly probable.

This somewhat unexpected tendency of tris-bidentate complexes to distort towards a trigonal-prismatic geometry in which the ligand planes are more nearly parallel to the pseudo- C_3 axis than is the case for octahedral symmetry, or more correctly for the ML_6 -core to distort toward D_{3h} symmetry, is analysed more fully in section 8.2.2.

8.2.2 Repulsive Potential of the ML_6 -Core

(1) The majority of complexes for which distortion parameters are tabulated in section 8.1 are not of immediate relevance to an evaluation of the current models for CD-absolute configuration correlations of trigonal-dihedral transition metal complexes. Many, however, correspond to structures for which the single-crystal polarized absorption spectra have been determined. Since the distortion of the ML_6 -core is usually incompletely specified for tris(bidentate) complexes a comprehensive tabulation of the relevant parameters for those structures for which positional coordinates are available seemed desirable: more structures have been published recently and the tables of section 8.1 are no longer complete. Several other structures, at present available only as preliminary communications, should shortly appear as full papers. However, the data which are presented in section 8.1 are sufficiently comprehensive

to permit a discussion of the ML_6 -core distortion in tris-bidentate D_3 complexes.

The expectation^{436,437} that tris-bidentate complexes should exhibit geometries closely octahedral is founded on a $1/r$ repulsive electrostatic potential function. The summation, $\Sigma 1/r$, over the fifteen interaction vectors of the ML_6 -core is smaller for an O_h geometry than for a D_{3h} arrangement, maintaining fixed chelate ring dimensions $b = a/2$, i.e. $\alpha = 90^\circ$. However, most bidentate ligands subtend angles other than 90° at the metal atom and the ML_6 polyhedron cannot attain O_h symmetry in such cases; a geometry in which the three chelate rings remain mutually orthogonal is still possible and is implicit in several theoretical models.

$\beta = 54.74^\circ$ for a D_3 complex having three mutually orthogonal chelate rings; the data listed in Tables 8.1-8.9 indicate that this geometry rarely obtains and that in general β increases with decreasing α . In this discussion of the distortion of the ML_6 -core of a D_3 tris(bidentate) complex from the mutually orthogonal arrangement of ligands (ORTH) towards D_{3h} trigonal-prismatic geometry (TP), the dimensions of the chelate ring are considered invariant. Three reference geometries are important; they are characterized as follows -

- (i) TP, $\omega = 0^\circ$, $\beta = 90^\circ$, $\gamma = 120^\circ$ (interligand plane dihedral angle),
 $h = b : (\alpha, a, b)$.
- (ii) ORTH, $\beta = 54.74^\circ$, $\gamma = 90^\circ$, $h = b\sqrt{(2/3)} : (\alpha, a, b)$.
- (iii) TAP (= trigonal antiprismatic ML_6 -core, D_{3d} symmetric),
 $\omega = 60^\circ : (\alpha, a, b)$.

A fourth trivial geometry is the completely flattened arrangement having the three ligands coplanar -

$$(iv) \quad \omega = \alpha, \beta = 0^\circ, \gamma = 0^\circ, \delta = 0 : (\alpha, \alpha, b).$$

When $\alpha = 90^\circ$ the ORTH and TAP arrangements are identical and the ML_6 -core has O_h symmetry. Distortion of $M(L-L)_3$ from an O_h ML_6 arrangement to D_{3h} is facilitated if an attractive potential operates between the ligators of the same trigonal face and a repulsive potential between the donor atoms, of adjacent ligands, on opposing faces. Discrimination of this form is theoretically possible with a Morse-shaped potential function of the type used to represent non-bonded van der Waals (vdW) interactions, but evaluation for an idealized CoN_6 core ($\alpha = 2.0 \text{ \AA}$, $\alpha = 90^\circ$) showed the intra-trigonal face N...N interactions to be dominant and strongly repulsive in a D_{3h} geometry.^{†2}

Although the donor atoms in transition metal complexes are usually assigned only quite small residual charges the interatom vectors are such that electrostatic interactions are worthy of consideration; these coulombic

^{†2} Based on the N...N non-bonded potential function of A.M. Liquori, A. Damiani and G. Elefante, *J. Mol. Biol.*, **33**, 439 (1968), quoted in ref. 417, the D_{3h} arrangement was destabilized by ca. 9 kcal mole⁻¹ with respect to the O_h geometry. Inclusion of the repulsive N...N non-bonded interactions reportedly⁴¹⁷ has little effect on the final minimized geometries of pseudo-octahedral polyamine species where the angular distortion about the central Co atom is dominated by an N-Co-N angle-bending function minimizing at $\alpha = 90^\circ$; they were included in the tris(en/pn) calculations (parameters listed in Table 8.1, nos. 22-25) but were omitted from the analysis of the six-membered ring $Co(tn)_3$ complex (Table 8.2, nos. 3-5) and the bis(tridentate) $Co(tame)_2$ (Table 8.8A, nos. 3 and 4).

interactions were not explicitly included in the energy minimization calculations of the $\text{Co}(\text{diamine})_3$ and $\text{Co}(\text{triamine})_2$ complexes.^{†3} Furthermore, the essentially crystal field approach²¹⁹ adopted in interpreting many electromagnetic properties of pseudo-octahedral transition metal complexes makes an attempted description of the geometric distortion of tris-bidentate complexes in terms of a charged ML_6 -core a worthwhile exercise. Independently, Kepert⁴² has recently correlated the magnitude of the trigonal twist in tris-bidentate complexes with the size of the ligand bite on the basis of a simple electrostatic repulsive potential operative between the six donor atoms of the ML_6 -core; his treatment is entirely analogous to that summarized here. The values for the ML_6 -distortion parameters calculated by Kepert⁴² correspond exactly with those derived in this work using program AZIMUTH. Other limited compilations of distortion parameters characterizing the ML_6 -core geometry have been published, for example by Piper and Carlin,²³⁷ Tomlinson²⁴¹ and Holm and co-workers;⁴⁴¹ the latter group

^{†3} As Dr. M.R. Snow has pointed out,⁴²⁹ full energy minimization of the tris-diamine complexes closely reproduces the distortions observed in the solid-state, particularly for the five-membered ring complexes. In these calculations, however, a "cut-off" was applied to exclude contributions from the large number of non-bonded interactions at distances greater than 1.16σ , where σ is the sum of the relevant vdW radii; inclusion of these weakly attractive vectors may alter the complex ion geometry at the energy minimum but the direction of further distortion cannot be decided without making comprehensive minimization calculations.

have also studied ML_6 -core distortion in trigonally symmetric hexadentate complexes.³⁴³ All derived parameters listed in these works are in substantial agreement.

(2) Vector Analysis.

Given a chelate ring of fixed dimensions, a D_3 symmetric tris(bidentate) complex has one independently variable parameter; Kepert⁴² used the "half angle of twist" (i.e. $\omega/2$). We had previously chosen ω which resulted in mathematical expressions somewhat more cumbersome than those derived by Kepert; however, since the program used to calculate the electrostatic potential was continually modified to enable elucidation of all features of the theoretical curves, a representative listing is not possible and the formulae for the inter-donor atom vectors are given instead.

Using the nomenclature of Figure 8.1 and the angle and length parameters defined previously (sections 7.3 and 8.1) the following relationships are obtained -

$$\begin{aligned} \text{Dimensions of the chelate ring: } M-A_1 &= a, A_1 \dots A_4 = b, \angle A_1 M A_4 = \\ &\alpha = 2 \arcsin (b/2a). \end{aligned}$$

Program VECTOR was written to increment $\sin\beta$ in the range $0 \rightarrow 1$:

$$h = b \sin\beta$$

$$\text{and } \omega = 2 \arctan (\cos\beta \cdot \tan(\alpha/2)) = 1 - (b^2 - h^2)/2d^2$$

where $d = (a^2 - h^2/4)^{1/2}$ is the projection of MA_1 on the plane orthogonal to the C_3 axis. The three intra-ligand bites of fixed length

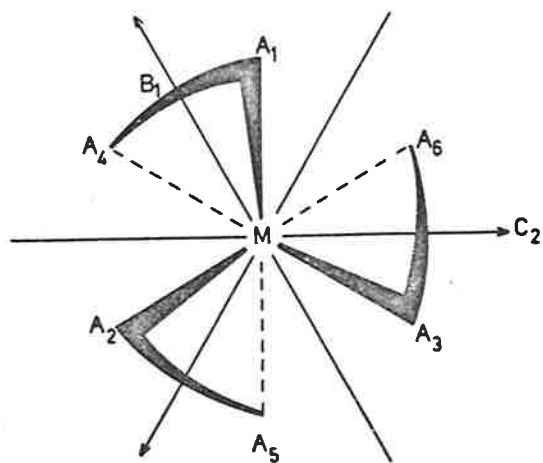


FIGURE 8.1: Λ - D_3 GEOMETRY.

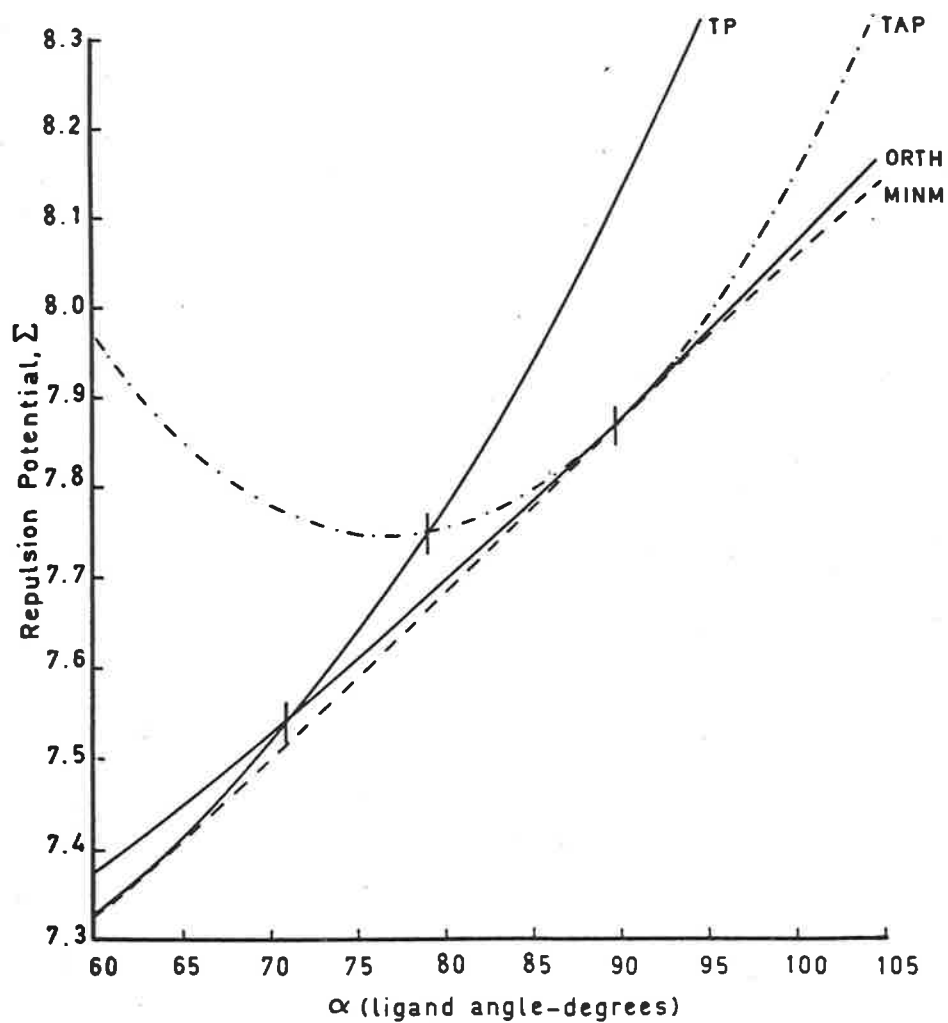


FIGURE 8.2: REPULSION POTENTIAL VERSUS α FOR A D_3 SYMMETRIC ML_6 -CORE.

b were excluded from the potential sum. There are six vectors between donor atoms related by the C_3 operation, e.g. $A_1 \dots A_2$, of length

$$V_3 = \sqrt{3}.d.$$

The six interaction vectors between donors on opposing trigonal faces divide into two groups,

(i) atoms related by a C_2 operation, e.g. $A_1 \dots A_6$,

$$V_2 = (h^2 + 2d^2 - 2d^2 \cos(120 - \omega))^{\frac{1}{2}},$$

and (ii) atoms related by a $C_2 + C_3$ operation, e.g. $A_1 \dots A_5$,

$$V_{32} = (h^2 + 2d^2 - 2d^2 \cos(120 + \omega))^{\frac{1}{2}}.$$

The total repulsive potential was calculated as

$$\Sigma = 6/V_3 + 3/V_2 + 3/V_{32}$$

for the $\sin\beta$ range $0 \rightarrow 1$ at various fixed values of α : the $\sin\beta$ value corresponding to the minimum Σ for a particular α was determined to four decimal places and ω and β computed. No attempt has been made to "weight down" the V_{32} vector contribution in pseudo-octahedral geometries where it corresponds to a "through-metal" interaction, i.e. the dielectric constant was assumed identical for all vectors. The model then is of a central metal atom, bearing zero electrostatic charge^{†4} and having no

^{†4} The metal atom is more usually considered to carry a small residual charge opposite in sign to that on the donor atoms. The approximation of zero "effective" charge is necessary to permit inclusion of $3/V_{32}$ at full weight; if the metal were credited with an oppositely signed charge to that on the donor atoms, sensible analysis would be difficult since the degree to which this repulsive component would be reduced could be expected to vary with $\rightarrow A_1MA_5$, being least for O_h symmetry where A_1-M-A_5 is linear.

directional bonding preference, coordinated to six identically charged donor atoms linked together in pairs and free to move within the restriction of D_3 symmetry in response to a $1/r$ repulsive potential.

(3) Summary of Analysis.

- (i) At O_h symmetry $V_3 = V_2$ and $V_{32} = 2\alpha$; for D_{3h} symmetry $V_2 = V_{32}$. Further discussion of the trends in the individual vectors as a function of α and β (or ω) is not warranted here.
- (ii) For fixed α the repulsive potential Σ increases with increasing α for a fixed value of β .
- (iii) $\Sigma_{TP} = \Sigma_{ORTH}$ at $\alpha = 71.0^\circ$; $\Sigma_{TP} = \Sigma_{TAP}$ at $\alpha = 79.2^\circ$; $\Sigma_{ORTH} = \Sigma_{TAP}$ at $\alpha = 90^\circ$ at which value the ML_6 -core is O_h symmetric. Σ_{TAP} is a minimum at $\alpha = 76.9^\circ$. Both Σ_{TP} and Σ_{ORTH} increase with increasing α but below $\alpha = 71.0^\circ$ the TP geometry is favoured relative to ORTH, the position of maximum relative favourability occurring at $\alpha = 50.0^\circ$.
- (iv) For $\alpha \leq \alpha_c. 58.9^\circ$, Σ_{TP} is lower than the repulsive potential of any other D_3 arrangement. For $\alpha > 58.9^\circ$, D_3 geometries having $\beta < 90^\circ$ and $\omega > 0^\circ$ are of lower potential, the position of the minimum moving to decreasing β (and increasing ω) with increasing α . As derived by Kepert,⁴² for $\alpha = 90^\circ$ a regular octahedral ML_6 -core has minimum energy.

The changes in Σ with changing α are summarized graphically in Figure 8.2: TP, TAP and ORTH have their previously defined meanings and MINM signifies

the minimum repulsive energy, as in point (iv) above, at a particular value of α .

(4) Discussion.

a) tris-bidentate complexes:

When $\alpha = 90^\circ$ the minimum potential corresponds to O_h symmetry irrespective of the exponential order of the repulsion. However, the values quoted in part (3) above for non-octahedral geometry are sensitive to the order of the repulsive law; e.g. for an r^{-6} potential (distance dependence of dipole-dipole and London dispersion potentials) discussed by Kepert,⁴² $\Sigma_{TP} = \Sigma_{ORTH}$ at $\alpha = 66.5^\circ$ and TP is most favoured relative to ORTH at $\alpha = 46^\circ$.

Because of the interdependence of the distortion parameters characterizing the ML_6 -core there are several valid ways of presenting the experimental data. A fully angular description seemed preferable; ω_{min} , twist angle at the minimum potential, versus α is approximately linear in the range spanned by the experimental data (α ca. $65-100^\circ$) and corresponds to Kepert's Figure 3 in which the bite b is really the ratio $b/a = 2\sin(\alpha/2)$ and $\theta_{min} = \omega_{min}/2$. ω_{min} and β_{min} calculated at 5° intervals in α over the range $60^\circ-105^\circ$ are listed in Table 8.10. The experimental data listed in Tables 8.1-8.8 are plotted against the theoretical ω_{min} vs α curve for the $1/r$ repulsive potential; tris(bidentate) complexes only are plotted, with the exclusion of the pseudo-trigonal prismatic structures. In Figure 8.3A those data for which the standard

deviation of α is given are represented as horizontal error bars extending one σ either side of the computed α value. Those structures for which no esd in α was given are plotted as discrete points in Figure 8.3B. Some overlap of points was unavoidable.

TABLE 8.10 ML_6 -CORE: β_{min} AND ω_{min} AT FIXED α VALUES FOR A $1/r$ POTENTIAL.

α (deg.)	β_{min} (deg.)	ω_{min} (deg.)
60	81.975	9.220
65	71.750	22.565
70	66.283	31.466
75	62.375	39.171
80	59.342	46.333
85	56.855	53.222
90	54.736	60.000
95	52.883	66.734
100	51.233	73.462
105	49.721	80.232

The experimental distortion of the ML_6 -core in most tris-bidentate complexes is well represented by this limited theoretical model. The extreme distortion of the tris(dithiolene) complexes $V(dpd)_3$, $Re(dpd)_3$ and $Mo(tfs)_3$ has been interpreted elsewhere as indicative of dominant inter-donor atom bonding between the sulphur atoms of the same trigonal face,^{348,351,389,438} i.e. the contribution $6/V_3$ is attractive in these cases; that the geometries of the tris-dithiolates containing four-membered

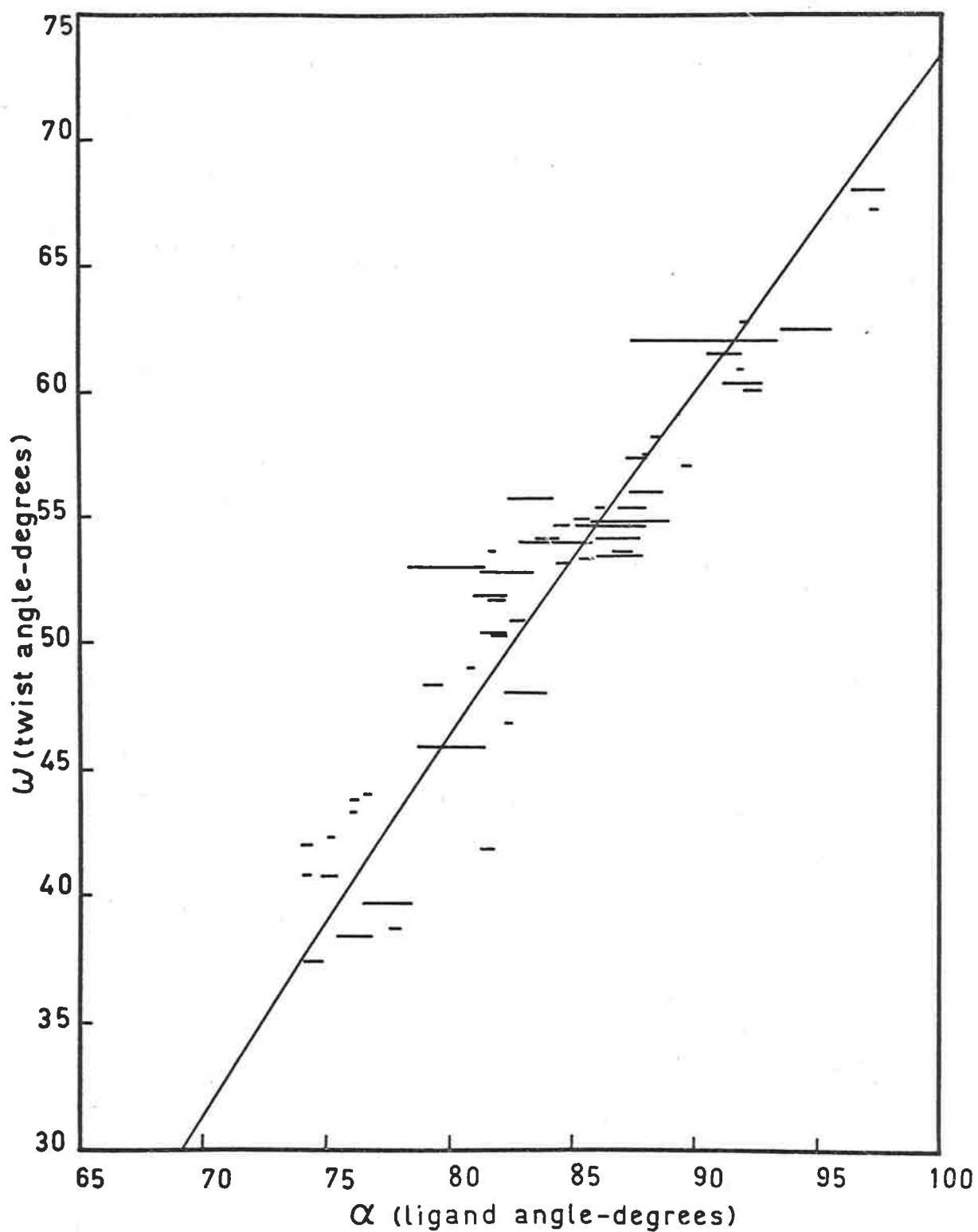


FIGURE 8.3A: PLOT OF EXPERIMENTAL ω VALUES VERSUS α (see text).

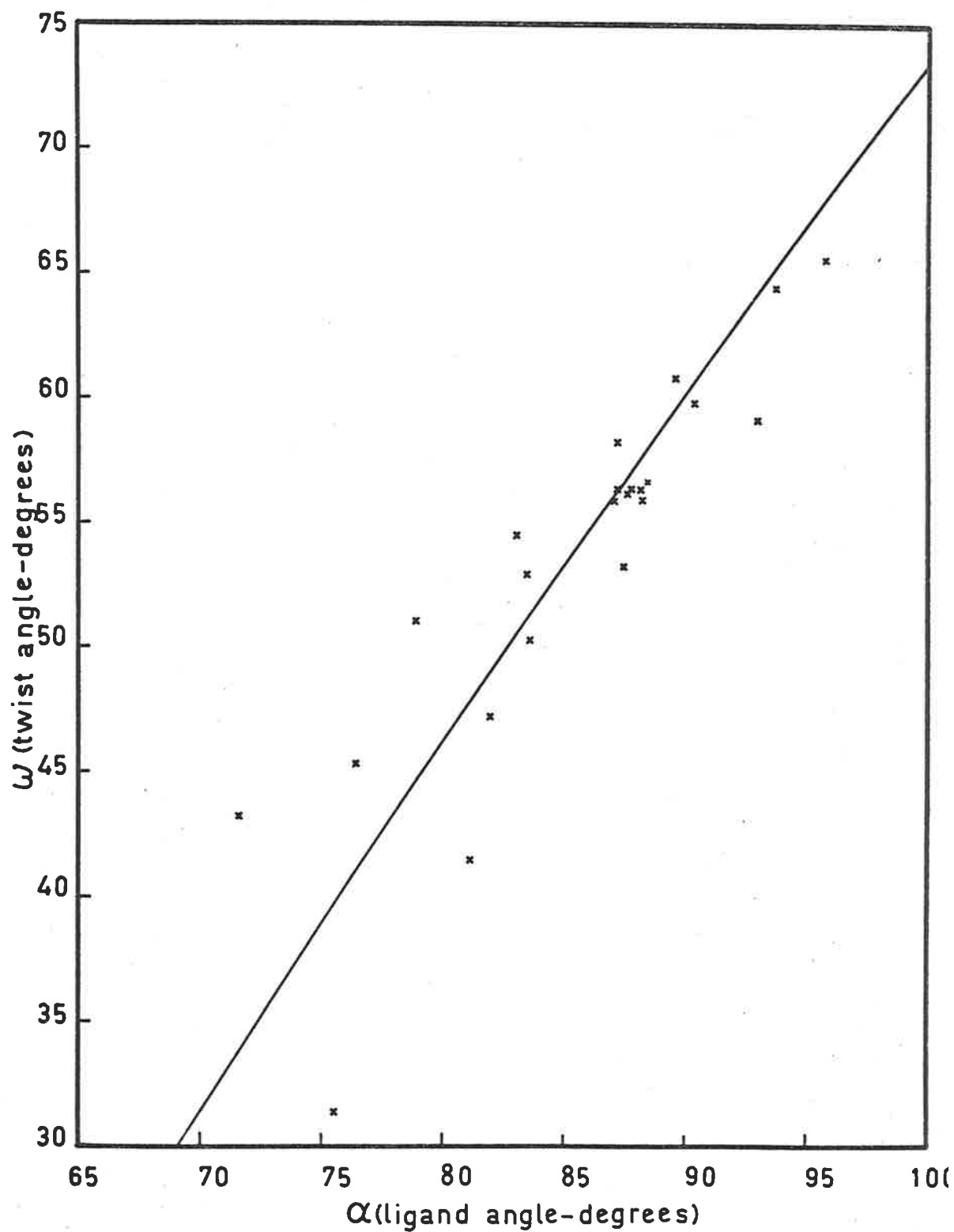


FIGURE 8.3B: PLOT OF EXPERIMENTAL ω VALUES VERSUS α (see text).

chelate rings bidentate through sulphur and of the anionic tris(five-membered ring) complexes^{426,448} and $\text{Co}(\text{thiox})_3^{3-}$ are more closely orthogonal suggests that in these complexes the electrostatic charge on the donor atoms dominates the potential field.^{389,436}

Failure during the present work of attempts to synthesize tris-complexes of Co(III) and Cr(III) comprising seven-membered chelate rings (e.g. with succinic acid and 1,4-diaminobutane) by the methods successfully applied to the synthesis of the analogous tris(six-membered ring) chelates offers some support to the concept of directional bonding preference in complexes of transition metals;² alternative rationalizations of this failure are possible, e.g. on the grounds of increased ligand bulk or extreme solubility. Despite the paucity of tris-complexes having α significantly greater than 90° the limited electrostatic repulsion model faithfully represents the ML_6 -core distortion over a wide α range without any weighting for the octahedral ML_6 geometry favoured for hexacoordinate transition metal complexes on the basis of ligand-field theory (but see refs. 343, 445 for calculations of the relative ligand field stabilization energies for octahedral, trigonal prismatic and twist distorted ML_6 geometries).

Non-involvement of the $4f$ -orbitals in the bonding scheme of lanthanide metal complexes is considered^{81,449,450} to result in essentially ionic metal-donor atom bonds uninfluenced by the directional preferences postulated for transition metal complexes. The geometry of discrete complexes should result primarily from the minimization of ligand-ligand repulsions in

the coordination sphere, taking cognizance of the fixed parameters in polydentate systems. It is therefore disturbing that the only six-coordinate tris-bidentate lanthanoid(III) complex for which the structure has so far been published,³⁵² $\text{Er}(\text{thd})_3$, adopts a distorted trigonal-prismatic geometry in the solid state, whereas the $1/r$ repulsion model predicts β ca. 63° , ω ca. 38° for $\alpha = 74^\circ$. By contrast, this monomer is considered to have a pseudo-octahedral geometry in the vapour phase, although the Er-O bond lengths reportedly differ from those in the solid state.⁴⁴⁹

The pseudo- D_{3h} geometry of $\text{Er}(\text{thd})_3$ raises the question of the contribution of non-donor ligand atoms to the distortion of the ML_6 -core in tris-bidentate complexes. For a D_3 complex, the smaller α the greater the distortion toward TP geometry. Since the ligand backbone atoms, taken in their two-fold related pairs, subtend angles at the metal smaller than the ligand angle, inclusion of these atoms in the present repulsion model with charges of the same sign as the donor atoms should result in a larger distortion towards TP geometry than is predicted solely on the basis of the repulsion forces operative within the ML_6 -core, i.e. Figure 8.3 should show a preponderance of experimental data lying to the low ω side of the theoretical ω_{\min} vs α curve. The scatter of experimental points either side of the theoretical line indicates that any contribution from the ligand backbone atoms to the electrostatic potential is small and random (but see part (b) of this discussion for further comment).

Since many of the vectors involving ligand backbone atoms, particularly

between donor atoms and backbone atoms, are of similar length to the inter-donor atom vectors, the most realistic interpretation of their lack of influence on the ML_6 -core distortion (within the electrostatic representation) is that the backbone atoms carry a vanishingly small residual charge (q_1) such that $(q_1q_2)/r$ is effectively zero for vectors involving non-donor atoms. However, in $Er(thd)_3$ the essentially ionic bonding between metal and ligand necessitates the delocalization of ca. $1e^-$ over the atoms of each β -diketone ring; in calculating the lattice energies of the related dimeric lanthanide chelates Boeyens^{449,451} has distributed this uni-negative charge as $-0.4e^-$ on the two oxygen donor atoms and $-0.2e^-$ on the central carbon atom (N.B. this leaves a +3 charge on the metal and in terms of footnote †⁴, Chapter 8, effectively negates the current treatment). Ignoring the charge on the metal ion, the charge distribution of the $Er(thd)_3$ complex can be allowed for in a pseudo- ML_9 calculation analogous to that outlined in part (b) of this discussion for tris-tridentates. Using the nomenclature of 8.2.2(b) the repulsion potential is calculated as

$$\Sigma = 6/V_3 + 3/V_2 + 3/V_{32} + 3/V_4 + 3/V_5$$

the vectors V_4 and V_5 involving the ring carbon atom which bears a charge half that localized on the donor atoms. In-putting $\alpha = 73.86^\circ$, $a = 2.223 \text{ \AA}$ and $f = 3.716 \text{ \AA}$ (average values over the three chelate rings calculated from the crystallographic coordinates) the minimum potential occurs at $\beta_{min} = 67.57^\circ$, $\omega_{min} = 32.01^\circ$. This resultant geometry is more distorted toward TP than that calculated for the ML_6 model, but is still

far removed from a D_{3h} situation.

Distortion of d -transition metal tris(β -diketonates) is well represented by the ML_6 electrostatic model and this suggests that attempted explanation of the $Er(thd)_3$ geometry simply in terms of a delocalization of charge over the chelate ring is naïve. Admittedly for the more covalent transition metal complexes the ring charge should more closely approach zero, but the same delocalization pattern applies⁴⁵² and the ratio of the charge on the ring carbons to that on the oxygen donors will be similar. Apart from the difference in α , the most notable difference between $Er(thd)_3$ and the tris(acac) complexes of the first row transition metals is the replacement of the methyl groups of each chelate ring by tertiary butyl groups. It has been suggested⁴⁴⁹ that $Er(thd)_3$ is forced into a TP geometry by the steric repulsion between these bulky substituents. Full energy minimization procedures are required to test this hypothesis since in the present analysis it is not possible to realistically represent the tertiary butyl groups, but some preliminary observations can be made.

The larger the distance of a ligand atom from the central metal the smaller its contribution to the potential sum; the quaternary carbon of the *t*-butyl group is ca. 4.6 Å from Er as opposed to an average Er-O bond length of 2.223 Å. Furthermore, the repulsive electrostatic potential operative between the charged donor oxygens is here considered to vary as r^{-1} whereas the non-bonded Buckingham-type potential, $E_{nb} = A \exp(-Bd) - c/d^6$, is dominated by the weakly attractive cd^{-6} dispersion term at the distances

separating the quaternary butyl carbons of adjacent chelate rings in $\text{Er}(\text{thd})_3$. The two-fold related quaternary carbon atoms subtend an angle of 68.3° at the metal atom; for this geometry a TP arrangement is more favourable than an ORTH geometry in the ratio 1.03/1.0, arguing on the basis of an r^{-6} attractive potential applied only to these six carbon atoms, but this attraction is surely negligible alongside the dominant electrostatic repulsion terms. In view of the above remarks and the postulated vapour phase geometry, the solid state geometry of $\text{Er}(\text{thd})_3$ seems inexplicable: intermolecular contacts in the crystal structure were not tabulated³⁵² and unfortunately we have overlooked the calculation of these from the crystal coordinates.

b) D_3 Symmetric tris(tridentate) complexes:

Despite the example of $\text{Er}(\text{thd})_3$, many lanthanide complexes do adopt the regular arrangements expected on the basis of minimum repulsion between the donor atoms of the ML_x -core.⁴⁵³⁻⁴⁵⁵ The structures of the tris-complexes of lanthanoid(III) ions with planar tridentate ligands, studied by Albertsson,⁴⁵⁶⁻⁴⁶¹ are particularly relevant to the present discussion of the electrostatic repulsion model. The idealized ML_9 -cores in these complex ions have the favoured tricapped trigonal-prismatic geometry,^{455,462} each planar tridentate ligand spanning a diagonal of one rectangular face, six oxygen donors sited at the prism corners and the three central oxygen (or nitrogen) donors coplanar with the metal atom and sited on two-fold symmetry positions above the midpoints of the rectangular

faces. The chiral ligand arrangement resembles that in a pseudo-octahedral tris(bidentate) complex and the ionic repulsion model developed above can be easily modified to describe the ML_9 -core geometry of these tris-tridentates.

If all nine donor atoms are assumed to bear identical charges the tridentate ligands can be described as fixed bite bidentates pivoting about the central M-L bond. Intra-ligand interactions were omitted as were the invariant vectors between the three central donor atoms coplanar with M. Two additional vectors are introduced to the tris-bidentate description: in terms of Figure 8.1, if B_1 is the central donor atom of what is now the planar tridentate ligand $A_1B_1A_4$, where $M-B_1 = f$, then for the tris-tridentate there are six vectors

$$V_4 = (f^2 + \alpha^2 - 2f \cdot d \cdot \cos(120 - \omega/2))^{1/2}$$

of type $B_1 \dots A_2$, $B_1 \dots A_6$ and another six

$$V_5 = (f^2 + \alpha^2 - 2f \cdot d \cdot \cos(120 + \omega/2))^{1/2}$$

of type $B_1 \dots A_3$, $B_1 \dots A_5$; ω is still the projection of α , i.e. angle A_1-M-A_4 . The repulsion potential becomes

$$\Sigma = 6/V_3 + 3/V_2 + 3/V_{32} + 6/V_4 + 6/V_5.$$

It was mentioned in part (a) of this discussion that inclusion of backbone atom contributions in the repulsion model should result in greater distortion toward TP geometry than is predicted on the basis of the donor atoms alone (see also part (c)). This is effectively the case in the present treatment of a tris(tridentate) complex where f is much shorter than a normally observed metal non-donor atom distance. ω and β

corresponding to the minimum repulsive potential for a fixed α value were calculated with the approximation that $\alpha = f$; these values, given in Table 8.11, should be compared with the corresponding values for an ML_6 -core listed in Table 8.10. The effect of changes in f/α , and in the relative charge distribution over the two types of donor atom site, on the position of the minimum potential has not been investigated.

TABLE 8.11 ML_9 -CORE: β_{min} AND ω_{min} AT FIXED α VALUES FOR A $1/r$ POTENTIAL.

α (deg.)	β_{min} (deg.)	ω_{min} (deg.)
60	90	0
75	80.167	14.936
90	63.667	47.849
105	56.550	71.393
120	52.133	93.513
135	49.283	115.174

However, since the equality of α and f is only approximate it is preferable to calculate ω_{min} and β_{min} precisely using the average bond lengths (α, f) and intra-ring angles (α) for the individual complexes. The results of these computations are summarized in Table 8.12A: α, α, β and ω were calculated from the crystal coordinates using program AZIMUTH and f was abstracted from the structure report. Literature sources, symmetry information and L...L (b) and θ characteristic of an ML_6 -core are given in Table 8.12B.

TABLE 8.12A DISTORTION PARAMETERS OF TRIS-TRIDENTATE COMPLEXES: MO_9^- AND MO_6N_3^- -CORES.

Complex : structure	α (deg.)	a (Å)	f (Å)	β (deg.)	β_{min}	ω (deg.)	ω_{min}
1. $\text{Yb}(\text{pyd})_3^{3-} : \text{Na}_3 \cdot \text{NaClO}_4 \cdot 10\text{H}_2\text{O}$	129.62	2.406(10)	2.43	50.90	50.12	106.57	107.58
2. $\text{Yb}(\text{pyd})_3^{3-} : \text{Na}_3 \cdot 14\text{H}_2\text{O}$	130.46	2.335(20)	2.38	50.26	49.93	108.36	108.73
3. $\text{Yb}(\text{pyd})_3^{3-} : \text{Na}_3 \cdot 13\text{H}_2\text{O}$	130.42	2.365(15)	2.51	50.02	49.80	108.55	108.83
4. $\text{Nd}(\text{pyd})_3^{3-} : \text{Na}_3 \cdot 15\text{H}_2\text{O}$	124.94	2.495(15)	2.58	53.22	50.93	97.83	100.83
5. $\text{Nd}(\text{oxd})_3^{3-} : \text{Na}_3 \cdot 2\text{NaClO}_4 \cdot 6\text{H}_2\text{O}$	125.63	2.428(6)	2.523	51.29	50.77	101.21	101.84
6. $\text{Nd}(\text{oxd})_3^{3-} : \text{Na}_3 \cdot 2\text{NaClO}_4 \cdot 6\text{H}_2\text{O}$	126.34	2.375(20)	2.52	51.30	50.55	102.05	102.95
7. $\text{Yb}(\text{oxd})_3^{3-} : \text{Na}_3 \cdot 2\text{NaClO}_4 \cdot 6\text{H}_2\text{O}$	128.92	2.339(6)	2.431	50.09	50.14	106.65	106.59
8. $\text{Yb}(\text{oxd})_3^{3-} : \text{Na}_3 \cdot 2\text{NaClO}_4 \cdot 6\text{H}_2\text{O}$	129.13	2.314(20)	2.46	51.63	50.02	105.08	106.99
9. $\text{Gd}(\text{oxd})_3^{3-} : \text{Na}_3 \cdot 2\text{NaClO}_4 \cdot 6\text{H}_2\text{O}$	127.38	2.406(10)	2.49	50.80	50.45	103.93	104.34

TABLE 8.12B SUPPLEMENTARY DATA ON TRIS-TRIDENTATE STRUCTURES OF

TABLE 8.12A.

<i>Structure</i>	<i>Space group</i>	<i>Complex Ion Site Symmetry</i>	<i>b</i> (Å)	θ (deg.)	<i>Ref.</i>
1	$P_{\bar{6}2c}$	D_3	4.354	45.39	461
2	P_{nna}	C_2	4.240	45.71	458
3	$P_{2_1/c}$	C_1	4.295	45.88	456
4	$P_{\bar{1}}$	C_1	4.425	44.73	457
5	R_{32}	D_3	4.320	46.04	459
6	"	"	4.239	45.86	460
7	"	"	4.222	46.20	459
8	"	"	4.180	44.92	460
9	"	"	4.313	46.00	460

Apart from complex ion no. 4, the experimental geometries are well represented by the theoretical model. Structure solutions nos. 5 and 7 are redeterminations of structures 6 and 8 respectively and are based on diffractometer data; all seven other structures were determined using Weissenberg equi-inclination film data. The computed esd's in the twist angles of structures 5 and 7 are $\pm 0.3^\circ$; for the structures solved using film data the bond length and angle errors are typically two to three times larger.

Although the experimental β and ω values lie within 3σ of the theoretical minima the tendency for the theoretical model to slightly

underestimate the extent of the distortion toward TP geometry (i.e. $\beta_{min} < \beta$, $\omega_{min} > \omega$) in all cases except structure 7 is worthy of note. This is precisely the trend to be expected if the non-donor atoms, excluded from the theoretical model, contribute to the structural distortion of the real complex ion. However, the effect is so small in these relatively "highly charged" pseudo-ionic lanthanide complexes that it can probably be safely ignored in discussion of the d -transition metal complexes (but see part (c)), particularly when the total charge on the complex is small or the metal-ligand bonding is more closely covalent.

In conclusion, it should be pointed out that the assignment of equal charge density to the two types of ligand donor atoms may be a source of error in these tris-tridentate calculations.

c) CRMALTCOPN and CADCOTHIOX:

Having elucidated the general principles of the first coordination sphere electrostatic repulsion model and applied it with some success to both D_3 symmetric tris(bidentate) and tris(tridentate) complexes, it is perhaps pertinent at this stage to make special mention of the geometries of the tris-complex ions in the CRMALTCOPN (Chapter 2) and CADCOTHIOX (Chapter 3) structures.

Both the $\text{Cr}(\text{mal})_3^{3-}$ and $\text{Co}(\text{thiox})_3^{3-}$ ions have α angles close to 90° (91.91° and 89.68° respectively). Although the observed trend in β (55.91° , 56.91°) and ω (60.19° , 56.98°) is as expected from the relative

magnitudes of α , on the basis of the ML_6 -core repulsion model β should be less than 54.74° for the former complex ion and almost exactly 54.74° for $Co(thiox)_3^{3-}$. It is difficult to evaluate the effective direction of further distortion due to non-bonded contacts and the extensive hydrogen bonding in the CADCOTHIOX lattice but the trigonal symmetry of the CRMALTCOPN structure permits a more rigorous evaluation. Strong hydrogen bonding is indicated between the $Co(pn)_3^{3+}$ and $Cr(mal)_3^{3-}$ ions sharing a common three-fold axis (Table 2.7 and Figure 2.3); its implications in terms of the CD spectrum of the microcrystalline diastereoisomer have been discussed in section 5.3. Structurally this hydrogen bonding scheme promotes distortion of both complex ions further toward trigonal prismatic geometry (by twist contraction) than is theoretically predicted by the ML_6 -core repulsion model. The β value for the (-) $Co(-)pn_3^{3+}$ cation in this structure is 59.93° ($\alpha = 83.24^\circ$, $\omega = 47.99^\circ$), the highest observed for any tris(five-membered ring) complex of Co(III) or Cr(III) — (see Table 8.1); theoretical values calculated for the r^{-1} potential for $\alpha = 83.24^\circ$ are β ca. 57.7° , ω ca. 51.0° . It is unsatisfactory in many cases merely to discuss the distortion of tris(bidentate) complex ions in terms of the limited ML_6 repulsion model without some appreciation of possible subsidiary effects due to close contacts in the particular crystal lattice.

Finally, it was intimated in parts (a) and (b) that the ligand backbone atoms, except in chelate rings having pronounced charge delocalization, should not greatly influence the ML_6 -core distortion.

While the larger than predicted β angles of the $\text{Co}(\text{thiox})_3^{3-}$, $\text{Cr}(\text{mal})_3^{3-}$ and $\text{Co}(\text{pn})_3^{3+}$ ML_6 -cores can be explained by incorporating varying degrees of backbone atom contribution, as for $\text{Er}(\text{thd})_3$ in part (a), these backbone atom repulsions have most effect on the inter-ligand plane dihedral angles. As mentioned in section 7.3, it is more correct to discuss the distortion of tris(bidentate) complexes in terms of ligand planes rather than the ML_6 -core since in many cases (even for supposedly planar chelate rings such as ox, thiox) the coordinated metal atom is displaced from the mean ligand plane. Once again $\text{Cr}(\text{mal})_3^{3-}$ and $\text{Co}(\text{thiox})_3^{3-}$ can be used to illustrate the argument. For $\text{Cr}(\text{mal})_3^{3-}$ in CRMALTCOPN the dihedral angle between three-fold related O.Cr.O planes is $91.7 (1.0)^\circ$ whereas that between the C.Cr.C planes, where C are the carboxyl carbon atoms, is $96.9 (1.0)^\circ$ — (Table 2.5); for $\text{Co}(\text{thiox})_3^{3-}$ the S.Co.S planes are inclined at $93.0 (6)^\circ$ while the average dihedral angle between the six-atom ligand planes is 97.7° . In both cases the larger second angle indicates that the ligand is more closely parallel to the C_3 axis than is the L.M.L donor atom plane.

d) Further structural anomalies:

As mentioned previously in this section, the observed geometries of tris(diamine)Co(III) complexes are well reproduced by the more conventional energy minimization approach without explicit consideration of the electrostatic charge distribution. The distortion of the CoN_6^- core in the five-membered ring complexes is found to be largely

independent of the ring conformation (see Table 8.1): for the six-membered ring complexes the core geometry is more sensitive to chelate ring conformation, although the variation is not embarrassingly large in terms of the ionic repulsion model formulated here. A lack of suitable potential functions, particularly as regards the steric influence of oxygen and sulphur lone-pair electrons, has prevented a more extensive application of the energy minimization procedure.

The closeness with which the experimental distortion of the ML_6 -core in tris-bidentates is represented by the r^{-1} electrostatic repulsion model is somewhat embarrassing^{†5} in view of the greater sophistication of the full energy minimization procedures. However, it is difficult to conceive of how electrostatic forces operative only in the first coordination sphere could twist the ML_6 -core of a bis(tridentate), e.g. $Co(TRI)_2^{3+}$ and $Co(tame)_2^{3+}$, from ideal D_{3d} symmetry although axial distortion, $\theta \neq 54.74^\circ$, due to the ligand backbone remains possible. For $Co(TRI)_2^{3+}$ interligand dispersion interactions between adjacent aromatic rings of the two ligands may be important^{33,463} and the twist in the energy minimized $\Lambda\Lambda-Co(tame)_2^{3+}$ results from non-bonded repulsion of the amine hydrogen atoms attached to the opposing trigonal nitrogen faces.

A more striking example is the structure²⁶³ of hexakis(urea)-titanium(III) iodide, $[Ti(OC(NH_2)_2)_6]I_3$, (and its isomorphous V(III)

^{†5} Perhaps the agreement is not so "embarrassing" when it is realized that quantum mechanical theory shows⁸³ that the force on any nucleus in a system of nuclei and electrons is exactly the classical electrostatic interaction.

analogue⁴¹¹), in which the cation has D_3 symmetry; although the TiO_6 -core shows only a very small axial compression ($\theta = 55.1^\circ$) there is an appreciable twist (ca. 5.5°) of the two equilateral triangular faces from the maximally staggered D_{3d} symmetry. The magnetic susceptibility and the splitting in the polarized crystal spectrum⁴⁶⁴ of $[Ti(urea)_6]I_3$ have been interpreted both in terms of an assumed axial compression and, more recently, the observed trigonal twist.^{262,411} Examination of the non-bonded interactions in the crystal lattice²⁶³ indicates that the observed twist distortion is probably favoured by a maximizing of strong hydrogen bonds between the iodide ions and the amine nitrogen atoms, although Figgis et al⁴¹⁰ invoke an intramolecular vdW interaction between the urea ligands as the probable cause. However, it is not possible to say to what extent this structural distortion is due to the Jahn-Teller effect which complicates the low temperature polarized absorption spectrum.^{244,464}

A final relevant example of a distorted geometry which cannot be predicted solely from a consideration of electrostatic repulsions within the ML_6 -core is the corundum lattice. $\alpha-Al_2O_3$, corundum, can be regarded⁴⁶⁵ as a slightly distorted hexagonal close-packed array of spherical oxide ions with the smaller Al^{3+} ions (these Al^{3+} ions can be substituted to varying degrees by other M^{3+} ions without disruption of the lattice, e.g. Cr^{3+} in ruby) occupying 2/3 of the octahedral interstices. The metal ions stack in pairs along the c axis of the lattice (space group $R\bar{3}c$) sharing a common trigonal face of a

distorted MO_6 octahedron.²¹⁷ The metal ions are not positioned at the centres of the interstices, as would be predicted from a simplified ML_6 point charge model, but are displaced along c in the direction of the adjacent unoccupied interstice. The shared trigonal face is relatively contracted and corresponds to the larger $M-O$ and smaller θ values listed for these structures in Table 8.7. The perpendicular distances of the trivalent metal ions from this shared face are (with distance to the opposite face in parentheses): Al_2O_3 1.326 (0.840), Cr_2O_3 1.324 (0.940), Fe_2O_3 1.441 (0.847), Ti_2O_3 1.295 (0.978), V_2O_3 1.391 (1.017) Å.

Elsewhere the axial displacement of the trivalent metal ions from the centres of the "octahedral" holes has been discussed⁴⁶⁶⁻⁴⁶⁸ in terms of coulombic repulsion between metal ions sharing a common interstitial face. However, this axial interaction can promote polar distortion only and the MO_6 polyhedron should retain C_{3v} symmetry. All five structures exhibit significant twisting of the trigonal oxide ion faces from a D_{3d} (or C_{3v}) arrangement having $\omega = 60^\circ$. (N.B. — in Table 8.7 ω is given as less than 60° corresponding to $\alpha < 90^\circ$: this implies nothing about the chiral sense of the trigonal twist since the lattice is centric.) The reason for the twist distortion is readily seen from an examination of the corundum lattice: the M^{3+} ions occupy three-fold symmetry sites and are surrounded in the basal plane (i.e. approximately constant z coordinate) by three nearest neighbour metal ions,^{217,468} each of which shares the shorter $0\dots0$ edge of the adjacent

occupied octahedral interstice. It is this 0...0 vector ($L-L$ in Table 8.7) which corresponds to $\alpha < 90^\circ$, $\omega < 60^\circ$.

Thus, in applying the point-charge description to the corundum structures it is necessary to take account of the charge on the metal ions, both the axial and trigonal twist distortions being understandable in terms of repulsion between metal ions occupying adjacent octahedral interstices having either an octahedral face or edge in common. The successful representation of many of the spectral and magnetic features observed for doped $\alpha\text{-Al}_2\text{O}_3$ by models incorporating coupling⁴⁶⁹⁻⁴⁷¹ between metal ions occupying adjacent interstices^{217,468} suggests that such considerations are also necessary for realistic analysis of the polarized crystal spectra.

It is, of course, not possible to explain the trigonal prismatic coordination^{465,472} of the metal in MoS_2 and WS_2 simply on the basis of a point charge model of an isolated MS_6 core.

e) Trigonal twist inversion:

The trigonal twist inversion was early proposed as a facile intra-molecular mechanism for the racemization of chiral tris(bidentate) transition metal complexes and has been invoked in solution^{441,447,473} and solid state⁴⁷⁴⁻⁴⁷⁸ studies. During the inversion process the pseudo-octahedral ML_6 -core passes through a "supposedly" higher energy trigonal-prismatic transition state in which the chelate rings are parallel to the C_3 axis. This and other intra-molecular twist models

can be considered⁴⁴⁴ as special cases of the general Bailar non-bond rupture mechanism.^{439,440}

There are two ways of viewing the trigonal-twist mechanism which are only equivalent when considering tris-bidentate complexes exhibiting ideal D_3 symmetry. The description most commonly used is of a twisting of one trigonal donor atom face about the C_3 axis relative to the opposing parallel face;^{447,473} the twist angle changes from $+\omega$ through 0° at D_{3h} symmetry to $-\omega$ for the enantiomeric configuration. An alternative description is possible in terms of a pivoting of the individual bidentate ligands about the two-fold axes of the D_3 complex, the tilt angle changing from $+\beta$ through 90° to $-\beta$. (We here modify our definition of positive ω and β given in footnote ⁸ to section 7.3 in order to emphasize the inversion of configuration.)

Both descriptions have some merit. The ω description is immediately applicable to the intra-molecular racemization of linked sexadentate complexes approximating C_3 symmetry^{445,473} and of mono- and bis-complexes containing cyclic tridentate ligands, e.g. $\text{Co}(\text{TRI})_2^{3+}$, whereas the β description in terms of tilted ligand planes is only an imaginary concept in the latter case. However, the ω description has often prompted interpretation^{441,444} of the trigonal twist mechanism as involving distortion of the complex from an ideally trigonal antiprismatic geometry in which the two triangular donor atom faces are maximally staggered, i.e. $\omega = 60^\circ$. For mono- and bis(cyclic-tridentate) complexes TAP is the sensible reference geometry, but for tris-bidentates the

ORTH arrangement having $\beta = 54.74^\circ$ ($\gamma = 90^\circ$) is a more realistic reference state from which to consider the degree of ML_6 distortion, since for a chelate ring of fixed dimensions Σ_{ORTH} is always less than Σ_{TAP} (see Figure 8.2). Furthermore, trigonal-antiprismatic geometry is unattainable for hypothetical (i.e. none known so far) tris-complexes having $\alpha < 60^\circ$ whereas the full β range $0-90^\circ$ remains valid.

Perhaps the most cogent argument for describing the trigonal-twist mechanism in tris-bidentates in terms of a change in β is that in such complexes the donor atoms of a trigonal face are not linked together and each bidentate ligand can be considered to move independently; since rotation of one chelate ring about the C_2 axis will affect the other two the motion is more "concerted" than "independent". This alternative description of the trigonal twist inversion mechanism assumes an increased importance in tris-bidentates containing non-identical ligands;⁴⁴⁷ in these cases the inversion of the chiral molecule is seldom realistically described by an average angle of twist of the two opposing pseudo-trigonal faces. Further, application of the "average-twist" formalism to the trigonal-prismatic complexes $Re(dpd)_3$, $V(dpd)_3$ and $Er(thd)_3$, where the chelate rings exhibit opposing chiral senses relative to the pseudo- C_3 axis of the complex, would not result in ideal D_{3h} symmetry.

Whichever way the trigonal-twist inversion is visualized, the preceding electrostatic analysis of ML_6 -core geometry in D_3 tris(bidentate) complexes has shown that the racemization process should not be regarded

simply as distortion from either an idealized TAP or ORTH geometry to a TP transition state, but rather as distortion from a precise minimum energy geometry characteristic of the chelate ring dimensions. If the r^{-1} potential is as faithful a representation of the ML_6 -core potential as comparison with experimental data suggests (Figures 8.3A and 8.3B), then the activation energies for the intra-molecular trigonal-twist racemization of tris(bidentate) complexes should correlate directly with the calculated potential difference between the minimum energy geometry and the D_{3h} arrangement, provided the electrostatic charge distribution over the complex can be adequately represented and the assumption of fixed chelate ring dimensions during the inversion process is valid.

The trends in the distortion geometry of the ML_6 -core have been indicated previously in this section. In Figure 8.2 the relative repulsion potentials for the three reference geometries ORTH, TAP and TP were plotted as functions of α ; the fourth curve, MINM, is a plot of the minimum potential. All potential sums (ΣML_6) were computed with $\alpha = 1.00$ and varying α , and hence the ligand bite b also varies; alternatively the potential corresponding to fixed ligand bite could have been computed as a function of α : the donor atom charge was taken as unity. An observation of particular relevance to discussion of the trigonal twist inversion mechanism is that for a fixed metal-donor atom bond length, α , the potential difference $\Sigma_{TP} - \Sigma_{MINM}$ increases with increasing α , i.e. the larger α the more energetically prohibitive the

attainment of a trigonal prismatic transition state.

Therefore, contrary to the conclusion of Stiefel and Brown,⁴⁴² the trigonal twist inversion mechanism for the intra-molecular racemization of tris-bidentate complexes should be more favourable the smaller the ligand angle α .

8.3 ASSESSMENT OF THE VALIDITY OF THE PK TRIGONAL-DISTORTION MODEL

On a crystal field basis the degree of geometric distortion necessary to produce a change in most spectral properties is small since often a lowering of the chromophore symmetry only is required. Given theoretical models which relate the experimentally determinable electromagnetic properties of complexes to distortions from an idealized geometry it is difficult to resist the temptation to correlate these observations with structural parameters which often are not significantly different from those characterizing the high symmetry reference state. The structure refinement of CRMALTCOPN (Chapter 2) is a case in point: $\alpha = 91.91 (68)^\circ$ and $\omega = 60.19^\circ$ for the (+) $\text{Cr}(\text{mal})_3^{3-}$ ion; the electrostatic r^{-1} repulsion model predicts $\omega = 62.5^\circ$. The esd in ω is ca. $\pm 0.45^\circ$ (i.e. $2/3$ the error in α since ω involves no z component); the difference from the theoretical value is significant even at a 3σ level but the distortion from $\omega = 60^\circ$, the trigonal antiprismatic reference geometry of the PK-model, is only 0.3σ .

An important question is the correctness of using structural parameters derived from complexes in the solid state in interpreting solution spectral properties. Distortion parameters are probably most legitimately transferable in cases where the geometry of the complex has been found to be largely invariant in several different structures and is in close agreement with the predictions of the repulsion model. However, even in these cases specific solvent and ion association effects in solution may promote distortions not observed in the solid state.

8.3.1 Co(III), Cr(III) N_6 Chromophores.(1) Co(en) $_3$ /(pn) $_3$ ³⁺.

a) Determination³⁰⁹ of the absolute configuration of (+) Co(en) $_3$ ³⁺ as Λ provided the necessary reference for the empirical and less certain theoretical models for absolute configuration/CD correlation of transition metal complexes; Kuhn and Bein^{183,321,322} and Piper and Karipides^{34,236,331} had predicted a Δ configuration.

Mason suggested, on the basis of exchange studies⁴⁷⁹ of the amine hydrogens in D₂O, that the PK-model limiting the non-donor atoms of the ligands to an electronically inert structural role was incorrect. However, subsequent experiments^{246,480,481} suggest that the amine hydrogens make negligible contributions to the dipole and rotatory strengths of the chromophore $d-d$ transitions.

The long wavelength positive solution CD band of (+) Co(en) $_3$ ³⁺ was assigned E_α symmetry from single crystal CD studies,^{192,193,273} but this assignment conflicts with an earlier polarized absorption crystal spectrum determination,²⁴⁵ which gave K positive for both Co(en) $_3$ ³⁺ and Cr(en) $_3$ ³⁺, and subsequent experiments^{246,247,253} showing significant vibronic structure in both the long wavelength absorption and CD bands; the importance of vibronic coupling contributions to the $d-d$ rotatory strength of Co(en) $_3$ ³⁺ has recently been questioned.^{13,41} As indicated in Chapter 6, we adopt the trigonal splitting formalism for the purpose of this discussion.

Early structural parameters³⁵⁴⁻³⁵⁶ for the Co(en) $_3$ ³⁺ ion in

various crystal lattices gave an inconsistent picture of the displacement of the six nitrogen donor atoms from idealized O_h symmetry: the first-order crystal field model required inordinately large trigonal splitting to explain the magnitude of the observed rotatory strengths.^{58,192,281} The small positive component under the high energy ${}^1A_{1g} \rightarrow {}^1T_{2g}$ magnetic-dipole forbidden band was assigned E_b symmetry, its small magnetic-dipole strength supposedly being borrowed from the lower energy E_α component and the intense charge transfer band, also E symmetric but having negative rotatory strength.^{25,58,192}

b) The first-order crystal field model predicts trigonal components of E_α and A_2 symmetry under the low energy ${}^1A_{1g} \rightarrow {}^1T_{1g}$ band; the equal, but oppositely signed, rotatory strengths of these two components should exactly cancel in the absence of trigonal splitting.^{34,41,270,280} The two unequal solution CD peaks observed under the envelope of the long wavelength absorption band of Co(en)_3^{3+} are interpreted^{191,192} as "residual wing overlaps" of the oppositely signed E_α and A_2 trigonal components, the rotatory strength of the solution E_α component being an order of magnitude less than that observed for the oriented single crystal.^{192,273}

Suggestions⁴⁸² that these components resulted solely from the presence of two or more conformers in equilibrium in solution were refuted when a similar solution CD spectrum was observed^{302,341,483} for the

conformationally locked (+) $\text{Co}((+)\text{pn})_3^{3+}$ ion, and microcrystalline KBr disc CD spectra²¹⁵ of (+) $\text{Co}(\text{en})_3^{3+}$ in the lattices used for the single crystal studies were shown to be identical with the aqueous solution spectra. The similarity of the CD spectra^{3,108,341} of the ideally D_3 symmetric tris(1el) (-) $\text{Co}((+)\text{chxn})_3^{3+}$ ion,³⁶¹ the C_3 symmetric *cis* (+) $\text{Co}((+)\text{pn})_3^{3+}$ ion and C_1 symmetric *trans* (+) $\text{Co}((+)\text{pn})_3^{3+}$ argues for a primary dependence on the microsymmetry of the CoN_6 -core rather than of the complex ion as a whole, although the observance³⁰² of a single long wavelength negative peak in the CD spectrum of (-) $\text{Co}((+)\text{pn})_3^{3+}$, together with an elaborate series of variable conformer solution studies,²⁶⁹ has demonstrated that conformational and vicinal effects play a minor role in the visible region of the spectrum, these contributions being generally additive^{269,483} to the dominant configurational rotatory strength. In some cases two components are observed²⁶⁹ under the T_{2g} band envelope although the idealized ML_6 -core microsymmetry is still D_3 .

c) The rotatory strengths of both the E_α and A_2 components change with increasing concentration of uninegative and dinegative anions.^{290,484,485} Tetrahedral and trigonal oxyanions, notably phosphate and selenite, enhance^{248,290,291} the negative A_2 component of (+) $\text{Co}(\text{en})_3^{3+}$ with an apparent concomitant reduction of the E_α rotatory strength. Again, observation²⁴⁸ of a similar effect for (+) $\text{Co}((+)\text{pn})_3^{3+}$ argues against a trivial change in conformer proportions being solely responsible

for the effect. A much smaller effect was observed for (-) $\text{Co}((+)\text{pn})_3^{3+}$ where the ligands are locked in the energetically less favourable "ob" conformation and the enhancement of A_2 in the case of (+) $\text{Co}(\text{en})_3^{3+}$ and (+) $\text{Co}((+)\text{pn})_3^{3+}$ ($\Lambda\delta\delta\delta$) was rationalized^{248,485} in terms of strong hydrogen bonding of the tetrahedral oxyanion to the favourably oriented amine hydrogen atoms of the trigonal nitrogen faces of the tris(1el) conformer, with resultant electronic coupling between the metal centred and oxyanion transitions. This model for oriented ion-pair formation receives some support from the crystal structure³⁵⁸ of $2[\text{Co}(\text{en})_3](\text{HPO}_4)_3 \cdot 9\text{H}_2\text{O}$ in which the three-fold axis of one biphosphate anion is approximately coincident with the pseudo- C_3 axis of the tris(1el) cation. In the isomorphous $[\text{Ni}(\text{en})_3](\text{SO}_4)$ and $[\text{Cu}(\text{en})_3](\text{SO}_4)$ structures,^{362,365} however, a two-fold axis of the sulphate ion lies approximately coincident with the C_3 axis of the tris(1el) cation, again with extensive hydrogen bonding to the trigonal amine hydrogen atoms. Solution nmr studies^{486,487} indicate a favouring of the tris(1el) conformer of $\text{Co}(\text{en})_3^{3+}$ at high phosphate concentration.

Excess anion is commonly used in these solution studies and the modifying effect on the CD spectrum of the 1:1 cation-anion pair due to higher order outer-sphere complexes has been studied;^{67,291,488} in most cases, however, the precise cation:anion ratio must be uncertain. This so-called gegenion effect with PO_4^{3-} was proposed^{188,248} as a means of assigning the E_α and A components of the T_1 octahedral transition in $\text{Co}(\text{III})$ and $\text{Cr}(\text{III})$ tris-diamine complexes, but in view

of the conflicting assignments^{36,96,189,190} made for $\text{Co}(\text{tn})_3^{3+}$ it is doubtful that the proposed^{248,291} charge-transfer mechanism is correct. The similarity of the CD spectrum⁴⁸⁹ of the "capped" sexadentate $\text{Co}(\text{sen})^{3+}$, $\text{sen} = \text{CH}_3\text{C}(\text{CH}_2\text{NHCH}_2\text{CH}_2\text{NH}_2)_3$, to that of (+) $\text{Co}(\text{en})_3^{3+}\text{-PO}_4^{3-}$ suggests that the gegenion effect is more correctly viewed as a vicinal effect reflecting the production of new asymmetric centres at the primary amine donor atoms.

(2) $\text{Co}(\text{tn})_3^{3+}$.

d) (-) $\text{Co}(\text{tn})_3^{3+}$ was shown to have a Λ absolute configuration by a full X-ray structure determination.^{120,490} Whereas the ligand angle, α , had been found to be less than 90° in all Co(III) and Cr(III)-en rings (see Table 8.1), apart from the doubtful case³⁵⁵ of $[\text{Co en}_3]\text{Cl}_3 \cdot 3\text{H}_2\text{O}$ (number 3 in Table 8.1) unfortunately quoted by Piper and Karipides^{34,35,237} in the original treatment of the PK-model, the α angles for $\text{Co}(\text{tn})_3^{3+}$ averaged 94.5° . Provided the CD components of this tris(six-membered ring) complex ion could be assigned, the expansion in ligand angle suggested that a test of the validity of the PK-model as opposed to Mason's E_α -sign model should be possible.

e) The $\text{Co}(\text{tn})_3^{3+}$ ion in the monoclinic $(-)[\text{Co tn}_3]\text{Br}_3 \cdot \text{H}_2\text{O}$ structure^{120,490} is not restricted to any crystallographic site symmetry but all three Co-tn rings adopt chair conformations, the complex ion having pseudo- C_3 symmetry.

The aqueous solution CD spectrum of $\Lambda(-)$ $\text{Co}(\text{tn})_3^{3+}$ shows^{60,67} a minor positive long wavelength peak and a dominant negative component at higher energy under the ${}^1A_{1g} \rightarrow {}^1T_{1g}$ band envelope; a smaller negative component occurs under the high energy ${}^1A_{1g} \rightarrow {}^1T_{2g}$ band. Addition of sodium selenite or phosphate enhances the dominant negative component at the expense of the longer wavelength positive component.^{189,190}

Without a realistic appreciation of the relative strain energies of the possible $\text{Co}(\text{tn})_3$ conformers, it was argued^{189,190} that the tris-chair conformer dominated the solution spectrum and that the relative enhancement and diminution of the long wavelength CD components proceeded by a mechanism entirely analogous to the ion-pairing suggested for $\text{Co}(\text{en})_3^{3+}-\text{PO}_4^{3-}$. On this basis the longer wavelength positive component was assigned E_α symmetry and the dominant negative component as A_2 ; this assignment was in contradiction of the more general rule that the E_α component exhibit dominant rotatory strength.^{58,191}

Arguing incorrectly in terms of α it was intimated^{189,190} that the PK-model was invalid since the E_α component was positive for both $\Lambda(+)$ $\text{Co}(\text{en})_3^{3+}$ and $\Lambda(-)$ $\text{Co}(\text{tn})_3^{3+}$ for which α is respectively $< 90^\circ$ and $> 90^\circ$.

f) However, a recent single crystal CD spectrum³⁶ of $\Lambda(+)[\text{Co}(\text{tn})_3]\text{Cl}_3 \cdot 4\text{H}_2\text{O}$ has suggested that the E_α component for $\text{Co}(\text{tn})_3^{3+}$ is in fact the higher energy dominant component, i.e. for

$\Lambda(-)$ $\text{Co}(\text{tn})_3^{3+}$ E_α is dominant and negative. This assignment seemingly supports the first-order crystal-field model based on the ML_6 -core distortion, both in the reversal of E_α rotatory strength (equations 7.1 and 7.2) and the inversion in the energy ordering of the trigonal components (eq. 7.3), although once again it was implicitly assumed that $\alpha > 90^\circ$ necessarily means $\omega > 60^\circ$ and $\theta < 54.74^\circ$.

These conflicting solution and single-crystal assignments prompted the following consideration of the $\text{Co}(\text{en})_3/(\text{tn})_3$ system: (see also ref. 96).

(3) Geometry of $\text{Co}(\text{en})_3^{3+}$ and $\text{Co}(\text{tn})_3^{3+}$.

g) A chelated ethylenediamine ligand can adopt two minimum energy, mirror-image skew conformations, λ and δ ,^{127,128} in which the ring hydrogen atoms are maximally staggered. Conformational energy calculations^{109,491,492} show that when three en ligands are bidentate to the same metal atom, the conformer having all three C-C bonds approximately parallel (lel) to the pseudo- C_3 axis has a lower strain energy (enthalpy) than that in which the en ring C-C bonds are more obliquely inclined (ob) to the C_3 axis, although the enthalpy difference, ΔH , is significantly less than the $1.8 \text{ kcal mol}^{-1}$ derived by Corey and Bailar^{1,2} using rigid models and hard-sphere non-bonded interaction potentials. The lowest energy tris(lel) conformer is $\Lambda(\delta\delta\delta) \equiv \Lambda(\lambda\lambda\lambda)$; the higher energy tris(ob) form is $\Lambda(\lambda\lambda\lambda) \equiv \Lambda(\delta\delta\delta)$. The minimized conformers quoted in Table 8.1 have a calculated ΔH of $0.58 \text{ kcal mol}^{-1}$;

substitution of a methyl group at the favoured equatorial position on a ring carbon atom, i.e. pn, has negligible effect on this energy difference ($\Delta H = 0.65 \text{ kcal mol}^{-1}$ for the isomers of Table 8.1).

h) Mixed conformers, i.e. $\Lambda(\delta\delta\lambda)$ and $\Lambda(\delta\lambda\lambda)$, have intermediate enthalpies.¹⁰⁹ In earlier discussions³⁰² of solution spectra of Co(en)_3^{3+} the fractions of the various conformers have been quoted as $(\text{lel})_3 : (\text{lel})_2\text{ob} : \text{lel}(\text{ob})_2 : (\text{ob})_3 = 59 : 29 : 8 : 4$ ^{150,311} but it is now more generally recognized^{240,492,493} that the statistical entropy term^{341,494} may favour a slight excess of the higher enthalpy $(\text{lel})_2\text{ob}$ conformer, i.e. $\Lambda(\delta\delta\lambda) \equiv \Lambda(\lambda\lambda\delta)$.⁴⁸⁷ The question of conformer proportions in the tris(five-membered diamine ring) complexes of Co(III) and Cr(III) is not important in assessing the predictions of the PK-model since $\omega < 60^\circ$ independent of conformation (Table 8.1); there is, however, some variance in $\theta < \text{or} > 54.74^\circ$ but for this discussion we will consider the CoN_6 -core as showing axial compression ($\theta > 54.74^\circ$). Of course, that the conformational and vicinal effects contribute to the $d-d$ rotatory strength at all is contrary to the basic premise of the PK-model that atoms outside the ML_6 -core are electronically inert.

However, the question of conformer proportions is important in interpreting the solution CD spectra since a significant portion of the visible transition rotatory strength could arise from conformers other than the tris(lel) form.^{269,341,482} More importantly, the

changes observed in the aqueous solution CD spectra on the addition of phosphate or selenite ions may reflect a change in the conformer proportions⁴⁹⁴ as much as any specific vicinal or electronic effect - but see (b) and (c) above for arguments against ascribing the observed spectral changes solely to an alteration of conformer proportions.

i) As for cyclohexane, six-membered M-tn rings can adopt a variety of conformations having differing degrees of stagger of the substituent hydrogen atoms around the chelate ring. Excluding the non-symmetric forms there are four conformations of particular interest. The symmetrical chair and boat forms are both mirror symmetric and should make no individual conformational contribution to the rotatory strength.¹²⁷ There are two C_2 symmetric skew forms, analogous to the λ and δ forms of the Co-en ring, and these should make oppositely signed ring conformational contributions to the rotatory strength.

Examination of Dreiding models shows the tris(boat) conformer to be least favoured because of close contact between the methylene hydrogens on the central carbon atom of a tn ring and the amine hydrogens of an adjacent ligand. In early discussions^{189,190} the tris(chair) conformer was considered predominant although the possibility of low energy skew conformers had been mentioned elsewhere.^{67,182,495} As with Co(en)_3^{3+} , the backbone carbon atoms of the λ and δ skew tn conformers lie parallel or oblique to the C_3

axis of the $\text{Co}(\text{tn})_3^{3+}$ complex depending on whether the absolute configuration of the ion is Λ or Δ . By analogy⁹⁶ with $\text{Co}(\text{en})_3^{3+}$, the tris(tn) conformer having the CoCCC planes of all three ligands more nearly parallel to the C_3 axis than the respective CoNN plane is called tris(lcl); the tris(ob) conformer has the CoCCC planes more oblique than the CoNN planes.

Energy minimization calculations^{94,372} gave a tris(lcl) conformer $0.77 \text{ kcal mol}^{-1}$ lower in enthalpy than the tris(chair) conformer; the tris(ob) conformer was $5.06 \text{ kcal mol}^{-1}$ more strained than the tris(chair). Independent calculation³¹² of the relative energies has inverted the tris(lcl) and tris(chair) energy order ($\Delta H = 0.60 \text{ kcal mol}^{-1}$) but the reliability of all these computed enthalpy differences is probably no better than $\pm 1 \text{ kcal mol}^{-1}$;⁴²⁹ the important conclusion is that the tris(lcl) and tris(chair) conformers have similar minimum enthalpies. Yet another study^{182,313} has indicated a slight favouring of the tris(lcl) conformer but more importantly it has been suggested³¹² that strong inter-ring non-bonded repulsions destabilize "mixed" conformers relative to the trigonally symmetric forms even allowing for the statistical entropy term favouring the non- C_3 species (but contrast refs. 313, 496). No realistic assessment of specific solvation effects can be made in these essentially vapour phase calculations: the most important omission, however, has been any attempt to calculate relative conformer enthalpies for particular ion-pairing models

with tetrahedral oxyanions. Experimentally, the nature of the anion has been shown⁴⁹⁷ to markedly alter the conformer equilibrium for polydentate Co(III) species.

NMR studies indicate rapid conformational flipping of chelated en^{486,492,493,498} and tn^{162,166} ligands in solution, but on the addition of phosphate there is a degree of conformational ordering not inconsistent with ion-pairing through specific hydrogen bonding.^{493,499,500} In view of the different geometries of the CoN₆-cores in the energy-minimized tris(1e1) and tris(chair) Co(tn)₃³⁺ conformers, namely $\alpha = 88.1^\circ$, $\omega = 56.3^\circ$ and $\alpha = 93.73^\circ$, $\omega = 64.31^\circ$ respectively, and the sign inversion of the rotatory strength, $R'_{E\alpha}$, predicted by the PK-model for a change in the sign of $\theta - \omega$ without changing the absolute configuration, some appreciation of the relative favourability of the proposed Co(en)₃³⁺/Co(tn)₃³⁺-PO₄³⁻ ion pairs is needed.

j) — this subsection abstracted from ref. 96 with minimum modification.

Without a realistic force constant representation of a phosphate ion, energy minimization calculations are not possible; however, assuming the model proposed by Mason and co-workers,^{190,248,485} i.e. hydrogen bonding of the oxyanion to the amine hydrogens of a trigonal face, the orientation of the N-H bonds in the various energy-minimized conformers of Co(en)₃ and Co(tn)₃ can be meaningfully

compared. The parameters characterizing the trigonal faces were derived using program NHANGLE (Appendix VI) and are summarized in Table 8.13.

TABLE 8.13 GEOMETRY OF THE MOST FAVOURABLY ORIENTED N-H BONDS IN THE ENERGY-MINIMIZED TRIS-DIAMINE COMPLEXES.

<i>Complex Ion</i>	<i>Ligand Conformation</i>	<i>N...N (Å)</i>	<i>H...H (Å)</i>	<i>Inclination of N-H to C₃ axis (deg.)</i>	
Co(en) ₃	(1e1) ₃	2.79	2.36	14.87	
	(ob) ₃	2.80	2.62	30.49	
Co(tn) ₃	(chair) ₃ {	face 1	2.79	2.55	32.86
		face 2	2.80	2.34	24.83
	(1e1) ₃	2.80	2.34	22.98	

The tris(chair) form of Co(tn)₃ has C₃ symmetry only, face 1 resembling the trigonal faces of tris(ob) Co(en)₃ and face 2 the trigonal faces of tris(1e1) Co(tn)₃. The tetrahedral PO₄³⁻ ion was taken to have O...O vectors of 2.50 Å¹⁸⁹ (for P-O = 1.534 Å⁷⁴) and linearity of the N-H...O hydrogen bonds (to within 25°)^{501,502} was considered important, without being concerned with the orientation of the oxygen lone pairs.⁵⁰³ For the tris(1e1) conformers of Co(en)₃ and Co(tn)₃ (namely N...N = 2.80 Å, H...H = 2.35 Å, and with N-H = 0.99 Å, O...O = 2.50 Å) the formation of linear N-H...O bonds of length 2.73-3.22 Å⁷⁴ requires that the N-H bonds be

skewed $36-32^\circ$ relative to the C_3 axis with the phosphorous atom $2.7-3.2$ Å above the trigonal nitrogen plane. Similarly for face 1 of tris(chair) $\text{Co}(\text{tn})_3$ having $\text{H}\dots\text{H} = 2.55$ Å, the ideal inclination of the N-H bonds to the C_3 axis is $23-20^\circ$, the phosphorous atom being $3.0-3.5$ Å from the nitrogen atom plane. The commonly quoted^{189,248} criterion of N-H bonds parallel to the C_3 axis of the complex is less satisfactory.

The CRMALTCOPN structure refinement indicated a significant trigonal twist ($\omega = 48^\circ$) of the $\Delta(-)$ $\text{Co}((-)\text{pn})_3^{3+}$ ion which could be rationalized in terms of strong hydrogen bonding with the adjacent $\text{Cr}(\text{mal})_3^{3-}$ anions. This distortion emphasizes the limitations of the present approach in considering the interaction of the PO_4^{3-} ion with a "rigid" energy-minimized tris-diamine conformer. Indeed, from an examination of Dreiding models it seems that bifurcated hydrogen bonds are even possible between an axially oriented PO_4^{3-} ion and the amine hydrogens of the energetically less favourable tris(ob) $\text{Co}(\text{en})_3^{3+}$ and $\text{Co}(\text{tn})_3^{3+}$ conformers.

(4) CD Spectra of $\text{Co}(\text{tn})_3^{3+}$: an interpretation.

k) From the preceding discussion it seems that the N-H bonds of the tris(1el) $\text{Co}(\text{tn})_3$ conformer are no less favourably oriented for formation of an axial ion pair with PO_4^{3-} than are those of the tris(chair) form. In the light of this observation we suggested that if the PK-model has any validity, the long wavelength positive

component observed in the solution CD spectrum¹⁹⁰ of $\Lambda(-) \text{Co}(\text{tn})_3^{3+}$ is the E_α component of the twist contracted ($\omega = 56.3^\circ$) tris(1e1) conformer while the positive higher energy E_α band in the single crystal CD spectrum³⁶ of $\Lambda(+)[\text{Co}(\text{tn})_3]\text{Cl}_3 \cdot 4\text{H}_2\text{O}$ arises from the twist expanded ($\omega = 64.31^\circ$) tris(chair) conformer. However, the structure of the tetrahydrate is unknown and the orientation of the pseudo- C_3 axes of the complex ions was determined by an nmr technique; thus the conformation of the cation could be other than the regular tris(chair). Saito has recently shown⁴¹⁸ the trichloride-monohydrate to be isostructural with monoclinic $(+)[\text{Co}(\text{tn})_3]\text{Br}_3 \cdot \text{H}_2\text{O}$ but it is not known whether the tetrahydrate merely corresponds to a super-hydrated modification or is a structurally different form.

1) Mason and co-workers²⁹² have recently published an elegant investigation of the $\text{Co}(\text{tn})_3^{3+}$ system which seems to confirm our hypothesis⁹⁶ of a conformational equilibrium in aqueous solution at room temperature, with the tris(chair) conformer apparently being marginally favoured energetically.

The microcrystalline CD spectrum²⁹² of $\Lambda(+)[\text{Co}(\text{tn})_3]\text{Br}_3 \cdot \text{H}_2\text{O}$ in a KBr matrix was shown to be identical with the oriented single-crystal CD spectrum³⁶ of $\Lambda(+)[\text{Co}(\text{tn})_3]\text{Cl}_3 \cdot 4\text{H}_2\text{O}$; both showed only a single positive component at ca. $20.7 \times 10^{-3} \text{ cm}^{-1}$ under the envelope of the ${}^1A_{1g} \rightarrow {}^1T_{1g}$ absorption band. This disc spectrum therefore

suggests negligible trigonal splitting of the ${}^1E_\alpha$ and 1A_2 trigonal components. More importantly, variable temperature studies^{67,292} of ethylene-glycol/water solutions of $\Delta(+)$ $\text{Co}(\text{tn})_3^{3+}$, analogous to those conducted earlier with the tris(en)/(pn) complexes,^{269,341} showed a marked increase in the rotatory strength of the high energy positive component at the expense of the minor negative longer wavelength band on lowering the temperature from 330°K to 198°K, i.e. the solution CD spectrum tends towards that of the tris(chair) conformer on lowering the temperature.

Addition of phosphate or selenite^{189,190,292} produced changes in the CD spectrum similar to those observed on reduction of the solution temperature and it was argued²⁹² that ion association favoured the tris(chair) conformation.

m) Some points merit comment.

First, it has been shown^{165,282,288,481} elsewhere that the solvent can effect the transition rotatory strength of even conformationally rigid complexes and the variable temperature spectra cannot be regarded as proof of a more stable tris(chair) conformer without an appreciation of possible asymmetric solvent interactions in ethylene-glycol/water solution, see for example the temperature induced changes in the CD spectra of conformationally rigid organic chromophores,^{19,289} e.g. isofenchone, and $(+)$ $\text{Co}((+)\text{pn})_3^{3+}$ - ref. 269.

Secondly, interpreting the spectral change induced by addition

of polarizable oxyanions as primarily due to a change in conformer equilibrium neglects the earlier model^{248,485} which rationalized the enhancement of the 1A_2 component of tris(1el) Co(en)_3^{3+} (and also^{60,190} the $\text{Co}(\text{tn})_3^{3+}$ ion) in terms of electronic effects. To apply this latter model here would predict an increase in the concentration of the tris(1el) conformer relative to the tris(chair) as the temperature is lowered, if the two CD bands are interpreted as E_α and A_2 trigonal components to increasing energy for the former but A_2 and E_α for the latter conformer. However, in view of the single peak observed²⁹² in the KBr disc spectrum and the single peaks observed^{38,314} under the ${}^1A_{1g} \rightarrow {}^1T_{1g}$ band envelope for the three conformationally rigid $\text{Co}(\text{ptn})_3^{3+}$ complex ions it seems more likely that the two peaks observed in the room temperature solution CD spectrum of $\text{Co}(\text{tn})_3^{3+}$ are $E_\alpha - A_2$ composites reflecting negligible splitting of the trigonal components. None of the energy-minimized $\text{Co}(\text{tn})_3$ structures show polar angle distortions as large as that of the cation in $(-)[\text{Co}(\text{tn})_3]\text{Br}_3 \cdot \text{H}_2\text{O}$, ($\theta = 52.6^\circ$).

Third, calculation of relative isomer proportions on the basis of the CD component band areas assumes equal but oppositely signed rotatory strengths for the optically active transitions in the tris(1el) and tris(chair) conformers and implies that the population of all other species is negligible. The minor long wavelength solution component is thus attributed solely to the tris(1el) and the higher energy dominant component solely to the tris(chair) conformer: the

opposing signs of these two CD components contradicts the E_α sign model which correlates the sign of R_{E_α} with the absolute configuration of the complex. The positive E_α component in the single crystal CD spectrum of $\Lambda(+)[\text{Co}(\text{tn})_3]\text{Cl}_3 \cdot 4\text{H}_2\text{O}$ supports the PK-model if the conformer in the crystal lattice is indeed the trigonal twist expanded tris(chair).

(5) $\text{Cr}(\text{tn})_3^{3+}$.

n) In Chapter 5 the $(-)\text{Cr}(\text{tn})_3^{3+}$ ion was assigned a Λ configuration. Unlike $\text{Co}(\text{tn})_3^{3+}$, this complex ion shows^{60,67,190} only a single positive CD component under the long wavelength ${}^4A_{2g} \rightarrow {}^4T_{2g}$ absorption band in the 300°K aqueous solution spectrum. Addition of PO_4^{3-} diminished the rotatory strength of this component and gave a weaker negative band at shorter wavelength. The interpretation is therefore entirely analogous to that outlined above for $\text{Co}(\text{tn})_3^{3+}$.

$\Lambda(+)\text{Cr}(\text{en})_3^{3+}$ also gives^{27,60} a single positive aqueous solution CD component under the ${}^4A_{2g} \rightarrow {}^4T_{2g}$ band envelope; this, together with the similarity of the $(+)\text{Cr}(\text{en})_3^{3+}$ and $(-)\text{Cr}(\text{tn})_3^{3+}$ solution ORD curves suggests that the correlation of complex ion absolute configuration with the sign of the long wavelength Cotton effect may be as correct as any discussion in terms of distortion of the CrN_6 -core and CD component signs.

The ORD curve⁶⁰ of $\Lambda(-)\text{Co}(\text{tn})_3^{3+}$ shows only the short wavelength

features of the $\Lambda(+)$ $\text{Co}(\text{en})_3^{3+}$ curve but the CD spectra of both complex ions exhibit long wavelength positive components and short wavelength negative components under the ${}^1A_{1g} \rightarrow {}^1T_{1g}$ band envelope; again trivial comparison of the sign of the long wavelength CD component, regardless of transition symmetry or relative rotatory strength, correlates with the assigned absolute configuration. The relevant aqueous solution CD data for the $\text{Co/Cr}-(\text{en})_3/(\text{tn})_3$ system, abstracted from the literature, are collected in Table 8.14.

TABLE 8.14 AMBIENT TEMPERATURE AQUEOUS SOLUTION CD SPECTRA OF $\Lambda M(\text{aa})_3^{3+}$. (M = Co(III), Cr(III): aa = en, tn.)

Complex	low energy T_1 band		T_2 band	Ref.
	low frequency component	high frequency component		
(+) $\text{Co}(\text{en})_3^{3+}$	20.3 ^a (+1.89) ^b	23.4 (-0.17)	28.5 (+0.25)	27
(-) $\text{Co}(\text{tn})_3^{3+}$	18.80 (+0.067)	21.10 (-0.140)	27.80 (-0.015)	314
(+) $\text{Cr}(\text{en})_3^{3+}$	21.9 (+1.49)		28.5 (-0.08)	27,504
(-) $\text{Cr}(\text{tn})_3^{3+}$	20.9 (+0.34)			504

a. ν_{max} , $\times 10^{-3} \text{ cm}^{-1}$.

b. $\Delta(\epsilon_{\parallel} - \epsilon_{\perp})$.

c. similar compilations of optical rotatory strengths are given in ref. 60 (pp. 227-230) in *Biot* ($= 10^{-40}$ c.g.s. units) units.

(6) $\underline{\text{Co}(\text{ptn})}_3^{3+}$.

o) 2,4-diaminopentane, ptn, exists as *meso* (R,S) and *racemic* (R,R and S,S) forms. The ligand forms six-membered puckered chelate rings, analogous to tn, bidentate through the amine nitrogens. However, the steric requirement that the exocyclic methyl groups occupy equatorial rather than axial sites locks the chelate ring in various conformations and for the tris-complexes of the resolved R,R- (or S,S-) ligand the absolute configurations are predictable.

A crystal structure refinement³⁷¹ of $(+)_{546}[\text{Co}(\text{R,R-ptn})_3]\text{Cl}_3 \cdot 2\text{H}_2\text{O}$ has confirmed the high energy Λ -tris(ob) conformation expected on the basis of the preparative procedure, the nmr spectrum, and the positive sign of the long wavelength CD component.^{38,314}

$(-)_{546}[\text{Co}(\text{R,R-ptn})_3](\text{ClO}_4)_3 \cdot \text{H}_2\text{O}$ was prepared in the presence of activated charcoal and therefore should be the conformationally less strained Δ tris(lel) conformer; it exhibits a single negative CD component under the long wavelength ${}^1A_{1g} \rightarrow {}^1T_{1g}$ band envelope. The structure of this salt has not yet been solved³⁷⁰ but the distortion parameters (Table 8.2) derived for the $(+)_{546} \text{Co}(\text{R,R-ptn})_3^{3+}$ ion are in excellent agreement with those obtained for the energy minimized^{94,372} tris(ob) $\text{Co}(\text{tn})_3$ conformer. The skew ligands should make mirror image conformational contributions (as well as a vicinal contribution) to the transition rotatory strengths and this may account for the greater observed^{38,314} rotatory strength of $\Lambda(+)_546 \text{Co}(\text{R,R-ptn})_3^{3+}$ compared to $\Delta(-)_546 \text{Co}(\text{R,R-ptn})_3^{3+}$. Single crystal CD spectra have

not been reported: $(+)_{546}[\text{Co}(\text{R,R-ptn})_3]\text{Cl}_3 \cdot 2\text{H}_2\text{O}$ is orthorhombic ($P_{2_1^2_1^2_1}$) with the pseudo- C_3 axis of the complex ion aligned approximately parallel to the b crystallographic axis and one C_2 axis parallel to the c axis — this structure should be ideal for polarized spectral if not single crystal CD measurements.

p) However, although these $\text{Co}(\text{R,R-ptn})_3^{3+}$ complexes are important in so far as they provide rigid conformers for comparison with the conformationally more labile $\text{Co}(\text{tn})_3^{3+}$ ion, they afford no novel test of the PK-model since the CoN_6 -cores of both the tris(ob) and tris(1el) energy minimized $\text{Co}(\text{tn})_3$ conformers have ω ca. 56.5° .

meso (R,S-ptn) is configurationally non-stereospecific; the tris-complex was resolved with silver(+)tartrate.³⁸ On chelation R,S-ptn will lock in the ideally mirror symmetric chair conformation for which there can be no individual ring conformational or vicinal effect. $(-)_{546} \text{Co}(\text{R,S-ptn})_3^{3+}$ gives^{38,314} a single long wavelength negative CD component at marginally higher frequency than that observed for the tris(1el) conformer (see Table 8.15). Apart from the charge transfer region, the succession of peaks and troughs in the superposition of the Λ tris(1el) and $?(-)_{546}$ tris(chair) spectra corresponds with that in the $\Lambda(-) \text{Co}(\text{tn})_3^{3+}$ aqueous solution spectrum:^{60,190} this, together with the observation of only a single long wavelength CD component in the aqueous

solution spectra of all three $\text{Co}(\text{ptn})_3^{3+}$ conformers, supports the rationalization of the $\text{Co}(\text{tn})_3^{3+}$ spectrum in terms of a conformer equilibrium between these two low strain energy forms.

Therefore, consistent with the PK-model ($\omega = 64.3^\circ$ for the energy minimized $\text{Co}(\text{tn})_3$ chair conformer) we predict a Λ configuration for $(-)_546 \text{Co}(\text{R,S-ptn})_3^{3+}$, contrary to the literature correlation^{38,314} via the E_a sign model. Unfortunately the crystal structure of $(-)[\text{Co}(\text{R,S-ptn})_3](\text{ClO}_4)_3 \cdot 3\text{H}_2\text{O}$ has not yet been solved³⁷⁰ and the effect of polarizable oxyanions on the solution CD spectra has not been reported.

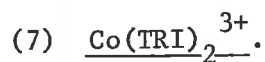
TABLE 8.15 APPROXIMATE POSITION AND PEAK HEIGHT OF $\text{Co}(\text{ptn})_3^{3+}$ CD COMPONENTS.^a

<i>Complex ion</i>	<i>low energy T₁ band</i>	<i>high energy T₂ band</i>
$\Lambda(+)_546 \text{Co}(\text{R,R-ptn})_3^{3+} : \text{ob}$	20.83 ^b (+2.690) ^c	28.41 (-0.283)
$\Delta(-)_546 \text{Co}(\text{R,R-ptn})_3^{3+} : \text{lel}$	19.61 (-0.586)	28.57 (+0.066)
$?(-)_546 \text{Co}(\text{R,S-ptn})_3^{3+} : \text{chair}$	19.69 (-0.548)	28.17 (-0.013)

a. from ref. 314.

b. frequency, $\times 10^{-3} \text{ cm}^{-1}$.

c. $\Delta(\epsilon_l - \epsilon_r)$.



q) The geometric distortion of the CoN_6 -core in the bis(cyclic tri-imine),⁴⁶³ $(+)_546[\text{Co}(\text{TRI})_2]\text{I}_3 \cdot 3\text{H}_2\text{O}$, was considered³³ to provide

"strong evidence ... for the metal-centred optical activity arising from the extant twisted crystal fields"; the parameters characterizing the CoN_6 -core are given in Table 8.8A. The ω contraction (52.3°) is defined in the Λ sense of the ligand skew and is analogous to the trigonal twist contraction of the CoN_6 -core in Co(en)_3^{3+} derivatives. Unlike Co(en)_3^{3+} , however, the first coordination sphere exhibits significant axial elongation ($\theta = 52.2^\circ$) and on the basis of the crystal field model (equation 7.3) the E_α and A_2 components should invert in energy from the Co(en)_3^{3+} assignment. However, the literature assignment³³ was simply made by comparison with Co(en)_3^{3+} , namely E_α dominant, +ve, at long wavelength and A_2 , minor -ve, at shorter wavelength. A single crystal assignment is required for this system, particularly since the electronic spectrum bears no resemblance to the visible absorption spectra of $\text{Co(diamine)}_3^{3+}$ complexes.

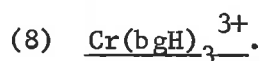
r) More important than this uncertainty in component assignment is the conclusion³³ that the $d-d$ rotatory strength arises from a twisted CoN_6 -core rather than from the inherent chirality of one coordinated cyclic tri-imine ligand. Although this interpretation may be correct, the wisdom of basing the argument on the failure⁵⁰⁵ to observe any CD maxima at wavelengths longer than 360 nm for the resolved monochelated (+)₅₄₆ $\text{Ni(TRL)(H}_2\text{O)}_3^{2+}$ ion is questionable when it is known^{21,23,24} that the CD spectra of Ni(dipy)_3^{2+} and

Ni(phen)_3^{2+} in the 400-700 nm wavelength range are also notoriously weak despite significant distortion of the NiN_6 -core from O_h symmetry ($\omega = 45.9, 48.2$: see Table 8.3).

Analysis of the geometry of the NiN_3O_3 -core in the structure⁴⁰⁴ of racemic $[\text{Ni}(\text{TRI})(\text{H}_2\text{O})_2\text{NO}_3]\text{NO}_3$ reveals the N_3 triangle to be twisted by $\omega = 57.5^\circ$ from an eclipsed position relative to the O_3 plane, the contraction being in the sense of the ligand chirality. To extend this geometry to the (+)₅₄₆ $\text{Ni}(\text{TRI})(\text{H}_2\text{O})_3^{2+}$ species in solution is tenuous but not unrealistic.

s) Not only is a single crystal study of $\text{Co}(\text{TRI})_2^{3+}$ desirable but also a thorough solution and solid state study of an active $\text{Co}(\text{TRI})\text{X}_3^{n+}$ species, preferably having $\text{X} = \text{NH}_3$. The $\text{Co}(\text{tame})_2^{3+}$ system presently being investigated by R.J. Geue was designed in the hope that the CoN_6 -core of the chiral species would show minimal trigonal twist, the gauche alkyl chains providing the sole chiral effect and thus affording a novel test of the R-model⁴¹ with all non-hydrogen atoms having $\theta < 54.74^\circ$, unlike $\text{Co}(\text{en})_3^{3+}$ where they all have $\theta > 54.74^\circ$. However, from the energy-minimization calculations³⁷² it seems that the repulsion between the amine hydrogen atoms of opposing trigonal faces is sufficiently strong to promote appreciable twisting of the two N_3 planes from a trigonal antiprismatic geometry ($\omega = 56.2^\circ$ in the Λ sense of ligand chirality, Table 8.8A) - it is not clear to what extent this

calculated distortion is limited by the $\text{NCoN} = 90^\circ$ angle bending potential.



t) Generally a configurationally active tris-bidentate transition metal complex also exhibits chiral distortion of the ML_6^- core from O_h symmetry and unless the chelated ligand expands the twist angle, ω , the CD correlations of the PK^- and E_α sign models are identical.

The absolute configuration of $(-)\text{Cr}(\text{biguanide})_3^{3+}$ has recently been determined³²³ as Λ by X-ray structure analysis of the least soluble $(+)$ -10-camphorsulphonic acid salt. Although the metal $d-d$ transitions are optically active the assignment³²³ of the CD components from the effect of PO_4^{3-} ion on the solution rotatory strengths seems doubtful since hydroxyl ion reportedly^{506,507} induces similar changes. The conclusion³²³ that a negative E_α component corresponds to a Λ (C_3) configuration about Cr(III) is confusing in view of earlier spectral assignments^{27,28} for $(+)\text{Cr}(\text{en})_3^{3+}$ and $(+)\text{Cr}(\text{ox})_3^{3-}$. Also, the assignment³²³ of a Λ absolute configuration to $(-)\text{Co}(\text{bgH})_3^{3+}$ on the basis of the ligand transitions is particularly questionable when both this and the $(-)\text{Cr}(\text{III})$ ion form least-soluble $(+)\text{bromo-camphor-}\pi\text{-sulphonates}$ of identical composition⁵⁰⁸ and the visible CD spectra of these $(-)$ ₅₈₉ enantiomers are almost superimposable.^{323,508} There is, however, some doubt as to the isomorphism of the least-

soluble camphor-sulphonates.⁴¹⁹

The aqueous solution CD components for the tris(biguanides), abstracted from ref. 508, are listed in Table 8.16. Since conflicting assignments^{323,508} have been made of the long wavelength CD components, a single crystal polarized absorption and CD study is required. The negative sign of the longest wavelength component for $\Lambda(-)$ $\text{Cr}(\text{bgH})_3^{3+}$ contradicts the empirical relationship observed for the Λ $\text{Co}(\text{III})$ and $\text{Cr}(\text{III})$ tris(diamine) complex ions.

TABLE 8.16 AQUEOUS SOLUTION CD COMPONENTS OF $(-)$ $\text{M}(\text{bgH})_3^{3+}$.

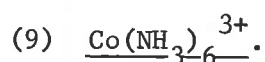
Complex ion	long wavelength T_1 band		ΣR_{T_1}	short wavelength T_2 band
	long λ component	short λ component		
?(-) $\text{Co}(\text{bgH})_3^{3+}$	513 (-3.49) ^a	455 (+4.68)	+	364 (-1.81)
$\Lambda(-)$ $\text{Cr}(\text{bgH})_3^{3+}$	522 (-2.73)	460 (+4.14)	+	375 (-1.28)

a. wavelength, nm: (and in parentheses, $\epsilon_l - \epsilon_r$).

u) The biguanide ligand gives planar six-membered chelate rings bidentate through nitrogen; the ligand angle α should be close to 90° . In the preliminary report of the structure of the $(-)$ $\text{Cr}(\text{bgH})_3^{3+}$ complex "all" the N-Cr-N angles were quoted³²³ as 90° within experimental error, conforming to ideal O_h symmetry of the CrN_6 -core if the six metal-donor atom bond lengths are identical. Unfortunately, difficulty in positioning all atoms of the large anions has delayed the structure refinement: although crystal coordinates were not

available it has been confirmed⁴¹⁹ that the geometry of the CrN_6 -core is octahedral and "unlikely to alter significantly in subsequent refinement cycles".

Faced with this rather unsatisfactory result we are forced to conclude that the CrN_6 -core is O_h symmetric with $\omega = 60^\circ$. Thus, if this geometry is maintained in aqueous solution, the observation of non-vanishing $d-d$ rotatory strength contradicts the PK-model (equation 7.1). Obviously an accurate structure analysis of a more suitable derivative, e.g. the active trichloride⁵⁰⁹ which crystallizes readily,⁵⁰⁸ is required.



v) The rotatory strength induced²⁹⁶ in the $d-d$ transitions of the ideally O_h symmetric $\text{Co}(\text{NH}_3)_6^{3+}$ ion on crystallization as the tri((+)-bromocamphor- π -sulphonate) was mentioned in section 6.3; until a structure analysis of this salt is made the role of the anion will be uncertain, i.e. whether it is dissymmetrically hydrogen bonded to the cation, whether it distorts the CoN_6 -sphere appreciably or whether it simply provides a non-centric crystal environment.

A similar induction of rotatory strength in the long wavelength ${}^1A_{1g} \rightarrow {}^1T_{1g}$ transition is observed^{510,511} on the addition of a large excess of (+)-tartrate or (+)-10-camphorsulphonate to an aqueous solution of $\text{Co}(\text{NH}_3)_6^{3+}$. The effect has been attributed^{510,511} to the formation of a chiral outer-sphere complex in which the tartrate ion

forms a "pseudo"-chelate ring by hydrogen bonding to adjacent ammine ligands. The inert Co(en)_3^{3+} ion gives⁵¹¹ a similar effect with these two anions which is not explicable in terms of a displacement of the isomer equilibrium,^{71,512} i.e. the common rationalization of the so-called Pfeiffer effect.²⁹³

(10) Co(III), Cr(III) N_6 Summary.

w) The α and ω values listed for the MN_6 -cores in Tables 8.1 and 8.2 are significantly different from the octahedral values in most cases; the θ values are generally closer to the O_h value and for some complexes the average values for the opposing triangular faces lie either side of 54.74° . This proximity of the polar angle in these complexes to the undistorted nodal value is reflected in the uncertainty of the experimentally determined trigonal splittings, K , of the Co(III) and Cr(III) tris(diamines). The opposing energy ordering of ${}^1E_\alpha$ and 1A_2 derived from the polarized absorption spectrum and the single crystal CD studies of Co(en)_3^{3+} remains a matter of concern; equally puzzling is the large trigonal splitting derived from the solution magnetic circular dichroism study ($K = -1500 \text{ cm}^{-1}$) compared with the vanishingly small values obtained from the low temperature single crystal studies. However, the change from K -ve to K +ve observed in the single crystal CD spectra of Co(en)_3^{3+} and Co(tn)_3^{3+} supports the crystal-field model (equation 7.3) as applied to the CoN_6 -core in isolation.

x) The PO_4^{3-} assignment of component symmetry has been shown to be unreliable and the tacit assumption of E_α dominance is particularly hazardous in cases where conformational and vicinal effects are probable, even though the second-order R-model attributes a much smaller rotatory strength to these chiral sources than to the chiral ligand distribution about the metal atom.

While it seems that there is no simple over-riding empirical relationship between the absolute configuration of D_3 metal complexes containing MN_6 ($M = \text{Co(III)}, \text{Cr(III)}$) chromophores and their signed $d-d$ rotatory strength, e.g.

- i) with the sign of the long wavelength CD component,
- ii) with the signed rotatory strength of the long wavelength T_1 magnetic-dipole allowed transition,
- iii) with the signed rotatory strength of the T_2 symmetric magnetic-dipole forbidden transition,

one or more of these correlations usually holds within a restricted class of complex.

There is no unambiguous evidence supporting the MN_6 -core distortion, represented by the PK-model, as the sole contributing factor to the rotatory strength of these transition metal chromophores, but some indication that such a chiral distortion may induce finite rotatory strength in the optically-active metal-centred $d-d$ transitions.

8.3.2 Co(III), Cr(III) O₆ Chromophores.(1) Chromium corundum: ruby.

a) α -Al₂O₃, corundum, conforms to the centric space group $R\bar{3}c$ (No. 167). Substitution of the Al³⁺ ions to varying degrees by transition metal ions gives certain gemstones (e.g. Cr³⁺ gives ruby; Fe²⁺, Fe³⁺ and Ti⁴⁺ together give blue sapphire) the colours of which depend not only on the nature of the "impurity" ion but also its relative concentration,^{217,259,513} the temperature²⁵⁹ and pressure.⁵¹⁴ This concentration dependence suggests,^{259,513} among other possibilities, a concerted distortion of the ideally hexagonal close-packed oxide ion lattice resulting from the inclusion of ions having larger ionic radii than Al³⁺. The hexagonal lattice constants change from $a = 4.763$, $c = 13.003$ Å for Al₂O₃,⁴⁰³ to $a = 4.770$, $c = 13.020$ Å for a synthetic ruby containing 5.2 mole % of Cr₂O₃,⁵¹⁵ to $a = 4.954$, $c = 13.584$ Å for Cr₂O₃.⁴⁰³ see also the compilation of lattice constants in ref. 516. The relevant features of the MO₆-core distortion in the pure corundum type structures were discussed in section 8.2.2.

The oxides and fluorides are the most ionic compounds of the transition metal ions and their spectral properties should be most suited to interpretation in terms of a point-charge crystal field model^{221,339} although the failure of such a model to satisfactorily explain the ⁴A₂ zero-field splitting of Cr³⁺ in ruby has been indicated.⁵¹⁷ We are not concerned with the hexafluorides in this

work since they are of little relevance to the tris(bidentate) complexes: several polarized spectral and magnetic studies of transition metal ions in various host fluoride lattices have been published.^{235,518,519} The availability of large well-formed natural crystals of the various gem corundums and the ability to synthetically produce the substituted structures, having varying concentrations of the impurity ions, to high degrees of crystal perfection has enabled a thorough study of the spectral properties of the impurity ions in a trigonally distorted MO_6 environment. The polarized optical spectra of Ti^{3+} , V^{3+} , Cr^{3+} , Mn^{3+} , Co^{3+} and Ni^{3+} in corundum single crystals have been studied by McClure²²¹ and interpreted in terms of a static C_3 point charge model.

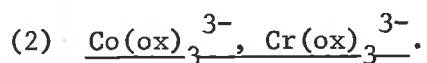
b) For Cr^{3+}/Al_2O_3 both the ${}^4A_{2g} \rightarrow {}^4T_{2g}$ and the ${}^4A_{2g} \rightarrow {}^4T_{1g}$ transitions were shown^{221,228} to split to give a higher energy A symmetric component, K ca. -500 cm^{-1} . For Co^{3+}/Al_2O_3 the trigonal splitting of both octahedral bands was smaller but of identical sign,²²¹ K ca. -360 cm^{-1} .^{219,221} It was concluded that the static *ungerade* distortion of the oxide ion lattice was the major intensity giving source, the appreciable intensity of the high energy ${}^4A_2 \rightarrow {}^4A_2$ Cr^{3+} component (π -polarization) indicating a chromophore symmetry lower than D_3 . Vibronic contributions to the band strengths at room temperature (and lower) were shown to be small and the complication of Jahn-Teller distortion of the $Cr^{3+} {}^4T_2$ excited state was not explicitly introduced

to the theoretical interpretation.²¹⁹

The Cr^{3+} ion in Cr_2O_3 is significantly displaced along the three-fold axis of the distorted octahedral interstice (Table 8.7 and section 8.2.2). Since the distortions of the five corundums are qualitatively similar it is reasonable to assume that the field experienced by the impurity ions in the Al_2O_3 host lattice is adequately described in terms of the distortions of the "pure" lattices.³³⁹ The M-O vectors to the shared triangular face subtend polar angles $< 54.74^\circ$ at the c axis while those to the opposing face subtend angles greater than the octahedral value; the average value of 55.12° indicates an insignificant average axial compression as does the inter-trigonal plane distance (2.264 \AA) compared to the value for ideal O_h symmetry (2.295 \AA) having $v_{\text{M-O}} = 1.988 \text{ \AA}$. However, it has been argued^{221,259,339} that the shorter of the two M-O vectors should dominate the spectral properties and in view of the inverse power of the radial dependence of the theoretical crystal-field treatments²¹⁹ this seems reasonable. For Cr_2O_3 $\Delta_{\text{M-O}} = 0.05 \text{ \AA}$ while $\Delta_{(h/2)} = 0.384 \text{ \AA}$ is perhaps more significant; the polar angles subtended by the long and short vectors are 48.86° and 61.38° respectively, the latter corresponding to a significant axial compression from O_h geometry.

c) But K is not simply indicative of the axial trigonal compression. Equation 7.3 gives only the polar angle dependence;

elsewhere^{411,520} it has been shown that the trigonal twist distortion ($\omega \neq 60^\circ$) of the ML_6 -core from D_{3d} symmetry contributes indirectly to the trigonal splitting of the triplet state via the off-diagonal matrix elements of the wave function, using the point charge crystal-field approximation. The axial distortion ($\theta \neq 54.74^\circ$) exerts a more direct influence through the diagonal matrix elements but where such distortion is small the trigonal splitting pattern is more correctly interpreted in terms of ω , e.g. as for $[Ti(urea)_6].I_3$ and its vanadium analogue.^{262,411} Thus, although both the corundum^{403,434} and hexakis(urea)^{263,411} structures are centric (R_{3c}^-), individual ML_6 -cores in both are appreciably twist distorted (Tables 8.7 and 8.8A). However, the trigonal twist of the "oxygen faces" in the corundum lattice has seldom been considered in discussions of the spectral properties of these structures.



d) Polarized crystal absorption²⁰⁷ and CD spectra^{27,184} have been recorded for these strongly absorbing anions diluted in the colourless, trigonal $NaMg[Al_2O_3].9H_2O$ host lattice. The major intensity giving source was again considered to be the static axial distortion of the MO_6 -core rather than vibronic coupling to *ungerade* modes.^{†6} For Cr^{3+} the 4A_1 component occurred at lower frequency

^{†6} Both the single crystal polarized absorption spectrum²⁰⁷ and the solution MCD²⁴⁹ support this interpretation.

than 4E_g ($K = +300 \text{ cm}^{-1}$ from the polarized absorption spectrum²⁰⁷) whereas for Co(ox)_3^{3-} the energy ordering of 1E_g and 1A_2 under the long wavelength octahedral band was reversed^{207,237} ($K = -150 \text{ cm}^{-1}$). The single crystal CD assignments^{27,184} confirmed this energy ordering and showed positive rotatory strength for the E_g components of (-) Co(ox)_3^{3-} and (+) Cr(ox)_3^{3-} ; the present X-ray work has confirmed^{87,93} the Λ configuration predicted for both complex ions.

e) The solution CD spectra^{27,184} (CD spectra of these and other Co(III), Cr(III) O_6 complexes summarized in Table 8.17) of these ions have been discussed at length in Chapter 5 and will not be reconsidered in detail here. For (-) Co(ox)_3^{3-} a large single CD peak only is observed in the solution spectrum under the envelope of the ${}^1A_{1g} \rightarrow {}^1T_{1g}$ band while three components occur under the higher energy ${}^1A_{1g} \rightarrow {}^1T_{2g}$ band; the long wavelength positive solution peak has a rotatory strength ca. 1/10 that of the 1E_g peak in the oriented crystal spectrum and is only marginally shifted in wavelength (620 nm, crystal; 617 nm solution) consistent with a small trigonal splitting.²⁷ The single crystal assignment gives an 1E_b component of the same sign as 1E_g but ca. 1/10 its rotatory strength; the tentative solution assignment²⁷ is inconsistent. The origin of the other two minor components at slightly higher frequency remains unexplained since solution studies^{185,186} have indicated negligible contamination by lower symmetry species.

The solution ${}^4E_\alpha$ component of (+) $\text{Cr}(\text{ox})_3^{3-}$ has ca. 1/3 the rotatory strength of the single crystal band but the rotatory strength of the 4E_b component is unchanged; the 4E_b component is negative in apparent contradiction of equation 7.5. The ${}^4E_\alpha$ component shifts 9 nm to shorter wavelength from crystal to solution consistent with a partial cancellation of the longer wavelength 4A_1 component.

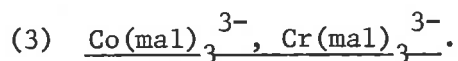
f) The crystal structure of $\text{NaMg}[\text{Al}(\text{ox})_3] \cdot 9\text{H}_2\text{O}$ has not been refined although it has been shown²⁰⁷ that the lattice conforms to the trigonal space group $P\bar{3}1c$ ⁺⁷ with the three-fold axes of the complex ions aligned parallel to the crystallographic *c* axis; the metal atoms occupy sites of 32-point symmetry.

Few structures of tris(oxalate) ions have been published and of the four listed in Table 8.5 least-squares esd's in the bond lengths and angles are available only for the poorly refined KNIPHECOOX structure of Chapter 4. Despite this lack of accurate structural data, the MO_6 -cores of these tris(five-membered ring) complexes reveal

⁺⁷ In this centric space group there must be equal numbers of Λ and Δ chiral tris(oxalate) ions. By substituting only one enantiomer of the "impurity" ion, (-) $\text{Co}(\text{ox})_3^{3-}$ say, a crystal containing $\Lambda(-)\text{Co}(\text{ox})_3^{3-}$ and an excess of $\Delta(?)\text{Al}(\text{ox})_3^{3-}$ ions is obtained. The assumption that any optically active transitions of $\text{Al}(\text{III})$ lie at too high a frequency to interfere with those of $\text{Co}(\text{III})$ is implicit in the single crystal CD studies.

a consistent distortion from O_h symmetry; $\alpha < 90^\circ$, $\theta > 54.74^\circ$, $\omega < 60^\circ$ but β is inconsistent. A suggestion²⁰⁷ that the negative value of K for Co(ox)_3^{3-} reflects an α angle greater than 90° is untenable and comparison with the less certain trigonal splitting parameters³⁵ of the Co(en)_3^{3+} and Cr(en)_3^{3+} ions^{192,245,251,252} suggests that for tris(complexes) having $\alpha < 90^\circ$, or more correctly $\theta > 54.74^\circ$, $K_{\text{Cr(III)}}$ is positive while $K_{\text{Co(III)}}$ is negative,^{70,191} although this is certainly at variance with the predictions of the crystal-field model. Furthermore, the sign reversal from Cr(ox)_3^{3-} to Cr_2O_3 is unexplained.

D_3 complexes having $\omega < 60^\circ$ provide no unique test of the PK-model (equations 7.1 and 7.2) as opposed to the E_α -sign model; the failure to observe E_α and E_b components of the same sign for (+) Cr(ox)_3^{3-} is contrary to the prediction of the second-order R-model but is in agreement with a similar finding for the tris(en) and tris(pn) Cr(III) complexes.



g) The complex ions (+) Cr(mal)_3^{3-} and (-)₆₀₀ Co(mal)_3^{3-} have both been assigned a Λ absolute configuration on the basis of the X-ray structure of CRMALTCOPN (Chapter 2).^{93,187} The solution and solid state CD spectra have been discussed at length in Chapter 5 in terms of E and A trigonal components.

The trigonal component ordering for Cr(mal)_3^{3-} was derived from

a polarized absorption spectrum²⁹ of the anion diluted in a $(\text{NH}_4)_3[\text{Fe mal}_3]$ host lattice of undetermined structure; it was argued²⁹ from comparison of the polarized spectrum of this matrix with that of $\text{Cr}(\text{ox})_3^{3-}$ in the trigonal $\text{NaMg}[\text{Fe ox}_3] \cdot 9\text{H}_2\text{O}$ host lattice that the three-fold axes of the $\text{Cr}(\text{mal})_3^{3-}$ ions were also aligned parallel, "or nearly so", to a crystal optic axis. It is, of course, unrealistic to suggest that the two complex salts are isostructural. The extinction coefficient ratio ($\epsilon_\pi/\epsilon_\sigma = 1.4$) for the ${}^4A_2 \rightarrow {}^4T_2$ long wavelength Cr(III) band agreed well with that found for $\text{Cr}(\text{ox})_3^{3-}$, 1.46, in the $\text{NaMg}[\text{Fe ox}_3] \cdot 9\text{H}_2\text{O}$ crystal.^{29,207} Unfortunately the high energy ${}^4A_2 \rightarrow {}^4T_1$ $\text{Cr}(\text{mal})_3^{3-}$ band was not interpretable because of strong overlap by the iron bands.

K was -180 cm^{-1} with ${}^4E_\alpha$ lying lower in energy than 4A_1 , opposite the splitting order found²⁰⁷ for $\text{Cr}(\text{ox})_3^{3-}$. The reversed component ordering and the increase in the absolute magnitude of K from $\text{Cr}(\text{mal})_3^{3-}$ to $\text{Cr}(\text{ox})_3^{3-}$, $K = +300 \text{ cm}^{-1}$, are consistent with greater trigonal distortion in the tris(oxalate) ion and a change from axial elongation ($\theta < 54.74^\circ$) to axial compression ($\theta > 54.74^\circ$). Hatfield²⁹ correctly anticipated a ligand angle, $\alpha > 90^\circ$, in the tris(malonato) Cr(III) ion.

h) Some doubt remains concerning the validity of this single crystal assignment for $\text{Cr}(\text{mal})_3^{3-}$. $\text{Al}(\text{mal})_3^{3-}$ would have been a more suitable diluent ion, allowing the polarization of the high energy

${}^4A_2 \rightarrow {}^4T_1$ band to be measured, thus permitting an empirical assessment of the importance of vibronic coupling to the $d-d$ intensity mechanism.

The structure, or at least the space group and unit cell data, of the host lattice should be determined; if the unit cell is not trigonal or hexagonal with the pseudo- C_3 axes of the complex ions aligned parallel to the crystallographic c axis, the full crystal structure is required since, in order to derive meaningful polarization intensity ratios, the inclination of the pseudo-symmetry axes of the complex ion to the crystal optic axes must be known.

The CD spectrum of $\text{Cr}(\text{mal})_3^{3-}$ in the $(\text{NH}_4)_3[\text{Fe mal}_3]$ host lattice has not been recorded and until it is there remains the possibility that, as with $\text{Co}(\text{en})_3^{3+}$, the component energy ordering and the degree of trigonal splitting determined by the polarized crystal spectral method and the CD technique will not correspond. This query becomes even more significant when it is seen that the long wavelength solution CD component,^{27,28,240} assigned ${}^4E_\alpha$ from the polarized crystal spectrum, has ca. 1/2 to 1/3 the rotatory strength of the 4A_1 component, whereas the E_α component is more usually considered dominant. Conformational lability of the six-membered Cr-malonate rings in solution could be responsible; the ${}^1E_\alpha$ and 1A_2 components for $\text{Co}(\text{mal})_3^{3-}$ have approximately similar rotatory strengths (Table 8.17).

- i) As can be seen from the geometry of the energy minimized

$\text{Co}(\text{tn})_3^{3+}$ complex ions, the distortion of the ML_6 -core reflects the detailed ring conformation; core angular distortion parameters were calculated for the C_3 and D_3 symmetric complex ions only, although conformationally mixed species are feasible. The malonate ion forms analogous six-membered ring complexes, the important difference from tn being that the carbon atom (carboxyl) attached to the donor oxygen atom is sp^2 -planar whereas that attached to the donor nitrogen of tn is sp^3 -tetrahedral. Given this further restriction in the malonate case it is still possible for the isolated chelate ring to adopt a variety of conformations including mirror-symmetric boat and chair forms and λ and δ two-fold symmetric skew conformations; in addition, partially flattened conformers are also attainable, these being energetically prohibitive for a bidentate tn ligand.

With this wide variety of possible conformations and in the absence of any assessment of their relative energies it is not realistic to consider the solution conformation to be precisely that found in the CRMALTCOPN structure refinement (Chapter 2). It was previously indicated⁹³ that the angular parameters characterizing the CrO_6 -core of $\Lambda(+)$ $\text{Cr}(\text{mal})_3^{3-}$ in CRMALTCOPN offered support, albeit at a low-level of significance, for the PK-model of optical activity in D_3 transition metal complexes. However, on alteration of the weighting scheme and subsequent refinement to convergence, the CrO_6 -core became more elongated axially; as indicated earlier, the resulting value of ω , $60.19 (45)^\circ$, was insignificantly different

from the D_{3d} nodal value of 60° . Thus the CrO_6 -core distortion can no longer be regarded as supporting the PK-model; indeed, analogous to $Cr(bgH)_3^{3+}$, the PK-model predicts zero optical activity in the $d-d$ transitions.

In section 5.3 the reduced rotatory strength of the $Cr(mal)_3^{3-}$ ${}^4A_2 \rightarrow {}^4T_2$ band relative to that of $Cr(ox)_3^{3-}$ was mentioned in reference to the "ring size effect". However, it could equally well be that the ca. 1/10 reduction reflects a more closely D_{3d} (or C_{3v}) symmetric CrO_6 -core in the former case and that *ungerade* distortion of this core does make a significant, as opposed to "sole", contribution to the $d-d$ transition rotatory strength, although it should be re-emphasized that the rotatory strength of the "so-called" E_α component for both $Cr(mal)_3^{3-}$ and $Co(mal)_3^{3-}$ relative to that of E_α *pn* (see Chapter 5) is increased in the microcrystalline CD spectrum (where the MO_6 -core is closely D_{3d}) compared to the ratio observed in aqueous solution. Since the malonate rings in the CRMALTCOPN structure adopt an almost mirror symmetric flattened chair (or boat) conformation any conformational contribution to the $Cr(III)$ O_6 region of the diastereoisomer spectrum must be minimal.

j) $\theta = 53.47^\circ$ reflects a small axial elongation of the CrO_6 -core of $Cr(mal)_3^{3-}$ in the CRMALTCOPN structure from octahedral geometry. Because of band overlap in solution CD spectra the precise component peak frequencies can be determined only by Gaussian analysis

and hence the magnitude of the trigonal splitting is not directly comparable with that derived from oriented single crystal determinations. For instance, for $\text{Cr}(\text{mal})_3^{3-}$ the aqueous solution CD spectrum gives K ca. -2190 cm^{-1} and for $\text{Co}(\text{mal})_3^{3-}$, K ca. $+1850 \text{ cm}^{-1}$, without Gaussian analysis. The reversal in component energy ordering, i.e. in the sign of K , is in agreement with Burer's correlation¹⁹¹ for D_3 complexes containing non- π -bonding ligands.

k) The CRMALTCOPN structure, or that of the analogous Co(III) derivative, should be re-refined using an excess of accurately determined diffractometer intensities. The polarized single-crystal absorption spectrum and the single crystal CD spectrum must be determined for the known structure, in view of the probable conformational lability in solution.

(4) Co(acac)₃, Cr(acac)₃.

1) Unlike the six-membered M-malonate chelate ring the M-acac ring should remain closely planar due to π -delocalization. While this ring planarity and consequent mm -symmetry means there can be no ring conformational contribution to the optical rotatory strength of chiral $\text{M}(\text{acac})_3$ complexes, the conjugated ligand introduces additional features not allowed for by the simple electrostatic crystal field model.^{219,224,254} The interligand coupling resembles that used in explaining the strong rotatory power of the $\pi \rightarrow \pi^*$ ligand transitions

in the tris(phen)- and tris(dipy)M(II) and M(III) complexes;^{21,22,199} the absolute configuration of (+) Si(acac)₃⁺ has been predicted to be Λ on the basis of the exciton theory.^{333,521}

The polarized-crystal spectra of M(III)(acac)₃, (M(III) = Co, Cr, Mn, Fe, Ti, V), in a colourless Al(acac)₃ host lattice were determined by Piper et al.^{237,239,242} The pure Co,^{85,86} Cr^{112,393} and Al⁸⁵ complexes crystallize in the monoclinic space group P_{2_1}/c but the precise geometric distortion of the CoO₆-core is significantly different from that of the MO₆-cores of the other two, particularly in the α and ω values (see Table 8.6). N.B.—The Mn(acac)₃ structure⁸⁶ determined by Morosin and Brathovde is reputed⁴²⁹ to be the structure of Co(acac)₃ — see the notes appended to Table 8.6.

m) Despite complications due to overlapping charge-transfer bands and the unfavourable alignment of the pseudo-C₃ axes of the tris(bidentate) molecules with respect to the optic axes of the monoclinic host lattice, Piper et al were able to derive the following^{237,242} trigonal splitting parameters for the long wavelength $d-d$ transition (T_1 symmetric); Co(acac)₃ $K' = +600$, Cr(acac)₃ $K' = +530 \text{ cm}^{-1}$. The ionic model fails to predict the larger trigonal splittings observed for the tris(acac) complexes relative to the tris(ox) ions or the appreciable intensity of the higher energy T_2 symmetric band in the π -polarization for Cr(acac)₃: it was concluded²³⁷ that this failure of the point-charge model was due to the greater π -

covalency of the acac ligand. Barnum⁵²² and Hanazaki et al²²⁴ showed that the splitting in the $M(\text{acac})_3$ spectra was best attributed to metal t_2 /ligand π -orbital interaction, whereas for the tris(oxalato) complexes the splitting is adequately described by the trigonal electrostatic field approximation.²³⁶

n) Since the ionic crystal field model fails to predict the sign and magnitude of the trigonal splitting parameter for the T_1 symmetric octahedral band of Co and $\text{Cr}(\text{acac})_3$, it is probably naïve to even consider applying it to a description of the optical rotatory power.

As indicated in Table 8.6 several structures of racemic $M(\text{III})(\text{acac})_3$ complexes have been reported. However, their ionic neutrality makes complete optical resolution difficult and although several chromatographic resolutions have been achieved^{150,264,523} the absolute configuration of $\text{Co}(\text{acac})_3$ was only recently determined.⁵²⁴ The Bijvoet technique of anomalous X-ray dispersion was used⁵²⁴ to show that $(-)_546 \text{Co}(\text{acac})_3$, as a "quasiracemate" with $\text{Al}(\text{acac})_3$, has the Λ absolute configuration: the solution CD spectrum⁵²⁴ showed a dominant positive high energy component under the ${}^1A_{1g} \rightarrow {}^1T_{1g}$ band envelope and this was assigned as E_α on the basis of the positive K value determined from the polarized crystal spectrum.²⁴²

The average ω value for $\text{Co}(\text{acac})_3$ from the two independent structure determinations^{85,86} listed in Table 8.6 is 68° , a highly

significant distortion from the D_{3d} value of 60° (given that the esd in α is 0.2° and 0.6° for the two structures). Furthermore, for α ca. 97° , the electrostatic repulsion model outlined in section 8.2 predicts ω ca. 69.5° and the distortion parameters defining the CoO_6 -core in the pure racemic structure can be expected to change only marginally in the $\text{Al}(\text{acac})_3$ lattice or in solution.

Before summarizing the results for the five- and six-membered ring tris(bidentate-oxygen chelate) complexes there is one other tris(β -diketone) which merits discussion.

(5) *trans*-Cr((+)atc)₃.

o) (+)-3-acetylcamphorate ion forms six-membered planar chelate rings (with suitable transition metals) in which the ligand π -electron delocalization pattern should be identical with that of an M-acac ring. The substituents external to the chelate rings confer differing degrees of favourability on the four possible isomers (2 optical x 2 geometric) of the tris((+)atc) complexes due to steric crowding.¹¹⁴ With the absolute configuration of the camphor moiety already known,⁵²⁵ the absolute configuration of (+) Cr((+)atc)₃ was assigned as Λ by internal comparison and confirmed by analysis of Friedel pairs.¹¹⁴

The high energy dominant positive CD component under the long wavelength absorption band was assigned E_α symmetric by comparison with the polarized crystal spectra of $\text{Co}(\text{acac})_3$ and $\text{Cr}(\text{acac})_3$, (see

above), but details of the absorption spectrum were not given.¹¹⁴ Possible vicinal contributions to the $d-d$ rotatory strength from the active β -diketone ligands were not explicitly considered, nor were possible complications due to the strong charge-transfer and intra-ligand $\pi \rightarrow \pi^*$ transitions. The long wavelength CD spectrum is similar to that of $(-)_546 \text{Co}(\text{acac})_3$.⁵²⁴

p) From Table 8.6 it can be seen that the distortion angles characterizing the CrO_6 -core in $(+) \text{Cr}((+)\text{atc})_3$ are quite similar to those derived from racemic $\text{Cr}(\text{acac})_3$ —Morosin:¹¹² the β angle is slightly smaller and α is slightly larger in the $(+) \text{atc}$ derivative; consequently the trigonal twist angle, ω , is some 1.2° larger ($\omega = 62.7^\circ$). The electrostatic repulsion model (section 8.2) predicts $\omega = 62.6^\circ$ for $\alpha = 92^\circ$; this, together with the ligand rigidity, suggests that the CrO_6 -core geometry in aqueous solution will not be very different from that in the monoclinic (P_{21}) structure.^{114,115}

(6) Co(III), Cr(III) O_6 Summary.

q) Mindful of the above reservations the following table (Table 8.17) correlating the structural and spectral properties of the tris(bidentate) MO_6 type complexes can be presented.

The empirical trigonal splitting parameters, K , determined for the axially contracted $\text{Cr}(\text{ox})_3^{3-}$ ion and the axially elongated $\text{Cr}(\text{mal})_3^{3-}$ ion are inconsistent with those determined for the

TABLE 8.17 RELEVANT STRUCTURAL AND CD DATA FOR MO₆-CORES OF Λ TRIS-BIDENTATE Co(III), Cr(III) COMPLEXES.

<i>Complex</i>	4A_1 or 1A_2	E_α	<i>ref. 1</i> ^a	<i>ref. 2</i> ^b	ω	θ	<i>ref. 3</i> ^c
(-) Co(ox) ₃ ³⁻	(ca. 16.35)	16.2 (+3.30) ^d	27,207	27	54.1	56.4	87
(+) Cr(ox) ₃ ³⁻	15.9 (-0.58)	18.1 (+2.83)	27,207	27	50.3	56.3	384
(-) ₆₀₀ Co(mal) ₃ ³⁻	15.1 (+1.06)	16.9 (-1.00)	Ch.5,29	Ch.5	-	-	-
(+) Cr(mal) ₃ ³⁻	18.3 (+0.29)	16.1 (-0.12)	29	Ch.5	60.2	53.5	Ch.3
(-) ₅₄₆ Co(acac) ₃	ca. 15 (-2) ^e	ca. 18 (+5) ^e	237,242	524	67.9	52.8	85
(+) <i>trans</i> -Cr((+)atc) ₃	16.3 (-1.8)	18.6 (+3.7)	114,237	114	62.7	54.5	115

a. *ref. 1* = assignment of trigonal components.

b. *ref. 2* = reference for CD data.

c. *ref. 3* = reference for structural data (see section 8.1 also).

d. component frequency, $\times 10^{-3} \text{ cm}^{-1}$ (in parentheses, $\epsilon_L - \epsilon_R$).

e. these CD peak values from graph only.

corresponding Co(III) ions and the axially elongated Co(III) and Cr(III)(acac)₃ complexes. The negative splittings determined for Co/Al₂O₃ and Cr/Al₂O₃ are consistent with axial compression of the MO₆-core but this core is grossly distorted from D₃ symmetry.

The Co and Cr(mal)₃³⁻ absolute configurations contradict the simple empirical model which predicts E_{α} positive for a Λ tris(bidentate) complex and, within the limits of the accuracy of the structure determination, the observed activity of the Cr(mal)₃³⁻ ion in the microcrystalline CD spectrum of CRMALTCOPN contradicts the first order PK-model. The absolute configurations of the tris(β -diketone) complexes are at variance with the PK-model which predicts, by comparison with $\Lambda(+)$ Co(en)₃³⁺, E_{α} negative for a Λ configuration having a twist expansion of the ML₆-core about the C₃ axis.

8.3.3 MS₆ Chromophores.

(1) (+) Co(thiox)₃³⁻.

a) In discussing the trigonal splitting of the triply-degenerate excited octahedral states of the tris(ox), tris(en) and tris(acac) complexes Piper and Carlin intimated²³⁷ that the polar placement of the donor atoms was in all cases so close to octahedral, i.e. $\theta = 54.74^{\circ}$, and so inaccurately determined by the structural refinements then available that the sign of K was indicative of an axially compressed chromophore in all cases. This they considered to reflect not so much the distortion of the ML₆-core from O_h but rather the

appreciable electron density of the ligand backbone, these atoms having $\theta > 54.74^\circ$: obviously this interpretation corresponds to the R-model which attributes all ligand atoms with a smaller or greater electronic role depending on their proximity to the angular nodal planes and their relative electrostatic charges.

b) However, the observed reversal of the trigonal component energy ordering from Cr(ox)_3^{3-} to Cr(mal)_3^{3-} and from Co(en)_3^{3+} to Co(tn)_3^{3+} suggests that the tris(β -diketonates) merit separate consideration (see section 8.3.2). The (+) Co(thiox)_3^{3-} ion had been assigned the Λ configuration on the basis of solution CD studies^{27,134} in which the energy ordering of the ${}^1E_\alpha$ and 1A_2 components was reversed from that of Co(ox)_3^{3-} . Comparison of expected C-S and C-O bond lengths⁷⁴ in "idealized" thiox and ox ligands suggested that whereas the latter ligand should always subtend an angle $\alpha < 90^\circ$ at the chelated metal, the Co(III) thiox five-membered ring should have α ca. 90° .

Leaving aside the complication of increased π -delocalization in the Co(thiox)_3^{3-} ion, the reversed component energy ordering should be understandable in terms of a change in θ from $> 54.74^\circ$ for Co(ox)_3^{3-} to $< 54.74^\circ$ for Co(thiox)_3^{3-} , on the basis of equation 7.3. For $\alpha = 90^\circ$ the r^{-1} electrostatic repulsion model (section 8.2) predicts O_h symmetry for the "isolated" ML_6 -core; as pointed out already, however, the ligand backbone atoms can be expected to

promote a small distortion in the direction of a D_{3h} trigonal-prismatic geometry for a tris-complex. Therefore, although α for $\text{Co}(\text{thiox})_3^{3-}$ should be closely 90° , this supplementary distortion should give an axially elongated ($\theta < 54.74^\circ$) twist contracted ($\omega < 60^\circ$) CoS_6 -core. The structure of CADCOTHIOX (Chapter 3) verifies that this is indeed the case (Table 8.5 and section 8.2). For $\text{Co}(\text{thiox})_3^{3-}$ $\alpha = 89.68 (15)^\circ$, $\theta = 53.79^\circ$, $\omega = 56.98^\circ$; the esd's in θ and ω are of the same order as for α and the differences from the O_h values are significant.

c) This change in K is not the only point of relevance of the $\text{Co}(\text{thiox})_3^{3-}$ ion. Since for both $\text{Co}(\text{ox})_3^{3-}$ and $\text{Co}(\text{thiox})_3^{3-}$ $\omega < 60^\circ$, the E_α component of the long wavelength T_1 symmetric octahedral band should have a positive rotatory strength for the Λ configuration by comparison with (+) $\text{Co}(\text{en})_3^{3+}$, on the basis of the first-order trigonal crystal-field model (eqns. 7.1 and 7.2); this is as found.^{27,134} Thus both the energy ordering of the trigonal components and the signed rotatory strengths of the E_α components in the CD spectra support the PK-model.

However, the electrostatic point-charge model must be extended to second order to predict the signed net rotatory strength of the T_1 band (eqns. 7.4 and 7.5). Although equation 7.4 should be applied to the trigonal-dihedral complex *in toto*, it can be applied to the ML_6 -core in isolation to test the validity of the PK-model which

attributes the rotatory strength of the $d-d$ transitions to the chiral distortion of the first-coordination sphere alone. The correlation of R''_{netT_1} with R'_{E_a} and K is given in Table 7.1 but note that the signs R''_{netT_1} were derived for equations 7.2 and 7.3 as written: using $\Lambda(+)\text{Co(en)}_3^{3+}$ as reference, however, i.e. geometry no. 1 of Table 7.1, R'_{E_a} +ve, K -ve and the signs of R'_{E_a} and K for all four classes of distortion (Table 7.1) invert from + to - (or - to +) but the signs of R''_{netT_1} are unchanged since it is the negatively signed product of the *gerade* (K) and *ungerade* (R'_{E_a}) functions.

Co(ox)_3^{3-} corresponds to geometry 1 and Co(thiox)_3^{3-} to geometry 3 of Table 7.1. Solely on the basis of the ML_6 -core distortion, therefore, R''_{netT_1} should be +ve for $\Lambda\text{Co(ox)}_3^{3-}$ and -ve for $\Lambda\text{Co(thiox)}_3^{3-}$; the experimental²⁷ values are +3.30 and +2.6 respectively contrary to the prediction from the second-order equation 7.4. This observed positive net rotatory strength correlates with the Λ absolute configuration, i.e. equation 7.4 taken over the whole complex, for the M(ox)_3^{3-} , M(mal)_3^{3-} ($\text{M} = \text{Co(III)}, \text{Cr(III)}$), Co(acac)_3 , Cr((+)atc)_3 and Co(thiox)_3^{3-} complexes irrespective of the precise distortion of the ML_6 -core or ligand π -bonding effects: this relationship does not appear to hold for the $\text{Co(en)}_3/(\text{tn})_3$ system however (see section 8.3.1).

(2) Six-membered ring complexes.

d) Preliminary communications of the $\text{Rh(sacsac)}_3^{402}$ and

$\text{Fe}(\text{sacsac})_3$ ³⁹⁹ structures have been published; their MS_6 -core distortion parameters are presented in Table 8.6. $\text{Co}(\text{sacsac})_3$ ⁵²⁶ and $\text{Cr}(\text{sacsac})_3$ ⁵²⁷ have been synthesized but their crystal structures have not yet been reported: none of these four neutral complexes has so far been resolved.

As with the ox/thiox ligands the dithioacetylacetonate ligand promises a larger value of the ligand angle, α , than is the case in the $\text{M}(\text{acac})_3$ complexes. The effect is accentuated in the case of the $\text{Fe}(\text{III})(\text{acac})_3/(\text{sacsac})_3$ complexes by the change from high spin^{258,431,528} ($r_{\text{Fe}} = 0.645 \text{ \AA}$)⁵²⁹ to low spin^{399,530} ($r_{\text{Fe}} = 0.55 \text{ \AA}$)⁵²⁹ $\text{Fe}(\text{III})$ respectively: for $\text{Fe}(\text{acac})_3$ the relevant distortion parameters are, with those for $\text{Fe}(\text{sacsac})_3$ in parentheses $-\alpha = 1.992$ (2.254) \AA , $b = 2.744$ (3.269) \AA , $\alpha = 87.06^\circ$ (92.98 $^\circ$).

(3) Four-membered ring complexes.

e) Tris(four-membered ring) complexes bidentate through sulphur have received increasing attention recently with the measurement of single crystal polarized absorption spectra,^{241,243,383} magnetic susceptibilities^{380,531} and the accurate determination of several relevant structures. The greater distortion of the ML_6 -core from O_h symmetry in these complexes than that found for the larger ring complexes makes them ideal for testing the validity of the crystal-field model for the trigonal splitting of degenerate ground and excited states. None of these complexes has been resolved as yet

so we are concerned only with equation 7.3.

The spectral interpretation is usually made solely in terms of the polar angle, θ , although the trigonal twist of the ML_6 -core contributes indirectly to K (see section 8.3.2) and may make the dominant contribution to the trigonal splitting in cases where θ ca. 54.74° . Tomlinson²⁴¹ has introduced the ligand tilt relative to the C_3 axis, i.e. $90-\beta$, as an independent variable but concluded that changes in this angle have little effect on the energy ordering of the trigonal components. Furthermore, Tomlinson indicated that the point-charge model of the MS_6 -cores of these tris-complexes having $\alpha < 90^\circ$ correctly predicted an A term lower in energy than the E component: this agrees with the more usual discussion in terms of θ , i.e. K positive for axial trigonal compression, but is, of course, at variance with the single crystal CD assignments^{27,192} for $Co(en)_3^{3+}$ and $Co(ox)_3^{3-}$.

f) The angular distortion parameters of several tris(four-membered ring) complexes are given in Table 8.4. The trigonal splitting parameters²⁴¹ of some relevant Co(III) and Cr(III) complexes (diluted as 1-10% "impurities" in the corresponding monoclinic indium host lattices) are collected in Table 8.18.

TABLE 8.18 TRIGONAL SPLITTING IN SOME MS_6 CHROMOPHORES.

Complex	$K, \text{ cm}^{-1}$
$\text{Cr}(\text{dtc})_3$	+500
$\text{Cr}(\text{etp})_3$	+150
$\text{Cr}(\text{eps})_3^a$	+400
$\text{Co}(\text{dtc})_3$	+200
$\text{Co}(\text{etp})_3$	+150

a. eps = 0,0'-diethylphosphorodiselenate
(as for etp but with both S donors replaced by Se).

In spite of the C_2 symmetry of the complexes in the lattices used for measuring the polarized absorption spectra, the polarization of the absorption bands conforms closely to that expected for D_3 symmetry and the small temperature dependence of the band intensities confirms a static rather than vibronic mechanism.^{241,243}

The negative trigonal splitting ($K = -130 \text{ cm}^{-1}$) observed³⁸³ for $\text{V}(\text{etp})_3$ was inexplicable²⁴¹ on the basis of α since the ligand angle is significantly less than 90° for all these complexes (Table 8.4). However, comparison of the average polar angles for these complexes suggests an explanation for this apparent anomaly in terms of equation 7.3: for all $\text{Co}(\text{III})$ and $\text{Cr}(\text{III})$ derivatives in Table 8.4 $\theta > 54.74^\circ$ whereas for $\text{V}(\text{etp})_3$ $\theta = 54.09^\circ$ (value for no. 15), ca. 3σ to the low side of the nodal value. Note, however, that Lebedda and Palmer²⁴³ have found K positive for all three $\text{M}(\text{etp})_3$ complexes

(M = Co(III), Cr(III), V(III)) from the polarized crystal spectra of the complexes again diluted in the indium host lattice;

$V(etp)_3$, K ca. $+40 \text{ cm}^{-1}$, $Co(etp)_3$ $+590 \text{ cm}^{-1}$, $Cr(etp)_3$ $+670 \text{ cm}^{-1}$.

The differences between the two independent determinations are disturbing.

g) The solution MCD spectrum⁵³² of $Cr(etp)_3$ showed the ${}^4T_{2g}$ band to be trigonally split by K ca. $+480 \text{ cm}^{-1}$ but MCD could not resolve the trigonal splitting in the $Cr(exan)_3$ or $Cr(dtc)_3$ complexes. This is surprising because the dtc and exan ligands subtend smaller α angles at the metal (Co(III), Cr(III)) than does etp. Since the inclination, β , of the ligand planes is similar in these tris(complexes) the MS_6 -cores of the dtc and exan complexes should show a greater trigonal compression than those of the corresponding etp derivatives.

h) The assignment of $K > 0$ for trigonal axial compression is at variance with the $Co(ox)_3^{3-}$ and $Co(thiox)_3^{3-}$ assignments where for the former $\alpha < 90^\circ$, $\theta > 54.74^\circ$, $K = -150 \text{ cm}^{-1}$ and for the latter α ca. 90° , $\theta < 54.74^\circ$, $K > 0$.

Resolution²¹⁴ of $Co(CO_3)_3^{3-}$ indicates that the complex ion most probably comprises three bidentate carbonate ligands, i.e. three four-membered chelate rings. However, it is not possible on the basis of the published diastereoisomer CD spectrum to make a definitive assignment of the ${}^1E_\alpha$ and 1A_2 trigonal components (see section 5.3). Analogous to the tris(four-membered ring) complexes bidentate through

sulphur, the Co-CO_3^{2-} ring should have α appreciably less than 90° , possibly of the order of 70° ($\alpha_{\text{OCoO}} = 68.8 (5)^\circ$ in $\text{Co}(\text{tn})_2(\text{CO}_3)^+$, ref. 94) for which value θ is necessarily always greater than 54.74° irrespective of the value of β . This tris-complex ion therefore affords a unique test of the crystal-field model, provided a valid assignment of the trigonal components can be made.

8.3.4 Miscellaneous Chromophores.

a) Although it seems that the PK-model alone cannot account for the optical activity of tris(bidentate) transition metal complexes this does not imply that an *ungerade* distortion of the first coordination sphere from holohedric symmetry makes zero contribution to the rotatory strength of the $d-d$ transitions.

The case of $\text{Co}(\text{NH}_3)_6^{3+}$ crystallized with (+) bromo-camphorsulphonate²⁹⁶ was mentioned in section 8.3.1. Without an accurate crystal structure analysis, however, it is not possible to identify the source of the electronic transition rotatory strength although both distortion of the CoN_6 -core and the asymmetry of the crystal environment beyond the first coordination sphere are likely originators.

b) A similar induction of non-vanishing rotatory strength in the electronic transitions of a formally non-chiral chromophore has been observed⁵³³ for the tetrahalides of Sn(IV), Ti(IV) and Zr(IV)

in dimethylformamide solutions of (+) tartaric and (+) malic acids. The CD of the absorption bands has been attributed to dissymmetric distortion of the hexa-coordinate $\text{MX}_4(\text{DMF})_2$ species (DMF = dimethylformamide) resulting from outer-sphere coordination of the environment compound. Although inner-sphere coordination of the acid anion is considered unlikely⁵³³ there is no reason, in terms of the second-order R-model, why outer-sphere attachment of a chiral molecule should not induce finite rotatory strength in the metal centred transitions without also distorting the mirror symmetric MX_4L_2 core.

c) A pertinent polydentate example is the base-induced sign inversion of the long wavelength (550 nm) CD band of $[\text{Ti}(\text{III})\text{PDTA}]^-$, (PDTA = (-) 1,2-propylenediaminetetraacetate). This pH-reversible inversion has been attributed⁵³⁴ to a partial relieving of ligand strain as one coordinated carboxyl group is replaced by an hydroxyl ion,⁵³⁵ the hexadentate ligand becoming pentadentate, without altering the chiral displacement of the four remaining chelate rings around the Ti(III) ion or changing the conformation of the stereospecific ligand: there is no concomitant change in the charge transfer region of the CD spectrum.⁵³⁴ Since a similar inversion of $\bar{d}-\bar{d}$ rotatory strength was not observed for the analogous less-strained EDTA complex of the smaller Co(III) ion it was argued⁵³⁴ that the sign change in the $[\text{Ti}(\text{III})\text{PDTA}]^-$ case was due to modification of the crystal-field resulting from displacement of

the ligator atoms of the polydentate relative to their positions in the highly strained hexadentate species. It was concluded⁵³⁴ that the rotatory strength of the metal centred $d-d$ transitions seemed to be dominated, at least in this case, by the *ungerade* displacement of the ligand donor atoms from O_h symmetry rather than by the chiral arrangement of chelate rings.

d) Matsumoto and Kuroya^{89,90} have commented on the CD of (+) $\text{Co}(\text{mal})_2(\text{en})^-$ in reference to the PK-model. However, not only is their discussion in terms of ligand angle, α , incorrect but it is apparent from examination of the PK-model that, because of the use of an ideally D_3 symmetric reference geometry, the model cannot be meaningfully applied to complexes of lower idealized micro-symmetry. Although the A symmetric component of the bis-complex, idealized symmetry C_2 , can be regarded as derived from the E_α component of the higher symmetry tris-complex,^{3,58} description of the $\text{Co}(\text{mal})_2(\text{en})^-$ ion relative to its pseudo- C_2 axis should be more satisfactory.

Both $\Delta(+)[\text{Co mal}_2 \text{ en}]^-$ and $\Delta(-)[\text{Co ox}_2 \text{ en}]^-$ were previously assigned³⁰ negative A symmetric components in their solution CD spectra. The "three-fold" distortion parameters for the two structure determinations of the former ion are given in Table 8.8A: for the three angular parameters α , θ and ω the values for the en ring and the two malonate ligands lie either side of the O_h nodal values of 90° , 54.74° and 60° respectively. Clearly a trivial interpretation

in terms of the PK-model is untenable. Parameters for $[\text{Co ox}_2 \text{ en}]^-$ are not available but they should not differ greatly from those given (Table 8.8A) for $\text{Cr(ox)}_2(\text{en})^-$ which are similar for both types of five-membered chelate ring. Given this correspondence, however, there still remains the error of interpreting the spectral properties of a C_2 chromophore in terms of a D_3 model.

It has been argued^{30,316} that the increased rotational strength of the $d-d$ transitions which accompanies the decreasing ring strain in $\text{Co(ox)}_2(\text{en})^-$, $\text{Co(mal)}_2(\text{en})^-$ and some other model complexes of Co(EDTA)^- contradicts the prediction of the PK-model that the optical activity be greater the greater the displacement of the donor atoms from octahedral symmetry. However, this conclusion is not supported by a similar study³¹⁷ of the carbonato, oxalato and malonato Co(III) complexes containing the tetradentate ethylenediamine- N,N' -diacetate ligand.

e) Few structures of tris-bidentate complexes having three ligand angles, α , greater than 90° have been reported and even less of resolved species of such complexes. Despite what has been said above about C_2 symmetric chromophores, one complex merits some comment. (-) $\text{Co(acac)(tn)}_2^{2+}$ contains two types of six-membered chelate ring:^{122,405} the α , θ and ω values for the acac and tn chelate rings are mutually consistent but the β values lie either side of the orthogonal value of 54.74° (Table 8.8A); the average values are

$\alpha = 95.76^\circ$, $\theta = 52.90^\circ$, $\omega = 65.51^\circ$, $\beta = 54.41^\circ$. The absolute configuration was determined¹²² as Δ by X-ray diffraction and the aqueous solution CD spectrum showed a single negative component at long wavelength which was taken as an E_α derivative; again it was argued¹²² that the PK-model was not supported.

Apart from the invalidity of testing the D_3 PK-model with the core-distortion parameters of a pseudo- C_2 complex there is the question of the probable conformational lability of the chelated tn ligands in solution. The opposing distortion senses of the various energy-minimized $\text{Co}(\text{tn})_3^{3+}$ conformers (Table 8.2) were discussed in section 8.3.1. Not only do skew conformers of tn subtend angles at Co less than 90° but they should also make a conformational contribution to the rotatory strength analogous to that attributed to coordinated en. In this respect the similarity^{122,319} of the long wavelength CD spectra of $(-)\text{Co}(\text{acac})(\text{tn})_2^{2+}$ and $(-)\text{Co}(\text{acac})(\text{en})_2^{2+}$ is noteworthy since, as for the $\text{Co}(\text{mal})_2(\text{en})^-$ ion, the donor atoms of the five- and six-membered chelate rings should exhibit opposing senses of chiral distortion from the D_{3d} reference geometry.

Not only are single crystal polarized absorption and CD spectra of the relevant structures required but also the correct description of the complexes with reference to the pseudo- C_2 axis of the chromophore.

8.4 CONCLUDING REMARKS

The discussion which constitutes this chapter is based on the simplest possible representation of a transition metal complex, namely a crystal-field model having small residual electrostatic charges localized on the metal and ligand donor atoms: the ligand backbone was generally taken to be electronically inert and considered to play only a minor structural role in so far as it distorts the ligand angle, α , from 90° . In this work we have restricted our attention to pseudo trigonal-dihedral ML_6 -core geometries and more particularly to tris-bidentate transition metal complexes, but similar examination of tetrahedral and higher coordination complexes should also be possible. The crystal-field model is still widely applied to the discussion of spectral and magnetic properties of transition metal complexes, it being maintained that, although quantitative estimation of the parameters of interest is not possible without a more sophisticated representation of the ligand field, the symmetry determined nodal properties are still adequately represented by the simple electrostatic model.

Few transition metal complexes have been adequately studied (i.e. solution and solid state absorption and CD spectra, theoretical calculation of energy levels and spectromagnetic properties, accurate structure determinations of the lattices used in the measurement of the solid state electromagnetic properties) to permit comprehensive evaluation of all the theoretical models proposed to describe the

properties of this wide class of compounds. Often the precision of the experimentally determined structural parameters is inadequate or the empirical variation of the chemically equivalent bond lengths and angles is inconsistent with the molecular symmetry indicated by the spectral properties.

In Chapter 6 an attempt was made to outline the interpretation of the electronic spectra which has been adopted in this final chapter. This was necessary in order to indicate the important theoretical features which were neglected in the present, somewhat idealized discussion of the experimental optical data. Not only is the paucity of suitable experimental data a limiting factor but the inability to apply the theoretical models at an adequate level of sophistication is also a serious restriction. The majority of the models summarized in Chapter 7 either defy application at this time or are restricted to such a narrow range of interest as to make comparison trivial: in fairness to Piper and Karipides it should be mentioned that they questioned the validity of comparing such dissimilar chromophores as Co(en)_3^{3+} and Co(ox)_3^{3-} and stressed the unsuitability of discussing the M(acac)_3 spectra without due consideration of the ligand π -covalency.

Thus, when it comes to applying the simplified crystal-field model of Piper and Karipides to the experimental optical-rotatory data in even the most qualitative way, there is no trigonal-dihedral Co(III) or Cr(III) complex of which it can be said without reservation

that interpretation of the observed rotatory strength is uncomplicated by either the possibility of significant vibronic coupling, ligand π -bonding effects, doubtful assignment of the trigonal components, conformational uncertainty or inadequate structural parameters. In discussing the individual complexes it has been necessary to indicate the possible importance of these factors in each case, thus making for a rather protracted analysis.

In many instances the broad spectral features suggest a primary dependence on the nature of the ML_6 -core and certainly the correspondence of the experimental ORD and CD spectra discussed in section 5.3 is not inconsistent with a model in which the characteristic peak and inflexion frequencies derive from the ML_6 -core but the signed rotatory strength reflects primarily the chiral displacement of the non-donor atoms around the metal centre. From what has been said about vicinal, conformational and environmental effects on the rotatory strengths of the optically active transitions of chiral transition metal complexes it seems that the optical CD is more sensitive to the "electronic structure" of the whole complex than is the absorption spectrum. It is not surprising, therefore, that the first-order crystal-field PK-model restricted to consideration of the ML_6 -core, should be found inadequate. A cursory examination of Richardson's second-order model suggests that it will prove no more successful than the PK-model.

Finally, there is a need not just for the accumulation of a

mass of experimental data but rather for the thorough investigation of compounds designed to fully test the proposed theoretical models. There is, of course, no reason why a single, necessarily incomplete model should be universally applicable to the properties of transition metal complexes, but the tendency to propose "all-embracing" theories on the basis of a limited data sample is hardly to be commended.

The following quotation from R.W. Parry (editorial, *Inorg. Chem.*, 1 (1962)) affords an appropriate conclusion;

"Theories change but quality experiments of science are eternal".

APPENDICES

APPENDIX I COMPUTER PROGRAMS USED IN CRYSTAL STRUCTURE ANALYSES.

<u>PROGRAM</u>	<u>FUNCTION</u>	<u>AUTHOR</u>	<u>ADAPTED LOCALLY BY</u>
1. PAPER	generate forms for recording film intensities.	M.R. Snow (1968) Dept. of Physical & Inorganic Chem., University of Adelaide.	
2. TDATA	test punched card data for mis-punching etc.	M.R. Snow (1967)	
3. FDP [†]	process the paper tape output by the diffractometer; convert to punched cards.	M.R. Taylor (1971) School of Physical Sciences, Flinders University of South Australia.	
4. AUFAC	least-squares interfilm scaling; weighting of raw data.	SUFFAC by G.L. Paul (1966) School of Chemistry, University of Sydney.	M.R. Snow
5. AULAC	least-squares interlayer scaling; index sorting.		
6. ABSCOR	application of absorption corrections by the analytical method.	N.W. Alcock (1969) Modified by R. Furina (1969).	M.R. Taylor
7. PREPFLS	data packing routine preliminary to program FOURIER.	F.R. Ahmed (1965) Division of Pure Physics, National Research Council, Ottawa.	M.R. Snow. J.B. Jones, Dept. of Geology, University of Adelaide.
8. FOURIER	compute FOURIER summations.		

(contd.)

APPENDIX I (contd.)

<u>PROGRAM</u>	<u>FUNCTION</u>	<u>AUTHOR</u>	<u>ADAPTED LOCALLY BY</u>
9. FORDAPB	compute Fourier summations with interpolation of peak heights and positions.	A. Zalkin (1968) Modified by J.A. Ibers, Department of Chemistry, Northwestern University.	M.R. Snow
10. FUORFLS	structure factor calculation and least-squares refinement.	A modified version of ORFLS. W.R. Busing, K.O. Martin, H.A. Levy (1962) ORNL-TM-305.*	M.R. Taylor
11. ORFFE	function and error program.	W.R. Busing, K.O. Martin, H.A. Levy (1964) ORNL-TM-306.*	M.R. Taylor
12. ORTEP	thermal ellipsoid plot.	C.K. Johnson (1965) ORNL-3794.*	M.R. Taylor
13. BLANDA	bond length and angle calculations.	J.F. Blount, University of Sydney.	M.R. Snow
14. PLANEH	calculate planes equations, inter-planar dihedral angles and position hydrogen atoms.	D.L. Smith (1964) Ph.D. Thesis, University of Wisconsin. Modified by J.F. Blount (1966).	M.R. Snow
15. PUTAB	list calculated and observed structure factors.	R.C. Elder. Modified by B. Foxman (1968).	M.R. Snow

† This program written for the IBM 1130 computer; all others in FORTRAN for the CDC 6400.

* Oak Ridge National Laboratory, Oak Ridge, Tennessee.

APPENDIX II REDUCTION OF THE PHOTOGRAPHIC DATA.

Intensities of the integrated photographic data were measured using a Nonius II microdensitometer linked to a Kipp and Zonen light spot galvanometer AL-1, the linearity of response of this combination having previously been verified for an optical density range of $0 \rightarrow 1.9$. A value for the plateau density and an average estimate of the local background were recorded for each observed reflection on all films of a reciprocal layer pack; reflections unobserved on the top film of a layer, i.e. having a plateau reading not measurably different from the average background, were marked (U in structure factor tables) and included with a background value only.

Using program AUFAC, the reflection intensities were scaled to the top film of each reciprocal layer by a non-iterative least-squares procedure[†] modified to incorporate estimation of the standard deviation of each observation. The weighted mean intensity, corrected for Lorentz and polarization effects but without application of absorption corrections, was output for each reflection together with its standard deviation. Individual observations showing large

† The inter-film and inter-layer scale factors were determined by a least-squares procedure described by Rae (A.D. Rae, *Acta Cryst.*, 19, 683 (1965)), developed by Paul (G.L. Paul, SUFFAC, a Fortran IV program for the least-squares determination of film factors) and extended locally by Snow (see Appendix I).

deviations from the mean intensity of a given reflection were listed and examined for mispunching and mismeasurement.

The weighted mean intensities (and their standard deviations) from AUFAC were input to program AULAC and the inter-layer scale factors determined by a least-squares fitting analogous to that applied in AUFAC. The weighted mean intensities and sigmas were output in a format suitable for introduction to the structure factor calculating program (FUORFLS) and the programs for computing Patterson and Fourier maps (FOURIER and FORDAPB).

AUFAC - inter-film scaling.

For an observed reflection h on film i the scaled intensity is given as

$$I_{h_i} = \left[\ln \left(\frac{\text{Background}_i}{\text{Spot density}_i} \right) \right] \times k_i \times 100$$

and the standard deviation of the unscaled intensity, i.e.

$I_u = I_{h_i} / 100$, is

$$\begin{aligned} \sigma_u &= a I_u + b \times k_i \quad (\text{when } I_u \geq c \times k_i) \\ \text{and } \sigma_u &= d \times k_i \quad (\text{when } I_u < c \times k_i). \end{aligned}$$

The weights, w_{h_i} , assigned to the individual observations in the least-squares determination of film factors are assumed proportional to $1/\sigma_{h_i}^2$, the standard deviation of the scaled reflection h on the i^{th} film being

$$\sigma_{h_i} = \sigma_u \times \sqrt{EOF/a} \times 100.$$

Here k_i is the scale factor for the i^{th} film and EOF_α is the least-squares error of fit from the inter-film scaling procedure. If the slope, α , is too small or the cut-off, c , too high relative to the distribution of unscaled intensities, the weights applied to the data are largely independent of the reflection intensity leading to a relative "over-weighting" of the more intense reflections in the least-squares structure refinement cycles. AUFAC outputs a new weighting scheme (i.e. a, b, c, d) after determining the scale factors and this can be resubmitted with the corrected data thus providing a means of improving the least-squares fit of the raw data.

For unobserved reflections

$$I_{unobs} = \left[\ln \left(\frac{\text{Background}_i}{\text{Background}_i - BGF} \right) \right] \times S \times 100$$

$$\text{and } \sigma_{unobs} = I_{unobs} \times T/S \times \sqrt{EOF_\alpha}$$

where BGF is an average value for the background intensity fluctuation on the top film and S and T are constants having the values 0.500 and 0.346 respectively for non-centric film data.⁴³

The weighted mean intensity of a reflection on reciprocal layer j is calculated as

$$\bar{I}_{h_j}^{uns} = \frac{\sum_i (w_{h_i} / k_i) I_{h_i}}{\sum_i (w_{h_i} / k_i^2)}$$

The standard deviation, $\sigma_{h_j}^{uns}$, is estimated from the agreement between multiple observations of a reflection on the individual films of a reciprocal layer pack. Unobserved and unreliable reflections were

not included in the least-squares determination of inter-film and inter-layer scale factors.

AULAC — inter-layer scaling.

The least-squares inter-layer scale factors, k_j , are applied to the mean intensities from AUFAC such that

$$\bar{I}_{h_j} = \bar{I}_{h_j}^{uns} \times k_j$$

for all reflections. For an unobserved reflection on layer j

$$\bar{\sigma}_{h_j} = \sigma_{unobs} \times k_j$$

but for observed reflections the standard deviation of the mean intensity is modified to incorporate the least-squares error of fit of the inter-layer scaling process

$$\bar{\sigma}_{h_j} = \bar{\sigma}_{h_j}^{uns} \times k_j \times \sqrt{EOF_b}.$$

The scaled mean intensity, \bar{I}_h , and its standard deviation, $\bar{\sigma}_h$, are then computed for each unique reflection by a method analogous to that applied in AUFAC. Where unobserved or unreliable reflections occur in combination with an observed intensity only the observed reflection contributes to the mean.

The observed structure factor and its standard deviation input to the least-squares structure refinement (FUORFLS) are

$$|F_o| = \sqrt{\bar{I}_h}$$

$$\sigma_{F_o} = \frac{\bar{\sigma}_h}{2 \times |F_o|}$$

for all reflection types.

In the case of the NADCOMALEN structure (see Chapter 1), subsequent analysis of the least-squares structure refinement outputs showed the weighting scheme derived in program AUFAC to be unsatisfactory and a significant improvement in the estimated standard deviations of the atomic positional and thermal parameters was achieved by the application of a Cruickshank-type weighting scheme^{44a} to the data set.

primary references for this Appendix

AUFAC and AULAC manuals (see Appendix I).

ref. 45, 46.

APPENDIX III DIFFRACTOMETER DATA COLLECTION AND REDUCTION.

The reflection intensities for the CADCOTHIOX structure (Chapter 3) were collected using a Buerger-Supper equi-inclination diffractometer on line to a PDP-8/L computer; Philips counting electronics were used. This diffractometer employs the ϕ (or ω) scan technique (stationary counter, rotating crystal), the operation being identical with that described by Freeman and co-workers.^{47,48} Data were measured over an 2θ range of $10-140^\circ$, the output being in the form of a tele-type line print-out and an eight channel binary code punch tape. The output for a measured reflection consists of the indices hkl , the scan speed, the peak count and the background count either side of the peak in ϕ . Reflections having count rates outside the linear range of the counter were automatically remeasured with an aluminium foil attenuator inserted between the tube window and the crystal. Two metal slides with circular holes subtending angles ranging $2.5^\circ-4.0^\circ$ at the crystal, placed between the crystal and the counter window, served to collimate the diffracted beam. The correct choice of aperture is important in keeping the background intensity contribution to the peak count minimal but no reflection should be limited by the aperture size. The aperture size should be increased with increasing equi-inclination angle, μ , to allow for greater beam divergence but an aperture greater than optimum merely increases the standard deviation without increasing the integrated reflection intensity. The aperture size for each reciprocal layer was checked

against the intensity profiles of several low order peaks.

The scan range for a reflection hkl is calculated as

$$\Delta\phi = \phi_{\lambda} + \phi_D + \phi_M + \phi_E$$

where ϕ_{λ} is due to wavelength dispersion, ϕ_D to divergence of the X-ray beam, ϕ_M to crystal mosaicity and ϕ_E allows for possible errors in the crystal settings. These factors are rigorously defined in references 47 and 48. The mosaicity factor was experimentally determined as 1.15° by measuring peak profiles of several zero layer reflections; other constants were assigned the values quoted in refs. 47, 48. ϕ_M is assumed constant for all values of $\sin\theta$ ($2\theta = T$) but ϕ_{λ} , ϕ_D and ϕ_E are functions of T and μ .

In the variable scan-speed data collection procedure a reflection is initially measured at the maximum scan speed ($1/3$ deg. sec⁻¹). For a reflection having crystal and counter setting angles ϕ and T respectively, the counter remains fixed at angle T throughout the measurement cycle. The background count, B_1 , at position $(\phi - \frac{1}{2}\Delta\phi)$ is accumulated for $t/2$ seconds where $t = \frac{\Delta\phi}{\text{scan speed}}$; the integrated peak count, P , is measured with the crystal moving through $\Delta\phi$ degrees in t seconds and then, with the crystal again stationary, background B_2 is determined at $(\phi + \frac{1}{2}\Delta\phi)$.

Following the preliminary fast scan the control program performs the following tests -

- i) tests that the reflection count rate is within the linear range of the counter; in the present case $\frac{\text{peak count}}{\text{scan range}}$ was

required to be less than 4000. If this condition was not satisfied an Al attenuator was inserted in the primary beam and the reflection remeasured.

ii) tests for background imbalance;

$$|B_1 - B_2| < 6(\sigma_B) + 0.01 (I)$$

$$\text{where } \sigma_B = \sqrt{B_1 + B_2}.$$

If this inequality was failed (perhaps due to the presence of an intense Laue streak from a lower order reflection or non-centering of the peak in the scan range due to a slight mis-setting of the crystal) the scan range was incremented by 0.5° and the reflection remeasured.

iii) tests that σ_I/I lies within the specified limits of precision; if not a new scan speed ($0.05 \leq \delta \leq 1/3 \text{ deg. sec}^{-1}$) was calculated so that remeasurement of the reflection at this speed gave the desired precision.

$$\delta = \frac{1}{3} \left\{ \frac{R_E}{50} \right\}^2 \left\{ \frac{P - (B_1 + B_2)}{P + (B_1 + B_2)} \right\}^2 \text{ deg. sec}^{-1}$$

where R_E is the expectation value of the residual R_1 assuming the experimental errors to be random. For this data collection process

$$R_E (= \frac{\alpha_F}{|F_O|})$$

was fixed at 4%.

The three counts B_1 , P and B_2 from the slow scan are output.

Program FDPTP was used to calculate the intensity, corrected for Lorentz and polarization effects, and its standard deviation, based on counting statistics, for each reflection. Punch cards of format suitable for input to the absorption correction program, ABSCOR, and the inter-layer scaling program, AULAC, were output.

$$\text{Intensity } I = [P - (B_1 + B_2)] \times \delta'$$

$$\text{where } \delta' = \frac{\text{scan speed}}{\text{minimum scan speed}} = \frac{\delta}{0.05} = 20\delta.$$

The standard deviation of the peak intensity due to statistical fluctuations in the counting is given as

$$\sigma_I = [N + B_1 + B_2]^{\frac{1}{2}} \times \delta'$$

Reflections having $I \leq 2\sigma_I$ were excluded from the punch card deck and in a subsequent data rework those having $2\sigma_I < I \leq 3\sigma_I$ were designated "unobserved" and excluded from further least-squares refinement cycles without modification of their intensities or sigmas. Reflections having $|B_1 - B_2| > 3\sigma_B$ were checked on the films for background imbalance due to white radiation streaks. Several systematically absent reflections (form $\{h00\}$, $h = 2n + 1$) had significant peak intensities due to the extension of strong Laue streaks from the $h = 2n$ reflections along the axial rows: all systematic absences were excluded from the data set.

The diffractometer control program had a facility for repeated measurement of a "standard reflection" on each reciprocal layer; average values for the background and peak counts for the standard reflection were supplied and automatically re-determined every fifty

reflections testing the inequality

$$|I_S - I_R| < 5(\sigma_{I_S} + \sigma_{I_R})$$

where I_S is the average intensity supplied initially

and I_R the current measurement.

If the inequality is failed the standard is remeasured and if it fails again the data collection halts. No such halts were encountered although examination of the raw data revealed that the test was failed on the first pass several times. Only one set of values was included for each standard reflection of a layer in AULAC. Despite the apparent constancy of the standard reflection intensities there were some obvious examples of electronic malfunction and these data were excluded.

The integrated intensities were corrected for absorption using program ABSCOR. Both crystals were described as rectangular parallel-pipeds although a more rigorous description of the crystal shape is possible; indeed the differences in intensity of some of the zero layer $++0$ and $-+0$ c axis reflections (Table 3.1) indicate that a more accurate description may be needed^{44b} since such differences can not be due to anomalous dispersion effects. ABSCOR calculates the absorption corrections for polyhedral crystals by the analytical method developed by de Meulenaer and Tompa⁴⁹ and extended in Fortran form by Alcock.^{50,51} The corrected intensities were scaled using program AULAC which generates the observed structure factor modulus, $|F_O|$, and its standard deviation, σ_{F_O} . Collection of diffractometer data about two

or more axes using different crystals permits some assessment to be made in the least-squares scaling sequence of the random errors in the data set (see Appendix II).^{45,52}

primary references for this Appendix

FDTP and ABSCOR manuals (Appendix I).

refs. 47, 48, 50, 53.

APPENDIX IV MISCELLANEOUS NOTES ON THE CRYSTAL STRUCTURES.

1. Scattering factor curves:

Hydrogen ref. 73.

$\Delta f'$, $\Delta f''$ for all atoms ref. 74.

NADCOMALEN - Co^{+1} ref. 74;^a Na^{+1} , C, N, O ref. 75.

CRMALTCOPN - Co^{+2} , Cr^{+2} , C, N, O ref. 75.

CADCOTHIOX - Co^{+1} ref. 74;^a K^{+1} , Ca^{+2} , S, O, C ref. 75.

KNIPHECOOX - Co^{+2} , Ni^{+1} , Ni^0 , K^{+1} , C, N, O ref. 74.^a

a. Vol. III, table 3.3.1A.

Scattering curves corresponding to less than the formal valence of the complexed metal were used;⁷⁶ in view of the almost complete delocalization of charge over the whole complex ion suggested elsewhere⁷⁷ it may have been more suitable to use the zero-valent scattering factor curves. For the non-complexed Ca^{+2} , K^{+1} and Na^{+1} ions use of the ionic curves is probably a reasonable approximation.

2. Data presentation:

The errors in the lattice constants were not included in computation of the individual bond length and bond angle standard deviations, which were also not corrected for thermal vibration. The mean square amplitudes of thermal vibration were computed only for K^+ , Ca^{++} and Co in the CADCOTHIOX structure.

Average planes through four or more atoms are unweighted least-squares planes only; our version of ORFFE has not been

modified to compute interplanar dihedral angles for which one plane contains four or more atoms and the values (without esd's) for these angles were computed using PLANEH. The esd's of the deviations from the planes of best fit were not computed.

Standard deviations in the torsion angles were calculated as the error in the dihedral angle between the relevant three atom planes; a more satisfactory method of calculating these errors has recently been proposed.⁷⁸

3. Mean parameters:

The mean, \bar{x} , is the unweighted sum average; its estimated standard deviation, $\hat{\sigma}$, is computed^{45,79} as

$$\hat{\sigma} = \left(\sum_i (x_i - \bar{x})^2 / n(n-1) \right)^{1/2}$$

where x_i is an individual observation and n the number of independent observations. If $\hat{\sigma}$ is less than $\sigma_i/n^{1/2}$, then the latter value is given as the standard deviation of the mean.

4. Footnotes and comments of obviously general application to the data tables of all three structures are not subsequently restated but are implied in the data presentation.

APPENDIX V PROGRAM OCTANT.

Program OCTANT was originally written to calculate the octant sum for the ML_6 -core of a chiral D_3 complex according to the octant sign rule proposed by Hawkins and Larsen³²⁴ but using the orientation proposed by Mason.³⁰⁶ However, the preliminary results were random (the octant rule having been devised for an assumed orthogonal ML_6 coordination sphere which makes no contribution to the sum, see section 7.1) and the program was not extended to include the whole complex in the summation. The program can be easily modified to include all atoms of the complex or to calculate the relevant sums for the hexadecahedral, $F(D_{4h})$, and octahedral conformational, $F(O_h)$, rules both of which are defined in terms of Cartesian axes.

The relevance of this program to the present work is that it was readily adaptable to the calculation of a set of orthogonalized coordinates (in Å) for the ML_6 -core of a tris(bidentate) complex for which sufficient bond lengths and angles, but not coordinates, were available. The six bond lengths, M-L, and twelve interatom vectors, all involving one of the first three donor atoms in the atoms list, are used as input in the present modification of OCTANT. As this requires knowledge of some approximately 180° vectors, which are seldom quoted in preliminary structure communications, an alternative approach using only adjacent atom vectors, i.e. interbond angle 90° in O_h symmetry, in conjunction with the six M-L bond lengths would be preferable.

Evaluation of the octant sum, $\sum Z(X^2 - Y^2)$, requires that the complex be oriented such that one ligand (of a tris-bidentate complex) lies in the $Z = 0$ plane with one donor atom, L, on the $+X$ axis and the other on $+Y$. In reality the ligand angle, α , is seldom 90° and this idealized arrangement is unattainable; in program OCTANT the ML_6 -core is reoriented to approximate the required geometry as nearly as possible, maintaining a fixed right-handed set of reference axes (see the comment cards at the head of the program). The mathematics is simple vector geometry and needs no elaboration. Truncation effects, both in the computation cycle and in the starting vectors abstracted from the literature, can result in slightly different values for the output coordinates depending on the order in which the input vectors are supplied, but these uncertainties usually have only a minor effect on the AZIMUTH averages.

PROGRAM OCTANT(INPUT,OUTPUT)

C
 C PROGRAM TO CALCULATE INDIVIDUAL ATOM TERMS FOR THE OCTANT RULE OF HAWKINS
 C USES CRYSTAL COORDINATES, ORTHOGONALIZES AND REORIENTS ATOM SET TO GIVE
 C METAL(0,0,0) AND LIGATING ATOM(1) AT (X,0,0). ITS CHELATE MATE IS AT(X,Y,0).
 C LIGATING ATOM 2 HAS Y +VE, LIGATING ATOM 3 HAS Z DEFINED +VE.
 C SHOULD SUPPLY FIRST FOUR ATOMS IN ORDER NEEDED TO GIVE RIGHT
 C HANDED SET MA1,MA2,MA3. THEN LIGAND A1-A2 SPANS +X+Y WITH A3 AT +Z.
 C PROGRAM PRESENTLY RESTRICTED TO SEVEN ATOM INPUT. 1 METAL + COORD OCTAHEDRON.
 C CAN ALSO READ APPROPRIATE INTERATOM DISTANCES IN ANGSTROMS AND
 C CALCULATE ORTHOGONALIZED COORDINATES FOR METAL ATOM AND THE SIX ATOMS
 C OF THE COORDINATION SPHERE. BUTLER JAN-FEB/1972

C
 DIMENSION ATOM(7),XT(7),YT(7),ZT(7),TITLE(8),
 1A(7),B(7),C(7),D(7),X(7),Y(7),Z(7)
 2 FORMAT(1H1,X,8A10)
 3 FORMAT(6F10.7,I2)
 4 FORMAT(1H0,8X,1HA,8X,1HB,8X,1HC,7X,4HCOSA,7X,4HCOSB,7X,4HCOSC,
 12X,4HNATM,/,X,3F9.4,3F11.5,I6)
 12 FORMAT(X,* BOND LENGTH METAL TO *,A6,* IS *,F15.12,* ANGSTROM*)
 15 FORMAT(X,* INTERATOM DISTANCE *,A6,* TO *,A6,* IS *,F15.12,
 1* ANGSTROM*)
 20 FORMAT(1H0,7X,*ORTHOGONAL X,Y,Z IN ANGSTROMS*)
 21 FORMAT(8X,A6,3F15.7)
 61 FORMAT(1H0,8X,* OCTANT SUM = *,F35.30)
 62 FORMAT(1H0,X,* CONTRIBUTION OF ATOM *,A6,X,F25.20)
 100 FORMAT(I2)
 104 FORMAT(7A6)
 200 FORMAT(4F20.15)
 201 FORMAT(2F20.15)
 202 FORMAT(F20.15)
 203 FORMAT(3F20.15)
 300 FORMAT(X,/,X,4F20.15)
 301 FORMAT(X,2F20.15)
 302 FORMAT(X,F20.15)
 303 FORMAT(X,3F20.15)
 211 FORMAT(8A10)
 9002 FORMAT(A6,3F10.6)
 9005 FORMAT(1H0,2X,*ATOM*,16X,*X*,15X,*Y*,15X,*Z*,14X,*XT*,14X,*YT*,
 114X,*ZT*)
 9006 FORMAT(2X,A6,6F15.12)
 READ 100,NUM
 DO 600 ISKY=1,NUM
 READ 100,IN
 READ 211,TITLE
 PRINT 2,TITLE
 IF(IN.EQ.0)101,102
 101 READ 3,CA,CB,CC,COSA,COSB,COSC,NATM
 PRINT 4,CA,CB,CC,COSA,COSB,COSC,NATM

C
 C CALC OF ORTHOGONALIZED COORDS (AS IN AZIMUTH)
 SG=SQRT(1.-COSC*COSC)
 CR=(COSA-COSB*COSC)/SG
 CP=SQRT(1.-COSB*COSB-CR*CR)
 PRINT 9005
 DO 1 I=1,NATM
 READ 9002,ATOM(I),X(I),Y(I),Z(I)
 XT(I)=CA*X(I)+CB*COSC*Y(I)+CC*COSB*Z(I)
 YT(I)=CB*SG*Y(I)+CC*CR*Z(I)
 ZT(I)=CC*CP*Z(I)
 PRINT 9006,ATOM(I),X(I),Y(I),Z(I),XT(I),YT(I),ZT(I)
 1 CONTINUE

C

```

C METAL LIGAND BOND DISTANCES,A(N)
10 DO 11 N=2,7
   A(N)=SQRT((XT(1)-XT(N))**2+(YT(1)-YT(N))**2+(ZT(1)-ZT(N))**2)
   PRINT 12,ATOM(N),A(N)
11 CONTINUE

C
C INTERATOM DISTANCES,A(1) TO A(2-6)
13 DO 14 N=3,7
   B(N)=SQRT((XT(2)-XT(N))**2+(YT(2)-YT(N))**2+(ZT(2)-ZT(N))**2)
   PRINT 15,ATOM(2),ATOM(N),B(N)
14 CONTINUE

C
C INTERATOM DISTANCES,A(2) TO A(3-6)
17 DO 16 N=4,7
   C(N)=SQRT((XT(3)-XT(N))**2+(YT(3)-YT(N))**2+(ZT(3)-ZT(N))**2)
   PRINT 15,ATOM(3),ATOM(N),C(N)
16 CONTINUE

C
C INTERATOM DISTANCES,A(3) TO A(4-6)
18 DO 19 N=5,7
   D(N)=SQRT((XT(4)-XT(N))**2+(YT(4)-YT(N))**2+(ZT(4)-ZT(N))**2)
   PRINT 15,ATOM(4),ATOM(N),D(N)
19 CONTINUE
GO TO 103

102 READ 104,(ATOM(I),I=1,7)
   READ 200,(A(I),I=2,5)
   PRINT 300,(A(I),I=2,5)
   READ 201,(A(I),I=6,7)
   PRINT 301,(A(I),I=6,7)
   READ 200,(B(I),I=3,6)
   PRINT 300,(B(I),I=3,6)
   READ 202,B(7)
   PRINT 302,B(7)
   READ 200,(C(I),I=4,7)
   PRINT 300,(C(I),I=4,7)
   READ 203,(D(I),I=5,7)
   PRINT 303,(D(I),I=5,7)

C
C DERIVATION OF NEW COORDS
103 PRINT 20

C
C CENTRAL METAL
M=1
X(M)=0 $ Y(M)=0 $ Z(M)=0
PRINT 21,ATOM(M),X(M),Y(M),Z(M)

C
C LIGAND ATOM A(1)
M=2
X(M)=A(M) $ Y(M)=0 $ Z(M)=0
PRINT 21,ATOM(M),X(M),Y(M),Z(M)

C
C LIGAND ATOM A(2)
M=3
X(M)=(A(2)**2+A(3)**2-B(3)**2)/(2*A(2))
Y(M)=ABS(A(3)**2-X(M)**2)
Y(M)=SQRT(Y(M))
Z(M)=0
PRINT 21,ATOM(M),X(M),Y(M),Z(M)

C
C LIGAND ATOMS A(3)-A(6)
C Z COORD OF A(3) +VE SUCH THAT MA(1),MA(2),MA(3) CONSTITUTE
C A RIGHT HANDED SET.
DO 22 N=4,7
   X(N)=(A(2)**2+A(N)**2-B(N)**2)/(2*A(2))
   Y(N)=(-A(2)**2-C(N)**2+B(N)**2+2*A(2)*X(N)+Y(3)**2
   1+X(3)**2-2*X(N)*X(3))/(2*Y(3))

```



```

Z(N)=ABS(A(N)**2-X(N)**2-Y(N)**2)
Z(N)=SQRT(Z(N))
IF(N.EQ.4)23,24
C
C DETERMINE WHETHER Z(N) +VE OR -VE
24 TEST=(X(N)-X(4))**2+(Y(N)-Y(4))**2+(Z(N)-Z(4))**2
ZNEG=-Z(N)
TOAD=(X(N)-X(4))**2+(Y(N)-Y(4))**2+(ZNEG-Z(4))**2
VAL=D(N)**2
DIFF1=ABS(VAL-TEST)
DIFF2=ABS(VAL-TOAD)
IF(DIFF1.LE.DIFF2)23,25
25 Z(N)=-Z(N)
23 PRINT 21,ATOM(N),X(N),Y(N),Z(N)
22 CONTINUE
C
C FORMATION OF THE OCTANT SUM (Z**2)(X**2-Y**2)
HAWK=0
DO 60 N=4,7
ZS=Z(N)**2
XS=X(N)**2
YS=Y(N)**2
HT=ZS*(XS-YS)
HAWK=HAWK+HT
PRINT 62,ATOM(N),HT
60 CONTINUE
PRINT 61,HAWK
600 CONTINUE
END

```

APPENDIX VI PROGRAM NHANGLE.

Using previously orthogonalized coordinates (in Å) program NHANGLE calculates the inclination of the N-H bonds of tris(diamine) complexes relative to the C_3 axis of the complex ion. Unlike program AZIMUTH, the three-fold axis is defined as the line passing through the metal atom and the centroid of the donor atom triangle. For the energy minimized models for which this program was designed there is little difference between this definition of the C_3 axis and the definition chosen for the purpose of program AZIMUTH (see section 7.3) since all the complex ions are closely C_3 symmetric and their CoN_6 -cores almost ideally D_3 symmetric. The program has not been applied to any structural data since nothing new would be added to the argument concerning the relative stabilities of the various oriented ion-pairs in aqueous solution.

The angle between the C_3 axis and the inter-hydrogen atom vector for the two amino hydrogens bonded to the same nitrogen donor atom is also output. The mathematics merely involves calculation of the cosine of the desired angle as a function of the direction cosines of the relevant vector and the C_3 axis, i.e.

$$\cos(\text{ang.}) = l_1 l_2 + m_1 m_2 + n_1 n_2.$$

```

PROGRAM NHANGLE (INPUT,OUTPUT)
C
C INPUT CARDS COMPATIBLE WITH AZIMUTH. ORTHOGONALIZED COORDS ONLY.
C METAL ATOM NOT INPUT BUT MUST BE AT ORIGIN WITH RESPECT TO OTHER ATOMS
C PROGRAM CALCULATES ANGLE BETWEEN N-H BONDS AND C3 AXIS OF COMPLEX ION
C COORDS CAN BE IN ANGSTROMS OR ANY MULTIPLE THEREOF SINCE MAKES
C NO DIFF TO ANGLE CALCS BUT DOES AFFECT LENGTHS
C DATA DECK CARD1 NUM. OF CALCS TO BE DONE
C CARD 2 TITLE
C CARD 3-11 INPUT COORDS.3N ATOMS,3H1,3H2 ATOMS
C CARDS 2-11 MUST BE SUPPLIED FOR EACH SET OF COORDS TO BE PROCESSED
C BUTLER NOV 17-18/1970
C
COMMON TITLE(8),X(9),Y(9),Z(9),ATOM(9)
9000 FORMAT(8A10)
9001 FORMAT(2X,* BOND LENGTH *,A6,X,A6,* IS *,F10.6)
9002 FORMAT(A6,3F10.6)
9003 FORMAT(1H1,8A10)
9006 FORMAT(/,8X,A6,3(3X,F10.6))
9007 FORMAT(1H0,X,*CENTROID X= *,F10.6,3X,*Y= *,F10.6,3X,*Z= *,F10.6)
9008 FORMAT(2X,*CENTROID -ORIGIN DISTANCE =*,F10.6)
9009 FORMAT(2X,*DIRECTION COSINES C3 DL=*,F10.6,2X,*DM=*,F10.6,2X,
1*DN=*,F10.6)
9010 FORMAT(/,2X,*DIFFX=*,F10.6,2X,*DIFFY=*,F10.6,2X,*DIFFZ=*,F10.6)
9011 FORMAT(2X,*DA=*,F10.6,2X,*DB=*,F10.6,2X,*DC=*,F10.6)
9012 FORMAT(2X,*ANGLE BETWEEN C3 AXIS AND*,4X,A6,A6,* BOND IS*,F10.6)
9013 FORMAT(/,2X,*END DATA SET *,I4)
9018 FORMAT(I4)
9020 FORMAT(2X,*ANGLE BETWEEN C3 AXIS AND *,X,A6,A6,* VECTOR=*,F10.6)
9021 FORMAT(2X,*INTERATOM DISTANCE *,A6,X,A6,* IS*,F10.6)
READ 9018,IDAT
DO 1000 NCYC=1,IDAT
READ 9000,TITLE
PRINT 9003,TITLE
DO 1 I=1,9
READ 9002,ATOM(I),X(I),Y(I),Z(I)
PRINT 9006,ATOM(I),X(I),Y(I),Z(I)
1 CONTINUE
C
C CALCULATE CENTROID OF LIGAND ATOM TRIANGLE
C C3 FROM ORIGIN TO CENTROID
SUMX=X(1)+X(2)+X(3) $ SUMY=Y(1)+Y(2)+Y(3) $ SUMZ=Z(1)+Z(2)+Z(3)
CX=SUMX/3. $ CY=SUMY/3. $ CZ=SUMZ/3.
PRINT 9007,CX,CY,CZ
C
C ORIGIN CENTROID DISTANCE
DIST=CX*CX+CY*CY+CZ*CZ
DOC=SQRT(DIST)
PRINT 9008,DOC
C
C DIRECTION COSINES OF C3 AXIS
DL=CX/DOC $ DM=CY/DOC $ DN=CZ/DOC
PRINT 9009,DL,DM,DN
C
C NITROGEN HYDROGEN BOND LENGTHS AND DIRECTION COSINES
DO 2 II=1,3
M=II+3
12 DIFFX=X(M)-X(II) $ DIFFY=Y(M)-Y(II) $ DIFFZ=Z(M)-Z(II)
PRINT 9010,DIFFX,DIFFY,DIFFZ
EN=DIFFX*DIFFX+DIFFY*DIFFY+DIFFZ*DIFFZ
BLENH=SQRT(EN)
PRINT 9001,ATOM(II),ATOM(M),BLENH
DA=DIFFX/BLENH $ DB=DIFFY/BLENH $ DC=DIFFZ/BLENH

```

```
      PRINT 9011,DA,DB,DC
C
C ANGLE BETWEEN N-H BOND AND C3 AXIS
  COSTH=DA*DL+DB*DM+DC*DN
  THETA=ACOS(COSTH)
  ANG=THETA*57.2958
  PRINT 9012,ATOM(II),ATOM(M),ANG
  M=M+3
  IF (M-II.EQ.6) 12,10
C
C ANGLE BETWEEN C3 AND H-H NONBONDED VECTOR
  10 NA=II+3
  M=NA+3
  AX=X(NA)-X(M) $ AY=Y(NA)-Y(M) $ AZ=Z(NA)-Z(M)
  HHDIS=AX*AX+AY*AY+AZ*AZ
  HH=SQRT(HHDIS)
  PRINT 9021,ATOM(NA),ATOM(M),HH
  DCA=AX/HH $ DCB=AY/HH $ DCC=AZ/HH
  COSAL=DCA*DL+DCB*DM+DCC*DN
  ALPHA=ACOS(COSAL)
  ALPHA=ALPHA*57.2958
  PRINT 9020,ATOM(NA),ATOM(M),ALPHA
  2 CONTINUE
  PRINT 9013,NCYC
1000 CONTINUE
  END
```

BIBLIOGRAPHY

1. E.J. Corey and J.C. Bailar, Jr., J. Amer. Chem. Soc., 81, 2620 (1959).
2. D.A. Buckingham and A.M. Sargeson, Topics in Stereochem., 6, 219 (1971).
3. R.D. Gillard and P.R. Mitchell, Structure and Bonding, 7, 46 (1970).
4. J.M. Bijvoet, A.F. Peerdeman and A.J. van Bommel, Nature, 168, 271 (1951).
5. A.F. Peerdeman and J.M. Bijvoet, Acta Cryst., 9, 1012 (1956).
6. R.W. James, "The Crystalline State, Vol. II: The Optical Principles of the Diffraction of X-rays" (G. Bell and Son, Ltd., London, 1965).
7. A. Werner, Bull. Soc. Chim. France, Series 4, 11, 1 (1912).
8. P. Drude, "Lerbuch der Optik" (S. Hirzel, Leipzig, 1906: Eng. trans., Dover, New York, 1959).
9. A. Fresnel, Ann. Chim. Phys., 28, 147 (1825).
10. W. Kuhn, Z. phys. Chem., B4, 14 (1929).
11. W. Kuhn and E. Braun, Z. phys. Chem., B8, 281 (1930).
12. W. Moffitt and A. Moscowitz, J. Chem. Phys., 30, 648 (1959).
13. M.J. Harding, J. Chem. Soc. (Farad. II), 234 (1972).
14. W. Haidinger, Ann. Phys., 70, 531 (1847).
15. A. Cotton, Compt. rend., 120, 989, 1044 (1895).
16. A. Cotton, Ann. Chim. Phys., Series 7, 8, 347 (1896).
17. J.P. Mathieu, Ann. Phys., Series 11, 3, 371 (1935).
18. W. Moffitt, R.B. Woodward, A. Moscowitz, W. Klyne and C. Djerassi, J. Amer. Chem. Soc., 83, 4013 (1961).
19. C. Djerassi, Proc. Chem. Soc., 314 (1964).

20. P. Crabbé, "Optical Rotatory Dispersion and Circular Dichroism in Organic Chemistry" (Holden-Day, San Francisco, 1965).
21. S.F. Mason, *Inorg. Chim. Acta Revs.*, 2, 89 (1968).
22. B. Bosnich, *Inorg. Chem.*, 7, 178, 2379 (1968).
23. J. Hidaka and B.E. Douglas, *Inorg. Chem.*, 3, 1180 (1964).
24. J. Ferguson, C.J. Hawkins, N.A.P. Kane-Maguire and H. Lip, *Inorg. Chem.*, 8, 771 (1969).
- ~~25.~~ W. Moffitt, *J. Chem. Phys.*, 25, 1189 (1956).
26. D.H. Templeton, A. Zalkin and T. Ueki, *Acta Cryst.*, 21, Suppl., A154 (1966).
27. A.J. McCaffery, S.F. Mason and R.E. Ballard, *J. Chem. Soc.*, 2883 (1965).
28. A.J. McCaffery, S.F. Mason and B.J. Norman, *Proc. Chem. Soc.*, 259 (1964).
29. W.E. Hatfield, *Inorg. Chem.*, 3, 605 (1964).
30. B.E. Douglas, R.A. Haines and J.G. Brushmiller, *Inorg. Chem.*, 2, 1194 (1963).
31. D.A. Buckingham, L. Durham and A.M. Sargeson, *Aust. J. Chem.*, 20, 257 (1967).
32. H. Yoneda and Y. Morimoto, *Inorg. Chim. Acta*, 1, 413 (1967).
33. R.M. Wing and R. Eiss, *J. Amer. Chem. Soc.*, 92, 1929 (1970).
- ~~34.~~ T.S. Piper and A. Karipides, *Mol. Phys.*, 5, 475 (1962).
- ~~35.~~ A.G. Karipides and T.S. Piper, *J. Chem. Phys.*, 40, 674 (1964).
36. R.R. Judkins and D.J. Royer, *Inorg. Nuclear Chem. Letters*, 6, 305 (1970).

37. D.J. Royer, personal communication (1970).
38. F. Mizukami, H. Ito, J. Fujita and K. Saito, Bull. Chem. Soc. Japan, 43, 3633, 3973 (1970).
39. K. Saito, communication with M.R. Snow (1971).
40. Y. Saito, communication with M.R. Snow (1971).
41. F.S. Richardson, J. Phys. Chem., 75, 692 (1971).
42. D.L. Kepert, Inorg. Chem., 11, 1561 (1972).
43. W.C. Hamilton, Acta Cryst., 8, 185 (1955).
44. "Computing Methods and the Phase Problem in X-ray Crystal Analysis": Glasgow Conference, August 1960: Edited by R. Pepinsky, J.M. Robertson and J.C. Speakman (Pergamon Press, London, 1961).
 - (a) D.W.J. Cruickshank, D.E. Pilling, A. Bujosa, F.M. Lovell and M.R. Truter, Paper 6, p. 32.
 - (b) Y. Okaya and R. Pepinsky, Paper 28, p. 273.
45. G.H. Stout and L.H. Jensen, "X-ray Structure Determination" (Macmillan, London, 1968).
46. "Computing Methods in Crystallography", J.S. Rollett, Ed., (Pergamon Press, Oxford, 1965).
47. H.C. Freeman, J.M. Guss, C.E. Nockolds, R. Page and A. Webster, Acta Cryst., A26, 149 (1970).
48. J.M. Guss, C.E. Nockolds and A.M. Wood, "User Manual for a Computer Controlled Buerger-Supper Equi-inclination X-ray Diffractometer", (University of Sydney, 1970).
49. J. De Meulenaer and H. Tompa, Acta Cryst., 19, 1014 (1965).
50. "International Union of Crystallography. Commission on

Crystallographic Computing, Ottawa, 1969", F.R. Ahmed, S.R. Hall and C.P. Huber, Eds., (Munksgaard, Copenhagen, 1970).

51. N.W. Alcock, Acta Cryst., A25, 518 (1969).
52. S.C. Abrahams and E.T. Keve, Acta Cryst., A27, 157 (1971).
53. L. Srinivasan, Ph.D. Thesis, Flinders University (1972).
54. H.A. Levy, Acta Cryst., 9, 679 (1956).
55. W.C. Hamilton, Acta Cryst., 18, 502 (1965).
56. W.C. Hamilton and S.C. Abrahams, Acta Cryst., A26, 18 (1970).
57. R.S. Mulliken, J. Chem. Phys., 7, 14 (1939).
58. S.F. Mason, Quart. Rev., 17, 20 (1963).
59. W. Voigt, Ann. Phys., 18, 645 (1905).
60. F. Woldbye, "Studier Over Optisk Activitet", (Polyteknisk Forlag, Copenhagen, 1969).
61. J.P. Mathieu, J. Chim. Phys., 33, 78 (1936).
62. H. Eyring, J. Walter and G.E. Kimball, "Quantum Chemistry" (John Wiley and Sons, Inc., New York, 1949).
63. L. Rosenfeld, Z. Physik, 52, 161 (1928).
64. E.U. Condon, Rev. Mod. Phys., 9, 432 (1937).
65. A.D. Liehr, J. Phys. Chem., 68, 665 (1964).
66. D. Sutton, "Electronic Spectra of Transition Metal Complexes" (McGraw-Hill, London, 1968).
67. P.G. Beddoe, M.Sc. Thesis, University of East Anglia (1965).
68. R.D. Gillard, Progr. Inorg. Chem., 7, 215 (1966).
69. R.P. Feynman, R.B. Leighton and M. Sands, "The Feynman Lectures on Physics, Vol. I" (Addison-Wesley, Reading, Mass., 1965).

70. T. B urer, *Helv. Chim. Acta*, 46, 242 (1963).
71. S. Kirschner, *Coord. Chem. Rev.*, 2, 461 (1967).
72. F.P. Dwyer, I.K. Reid and F.L. Garvan, *J. Amer. Chem. Soc.*, 83, 1285 (1961).
73. R.F. Stewart, E.R. Davidson and W.T. Simpson, *J. Chem. Phys.*, 42, 3175 (1965).
74. "International Tables for X-ray Crystallography" (The Kynoch Press, Birmingham, U.K.: Vol. I 1965; II 1967; III 1968).
75. D.T. Cromer and J.T. Waber, *Acta Cryst.*, 18, 104 (1965).
76. K.N. Raymond, D.W. Meek and J.A. Ibers, *Inorg. Chem.*, 7, 1111 (1968).
77. L. Pauling, *J. Chem. Soc.*, 1461 (1948).
78. R.H. Stanford, Jr., and J. Waser, *Acta Cryst.*, A28, 213 (1972).
79. W.C. Hamilton, "Statistics in Physical Science" (Ronald Press, New York, 1964).
80. "Handbook of Chemistry and Physics", R.C. Weast, Ed., (The Chemical Rubber Co., Ohio: 47th Edtn., 1966).
81. F.A. Cotton and G. Wilkinson, "Advanced Inorganic Chemistry" (Wiley-Interscience, U.S.A., 1962).
82. N.L. Allinger, M.A. Miller, F.A. Van-Catledge and J.A. Hirsch, *J. Amer. Chem. Soc.*, 89, 4345 (1967).
83. J.O. Hirschfelder, C.F. Curtiss and R.B. Bird, "Molecular Theory of Gases and Liquids" (Wiley, New York, 1964).
84. G.N. Ramachandran in "Symmetry and Function of Biological Systems at the Macromolecular Level", Nobel Symposium 11 (1968).

85. P.-K. Hon, Ph.D. Thesis, University of Illinois (1964): University Microfilms, Inc., Ann Arbor, Michigan: Diss. Abs., 26, 1906 (1965).
86. B. Morosin and J.R. Brathovde, *Acta Cryst.*, 17, 705 (1964).
87. K.R. Butler and M.R. Snow, *J. Chem. Soc. (A)*, 565 (1971).
88. N.E. Kime and J.A. Ibers, *Acta Cryst.*, B25, 168 (1969).
89. K. Matsumoto and H. Kuroya, *Bull. Chem. Soc. Japan*, 45, 1755 (1972).
90. K. Matsumoto and H. Kuroya, *Bull. Chem. Soc. Japan*, 44, 3491 (1971).
91. J.W. Jeffrey, *Acta Cryst.*, A25, 153 (1969).
92. K.N. Raymond, P.W.R. Corfield and J.A. Ibers, *Inorg. Chem.*, 7, 1362 (1968).
93. K.R. Butler and M.R. Snow, *Chem. Comm.*, 550 (1971).
94. R.J. Geue and M.R. Snow, *J. Chem. Soc. (A)*, 2981 (1971).
95. P.F. Crossing, M.Sc. Thesis, University of Adelaide (1972).
96. K.R. Butler and M.R. Snow, *Inorg. Chem.*, 10, 1838 (1971).
97. K.N. Raymond and J.A. Ibers, *Inorg. Chem.*, 7, 2333 (1968).
98. B.W. Brown and E.C. Lingafelter, *Acta Cryst.*, 17, 254 (1964).
99. F.M. Jaeger, *Rec. Trav. Chim.*, 38, 171 (1919).
100. H.T.S. Britton and M.E.D. Jarrett, *J. Chem. Soc.*, 1728 (1935).
101. W. Lapraik, *Chemical News*, 67, 219 (1893).
102. J.C. Chang, *J. Inorg. Nuclear Chem.*, 30, 945 (1968).
103. G. Lohmiller and W.W. Wendlandt, *J. Inorg. Nuclear Chem.*, 32, 2430 (1970).
104. A.I. Vogel, "Quantitative Inorganic Analysis" (3rd Edtn., Longmans, London, 1961).

105. G.H. Cartledge and P.M. Nichols, *J. Amer. Chem. Soc.*, 62, 3057 (1940).
106. K.R. Ashley and K. Lane, *Inorg. Chem.*, 9, 1795 (1970).
107. M.J. Schmeil, I. Nakagawa, S. Mizushima and J.V. Quagliano, *J. Amer. Chem. Soc.*, 81, 287 (1959).
108. T.E. MacDermott, *Inorg. Chim. Acta*, 2, 81 (1968).
109. P.F. Crossing, personal communication.
110. P.F. Crossing and M.R. Snow, *J. Chem. Soc. (Dalton)*, 295 (1972).
111. M. Ito, F. Marumo and Y. Saito, *Acta Cryst.*, B27, 2187 (1971).
112. B. Morosin, *Acta Cryst.*, 19, 131 (1965).
113. R.F. Bryan, P.T. Greene, P.F. Stokely and E.W. Wilson, Jr., *Inorg. Chem.*, 10, 1468 (1971).
114. W.D. Horrocks, Jr., D.L. Johnston and D. MacInnes, *J. Amer. Chem. Soc.*, 92, 7620 (1970).
115. W.D. Horrocks, Jr., personal communication (1972).
116. S.C. Abrahams, *Quart. Rev.*, 10, 407 (1956).
117. R.J. Gillespie and R.S. Nyholm, *Quart. Rev.*, 11, 339 (1957).
118. K. Ramaswamy and P. Muthusubramanian, *J. Mol. Struct.*, 6, 205 (1970).
119. E.L. Eliel, *Svensk kem. Tidskr. (Eng. Trans.)*, 81, 22 (1969).
120. T. Nomura, F. Marumo and Y. Saito, *Bull. Chem. Soc. Japan*, 42, 1016 (1969).
121. G.D. Andreotti, L. Cavalca and P. Sgarabotto, *Gazz. Chim. Italiana*, 101, 494 (1971).
122. H. Kawaguchi, K. Matsumoto, H. Kuroya and S. Kawaguchi, *Chemistry Letters (Japan)*, 125 (1972).

123. E. Yasaki, I. Oonishi, H. Kawaguchi and Y. Komiyama, *Bull. Chem. Soc. Japan*, 43, 1354 (1970).
124. K. Matsumoto, S. Ooi and H. Kuroya, *Bull. Chem. Soc. Japan*, 43, 1903 (1970).
125. A. Pajunen, *Suomen Kem.*, B42, 15 (1969).
126. A. Pajunen, *Suomen Kem.*, B41, 232 (1968).
127. Commission on the Nomenclature of Inorganic Chemistry, *Inorg. Chem.*, 9, 1 (1970).
128. IUPAC Information Bulletin, No. 33, 68 (1968).
129. F.P. Dwyer and A.M. Sargeson, *J. Amer. Chem. Soc.*, 81, 2335 (1959).
130. "Advanced Methods of Crystallography", G.N. Ramachandran, Ed., (Academic Press, London, 1964).
 - (a) G.N. Ramachandran, p. 25.
 - (b) S. Ramaseshan, p. 67.
131. R. Srinivasan, *Advances in Structure Research by Diffraction Methods*, 4, 105 (1972).
132. J.H. Enemark, M.S. Quinby, L.L. Reed, M.J. Steuck and K.K. Walthers, *Inorg. Chem.*, 9, 2397 (1970).
133. E.W. Hughes, *J. Amer. Chem. Soc.*, 63, 1737 (1941).
134. J. Hidaka and B.E. Douglas, *Inorg. Chem.*, 3, 1724 (1964).
135. S. Merlino, *Acta Cryst.*, B24, 1441 (1968).
136. T. Brennan and I. Bernal, *J. Phys. Chem.*, 73, 443 (1969).
137. S. Merlino, *Acta Cryst.*, B25, 2270 (1969).
138. J.F. McConnell and A. Schwartz, *Acta Cryst.*, B28, 1546 (1972).

139. A.C. Villa, A.G. Manfredotti, C. Guastini and M. Nardelli, *Acta Cryst.*, B28, 2231 (1972).
140. L. Pauling, "Nature of the Chemical Bond", (3rd Edtn., Cornell Univ. Press, N.Y., 1960).
141. S. Asbrink, *Acta Cryst.*, A26, 385 (1970).
142. H.L. Yakel and I. Fankuchen, *Acta Cryst.*, 15, 1188 (1962).
143. J.W. Jeffrey and A. Whitaker, *Acta Cryst.*, 19, 963 (1965).
144. D.W. Engel, *Acta Cryst.*, B28, 1496 (1972).
145. M. Delépine, *Bull. Soc. Chim. France, Series 5*, 1, 1256 (1934).
146. M. Delépine and R. Charronat, *Bull. Soc. France Mineral.*, 53, 73 (1930).
147. P. Andersen, F. Galsbøl and S.E. Harnung, *Acta Chem. Scand.*, 23, 3027 (1969).
148. A. Werner, *Ber.*, 45, 1228 (1912).
149. F.M. Jaeger, *Bull. Soc. Chim. France, Series 5*, 4, 1201 (1937).
150. A.M. Sargeson in "Chelating Agents and Metal Chelates", Chapt. 5: F.P. Dwyer and D.P. Mellor, Eds., (Academic Press Inc., New York, 1964).
151. J.C. Bailar, Jr., and E.M. Jones, *Inorg. Synth.*, 1, 35 (1939).
152. R.C. Johnson, *J. Chem. Educ.*, 47, 702 (1970).
153. G.B. Kauffman, L.T. Takahashi and N. Sugisaka, *Inorg. Synth.*, 8, 207 (1966).
154. N.C. Kneten and S.T. Spees, Jr., *J. Inorg. Nuclear Chem.*, 33, 2437 (1971).

155. S.T. Spees and P.Z. Petrak, *J. Inorg. Nuclear Chem.*, 32, 1229 (1970).
156. K.A. Jones, R.J. Acheson, B.R. Wheeler and A.K. Galwey, *Trans. Faraday Soc.*, 64, 1887 (1968).
157. R.E. Hamm and R.H. Perkins, *J. Amer. Chem. Soc.*, 77, 2083 (1955).
158. H.F. Bauer and W.C. Drinkard, *J. Amer. Chem. Soc.*, 82, 5031 (1960).
159. M. Mori, M. Shibata, E. Kyuno and T. Adachi, *Bull. Chem. Soc. Japan*, 29, 883 (1956).
160. H.F. Bauer and W.C. Drinkard, *Inorg. Synth.*, 8, 202 (1966).
161. C.J. Dippel and F.M. Jaeger, *Rec. Trav. chim.*, 50, 547 (1931).
162. T.G. Appleton and J.R. Hall, *Inorg. Chem.*, 9, 1800, 1807 (1970).
163. C. Harries and T. Haga, *Ber.*, 31, 550 (1898); 32, 1191 (1899).
164. C.J. Dippel, *Rec. Trav. chim.*, 50, 525 (1931).
165. B. Bosnich and J.M. Harrowfield, *J. Amer. Chem. Soc.*, 94, 3425 (1972).
166. I.R. Jonasson, S.F. Lincoln and D.R. Stranks, *Aust. J. Chem.*, 23, 2267 (1970).
167. E. Pedersen, *Acta Chem. Scand.*, 24, 3362 (1970).
168. R.D. Gillard and P.R. Mitchell, *Inorg. Synth.*, 13, 184 (1972).
169. G.E. Ryschkewitsch and J.M. Garrett, *J. Amer. Chem. Soc.*, 90, 7234 (1968).
170. G.B. Kauffman and L.T. Takahashi, *Inorg. Synth.*, 8, 227 (1966).
171. G.T. Morgan and F.H. Burstall, *J. Chem. Soc.*, 2213 (1931).
172. F.H. Burstall and R.S. Nyholm, *J. Chem. Soc.*, 3570 (1952).
173. R.A. Palmer and T.S. Piper, *Inorg. Chem.*, 5, 864 (1966).

174. F.H. Burstall, *J. Chem. Soc.*, 173 (1936).
175. F.P. Dwyer, J.E. Humpoletz and R.S. Nyholm, *Proc. Roy. Soc. New South Wales*, 80, 212 (1946).
176. F.P. Dwyer and E.C. Gyarfaz, *Proc. Roy. Soc. New South Wales*, 83, 232 (1949).
177. A.M. Sargeson, personal communication (1972).
178. W.J. Robinson, personal communication (1972).
179. T.E. MacDermott and A.M. Sargeson, *Aust. J. Chem.*, 16, 334 (1963).
180. R.L.C. Russell, *Diss. Abs.*, 31, 1805 B (1970).
181. B.E. Douglas, communication with M.R. Snow (1972).
182. F. Woldbye, *Proc. Roy. Soc.*, A297, 79 (1967).
183. W. Kuhn, *Naturwiss.*, 26, 289 (1938).
184. A.J. McCaffery and S.F. Mason, *Proc. Chem. Soc.*, 388 (1962).
185. R.D. Gillard, S.H. Laurie and P.R. Mitchell, *J. Chem. Soc. (A)*, 3006 (1969).
186. A.L. Odell and D. Shooter, *J. Chem. Soc. (Dalton)*, 135 (1972).
187. M.R. Snow and K.R. Butler, *Proc. XIV ICCC, Toronto, Abstracts*, 390 (1972).
188. S.F. Mason and B.J. Norman, *Chem. Comm.*, 73 (1965).
189. J.R. Gollogly and C.J. Hawkins, *Chem. Comm.*, 689 (1968).
190. P.G. Beddoe and S.F. Mason, *Inorg. Nuclear Chem. Letters*, 4, 433 (1968).
191. T. Bürer, *Helv. Chim. Acta*, 46, 2388 (1963).
192. A.J. McCaffery and S.F. Mason, *Mol. Phys.*, 6, 359 (1963).

193. R.E. Ballard, A.J. McCaffery and S.F. Mason, Proc. Chem. Soc., 331 (1962).
194. J.H. Worrell, Inorg. Synth., 13, 195 (1972).
195. A.M. Sargeson, Transition Metal Chem., 3, 303 (1966).
196. T. Aoki, K. Matsumoto, S. Ooi and H. Kuroya, Proc. 21st Annual Meeting of the Chem. Soc. Japan, 1122 (1968).
197. A.J. McCaffery and S.F. Mason, Proc. Chem. Soc., 211 (1963).
198. I. Hanazaki and S. Nagakura, Inorg. Chem., 8, 648, 654 (1969).
199. A.J. McCaffery, S.F. Mason and B.J. Norman, J. Chem. Soc. (A), 1428 (1969).
200. F.P. Dwyer and E.C. Gyarfas, Proc. Roy. Soc. New South Wales, 83, 263 (1949).
201. G.K. Schweitzer and J.M. Lee, J. Phys. Chem., 56, 195 (1952).
202. A.J. McCaffery, S.F. Mason and B.J. Norman, Proc. VIII ICCC, Vienna, 109 (1964).
203. F.P. Dwyer and E.C. Gyarfas, Proc. Roy. Soc. New South Wales, 85, 135 (1951).
204. R.D. Gillard, R.E.E. Hill and R. Maskill, J. Chem. Soc. (A), 707 (1970).
205. S.F. Mason and B.J. Norman, J. Chem. Soc. (A), 1442 (1969).
206. R.G. Bray, J. Ferguson and C.J. Hawkins, Proc. XII ICCC, Sydney, 88 (1969).
207. T.S. Piper and R.L. Carlin, J. Chem. Phys., 35, 1809 (1961):
33, 608 (1960).

208. C.H. Johnson, *Trans. Faraday Soc.*, 31, 1612 (1935).
209. H. Krebs, J. Diewald, H. Arlitt and J.A. Wagner, *Z. anorg. Chem.*, 287, 98 (1956).
210. F.P. Dwyer and A.M. Sargeson, *J. Phys. Chem.*, 60, 1331 (1956).
211. W. Wahl, *Ber.*, 60, 399 (1927).
212. G.J. Burrows and K.H. Lauder, *J. Amer. Chem. Soc.*, 53, 3600 (1931).
213. F.P. Dwyer, T.E. MacDermott and A.M. Sargeson, *J. Amer. Chem. Soc.*, 85, 661, 2913 (1963).
214. R.D. Gillard, P.R. Mitchell and M.G. Price, *J. Chem. Soc. (Dalton)*, 1211 (1972).
215. A.J. McCaffery, S.F. Mason and B.J. Norman, *Chem. Comm.*, 661 (1966).
216. R.D. Gillard and G. Wilkinson, *J. Chem. Soc.*, 1368 (1964).
217. D. Reinen, *Structure and Bonding*, 6, 30 (1969).
218. E. König, *Inorg. Chem.*, 10, 2632 (1971).
219. C.J. Ballhausen, "Introduction to Ligand Field Theory" (McGraw-Hill, New York, 1962).
220. C.K. Jørgensen, "Modern Aspects of Ligand Field Theory" (North-Holland Pub. Co., Amsterdam, 1971).
221. D.S. McClure, *J. Chem. Phys.*, 36, 2757 (1962).
222. C.S.G. Phillips and R.J.P. Williams, "Inorganic Chemistry, Vol. 2" (Oxford, Clarendon Press, 1965).
223. K.V. Krishnamurty, G.M. Harris and V.S. Sastri, *Chem. Rev.*, 70, 171 (1970).
224. I. Hanazaki, F. Hanazaki and S. Nagakura, *J. Chem. Phys.*, 50, 265, 276 (1969).

225. M.R. Edelson and R.A. Plane, *Inorg. Chem.*, 3, 231 (1964).
226. A.S. Chakravarty, *J. Phys. Chem.*, 74, 4347 (1970).
227. N.K. Hamer, *Mol. Phys.*, 5, 455 (1962).
228. S. Sugano and Y. Tanabe, *J. Phys. Soc. Japan*, 13, 880 (1958).
229. F.A. Cotton, "Chemical Applications of Group Theory"
(Wiley-Interscience, New York, 1963).
230. E.B. Wilson, Jr., J.C. Decius and P.C. Cross, "Molecular
Vibrations" (McGraw-Hill, New York, 1955).
231. W.N. Shepard and L.S. Forster, *Theor. Chim. Acta*, 20, 135 (1971).
232. T. Yasui and B.E. Douglas, *Inorg. Chem.*, 10, 97 (1971).
233. Y. Kojima and M. Shibata, *Inorg. Chem.*, 10, 2382 (1971).
234. P.C. Healy and A.H. White, *J. Chem. Soc. (Dalton)*, 1883 (1972).
235. C.D. Flint, *Chem. Phys. Letters*, 11, 27 (1971).
236. T.S. Piper, *J. Chem. Phys.*, 36, 2224 (1962).
237. T.S. Piper and R.L. Carlin, *J. Chem. Phys.*, 36, 3330 (1962).
238. S.F. Mason, Plenary Lectures XII ICCG, Sydney, 335 (1969),
(Butterworths, London, 1970).
239. T.S. Piper and R.L. Carlin, *Inorg. Chem.*, 2, 260 (1963).
240. C.J. Hawkins, "Absolute Configuration of Metal Complexes" (Wiley,
New York, 1971).
241. A.A.G. Tomlinson, *J. Chem. Soc.*, 1409 (1971).
242. T.S. Piper, *J. Chem. Phys.*, 35, 1240 (1961).
243. J.D. Lebedda and R.A. Palmer, *Inorg. Chem.*, 10, 2704 (1971).
244. C.J. Ballhausen in "Spectroscopy in Inorganic Chemistry, Vol. 1",

- C.N.R. Rao and J.R. Ferraro, Eds. (Academic Press, New York, 1970).
245. S. Yamada and R. Tsuchida, *Bull. Chem. Soc. Japan*, 33, 98 (1960).
246. R. Dingle, *Chem. Comm.*, 304 (1965).
247. R. Dingle and C.J. Ballhausen, *Mat. Fys. Medd. Dan. Vid. Selsk.*, 35, No. 12 (1967).
248. S.F. Mason and B.J. Norman, *Proc. Chem. Soc.*, 339 (1964).
249. A.J. McCaffery, P.J. Stephens and P.N. Schatz, *Inorg. Chem.*, 6, 1614 (1967).
250. P.N. Schatz and A.J. McCaffery, *Quart. Rev.*, 23, 552 (1969).
251. H.U. Güdel, I. Trabjerg, M. Vala and C.J. Ballhausen, *Mol. Phys.*, 24, 1227 (1972).
252. R.L. Russell and B.E. Douglas, *Inorg. Chim. Acta*, 3, 426 (1969).
253. R.G. Denning, *Chem. Comm.*, 120 (1967).
254. L.E. Orgel, *J. Chem. Soc.*, 3, 3683 (1961).
255. T. Bürer, *Mol. Phys.*, 6, 541 (1963).
256. E. König and S. Kremer, *Theor. Chim. Acta*, 20, 143 (1971).
257. M. Gerloch, J. Lewis, G.G. Philips and P.N. Quested, *J. Chem. Soc. (A)*, 1941 (1970).
258. M. Gerloch, J. Lewis and R.C. Slade, *J. Chem. Soc. (A)*, 1422 (1969).
259. L.E. Orgel, *Nature*, 179, 1348 (1957).
260. S. Sugano, Y. Tanabe and H. Kamimura, "Multiplets of Transition Metal Ions in Crystals" (Academic Press, New York, 1970).
261. E. Duval, R. Lourat and R. Lacroix, *Phys. Stat. Sol. (b)*, 50, 627 (1972).

262. P.H. Davis and J.S. Wood, *Chem. Phys. Letters*, 4, 466 (1969).
263. P.H. Davis and J.S. Wood, *Inorg. Chem.*, 9, 1111 (1970).
264. T.S. Piper, *J. Amer. Chem. Soc.*, 83, 3908 (1961).
265. R.S. Cahn, C.K. Ingold and V. Prelog, *Angew. Chem. Int. Edn.*, 5, 385 (1966).
266. S.F. Mason, *Proc. Chem. Soc.*, 137 (1962).
267. L.I. Katzin and I. Eliezer, *Coord. Chem. Rev.*, 7, 331 (1972).
268. O.E. Weigang, Jr., *J. Chem. Phys.*, 42, 2244 (1965).
269. A.J. McCaffery, S.F. Mason, B.J. Norman and A.M. Sargeson, *J. Chem. Soc.*, 1304 (1968).
270. H. Poulet, *J. Chim. Phys.*, 59, 584 (1962).
271. W. Kuhn, *Trans. Faraday Soc.*, 26, 293 (1930).
272. F.S. Richardson, *Inorg. Chem.*, 11, 2366 (1972).
273. E. Drouard and J.P. Mathieu, *Compt. rend.*, 236, 2395 (1953).
274. S.K. Bose, *Indian J. Chem.*, 9, 493 (1971).
275. F.S. Richardson, *Inorg. Chem.*, 10, 2121 (1971).
276. C.E. Schäffer, *Proc. Roy. Soc.*, A297, 96 (1967).
277. O.E. Weigang, Jr., *J. Chem. Phys.*, 43, 3609 (1965).
278. S.E. Harnung, E.C. Ong and O.E. Weigang, Jr., *J. Chem. Phys.*, 55, 5711 (1971).
279. W.M. Reiff, *Chem. Phys. Letters*, 8, 297 (1971).
280. R. Engelman, *J. Chem. Phys.*, 45, 3862 (1966).
281. N.K. Hamer, *Mol. Phys.*, 5, 339 (1962).
282. R.G. Denning and T.S. Piper, *Inorg. Chem.*, 5, 1056 (1966).

283. B.H. O'Connor and D.H. Hale, *Acta Cryst.*, 21, 705 (1966).
284. C.A. Beevers and H. Lipson, *Z. Krist.*, 83, 123 (1932).
285. R. Strickland and F.S. Richardson, *J. Chem. Phys.*, 57, 589 (1972).
286. R. Grinter, M.J. Harding and S.F. Mason, *J. Chem. Soc. (A)*, 667 (1970).
287. P.L. Meredith and R.A. Palmer, *Chem. Comm.*, 1337 (1969).
288. B. Bosnich and J.M. Harrowfield, *J. Amer. Chem. Soc.*, 94, 989 (1972).
289. A. Moscovitz, C. Djerassi and K.M. Wellman, *Proc. Nat. Acad. Sci. U.S.A.*, 50, 799 (1963).
290. H.L. Smith and B.E. Douglas, *Inorg. Chem.*, 5, 784 (1966).
291. R. Larsson, S.F. Mason and B.J. Norman, *J. Chem. Soc. (A)*, 301 (1966).
292. P.G. Beddoe, M.J. Harding, S.F. Mason and B.J. Peart, *Chem. Comm.*, 1283 (1971).
293. P. Pfeiffer and K. Quehl, *Chem. Ber.*, 64, 2667 (1931): 65, 560 (1932).
294. V. Doron, W. Durham and D. Frazier, *Inorg. Nuclear Chem. Letters*, 7, 91 (1971).
295. R.C. Brasted, V.J. Landis, E.J. Kuhajek, P.E.R. Nordquist and L. Mayer in "Coordination Chemistry", S. Kirschner, Ed., (Plenum Press, New York, 1969).
296. B. Bosnich and J.M. Harrowfield, *J. Amer. Chem. Soc.*, 93, 4086 (1971).
297. E.W. Wilson and R.B. Martin, *Inorg. Chem.*, 9, 528 (1970).
298. C.T. Liu and B.E. Douglas, *Inorg. Chem.*, 3, 1356 (1964).
299. C.J. Hawkins, *Chem. Comm.*, 777 (1969).

300. F.R. Keene, G.H. Searle and S.F. Mason, *Chem. Comm.*, 893 (1970).
301. F.R. Keene and G.H. Searle, *Inorg. Chem.*, 11, 148 (1972).
302. A.J. McCaffery, S.F. Mason and B.J. Norman, *Chem. Comm.*, 49 (1965).
303. R. Larsson, G.H. Searle, S.F. Mason and A.M. Sargeson, *J. Chem. Soc.*, 1310 (1968).
304. B.E. Douglas and S. Yamada, *Inorg. Chem.*, 4, 1561 (1965).
305. S.K. Hall and B.E. Douglas, *Inorg. Chem.*, 8, 372 (1969).
306. S.F. Mason, *J. Chem. Soc. (A)*, 667 (1971).
307. S.F. Mason, A.M. Sargeson, R. Larsson, B.J. Norman, A.J. McCaffery and G.H. Searle, *Inorg. Nuclear Chem. Letters*, 2, 333 (1966).
308. J. Ferguson, *Progr. Inorg. Chem.*, 12, 159 (1970).
309. Y. Saito, K. Nakatsu, M. Shiro and H. Kuroya, *Bull. Chem. Soc. Japan*, 30, 795 (1957); *Acta Cryst.*, 8, 729 (1955).
310. M. Delépine, *Bull. Soc. Chim. France, Series 4*, 29, 656 (1921).
311. F.P. Dwyer, F.L. Garvan and A. Shulman, *J. Amer. Chem. Soc.*, 81, 290 (1959).
312. J.R. Gollogly and C.J. Hawkins, *Inorg. Chem.*, 11, 156 (1972).
313. S.R. Niketic and F. Woldbye, submitted for publication, preprint to M.R. Snow (1972).
314. F. Mizukami, H. Ito, J. Fujita and K. Saito, *Bull. Chem. Soc. Japan*, 45, 2129 (1972).
315. R.D. Gillard, *Inorg. Chim. Acta*, 1, 69 (1967).
316. C.W. van Saun and B.E. Douglas, *Inorg. Chem.*, 8, 1145 (1969).
317. C.W. van Saun and B.E. Douglas, *Inorg. Chem.*, 8, 115 (1969).

318. K. Yamasaki, J. Hidaka and Y. Shimura, *Bull. Chem. Soc. Japan*, 42, 119 (1969).
319. A.J. McCaffery, S.F. Mason and B.J. Norman, *J. Chem. Soc.*, 5094 (1965).
320. Y. Saito, *Pure Appl. Chem.*, 17, 21 (1968).
321. W. Kuhn and K. Bein, *Z. phys. Chem.*, B24, 335 (1934).
322. W. Kuhn and K. Bein, *Z. anorg. Chem.*, 216, 321 (1934).
323. G.R. Brubaker and L.E. Webb, *J. Amer. Chem. Soc.*, 91, 7199 (1969).
324. C.J. Hawkins and E. Larsen, *Acta Chem. Scand.*, 19, 185 (1965).
325. C. Djerassi, "Optical Rotatory Dispersion" (McGraw-Hill, New York, 1960).
326. F.S. Richardson, *J. Chem. Phys.*, 54, 2453 (1971).
327. S.F. Mason, *Chem. Comm.*, 856 (1969).
328. M. Shinada, *J. Phys. Soc. Japan*, 19, 1607 (1964).
329. A.D. Liehr, *J. Phys. Chem.*, 68, 3629 (1964).
330. A.D. Liehr, *Transition Metal Chem.*, 2, 165 (1966).
331. T.S. Piper and A.G. Karipides, *Inorg. Chem.*, 4, 923 (1965).
332. W. Moffitt, *J. Chem. Phys.*, 25, 467 (1956).
333. B. Bosnich, *Accounts Chem. Res.*, 2, 266 (1969).
334. S.F. Mason and B.J. Norman, *Inorg. Nuclear Chem. Letters*, 3, 285 (1967).
335. R.D. Gillard, R.E.E. Hill and R. Maskill, *J. Chem. Soc. (A)*, 1447 (1970).
336. S. Sugano, *J. Chem. Phys.*, 33, 1883 (1960).
337. E.U. Condon and G.H. Shortley, "Theory of Atomic Spectra" (Cambridge U.P., New York, 1951).

338. "The Concise Oxford Dictionary", H.W. Fowler and F.G. Fowler, Eds., (Oxford, Clarendon Press, 4th Edtn., 1959).
339. T.S. Piper and R.L. Carlin, *J. Chem. Phys.*, 33, 1208 (1960).
340. F.S. Richardson, personal communication (1972).
341. T.S. Piper and A. Karipides, *J. Amer. Chem. Soc.*, 86, 5039 (1964).
342. M. Ito, F. Marumo and Y. Saito, *Inorg. Nuclear Chem. Letters*, 6, 519 (1970).
343. E. Larsen, G.N. La Mar, B.E. Wagner, J.E. Parks and R.H. Holm, *Inorg. Chem.*, 11, 2652 (1972).
344. M. Gerloch and D.J. Mackey, *J. Chem. Soc. (A)*, 3030, 3040 (1970).
345. M.R. Snow, personal communication (1972), of work in C.E. Schäffer's research group.
346. G.B. Thomas, Jr., "Calculus and Analytic Geometry" (Addison-Wesley, Mass., 2nd Edtn., 1960).
347. A.C. Aitken, "Determinants and Matrices" (Oliver and Boyd, Edinburgh and London, 9th Edtn., 1962).
348. R. Eisenberg and H.B. Gray, *Inorg. Chem.*, 6, 1844 (1967).
349. R. Eisenberg, E.I. Stiefel, R.C. Rosenberg and H.B. Gray, *J. Amer. Chem. Soc.*, 88, 2874 (1966).
350. R. Eisenberg and J.A. Ibers, *Inorg. Chem.*, 5, 411 (1966).
351. R. Eisenberg and J.A. Ibers, *J. Amer. Chem. Soc.*, 87, 3776 (1965).
352. J.P.R. De Villiers and J.C.A. Boeyens, *Acta Cryst.*, B27, 2335 (1971).
353. M. Iwata, K. Nakatsu and Y. Saito, *Acta Cryst.*, B25, 2562 (1969).

354. K. Nakatsu, Bull. Chem. Soc. Japan, 35, 832 (1962).
355. K. Nakatsu, Y. Saito and H. Kuroya, Bull. Chem. Soc. Japan, 29, 428 (1956).
356. K. Nakatsu, M. Shiro, Y. Saito and H. Kuroya, Bull. Chem. Soc. Japan, 30, 158 (1957).
357. D.J. Hodgson, P.K. Hale and W.E. Hatfield, Inorg. Chem., 10, 1061 (1971).
358. E.N. Deusler and K.N. Raymond, Inorg. Chem., 10, 1486 (1971).
359. J.T. Veal and D.J. Hodgson, Inorg. Chem., 11, 597 (1972).
360. H. Iwasaki and Y. Saito, Bull. Chem. Soc. Japan, 39, 92 (1966).
361. F. Marumo, Y. Utsumi and Y. Saito, Acta Cryst., B26, 1492 (1970).
362. Mazhar-Ul-Haque, C.N. Caughlan and K. Emerson, Inorg. Chem., 9, 2421 (1970).
363. L.N. Swink and M. Atoji, Acta Cryst., 13, 639 (1960).
364. Y.I. Smolin, Soviet Physics Crystallog. (Eng. trans.), 15, 23 (1970).
365. D.L. Cullen and E.C. Lingafelter, Inorg. Chem., 9, 1858 (1970).
366. N.V. Podberezskaya, V.V. Bakakin and S.V. Borisov, J. Struct. Chem. (Eng. trans.), 10, 734 (1969).
367. H.J. Peresie and J.A. Stanko, Chem. Comm., 1674 (1970).
368. L.D.C. Bok, J.G. Liepoldt and S.S. Basson, Z. anorg. Chem., 389, 307 (1972).
369. N.V. Podberezskaya and S.V. Borisov, J. Struct. Chem. (Eng. trans.), 12, 1034 (1971).

370. Y. Saito, personal communication (1972).
371. A. Kobayashi, F. Marumo, Y. Saito, J. Fujita and F. Mizukami, *Inorg. Nuclear Chem. Letters*, 7, 777 (1971).
372. R.J. Geue, personal communication.
373. G. Albrecht, *Z. Chem.*, 3, 182 (1963).
374. B.A. Frenz and J.A. Ibers, *Inorg. Chem.*, 11, 1109 (1972).
375. Y. Watanabe and K. Yamahata, *Sci. Papers Inst. Phys. Chem. Research (Japan)*, 64, 71 (1970).
376. M. Bonamico, G. Dessy, V. Fares and C. Scaramuzza, *Ann. Chim. (Italy)*, 60, 644 (1970).
377. C. Furlani, P. Porta, A. Sgamellotti and A.A.G. Tomlinson, *Chem. Comm.*, 1046 (1969).
378. A. Avdeef, J.P. Fackler, Jr., and R.G. Fischer, *J. Amer. Chem. Soc.*, 92, 6972 (1970).
379. D.F. Lewis, S.J. Lippard and J.A. Zubieta, *Inorg. Chem.*, 11, 823 (1972).
380. P.C. Healy and A.H. White, *J. Chem. Soc. (Dalton)*, 1163 (1972).
381. S. Merlino and F. Sartori, *Acta Cryst.*, B28, 972 (1972).
382. H.V.F. Schousboe-Jensen and R.G. Hazell, *Acta Chem. Scand.*, 26, 1375 (1972).
383. C. Furlani, A.A.G. Tomlinson, P. Porta and A. Sgamellotti, *J. Chem. Soc. (A)*, 2929 (1970).
384. J.N. van Niekerk and F.R.L. Schoening, *Acta Cryst.*, 5, 499 (1952).
385. B.C. Dalzell and K. Eriks, *J. Amer. Chem. Soc.*, 93, 4298 (1971).

386. J.J. Flynn and F.P. Boer, *J. Amer. Chem. Soc.*, 91, 5756 (1969).
387. T.A. Hamor and D.J. Watkin, *Chem. Comm.*, 440 (1969).
388. J.N. van Niekerk and F.R.L. Schoening, *Acta Cryst.*, 5, 196 (1952).
389. C.G. Pierpont and R. Eisenberg, *J. Chem. Soc. (A)*, 2285 (1971).
390. D. van der Helm, L.L. Merritt, R. Degeilh and C.H. MacGillavry, *Acta Cryst.*, 18, 355 (1965).
391. B. Morosin and H. Montgomery, *Acta Cryst.*, B25, 1354 (1969).
392. J. Iball and C.H. Morgan, *Acta Cryst.*, 23, 239 (1967).
393. L.M. Shkol'nikova and E.A. Shugam, *Soviet Phys. Crystallog.* (Eng. trans.), 5, 24 (1960).
394. E.A. Shugam and L.M. Shkol'nikova, *Soviet Phys. Crystallog.* (Eng. trans.), 1, 378 (1956).
395. W.H. Watson, Jr., and Chi-Tsun Lin, *Inorg. Chem.*, 5, 1074 (1966).
396. M.R. Truter and B.L. Vickery, *J. Chem. Soc. (Dalton)*, 395 (1972).
397. M.D. Joesten, M.S. Hussain and P.G. Lenhert, *Inorg. Chem.*, 9, 151 (1970).
398. B.F. Hoskins, personal communication (1972).
399. R. Beckett, G.A. Heath, B.F. Hoskins, B.P. Kelly, R.L. Martin, I.A.G. Roos and P.L. Weickhardt, *Inorg. Nuclear Chem. Letters*, 6, 257 (1970).
400. P.E. Jones and L. Katz, *Acta Cryst.*, B25, 745 (1969).
401. L. Katz, personal communication (1972).
402. R. Beckett and B.F. Hoskins, *Inorg. Nuclear Chem. Letters*, 8, 683 (1972).
403. R.W.G. Wyckoff, "Crystal Structures", Vol. 2, pp. 6-8 (Wiley,

New York, 2nd Edtn., 1964).

404. E.B. Fleischer and E. Klem, *Inorg. Chem.*, 4, 637 (1965).
405. K. Matsumoto, personal communication (1972).
406. D.L. Johnston, W.L. Rohrbaugh and W. DeW. Horrocks, Jr.,
Inorg. Chem., 10, 1474 (1971).
407. U. Thewalt, *Chem. Ber.*, 104, 2657 (1971).
408. J.W. Lethbridge, L.S. Dent Glasser and H.F.W. Taylor,
J. Chem. Soc. (A), 1862 (1970).
409. A. Zalkin, J.D. Forrester and D.H. Templeton, *J. Amer. Chem. Soc.*, 88, 1810 (1966).
410. B.N. Figgis, L.G.B. Wadley and J. Graham, *Acta Cryst.*, B28, 187 (1972).
411. B.N. Figgis and L.G.B. Wadley, *J. Chem. Soc. (Dalton)*, 2182 (1972).
412. A. Kobayashi, F. Marumo and Y. Saito, *Acta Cryst.*, B28, 2709 (1972).
413. D. Witiak, J.C. Clardy and D.S. Martin, Jr., *Acta Cryst.*, B28, 2694 (1972).
414. O.P. Andersen, *J. Chem. Soc. (Dalton)*, 2597 (1972).
415. E.L. Muetterties and L.J. Guggenberger, *J. Amer. Chem. Soc.*, 94, 8046 (1972).
416. R.H. Boyd, *J. Chem. Phys.*, 49, 2574 (1968).
417. M.R. Snow, *J. Amer. Chem. Soc.*, 92, 3610 (1970).
418. Y. Saito, *Proc. XIV ICCS Toronto, Abstracts*, 91 (1972).
419. G.R. Brubaker, communication with M.R. Snow (1971-72).
420. G. Jacobs and F. Speke, *Acta Cryst.*, 8, 67 (1955).

421. D.E. Corbridge, Ph.D. Thesis, University of Leeds (1951).
422. M. Shiro and Q. Fernando, Chem. Comm., 350 (1971).
423. B.F. Hoskins and B.P. Kelly, Chem. Comm., 1517 (1968).
424. B.F. Hoskins and B.P. Kelly, Chem. Comm., 45 (1970).
425. J.N. van Niekerk and F.R.L. Schoening, Acta Cryst., 5, 475 (1952).
426. G.F. Brown and E.I. Stiefel, Chem. Comm., 728 (1970).
427. A.E. Smith, G.N. Schrauzer, V.P. Mayweg and W.S. Heinrich, J. Amer. Chem. Soc., 87, 5798 (1965).
428. V.M. Padmanabhan, Proc. Indian Acad. Sci. (A), 47, 329 (1958).
429. M.R. Snow, personal communication.
430. A. Forman and L.E. Orgel, Mol. Phys., 2, 362 (1959).
431. H.S. Jarrett, J. Chem. Phys., 27, 1298 (1957).
432. E.C. Lingafelter and R.L. Braun, J. Amer. Chem. Soc., 88, 2951 (1967).
433. P.E. Jones and L. Katz, Acta Cryst., B28, 3438 (1972).
434. R.E. Newnham and Y.M. De Haan, Z. Krist., 117, 235 (1962).
435. Y. Iitaka, I. Watanabe, I.T. Harrison and S. Harrison, J. Amer. Chem. Soc., 90, 1092 (1968).
436. E.L. Muetterties, J. Amer. Chem. Soc., 90, 5097 (1968).
437. R.J. Gillespie, Canad. J. Chem., 38, 818 (1960).
438. R. Eisenberg, Progr. Inorg. Chem., 12, 295 (1970).
439. J.C. Bailar, Jr., J. Inorg. Nuclear Chem., 8, 165 (1958).
440. R.C. Fay and T.S. Piper, Inorg. Chem., 3, 348 (1964).
441. S.S. Eaton, J.R. Hutchison, R.H. Holm and E.L. Muetterties, J. Amer. Chem. Soc., 94, 6411 (1972).

442. E.I. Stiefel and G.F. Brown, *Inorg. Chem.*, 11, 436 (1972).
443. R. Hultgren, *Phys. Rev.*, 40, 891 (1932).
444. C.S. Springer, Jr., and R.E. Sievers, *Inorg. Chem.*, 6, 852 (1967).
445. W.O. Gillum, R.A.D. Wentworth and R.F. Childers, *Inorg. Chem.*, 9, 1824 (1970).
446. F.A. Cotton and P. Legzdins, *Inorg. Chem.*, 7, 1777 (1968).
447. L.H. Pignolet, R.A. Lewis and R.H. Holm, *J. Amer. Chem. Soc.*, 93, 360 (1971).
448. E.I. Stiefel, Z. Dori and H.B. Gray, *J. Amer. Chem. Soc.*, 89, 3353 (1967).
449. J.C.A. Boeyens, personal communication (1972).
450. I. Grenthe, *Acta Chem. Scand.*, 26, 1479 (1972).
451. J.C.A. Boeyens, *J. Chem. Phys.*, 54, 75 (1971).
452. M. Kuhr and H. Musso, *Angew. Chem. Internat. Edn.*, 8, 147 (1969).
453. C.S. Erasmus and J.C.A. Boeyens, *Acta Cryst.*, B26, 1843 (1970).
454. J.P.R. De Villiers and J.C.A. Boeyens, *Acta Cryst.*, B27, 692 (1971).
455. L. Helmholtz, *J. Amer. Chem. Soc.*, 61, 1544 (1939).
456. J. Albertsson, *Acta Chem. Scand.*, 26, 985 (1972).
457. J. Albertsson, *Acta Chem. Scand.*, 26, 1023 (1972).
458. J. Albertsson, *Acta Chem. Scand.*, 24, 1213 (1970).
459. J. Albertsson, *Acta Chem. Scand.*, 24, 3527 (1970).
460. J. Albertsson, *Acta Chem. Scand.*, 22, 1563 (1968).
461. J. Albertsson, *Acta Chem. Scand.*, 26, 1005 (1972).
462. E.L. Muetterties and C.H. Wright, *Quart. Rev.*, 21, 109 (1967).

463. S.C. Cummings and D.H. Busch, *J. Amer. Chem. Soc.*, 92, 1924 (1970).
464. R. Dingle, *J. Chem. Phys.*, 50, 545 (1969).
465. A.F. Wells, "Structural Inorganic Chemistry" (Oxford U.P., 1962).
466. H.D. Megaw, *Acta Cryst.*, B24, 149 (1968).
467. W.H. Baur, *Trans. Amer. Cryst. Assoc.*, 6, 129 (1970).
468. J.B. Goodenough, *Progr. Solid State Chem.*, 5, 145 (1971).
469. K. Drager and A. Knappwost, *Z. phys. Chem.*, 81, 31 (1972).
470. C.A. Bates and R.F. Jasper, *J. Phys. C. Solid State Phys.*, 4, 2330, 2341 (1971).
471. J. Ferguson and P.E. Fielding, *Chem. Phys. Letters*, 10, 262 (1971).
472. R. Dickinson and L. Pauling, *J. Amer. Chem. Soc.*, 45, 1466 (1923).
473. S.O. Wandiga, J.E. Sarneski and F.L. Urbach, *Inorg. Chem.*, 11, 1349 (1972).
474. G.E. Humiston, *Diss. Abstr.*, B31, 3240 (1970).
475. G.E. Humiston and J.E. Brady, *Inorg. Chem.*, 8, 1773 (1969).
476. J.E. Brady, F. Dachille and C.D. Schmulbach, *Inorg. Chem.*, 7, 287 (1968).
477. H.E. Le May, Jr., in "Coordination Chemistry", S. Kirschner, Ed., (Plenum Press, New York, 1969).
478. C. Kutal and J.C. Bailar, Jr., *J. Phys. Chem.*, 76, 119 (1972).
479. S.F. Mason and B.J. Norman, *Chem. Comm.*, 48 (1965).
480. R.A.D. Wentworth, *Chem. Comm.*, 532 (1965).
481. E.A. Boudreaux, O.E. Weigang, Jr., and J.A. Turner, *Chem. Comm.*, 378 (1966).

482. F. Woldbye, *Rec. Chem. Progr.*, 24, 197 (1963).
483. B.E. Douglas, *Inorg. Chem.*, 4, 1813 (1965).
484. H.L. Smith and B.E. Douglas, *J. Amer. Chem. Soc.*, 86, 3885 (1964).
485. S.F. Mason and B.J. Norman, *J. Chem. Soc. (A)*, 307 (1966).
486. J.K. Beattie, *Accounts Chem. Res.*, 4, 253 (1971).
487. J.L. Sudmeier, G.L. Blackmer, C.H. Bradley and F.A.L. Anet, *J. Amer. Chem. Soc.*, 94, 757 (1972).
488. S.F. Mason, *Proc. Roy. Soc.*, A297, 3 (1967).
489. J.E. Sarneski and F.L. Urbach, *J. Amer. Chem. Soc.*, 93, 884 (1971).
490. Y. Saito, T. Nomura and F. Marumo, *Bull. Chem. Soc. Japan*, 41, 530 (1968).
491. J.R. Gollogly and C.J. Hawkins, *Inorg. Chem.*, 9, 576 (1970).
492. J.R. Gollogly, C.J. Hawkins and J.K. Beattie, *Inorg. Chem.*, 10, 317 (1971).
493. J.L. Sudmeier and G.L. Blackmer, *Inorg. Chem.*, 10, 2010 (1971).
494. F.P. Dwyer, A.M. Sargeson and L.B. James, *J. Amer. Chem. Soc.*, 86, 590 (1964).
495. S. Bagger, unpublished calculations (see refs. 60, 67, 313).
496. F.A. Journak and K.N. Raymond, *Inorg. Chem.*, 11, 3149 (1972).
497. F.R. Keene, personal communication (1971).
498. H. Elsbernd and J.K. Beattie, *J. Amer. Chem. Soc.*, 91, 4573 (1969).
499. L.R. Froebe and B.E. Douglas, *Inorg. Chem.*, 9, 1513 (1970).
500. J.L. Sudmeier and G.L. Blackmer, *J. Amer. Chem. Soc.*, 92, 5238 (1970).
501. J. Donohue, *J. Mol. Biol.*, 45, 231 (1969).

502. W.C. Hamilton and J.A. Ibers, "Hydrogen Bonding in Solids" (W.A. Benjamin, New York, 1968).
503. A.S.N. Murthy and C.N.R. Rao, *J. Mol. Struct.*, 6, 253 (1970).
504. S. Kaizaki, J. Hidaka and Y. Shimura, *Bull. Chem. Soc. Japan*, 43, 1100 (1970).
505. L.T. Taylor and D.H. Busch, *J. Amer. Chem. Soc.*, 89, 5372 (1967).
506. K. Igi, T. Yasui, J. Hidaka and Y. Shimura, *Bull. Chem. Soc. Japan*, 44, 426 (1971).
507. D.R. Boone, communication with M.R. Snow (1972).
508. K. Michelsen, *Acta Chem. Scand.*, 19, 1175 (1965).
509. Structure currently under investigation by M.R. Snow (1973).
510. S.F. Mason and B.J. Norman, *Chem. Comm.*, 335 (1965).
511. B. Norden, *Acta Chem. Scand.*, 26, 111 (1972).
512. E.C. Gyarfas and F.P. Dwyer, *Rev. Pure Appl. Chem.*, 4, 73 (1954).
513. J. Graham, *J. Phys. Chem. Solids*, 17, 18 (1960).
514. D.R. Stephens and H.G. Drickamer, *J. Chem. Phys.*, 35, 427, 429 (1961).
515. J.W. McCauley and G.V. Gibbs, *Z. Krist.*, 135, 453 (1972).
516. J.D.H. Donnay, G. Donnay, E.G. Cox, O. Kennard and M.V. King, *Amer. Cryst. Assoc. Monograph No. 5, Crystal Data, Determinative Tables* (2nd Edtn., 1963).
517. L.L. Lohr, Jr., and W.N. Lipscomb, *J. Chem. Phys.*, 38, 1607 (1963).
518. G.L. Allen, G.A.M. El-Sharkawy and K.D. Warren, *Inorg. Chem.*, 10, 2538 (1971).

519. J. Ferguson, H.J. Guggenheim and D.L. Wood, *J. Chem. Phys.*, 54, 504 (1971).
520. A.F. Schreiner and P.J. Hauser, *Inorg. Chem.*, 11, 2706 (1972).
521. E. Larsen, S.F. Mason and G.H. Searle, *Acta Chem. Scand.*, 20, 191 (1966).
522. E.W. Barnum, *J. Inorg. Nuclear Chem.*, 21, 221 (1961); 22, 183 (1961).
523. J.-Y. Sun, Ph.D. Thesis, University of Nth. Carolina (1967): *Diss. Abs.*, B28, 4482 (1968).
524. R.B. von Dreele and R.C. Fay, *J. Amer. Chem. Soc.*, 93, 4936 (1971).
525. F.H. Allen and D. Rogers, *Chem. Comm.*, 837 (1966).
526. G.A. Heath and R.L. Martin, *Aust. J. Chem.*, 24, 2061 (1971).
527. G.A. Heath and R.L. Martin, *Aust. J. Chem.*, 25, 2547 (1972).
528. G.A. Heath and R.L. Martin, *Aust. J. Chem.*, 23, 1721 (1970).
529. R.D. Shannon and C.T. Prewitt, *Acta Cryst.*, B25, 925 (1969).
530. W.M. Reiff and D. Szymanski, *Chem. Phys. Letters*, 17, 288 (1972).
531. R.G. Cavell, W. Byers and E.D. Day, *Inorg. Chem.*, 10, 2710 (1971).
532. P.J. Hauser, A.F. Schreiner, J.D. Gunter, W.J. Mitchell and M.K. De Armond, *Theor. Chim. Acta*, 24, 78 (1972).
533. V. Doron and W. Durham, *J. Amer. Chem. Soc.*, 93, 889 (1971).
534. K.P. Callahan, G.A. Ostrom and R.M. Wing, *Inorg. Chem.*, 9, 2605 (1970)
535. J. Podlahova and J. Podlaha, *J. Inorg. Nuclear Chem.*, 28, 2267 (1966).